METHODS OF CARBOHYDRATE FUNCTIONALIZATION AND DEFUNCTIONALIZATION

Laura L. Adduci

A dissertation submitted to the faculty of the University of North Carolina at Chapel Hill in partial fulfillment of the requirements for the degree of Doctor of Philosophy in the Department of Chemistry

Chapel Hill
2014

Approved by

Michel R. Gagné

Alexander J. M. Miller

Cynthia K. Schauer

Maurice S. Brookhart

Marcey L. Waters

ABSTRACT

LAURA L. ADDUCI: Methods of Carbohydrate Functionalization and Defunctionalization
(Under the direction of Michel R. Gagné)

Transformations of naturally abundant carbohydrates offer the potential to generate valuable chemicals from inexpensive chiral materials. Initial work described herein focuses on the oxidative addition of glycosyl halides to palladium(0) centers. This process models the first step of a non-radical cross-coupling cycle targeting the installation of a carbon-based fragment at the anomeric center of a carbohydrate, generating a *C*-glycoside. Although carbohydrates, as secondary alkyl halides, are particularly challenging substrates for oxidative addition, certain conditions provided glycosyl-palladium oxidative addition products. Subsequent investigations probed the stability and further reactivity of the isolated glucosyl palladium complexes to assess their suitability for further functionalization; they were found to be quite prone to elimination processes, which hindered attempts to elaborate this work to a cross-coupling cycle.

A second area of research focused on defunctionalization reactions to develop methods for biofeedstock syntheses. Initially, a hydrosilylative approach to carbohydrate deoxygenation was employed that involved catalysis by an iridium complex supported by a pincer ligand. Under iridium catalysis, the very active diethylsilane reduced all of the C-O bonds in a monosaccharide, resulting in the generation of *n*-hexane and, presumably through alkyl shift processes, 2-methylpentane and 3-methylpentane. The ratio of alkane product isomers varied for different carbohydrate starting materials.

Subsequently, complete hydrosilylative reduction of carbohydrates was catalyzed by commercially available Lewis acidic tris(pentafluorophenyl)borane. Several differences between the borane and iridium systems were observed. Notably, reactions catalyzed by borane proceeded more quickly than those catalyzed by iridium. This increased catalytic activity allowed the use of less active tertiary silanes, such as dimethylethylsilane and triethylsilane, as the reductive equivalent. Hydrosilylative reduction using these tertiary silanes proved to be selective for certain sites on the carbohydrate, affording partially deoxygenated compounds while retaining some of the carbohydrate stereochemistry. Close observation of the product stereochemistry revealed that certain substrates were epimerized during the course of the reaction. These data led to a proposed mechanism involving intramolecular cyclization to give a cyclic silyl oxonium species as an intermediate. The proposed cyclic intermediate was then independently generated and characterized. These intermolecular cyclization processes provide an explanation for an array of observations, suggesting that they may be quite prevalent in deoxygenation reactions of carbohydrates.

ACKNOWLEDGEMENTS

First and foremost, I would like to thank Professor Michel Gagné for allowing me to work in his laboratory. Mike insists on seeing the best in his students; his enthusiasm for chemistry and gentle encouragement have provided motivation in times of frustration and generated even more excitement when projects were going well.

Many former lab members had a significant impact on my first few years in lab. Dr. Colleen Munro-Leighton patiently taught me lab techniques, Swagelok skills, 2D NMR interpretation, and general lab upkeep procedures… in that order. Although we overlapped in the Gagné lab for less than a year, her email support has been constant over the past five years. Dr. Steve Andrews helped me with basic carbohydrate chemistry, and his narrations of lab procedures were always educational. Dr. Dieter Weber was always willing to share his knowledge and contribute new ideas to the group. Dr. Joe Sokol made sure I left lab every once in a while for trivia nights and book club meetings. Within lab, Joe was always up for troubleshooting the latest piece of misbehaving piece of lab equipment. Dr. Ryan Felix listened to me plan out ways to test various ideas, and provided insight whenever he could. Dr. Nikki Cochrane was always ready to chat about research approaches and potential safety issues.

Thanks to Dr. Mike Geier for sequestering Mee-Kyung to one room, for the most part. Thanks to Dr. Mee-Kyung Chung for running mass spec samples and providing advice on running columns. Thanks especially to Trandon Bender, Dr. Jen Dabrowski, Stephanie Kramer and Dr. Matt McLaughlin, the most recent members of "Team Sugar". Always ready to stop for a minute

to debate someone's newest research idea or ponder some confusing NMR data, these lab members have made it a pleasure to work in the carbohydrate subgroup. Thanks also to other members of the Gagné lab: Dr. Hongchao Zheng, Dr. Pippa Payne, Dr. Mike Bertucci, Ha Nguyen, Chrissy Roselli, and Mike Peruzzi for insightful comments on chemistry, lab life, and practice talks.

Thanks to Dr. Marc ter Horst and Dr. Ben Giglio in the NMR facility for giving me a place to escape from lab, and for humoring me when I wanted to talk (again) about ^{13}C NMR integration or the samplechanger. I would also like to thank the many users of the NMR facility who have sought my advice, given my suggestions a try, and genuinely thanked me for my help. These students and postdocs have done much to make me feel like a valued member of the UNC chemistry community. Thanks to the members of my committee, Professors Miller, Schauer, Brookhart, and Waters, and to Dr. Peter White for helping me with crystal structures and Dr. Sohrab Habibi for acquiring mass spectrometry data for the palladium structures.

Outside of UNC, thanks to the former residents of Brandeis's Mod 27. Oriana Fisher has been listening to me complain about chemistry since 2005. Generous with her time, she has never failed to give up an hour whenever I called to relate my latest lab story. Thanks also to Stephanie Chapin and Myka Held for being only an email or phone call away, even if our visits are few and far between. In addition, thanks to Ruth, Nick, and Calvin Baldasaro for 5 years (well, 2 years for Calvin) of dinners, board games, and walks on the trail. The biggest of thanks to Prof. Bruce Foxman, without a doubt the best professor at Brandeis, the reason that I am in grad school, and the person who showed me how much fun research can be. I am extremely thankful to have ended up in his lab for undergraduate research and kept in touch since then. Thanks to my family, especially to my grandparents for calling me every Friday for the last nine years, looking for Raleigh on the weather map every day, and admiring "those little stick diagrams" in my papers.

TABLE OF CONTENTS

LIST OF TABLES

LIST OF SCHEMES

LIST OF FIGURES

LIST OF ABBREVIATIONS AND SYMBOLS

°C	degrees Celcius
2-MP	2-methylpentane
3-MP	3-methylpentane
Å	angstrom
Ac	acetyl
α	alpha – opposite sides of pyranose ring (stereochemistry)
AIBN	2,2’-azobis(2-methylpropionitrile)
aq	aqueous
β	beta – same side of the pyranose ring (stereochemistry)
Bn	benzyl
Bz	benzoate
C-	carbon (linkage in saccharides)
δ	delta – chemical shift (NMR)
d	doublet (NMR)
D	dextrorotary (stereochemistry, relative to glyceraldehyde)
DMSO	dimethylsulfoxide)
eq.	equivalent
ESI	electrospray ionization
Et	ethyl
g	gram
µg	microgram
GCMS	gas chromatography – mass spectroscopy

h	hour
HRMS	high resolution mass spectrum
Hz	hertz (NMR coupling constants)
L	liter
L	levorotary (stereochemistry, relative to glyceraldehyde)
mL	milliliter
µL	microliter
λ	lambda - wavelength
M	molar – 1 mol / liter (concentration)
Me	methyl
MeOH	methanol
mg	milligram
$MgSO_4$	magnesium sulfate
MHz	megahertz
µL	microliter
min	minutes
mM	millimolar – 10^{-3} mol / liter (concentration)
mmol	millimole
mol %	mole percent (catalyst loading)
MS	molecular sieves
m/z	mass-to-charge ratio (mass spectrometry)
NMR	nuclear magnetic resonance
P	any unspecified protecting group

Ph	phenyl
1,10-phen	1,10-phenanthroline
Piv	pivaloate
PPh_3	triphenylphosphine
ppm	parts per million (NMR relative difference)
*i*Pr	*iso*-propyl
q	quartet (NMR)
R-	any unspecified carbon-containing group
rt	room temperature
σ	sigma – electrons involved in C-C single bonds
σ*	antibonding orbital in C-C single bonds
s	seconds
s	singlet (NMR))
t	triplet (NMR)
THF	tetrahydrofuran
TMEDA	*N,N,N',N''*-tetramethylethylenediamine
TMS	trimethylsilyl
TON	turnover number

Chapter 1 Introduction

1.1 *Carbohydrates in Nature*

Carbohydrates represent an attractive class of starting materials for organic synthesis. These naturally-occurring biological molecules consist mainly of carbon, oxygen, and hydrogen atoms and have the general formula $(CH_2O)_n$, where n is three or more.[1] Monosaccharides, for which n is generally between three and six, are often linked together to form di-, oligo-, and polysaccharides. Monosaccharides and disaccharides are frequently referred to colloquially as "sugars." Monosaccharides can be divided into aldose and ketose forms, where depending on whether the carbon chain terminates in an aldehyde or whether there is an internal carbonyl group.[2]

Within the group of monosaccharides, carbohydrates are usually named according to the stereochemical arrangement of their hydroxyl groups. Furthermore, each monosaccharide can adopt multiple isomeric structures.[1] For example, glucose can exist in an open chain aldohexose form, the more stable 6-membered hemiacetal pyranose form, or the less stable 5-membered hemiacetal furanose form (Figure 1.1).[1] The relative populations of each conformation depend on the environment of the carbohydrate. Glucose, for example, is usually found as the pyranose form in aqueous solutions under ambient conditions.[2]

[1] Miljkovic, M. *Electrostatic and Stereoelectronic Effects in Carbohydrate Chemistry*; Springer US: New York, 2014.

[2] Stoddart, J. F. *Stereochemistry of Carbohydrates*; John Wiley & Sons, I., Ed.; New York, 1971; pp. 32–33.

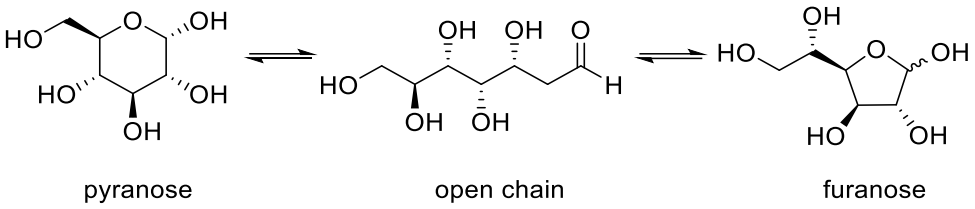

Figure 1.1: pyranose, open chain, and furanose forms of glucose

The carbon chain numbering scheme commonly used for carbohydrates assigns the hemiacetal carbon as C_1, and labels the carbons consecutively along the chain to C_6 (Figure 1.2).[2] One final difference between isomers of the same pyranose is the relative orientation of the substituents on both sides of the ethereal oxygen in the pyranose ring. In the α anomer, the hydroxyl group at C_1 and the CH_2OH group at C_5 are on opposite faces of the ring. The C_1-epimer, in which the C_1 and C_5 substituents are on the same face of the ring, is known as the β anomer.

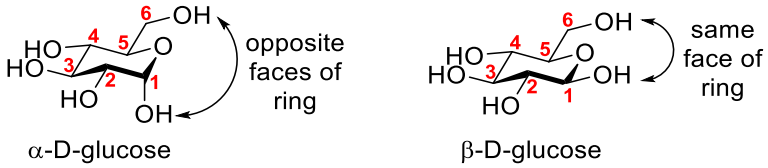

Figure 1.2: α and β anomers of glucose with numbering scheme

The distinction between α and β anomers is important because of the anomeric effect, a secondary orbital interaction between the non-bonding electrons of the ethereal oxygen and the σ* antibonding orbital of the C_1-X bond (Figure 1.3).[1] In the α anomer, the σ* antibonding orbital is oriented such that the non-bonding electrons from the ethereal oxygen can be donated into it. This serves to thermodynamically stabilize the molecule at the expense of weakening the C-X bond.[3] In the β anomer, the anomeric effect is not observed because the orientation of the σ* antibonding orbital of the C_1-X bond precludes overlap with the non-bonding electrons of the pyranose oxygen.

[3] Carey, F. A.; Sundberg, R. J. *Advanced Organic Chemistry*; 4th ed.; Plenum Publishers: New York, 2000.

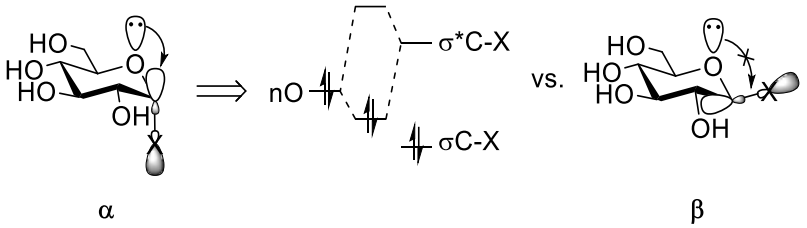

Figure 1.3: Anomeric effect stabilizes the α anomer relative to the βanomer

The relative stability of the α anomer in comparison to the β anomer allows for interesting reactivity. Namely, while the solution-phase equilibrium lies towards the α anomer for glycosyl halides, the β anomer is often more reactive due to its thermodynamic instability. Lemieux took advantage of this effect to achieve nucleophilic substitution using even poor nucleophiles such as alcohols (Scheme 1.1).[4] In this work, excess bromide in solution establishes an equilibrium between the α and β anomers, while the less thermodynamically stable β anomer further reacts with the weakly nucleophilic alcohol. The α anomer of the resulting *O*-glycoside usually predominates due to the increased stability of the α anomer relative to the β anomer resulting from the anomeric effect.

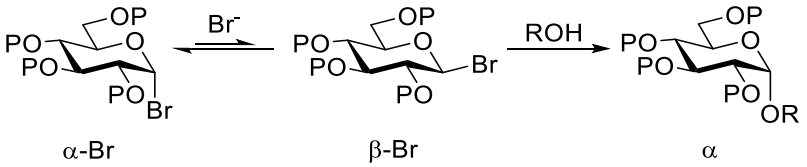

Scheme 1.1: Nucleophilic substitution of glucosyl bromide

From a synthetic chemistry perspective, carbohydrates are appealing starting materials. They are prevalent in nature and offer established stereochemistry. Their many C-O bonds provide sites for functionalization or substitution. However, they also present challenges to a synthetic chemist. The polarity of sugars renders them insoluble in most organic solvents, which limits the number of well-studied organic techniques that can be used to manipulate them. To overcome this

[4] Lemieux, R. U.; Hendriks, K. B.; Stick, R. V; James, K. *J. Am. Chem. Soc.* **1975**, *97*, 4056–4062.

insolubility, protecting groups are often used. However, protections and deprotections require additional synthetic steps, and protecting groups sometimes limit the tolerance for different reagents. Synthetic methods that aim to incorporate carbohydrates must take these considerations into account.

1.2 *Anomeric functionalization of carbohydrates*

1.2.1 Synthesis of C-glycosides

The synthesis of useful *C*-glycosides from naturally available *O*-glycosides has long been a goal for synthetic chemists.[5-9] *C*-glycosides are carbohydrates in which the hydroxyl group at C_1 has been replaced with a carbon-based fragment. *C*-glycosides are thought to have various beneficial medicinal properties. While metabolic processes readily decompose *O*-glycosides, C-glycosides are more resistant to these decomposition processes, resulting in a reduced dosage requirement for pharmaceuticals based on *C*-glycosides. A promising example of this comes from the synthesis of the *C*-glycosidic analog of KRN-7000, a galactosyl ceramide with immunostimulant properties (Figure 1.4).[10] To test the relative potencies of the *O*-glycoside and *C*-glycoside variations of this compound, mice were treated with 10 nanograms of either the *O*-glycosidic or *C*-glycosidic compound. They were then challenged with either malaria or melanoma. In the case of both diseases, the subjects that had been pre-treated with the *C*-glycoside had far fewer biomarkers of disease than the subjects that had been treated with the *O*-glycosides.

---

[5] Levy, D. E.; Tang, C. *The Chemistry of C-Glycosides*; Elsevier Science Ltd.: New York, 1995.

[6] Nicotra, F. *Top. Curr. Chem.* **1997**, *187*, 55–83.

[7] Giese, B.; Dupuis, J. *Angew. Chem. Int. Ed.* **1983**, *22*, 622–623.

[8] Du, Y.; Linhardt, R. J.; Vlahov, I. R. *Tetrahedron* **1998**, *54*, 9913–9959.

[9] Wellington, K. W.; Benner, S. A. *Nucleosides, Nucleotides and Nucleic Acids* **2006**, *25*, 1309–1333.

[10] Yang, G.; Schmieg, J.; Tsuji, M.; Franck, R. W. *Angew. Chem. Int. Ed.* **2004**, *43*, 3818–3822.

The authors suggest that the reduced propensity for the *C*-glycoside to decompose under physiological conditions has led to this increased potency, that is, a smaller dose of the *C*-glycoside gives similar effect as a larger dose of the *O*-glycosides because it will remain active for longer.

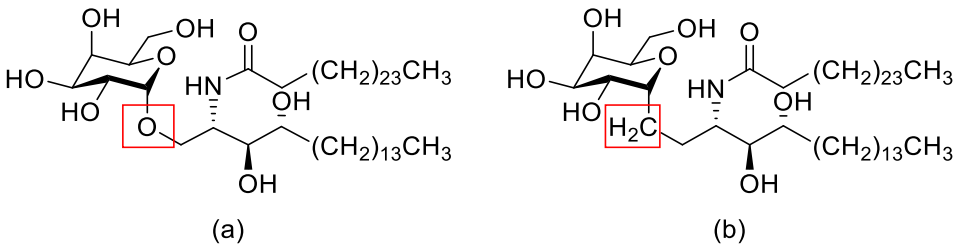

Figure 1.4: (a) KRN-7000 and (b) *C*-glycoside analog of KRN-7000

1.2.2 Methods of C-glycoside formation

C-glycosides have been synthetic targets for many years.[5] Accordingly, an array of methods has been developed. Many such methods are nucleophilic methods, in which an electrophilic site on the carbohydrate is attacked by a nucleophile, establishing a new bond between the carbohydrate and the nucleophile.[5] The addition of many nucleophiles require pre-activation of the carbohydrate by a Lewis acid. Some relatively strong Lewis acids can abstract the C_1 substituent entirely, leaving a carbocation that enjoys special stability due to interaction with the non-bonding electrons of the neighboring ethereal oxygen.[11] Many nucleophiles are then able to add to this oxocarbenium cation. Lewis acids such as BF_3 and $BiBr_3$[12] are typically used for this kind of activation. Silylium sources such as trimethylsilyltriflate (Me_3SiOTf)[13] iodotrimethylsilane (Me_3SiI)[14] also effect these types of transformations (Scheme 1.2). Allylations

[11] Kozikowski, A. P.; Sorgi, K. L.; Wang, B. C.; Xu, Z. *Tetrahedron Lett.* **1983**, *24*, 1563–1566.

[12] Komatsu, N.; Uda, M.; Suzuki, H.; Takahashi, T.; Domae, T.; Wada, M. *Tetrahedron Lett.* **1997**, *38*, 7215–7218.

[13] Hosomi, A.; Sakata, Y.; Sakurai, H. *Carbohydr. Res.* **1987**, *171*, 223–232.

[14] Hosomi, A.; Sakata, Y.; Sakurai, H. *Tetrahedron Lett.* **1984**, *25*, 2383–2386.

and related reactions can be accomplished in this way.[13] It is thought that, in these types of reactions, the stereochemistry of the intermediate oxocarbenium species directs the incoming nucleophile, giving rise to products that tend to favor the α anomer.[14]

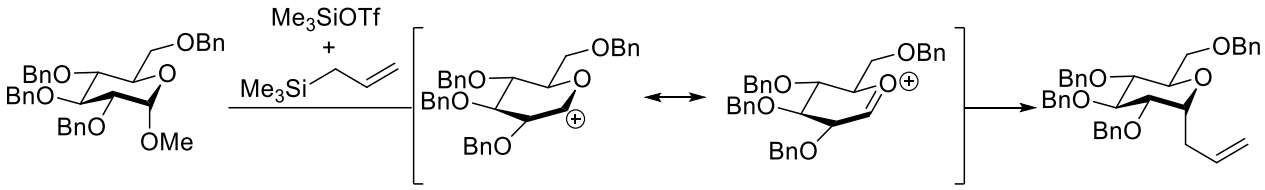

Scheme 1.2: Lewis acid assisted allylation of glucose

Some methods of *C*-glycoside formation depend on formation of radicals, sometimes mediated by Bu_3SnH (Scheme 1.3). These methods give a high selectivity for α anomer products due to the stability of the α radical relative to the β radical, which results from appropriate orientation of the radical to interact with electrons in the non-bonding orbital.[15] In addition, Giese and coworkers have shown that adoption of the boat form for glycosidic radical compounds orients the C_2 and C3 substituents axially, providing additional stabilization to the radical from neighboring C-O bonds.[16] While these methods are effective for generating *C*-glycosides,[17] they usually require excess amounts of the alkene, and the tin promoters are toxic. Other metal species such as manganese, titanium, and chromium have also been used to generate anomeric radicals.[5] However, the availability of mild methods of *C*-glycoside synthesis from glycosyl halides is still limited.

[15] Giese, B.; Dupuis, J. *Tetrahedron Lett.* **1984**, *25*, 1349–1352.

[16] Giese, B.; Dupuis, J. *Angew. Chem. Int. Ed.* **1983**, *22*, 622–623.

[17] Giese, B.; Dupuis, J.; Leising, M.; Nix, M.; Lindner, H. J. *Carbohydr. Res.* **1987**, *171*, 329–341.

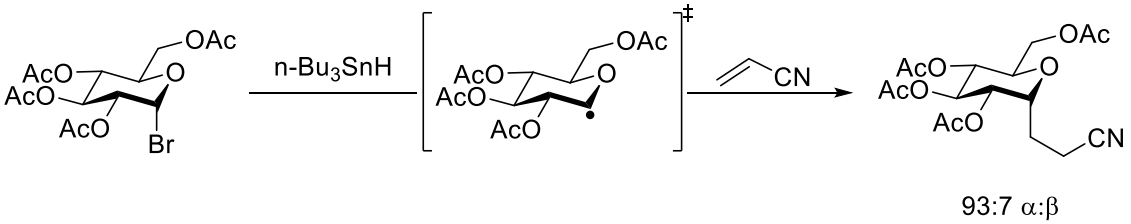

Scheme 1.3: reaction of an anomeric radical with acrylonitrile

Transition metal catalyzed cross-coupling offers potential as an effective method for *C*-glycoside synthesis. One of the biggest challenges to using traditional cross-coupling approaches with carbohydrates is the susceptibility of the glycosyl-metal intermediates to β-hydride or β-alkoxy elimination processes. Bulky pybox ligands were used to prevent these detrimental side reactions in a nickel-catalyzed Negishi reaction developed in the Gagné (Scheme 1.4).[18] By blocking the *cis* coordination site at the metal center, this ligand system allows the productive coupling pathway to outcompete the undesired elimination pathway. Using this system, various sugars (glucose, mannose, and galactose) with different protecting groups (relatively electron-rich benzyl groups or relatively electron-poor acetate groups) were treated with alkyl zinc bromide reagents to afford the desired glycosyl-alkyl compounds. Mannose sugars, which have axial C_2 substituents in contrast to the equatorial C_2 substituents of glucose and galactose, tended to give high selectivities for the α cross-coupling products, while glucose and galactose gave mixtures of diastereomers. Differences between benzyl-protected substrates and acetate-protected substrates were also evident: for the less activated acetate-protected sugars, use of the glycosyl bromide instead of the glycosyl chloride was necessary for the reaction to proceed. In contrast, for the more activated benzyl-protected sugars, the glycosyl bromide was too reactive and led to hydrolysis, but

[18] Gong, H.; Sinisi, R.; Gagné, M. R. *J. Am. Chem. Soc.* **2007**, *129*, 1908–1909.

the glycosyl chlorides worked well. This work represents exciting progress towards mild methods of *C*-glycoside generation.

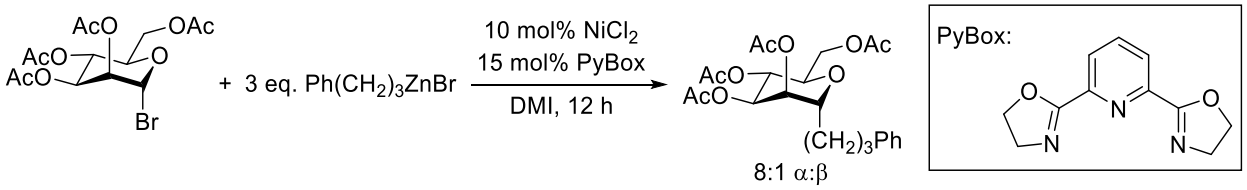

Scheme 1.4: *C*-glycosylation via nickel-catalyzed Negishi cross-coupling

In subsequent work, the scope of this methodology was expanded to include coupling to aryl zinc iodide, enabling the synthesis of *C*-aryl-glycosides (Scheme 1.5).[19] This was achieved by screening nickel sources and ligands, arriving at $Ni(COD)_2$/^{t}Bu-terpy in DMF as the optimal conditions. A variety of aryl groups were coupled to sugars, allowing a significant improvement over previous methods that were often limited to electron-rich arenes.[20]

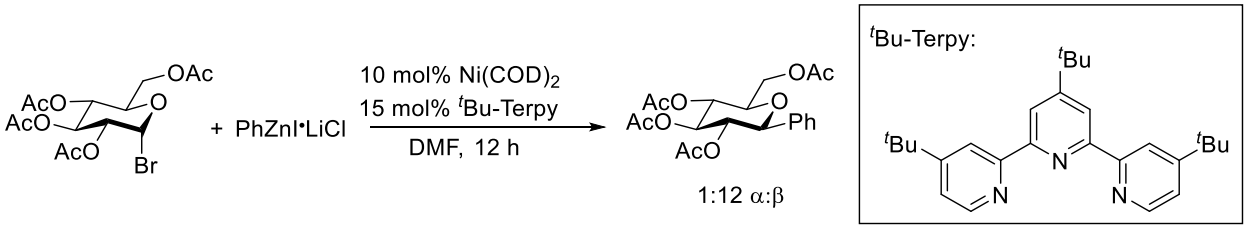

Scheme 1.5: *C*-aryl glycoside synthesis via Negishi cross-coupling reaction

Using a similar nickel/PyBox system, a reductive coupling method was developed in which an anomeric radical is generated and coupled to an electron-deficient alkene, giving an alkyl radical which was quenched using zinc as a terminal reductant (Scheme 1.6).[21] Potential side products include β-hydride or β-alkoxide elimination, hydrolysis, and overaddition, although

[19] Gong, H.; Gagné, M. R. *J. Am. Chem. Soc.* **2008**, *130*, 12177–12183.

[20] Jensen, A. E.; Knochel, P. *J. Org. Chem.* **2001**, *67*, 79–85.

[21] Gong, H.; Andrews, R. S.; Zuccarello, J. L.; Lee, S. J.; Gagné, M. R. *Org. Lett.* **2009**, *11*, 879–882.

reaction optimization provided a means to reduce yields of these undesired species. The most likely mechanism relies on radical intermediates.

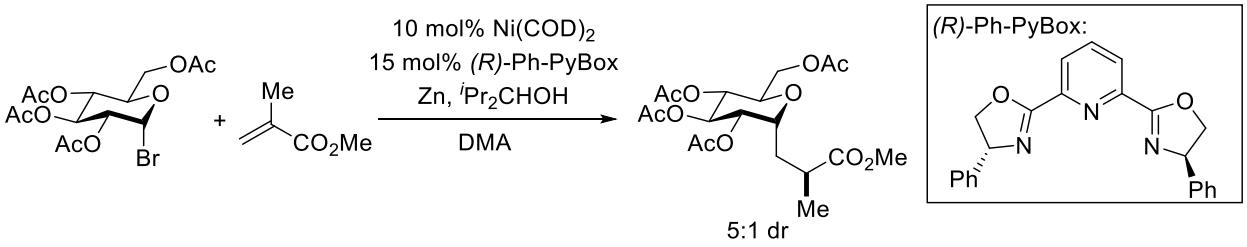

Scheme 1.6: Reductive coupling approach to *C*-glycosides

A final method of *C*-glycoside synthesis from the Gagné lab also involved a radical approach. In this photoredox system, visible light was used to activate $Ru(bpy)_3^{2+}$ to its metal-to-ligand charge transfer state, which could then be reduced by an amine to give a ligand-centered reducing equivalent (Scheme 1.7).[22] This complex then activates an anomeric glycosyl-bromide bond to give a glycosyl radical, which is trapped by an electron-deficient alkene. Subsequent radical quenching by a sacrificial $H^{\bullet}$ source then completes the reaction, giving the coupled *C*-glycoside product. This system worked well for a variety of electron-deficient alkenes, but the scale of the reaction was limited by the high molar extinction coefficient for compounds like $Ru(bpy)_3^{2+}$; Beer's law calculations indicated at practical catalyst concentrations, all of the visible light would be absorbed by the few millimeters of reaction mixture closest to the outside of the flask, leaving the majority of the flask essentially dark and unable to support catalysis.[23] By designing a photoflow reactor, in which the reaction mixture was irradiated by a series of LEDs as it progressed through a thin transparent tube, the reaction could be run on multi-gram scales.

[22] Andrews, R. S.; Becker, J. J.; Gagné, M. R. *Angew. Chem. Int. Ed.* **2010**, *49*, 7274–7276.

[23] Andrews, R. S.; Becker, J. J.; Gagné, M. R. *Angew. Chem. Int. Ed.* **2012**, *51*, 4140–4143.

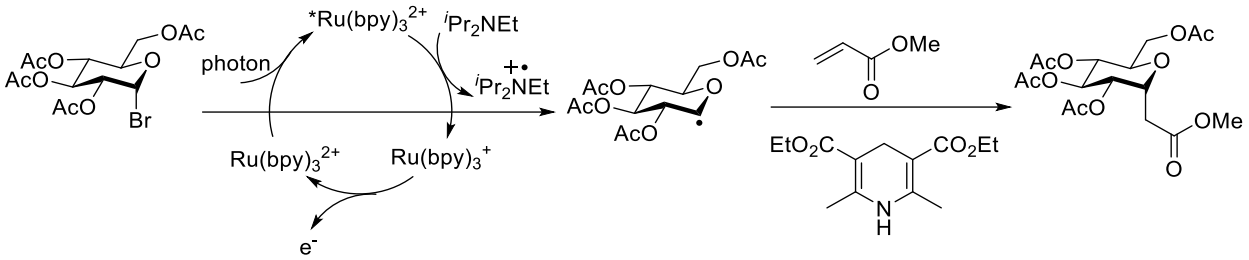

Scheme 1.7: Photoredox approach to *C*-glycoside synthesis

In further work, addition to an iridium(I) complex, $Ir(PMe_3)_2(CO)(Cl)$ or the PMe_3 derivative of Vaska's complex, was observed (Scheme 1.8).[24] The glucosyl-iridium complex was crystallized to determine its structure. It is thought that this glucosyl-metal complex was also generated via a radical process since both anomers of the sugars were observed. Also, addition to other similar complexes, such as $Ir(PPh_3)_2(CO)(Cl)$ was not observed, and it is known that the PMe_3 version of Vaska's complex can react through a radical or two-electron process, while the PPh_3 version is more prone to two-electron chemistry.[25] Furthermore, some substrates required the presence of AIBN, a radical initiator, to proceed, while others did not, suggesting that multiple different radical mechanisms may be at work.

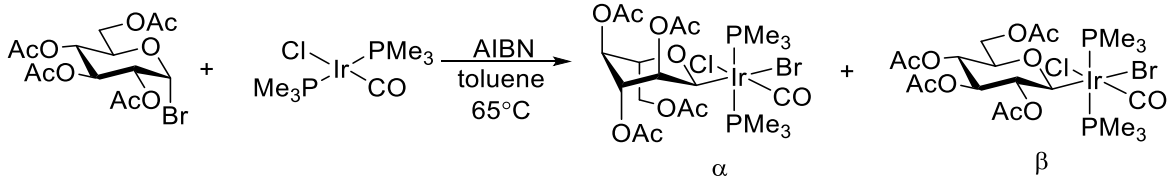

Scheme 1.8: Synthesis of glucosyl-iridium complexes

[24] Pelczar, E. M.; Munro-Leighton, C.; Gagné, M. R. *Organometallics* **2009**, *28*, 663–665.

[25] Labinger, J. A.; Osborn, J. A. *Inorg. Chem.* **1980**, *19*, 3230–3236.

1.2.3 Cross-coupling with secondary alkyl electrophiles

One difficulty of cross-coupling with carbohydrate substrates is that the sugar is a secondary alkyl electrophile. Although transition metal catalyzed cross-coupling has been intensely studied for decades, secondary alkyl electrophiles remain some of the most challenging substrates.[26] A typical cross-coupling, such as a Suzuki-Miyaura, Stille, or Buckwald-Hartwig reaction, begins with oxidative addition of a C-X bond to the metal center (Figure 1.5). Subsequent transmetallation with a suitable coupling partner followed by reductive elimination generates the desired cross-coupled product and turns over the catalytic cycle. While aryl and vinyl substrates work well in these processes, alkyl substrates present a greater challenge. Oxidative addition of alkyl halides to late transition metal centers is often slower than oxidative addition of aryls or vinyls because the C(sp^3)-X bond is more electron rich than the C(sp^2)-X bond, and oxidative addition, which formally reduces the C-X bond, is more facile for less electron-rich C-X bonds.[27] In addition, once alkyl substrates have added to the metal center, they are prone to β-hydride elimination, an undesirable side reaction that halts the progress of the catalytic cycle. π electrons, which can provide stabilizing interactions with the metal centers, are present in aryl and alkyl substrates, limiting the extent of β-elimination. For an oxidative addition product to continue through the catalytic cycle, the next desirable steps (transmetallation and reductive elimination) must outcompete β-elimination. As reductive elimination is generally slower for alkyl-based products than for aryl or vinyl products, alkyls are again more likely to undergo side reactions.[27]

[26] Rudolph, A.; Lautens, M. *Angew. Chem. Int. Ed.* **2009**, *48*, 2656–2670.

[27] Hartwig, J. F. *Organotransition Metal Chemistry: From Bonding to Catalysis*; University Science Books: Sausalito, 2010.

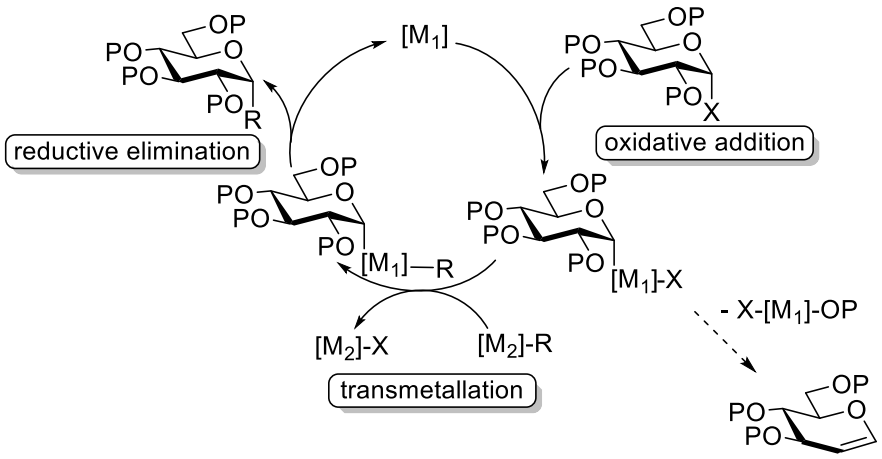

Figure 1.5: Targeted non-radical cross-coupling approach to *C*-glycosides

Despite the many challenges of cross-coupling reactions with alkyl electrophile substrates, much progress has been made with primary substrates.[28-32] Far fewer systems have been developed for use with secondary alkyl electrophile substrates, likely due to the higher energy barrier for oxidative addition of sterically hindered substrates. Fu and coworkers showed that, for branched primary substrates, branching closer to the halide significantly inhibits the rate of oxidative addition (Scheme 1.9).[33] In fact, for secondary alkyl electrophiles, no reactivity was observed.

[28] Cárdenas, D. J. *Angew. Chem. Int. Ed.* **2003**, *42*, 384–387.

[29] Terao, J.; Kambe, N. *Acc. Chem. Res.* **2008**, *41*, 1545–1554.

[30] Zhou, J.; Fu, G. C. *J. Am. Chem. Soc.* **2003**, *125*, 12527–12530.

[31] Frisch, A. C.; Beller, M. *Angew. Chem. Int. Ed.* **2005**, *44*, 674–688.

[32] Cong, H.; Fu, G. C. *J. Am. Chem. Soc.* **2014**, *136*, 3788–3791.

[33] Hills, I. D.; Netherton, M. R.; Fu, G. C. *Angew. Chem. Int. Ed.* **2003**, *42*, 5749–5752.

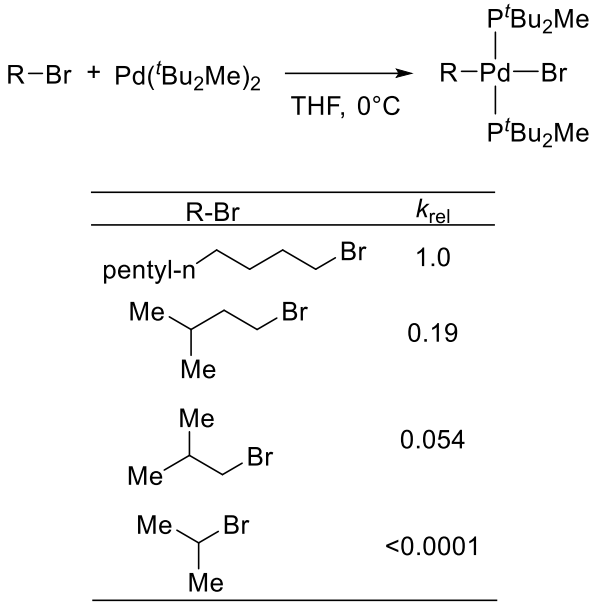

Scheme 1.9: Relative rates of oxidative addition to Pd(0) for primary, branched, and secondary alkyl electrophile substrates

The majority of transition metal-catalyzed reactions with secondary alkyl electrophiles have been nickel-catalyzed and likely proceed through radical mechanisms.[34-36] Such reactions include Negishi couplings using bulky ligands,[37] Suzuki couplings using aryl boronic acids and alkyl boranes,[38] and Stille couplings using monoorganotin reagents,[39] among other examples.[40] A recent example from the Gong group shows reductive electrophile coupling.[41] Complexes of other

[34] Anderson, T. J.; Jones, G. D.; Vicic, D. A. *J. Am. Chem. Soc.* **2004**, *126*, 8100–8101.

[35] Jones, G. D.; McFarland, C.; Anderson, T. J.; Vicic, D. A. *Chem. Commun.* **2005**, 4211–4213.

[36] Jones, G. D.; Martin, J. L.; McFarland, C.; Allen, O. R.; Hall, R. E.; Haley, A. D.; Brandon, R. J.; Konovalova, T.; Desrochers, P. J.; Pulay, P.; Vicic, D. A. *J. Am. Chem. Soc.* **2006**, *128*, 13175–13183.

[37] Zhou, J.; Fu, G. C. *J. Am. Chem. Soc.* **2003**, *125*, 14726–14727.

[38] Zhou, J.; Fu, G. C. *J. Am. Chem. Soc.* **2004**, *126*, 1340–1341.

[39] Powell, D. A.; Maki, T.; Fu, G. C. *J. Am. Chem. Soc.* **2005**, *127*, 510–511.

[40] Frisch, A. C.; Beller, M. *Angew. Chem. Int. Ed.* **2005**, *44*, 674–688.

[41] Wang, S.; Qian, Q.; Gong, H. *Org. Lett.* **2012**, *14*, 3352–3355.

first row transition metals, such as cobalt[42,43] and iron,[44,45] have also been shown to do similar couplings. Despite a few examples of palladium catalysis,[46,47] two-electron cross-coupling reactions of secondary alkyl electrophiles remain rare.[26]

In addition to the glucosyl-iridium complex isolated by our group, several other metal-carbohydrate complexes have been reported. Trainor and Smart reported the preparation of a glucospyranosyl iron compound via treatment of methyl-protected α-glucosyl bromide with sodium (η-5 cyclopentadienyl)dicarbonylferrate (NaFp) (Scheme 1.10).[48] The high nucleophilicity of the Fp^- anion likely drives this reaction. Although the authors report that this compound is isolated by column chromatography, they also mention that it is rapidly attacked by atmospheric oxygen. At -78°C, this reaction was diastereoselective for the α anomer, while at 25°C a 5:1 ratio of α to β anomers was observed. The authors attribute this decreased diastereoselectivity to α/β isomerization, noting that any β anomer formed will be kinetically trapped, giving the product of net retention. Although this is an important example of a carbohydrate-metal complex, it does not show susceptibility to CO insertion processes, limiting its utility in *C*-glycoside formation.

[42] Someya, H.; Ohmiya, H.; Yorimitsu, H.; Oshima, K. *Org. Lett.* **2007**, *9*, 1565–1567.

[43] Cahiez, G.; Chaboche, C.; Duplais, C.; Moyeux, A. *Org. Lett.* **2008**, *11*, 277–280.

[44] Sherry, B. D.; Fürstner, A. *Acc. Chem. Res.* **2008**, *41*, 1500–1511.

[45] Cahiez, G.; Duplais, C.; Moyeux, A. *Org. Lett.* **2007**, *9*, 3253–3254.

[46] Sustmann, R.; Lau, J.; Zipp, M. *Tet. Lett.* **1986**, *27*, 5207–5210.

[47] López-Pérez, A.; Adrio, J.; Carretero, J. C. *Org. Lett.* **2009**, *11*, 5514–5517.

[48] Trainor, G. L.; Smart, B. E. *J. Org. Chem.* **1983**, *48*, 2447–2448.

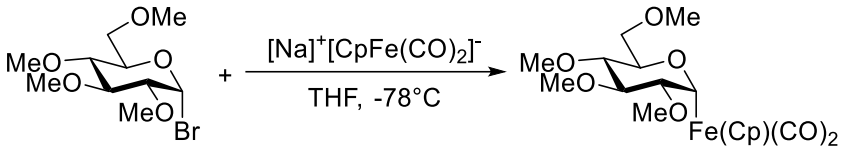

Scheme 1.10: Synthesis of glucosyl-iron complex

DeShong and coworkers reported several carbohydrate-metal complexes including a glucosyl-manganese complex produced from treatment of benzylbromo-α-D-glucose with sodium pentacarbonyl manganate(I) (Scheme 1.11).[49] Again, the highly nucleophilic character of the anionic transition metal precursor likely enables nucleophilic attack on the anomeric carbon center. DeShong reports that α-glucopyranosyl bromide and potassium pentacarbonylmanganate give exclusively the β product, while a mixture of α and β product results when tetrabutylammonium bromide is present. A subsequent report indicates that both the α and β glucosyl manganese complexes can undergo CO insertion when the complex is placed in a CO atmosphere, though the α complex seems to undergo carbonylation at a rate that is seven times faster than the β complex.[50] Although the α anomer undergoes faster CO insertion, the authors chose the β anomer of the CO insertion product to further elaborate with other nucleophiles via Reppe reactions. In this way, a variety of *C*-glycosyl esters were synthesized.

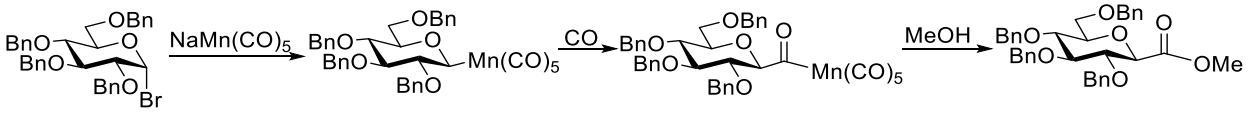

Scheme 1.11: Synthesis of glucosyl manganese complex, followed by carbonylation

[49] DeShong, P.; Slough, G. A.; Elango, V. *Carbohydr. Res.* **1987**, *171*, 342–345.

[50] DeShong, P.; Soli, E. D.; Slough, G. A.; Sidler, D. R.; Elango, V.; Rybczynski, P. J.; Vosejpka, L. J. S.; Lessen, T. A.; Le, T. X.; Anderson, G. B.; von Philipsborn, W.; Vöhler, M.; Rentsch, D.; Zerbe, O. *J. Organomet. Chem.* **2000**, *593-594*, 49–62.

An example of anomeric C-O activation comes from the Murai group, in which $Co_2(CO)_8$, under a CO atmosphere and in the presence of refluxing Me_3SiH or $MeEt_2SiH$, catalyzes a CO insertion into the C_1-O bond, followed by a silylation reaction (Scheme 1.12).[51] It is proposed that neighboring group assistance from the C_2 substituent aids in the selectivity of the reaction, in that the axial C_1 leaving group is activated by the neighboring C_2 group, rendering it susceptible to attack by the $Co(CO)_4^-$ nucleophile from the equatorial side.

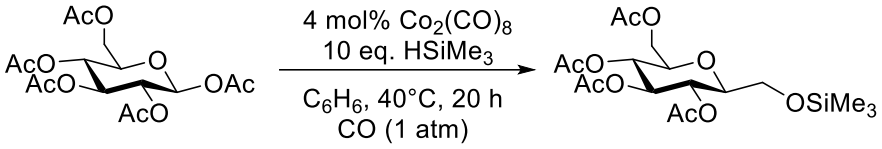

Scheme 1.12: Cobalt-catalyzed *C*-glycosylation

Another interesting report of an interaction between a carbohydrate and a metal center comes from Jones and Scott, who described in 1993 the synthesis of tetrabenzyl glucal from benzyl-protected glucosyl bromide (Scheme 1.13).[52] They propose that oxidative addition of the glucosyl bromide to the Pd(0) center occurs, followed quickly by β-hydride elimination. While it is possible that this reaction takes place via oxidative addition to the metal center followed by β-hydride elimination, it is also worth noting that the same product would result from base-catalyzed elimination from the glucosyl mesylate substrate.

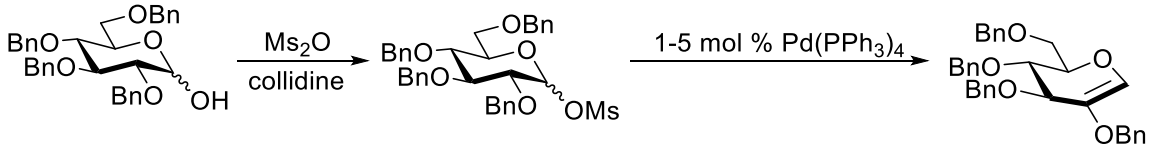

Scheme 1.13: Palladium(0)-catalyzed formation of tetra-benzyl glucal

[51] Chatani, N.; Ikeda, T.; Sano, T.; Sonoda, N.; Kurosawa, H.; Kawasaki, Y.; Murai, S. *J. Org. Chem.* **1988**, *53*, 3387–3389.

[52] Jones, G. S.; Scott, W. J. *J. Am. Chem. Soc.* **1992**, *114*, 1491–1492.

In summary, while there are methods for generating *C*-glycosides from glycosyl halides, the majority of these methods are thought to be based on radical transformations and are thus generally ineffective for the C-O activation that is necessary when starting from naturally occurring carbohydrates, without using an acid source to replace the anomeric oxygen-based substituent with a halide. New methods for these types of transformations are continually sought.

1.3 *Lewis acid catalyzed defunctionalization*

1.3.1 Biomass reduction

C-O bond cleavage in carbohydrates is also relevant for the transformation of biomass into biofuels and biofeedstocks, which has received increasing amount of attention recently as researchers look for replacements for bulk chemicals that have traditionally been derived from fossil fuels.[53] Schlaf summarized this challenge in 2006, stating that "an oxygen atom on every carbon – that is the problem!"[54] More specifically, carbohydrates are overfunctionalized for use as biofeedstocks and biofuels, so it is useful to develop efficient methods of removing oxygen content from biomass. Many methods have been developed by Schlaf,[55,54] Bullock, [56,57] Morris,[58]

[53] Ruppert, A. M.; Weinberg, K.; Palkovits, R. *Angew. Chem. Int. Ed.* **2012**, *51*, 2564–2601.

[54] Schlaf, M. *Dalton Trans.* **2006**, 4645–4653.

[55] Schlaf, M.; Thibault Michelle, E.; DiMondo, D.; Taher, D.; Karimi, E.; Ashok, D. *Int. J. Chem. React. Eng.*, 2009, *7*.

[56] Schlaf, M.; Ghosh, P.; Fagan, P. J.; Hauptman, E.; Bullock, R. M. *Adv. Synth. Catal.* **2009**, *351*, 789–800.

[57] Schlaf, M. *Dalt. Trans.* **2006**, 4645–4653.

[58] Meyer, N.; Lough, A. J.; Morris, R. H. *Chem. – A Eur. J.* **2009**, *15*, 5605–5610.

Dumesic,[59-62] and others[53] using ionic hydrogenations, catalysts supported by ionic liquids, and systems that operate at high temperature and pressures. The research on this topic is extensive and has been the subject of multiple reviews.[53,63] Nevertheless, a mild and selective system for the reduction of aldehydes, ketones, and alcohols has remained elusive. An ideal system might involve heterolytic cleavage of hydrogen gas to yield a proton that could activate C-O and a hydride that could perform a reduction. However, as systems for using H_2 in this manner are still in development, silanes such as Et_3SiH are often used as substitutes, allowing a silylium ion to be used as an activator and hydride to be the reducing agent.

1.3.2 Lewis acid assisted C-O reduction

Initial reports of Lewis acid assisted reduction used stoichiometric quantities of Lewis acids to activate carbonyl functionalities.[64] In these reactions, the polarization of the C-O bond is increased due to coordination of the Lewis acid, rendering the carbon more electrophilic and allowing for attack by an incoming nucleophile (Scheme 1.14). This method has been used to reduce carbonyls to alcohols using a BF_3/silane system.[65] In addition, this system can reduce alcohols and ethers to hydrocarbons, with selectivity for tertiary C-O bonds in preference to

[59] Roman-Leshkov, Y.; Barrett, C. J.; Liu, Z. Y.; Dumesic, J. A. *Nature* **2007**, *447*, 982–985.

[60] Kunkes, E. L.; Simonetti, D. A.; West, R. M.; Serrano-Ruiz, J. C.; Gärtner, C. A.; Dumesic, J. A. *Science* **2008**, *322*, 417–421.

[61] Serrano-Ruiz, J. C.; Braden, D. J.; West, R. M.; Dumesic, J. A. *Appl. Catal. B Environ.* **2010**, *100*, 184–189.

[62] Alonso, D. M.; Wettstein, S. G.; Dumesic, J. A. *Chem. Soc. Rev.* **2012**, *41*, 8075–8098.

[63] Corma, A.; Iborra, S.; Velty, A. *Chem. Rev.* **2007**, *107*, 2411–2502.

[64] Adlington, M. G.; Orfanopoulos, M.; Fry, J. L. *Tetrahedron Lett.* **1976**, *17*, 2955–2958.

[65] Fry, J. L.; Orfanopoulos, M.; Adlington, M. G.; Dittman, W. P.; Silverman, S. B. *J. Org. Chem.* **1978**, *43*, 374–375.

secondary and primary alcohols and ethers. Here, the boron-based Lewis acid likely activates the C-O bond, paving the way for the nucleophilic silane to donate a hydride (Scheme 1.15).

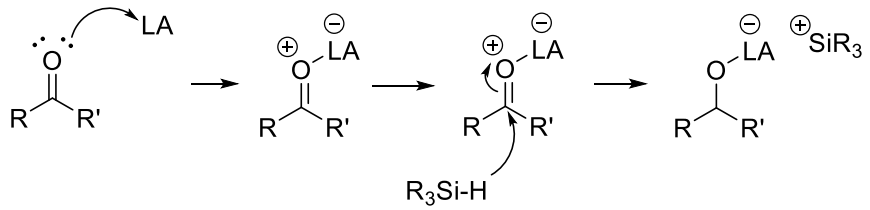

Scheme 1.14: Lewis acid assisted carbonyl reduction

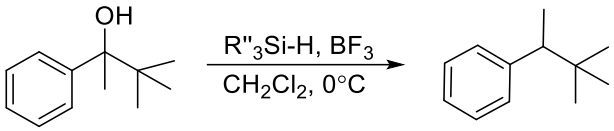

Scheme 1.15: BF_3-assisted reduction of a tertiary alcohol to a hydrocarbon

1.3.3 Catalytic reduction of C-O bonds

In the 1990's, it was reported that Lewis acidic tris(pentafluorphenyl)borane, $B(C_6F_5)_3$, in combination with a silane, is capable of catalytic reduction chemistry. Seminal work from the Piers group in 1996 demonstrated the reduction of aldehydes and ketones to alcohols and the reduction of esters to aldehydes by $B(C_6F_5)_3$ and Ph_3SiH.[66] The Piers group considered a mechanism in which $B(C_6F_5)_3$ coordinates to the carbonyl oxygen, supported by the observation that a solution of a carbonyl-containing substrate and $B(C_6F_5)_3$ gives an equilibrium favoring the adduct. Piers and coworkers were even able to characterize the carbonyl-$B(C_6F_5)_3$ adducts by small-molecule X-ray crystallography. In competitive binding experiments, they observe that the rate of $B(C_6F_5)_3$ binding follows the order of benzophenone > acetophenone >> ethyl benzoate (Scheme 1.16).

[66] Parks, D. J.; Piers, W. E. *J. Am. Chem. Soc.* **1996**, *118*, 9440–9441.

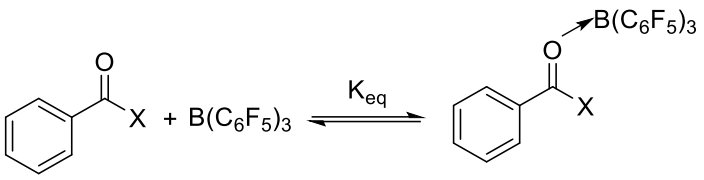

X	K_{eq} ($[M]^{-1}$)
H	2.1×10^4
Me	1.1×10^3
OEt	1.9×10^2

Scheme 1.16: Relative stabilities of carbonyl-$B(C_6F_5)_3$ adducts

However, they note that the observed rate of reaction is inversely dependent on the concentration of the substrate; increased substrate concentration leads to slower reactions. It is thought that the mechanism of activation here is different from so-called classical bond activation by Lewis acids. In contrast to a scenario in which the boron-based Lewis acid activates the C-O bond directly, here it is likely that the boron activates the silyl hydride (Scheme 1.17). Nucleophilic attack by the oxygen of a substrate then gives a disilyloxonium species and an equivalent of borohydride. The negatively charged borohydride can then add to the disilyloxonium, turning over the catalytic cycle and releasing silyl ether as a byproduct, in addition to the targeted reduction product. This suggests a mechanism in which the $B(C_6F_5)_3$ actually activates the silane (Si-H bond) instead of the carbonyl. Here, the substrate that coordinates the $B(C_6F_5)_3$ most weakly leaves the most uncoordinated $B(C_6F_5)_3$ available to interact with the silane, leading to a faster reaction (Scheme 1.18). Conversely, in competition experiments between benzophenone and ethyl benzoate, benzophenone is reduced preferentially. The observation that benzophenone is reduced in preference to ethyl benzoate during a competition experiment while the rate of ethyl benzoate reduction is faster than the rate of benzophenone reduction when the reactions are carried out in separate flasks suggests that the basicity of the carbonyl is important; the authors suggest that the more basic substrate is better able to abstract silyl cation from the silane/$B(C_6F_5)_3$ adduct.

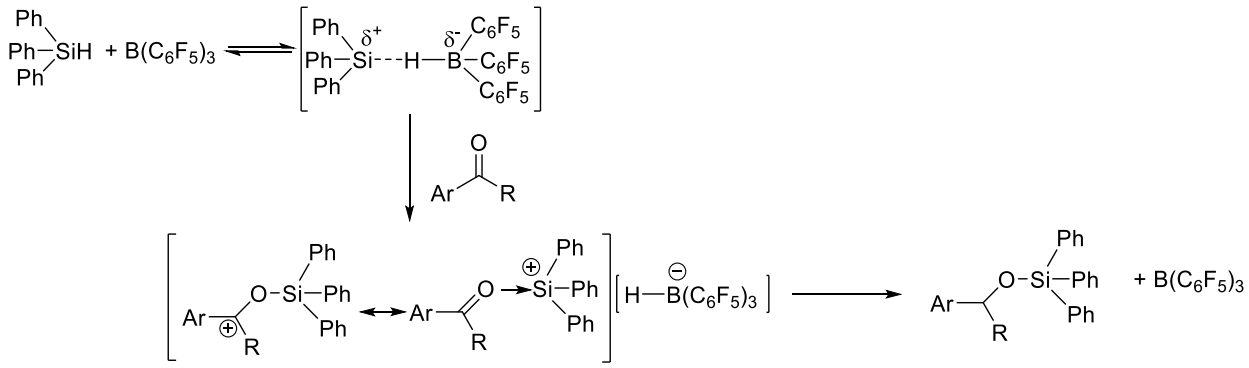

Scheme 1.17: Proposed mechanism of $B(C_6F_5)_3$-catalyzed reduction of carbonyls to silyl-protected alcohols

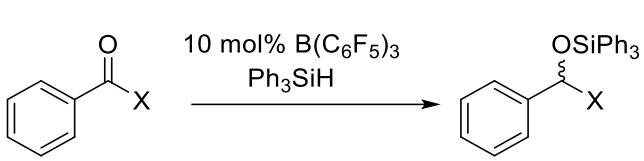

X	TON (hr^{-1})
H	19
Me	45
OEt	637

Scheme 1.18: Relative turn over numbers for reduction of carbonyls to alcohols

Several years after reporting the development of this catalytic system, the Piers group reported the results of an in-depth mechanistic investigation.[67] Their first group of studies focused on the interaction of $B(C_6F_5)_3$ with silane. Strong evidence towards borane activation of silane instead of activation of substrate would have been the observation of a borane-silane adduct in solution, but the Piers group was not able to observe that adduct, likely because the equilibrium lies too far towards the non-coordinated system. However, several other pieces of evidence indicate silane activation. Et_3SiH alone shows substantial coupling between the silyl hydride and the $Si\text{-}CH_2\text{-}CH_3$ groups in the proton NMR spectrum. When $B(C_6F_5)_3$ is added, the coupling is unobserved, indicating that $B(C_6F_5)_3$ enables a rapid exchange of the silyl hydride (Scheme 1.19). In addition, when a 1:1 mixture of Et_3SiH and Ph_3SiD is exposed to $B(C_6F_5)_3$, scrambling of the

[67] Parks, D. J.; Blackwell, J. M.; Piers, W. E. *J. Org. Chem.* **2000**, *65*, 3090–3098.

deuterium occurs, and approximately half of each silane becomes deuterium-labeled within minutes.

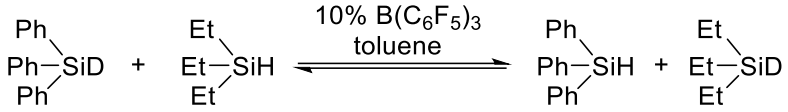

Scheme 1.19: Silane scrambling experiment

Further studies from the Piers group continued to examine the interaction of substrate with the transiently generated borane/silane adduct. In competition experiments between a more Lewis basic substrate and a less Lewis basic substrate, the more Lewis basic substrate is reduced preferentially (Scheme 1.20), although the rate of reduction is slower than the rate of reduction for the less Lewis basic substrate alone (Scheme 1.18). This observation indicates that nucleophilic attack on the borane/silane adduct by the carbonyl substrate is an important step of the catalytic cycle. Confirmation that silyl cation can coordinate to a ketone was provided by an experiment in which silyl cation was generated independently by treatment of Et_3SiH with $[Ph_3C][BAr^F_4]$ (BAr^F_4= tetrakis(pentaflurophenyl)borate), which had previously shown to generate $[Et_3Si][BAr^F_4]$ in situ.[68] Adding acetophenone to this ion pair resulted in changes in the NMR spectra of acetophenone: the carbonyl carbon shifted downfield by 21 ppm in the $^{13}C\{^1H\}$ spectrum while the methyl group shifted upfield by 0.11ppm in the ^1H spectrum.

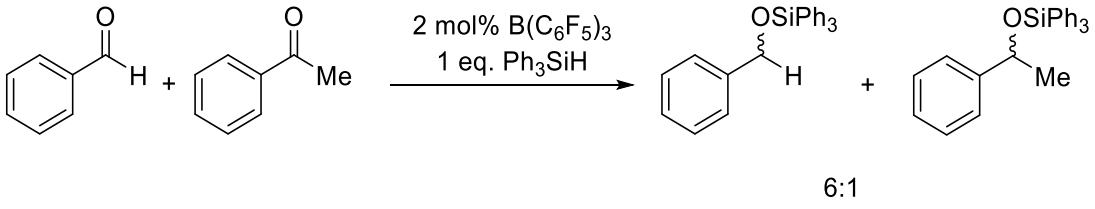

Scheme 1.20: Competition experiment between more Lewis basic and less Lewis basic substrates

[68] Lambert, J. B.; Zhang, S.; Ciro, S. M. *Organometallics* **1994**, *13*, 2430–2443.

One of the most challenging aspects of determining the mechanism of this reaction is distinguishing between borohydride ($[HB(C_6F_5)_3]^-$) and silane (Et_3SiH) as the hydride donor. Because the $[Et_3Si][BAr^F_4]$ adduct is able to catalyze the reaction when there is excess silane present, it is difficult to rule out silane as the hydride donor, as in this case, the reaction proceeds in the absence of borohydride. However, the Piers group argues that this is not the dominant mechanism when $B(C_6F_5)_3$ is used as the catalyst. They expose acetophenone to one equivalent of Et_3SiH in the presence of various catalysts, including $B(C_6F_5)_3$, $[Et_3Si][BAr^F_4]$, and $[Ph_3C][BAr^F_4]$. With $B(C_6F_5)_3$ used as the catalyst, all of the ketone is reduced to alcohol. However, in the other cases where "silyl cation" acts as the catalyst, half of the acetophenone is doubly reduced, giving ethylbenzene, while half of the starting material remains as unreacted ketone (Scheme 1.21). The authors ascribe this difference in product distribution to different hydride donors, indicating that Et_3SiH, which is the only possible hydride donor in the $[Et_3Si][BAr^F_4]$ and $[Ph_3C][BAr^F_4]$ cases, is not the hydride donor in the $B(C_6F_5)_3$ case.

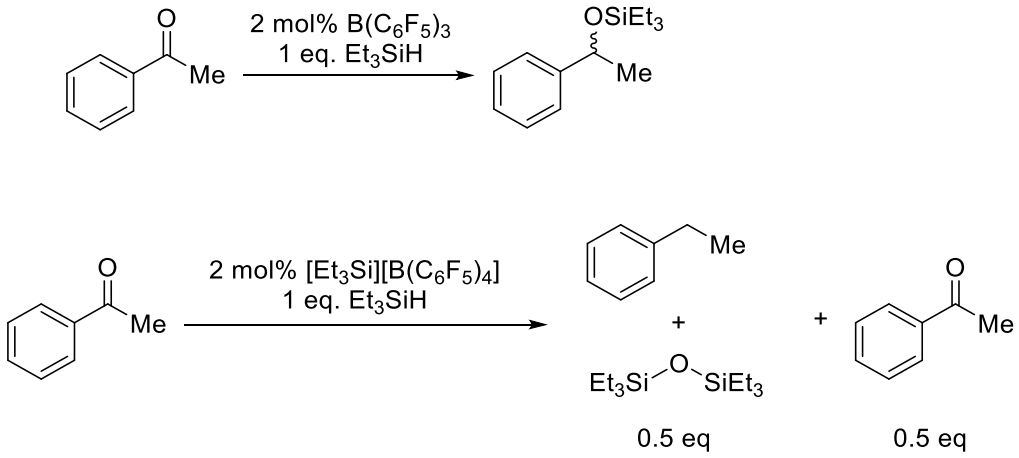

Scheme 1.21: Comparison of products from acetophenone reduction using two different catalysts

In addition, they use pre-formed $[^iPr_3Si][BAr^F_4]$ in combination with two equivalents of $^iPr_3SiH$ to reduce acetophenone to ethylbenzene, whereas the combination of $^iPr_3SiH$ and $B(C_6F_5)_3$ cannot catalyze reduction (Scheme 1.22), likely because the bulkiness of $^iPr_3SiH$ prevents it from

being activated by the also bulky $B(C_6F_5)_3$. Finally, a competition experiment between Ph_3SiD and $^iPr_3SiH$ was performed (Scheme 1.23). Since $^iPr_3SiH$ is a better hydride donor than Ph_3SiD, if silane were acting as the hydride donor it would be expected that the product would not be deuterated. In addition, since $B(C_6F_5)_3$ can activate Ph_3SiD but not $^iPr_3SiH$, the expected "borohydride" would be $D[B(C_6F_5)_3]^-$. The exclusive observation of deuterated ketone reduction product suggests that the hydride was delivered by the borodeuteride.

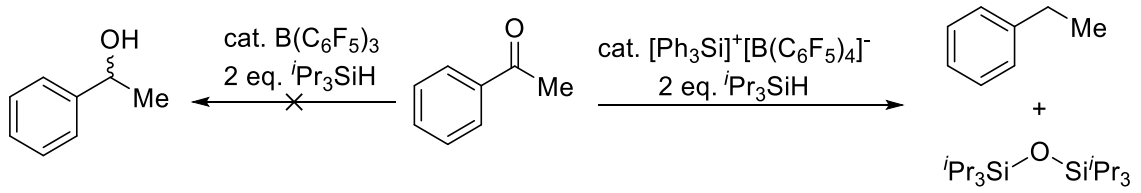

Scheme 1.22: Reduction of acetophenone by $^iPr_3SiH$ catalyzed only by pre-generated silylium ion

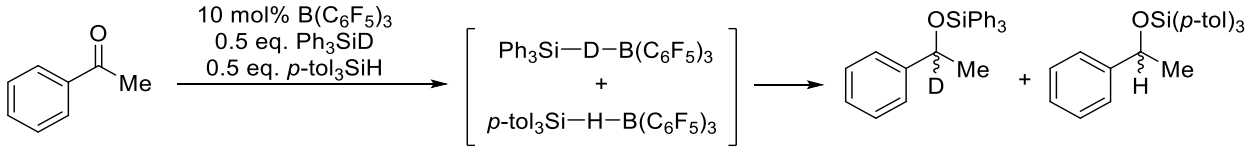

Scheme 1.23: Deuterium labeling experiment

1.3.4 Reduction of primary alcohols

A few years after the reduction of aldehydes and ketones was shown by the Piers group, the Yamamoto lab reported the reduction of primary alcohols and ethers to hydrocarbons by catalytic $B(C_6F_5)_3$ in combination with stoichiometric Et_3SiH (Scheme 1.24).[69] Under these conditions, aromatic alcohols, as well as most secondary and tertiary alkyl alcohols were not reduced. Instead, the hydroxyl groups were simply protected with triethylsilyl groups. The same product, that is, alcohol protection but not reduction, resulted when only one equivalent of

[69] Gevorgyan, V.; Rubin, M.; Benson, S.; Liu, J.-X.; Yamamoto, Y. *J. Org. Chem.* **2000**, *65*, 6179–6186.

triethylsilane was added instead of the optimum three equivalents, suggesting that unprotected alcohols undergo in situ protection (as reported by the Piers group for Ph_3SiH[70]) prior to reduction. The only secondary or tertiary alcohols to be reduced were the highly stabilized substrates Ph_2CHOH and Ph_3COH. Still, the reduction of primary alkyl alcohols and ethers represented a major step forward in the $B(C_6F_5)_3$-catalyzed conversion of highly oxygenated materials to more reduced compounds.

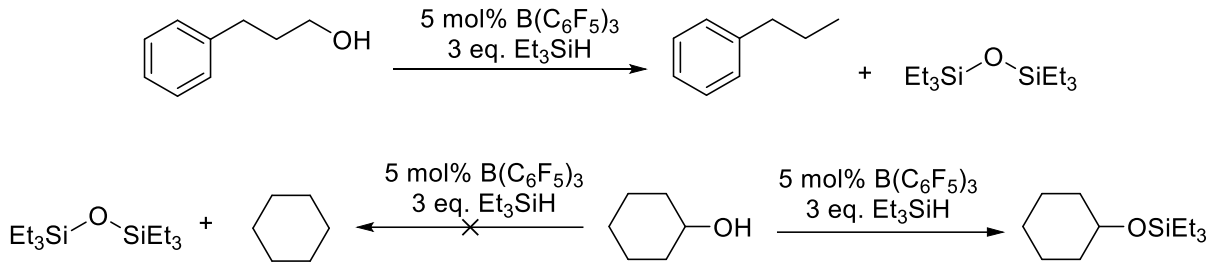

Scheme 1.24: Reduction of primary alcohols and silyl protection of secondary alcohols by $B(C_6F_5)_3/Et_3SiH$

1.3.5 Reduction of Secondary and Tertiary Alcohols

For a long time, the reduction of C-O bonds via $B(C_6F_5)_3$ was limited to primary substrates. For example, Yamamoto observed that octadecan-2-ol underwent only alcohol protection, not reduction, in the presence of $B(C_6F_5)_3$ and Et_3SiH. However, in 2006 McRae and coworkers disclosed their evidence that replacement of a tertiary silane with a secondary (diethyl) or primary (n-butyl) silane would allow for the reduction of secondary alcohols (Scheme 1.25).[71] In general, *n*-butylsilane tended to give a higher yield of reduced product than diethylsilane, although both were substantially more effective than tertiary silanes.

[70] Blackwell, J. M.; Foster, K. L.; Beck, V. H.; Piers, W. E. *J. Org. Chem.* **1999**, *64*, 4887–4892.

[71] Nimmagadda, R. D.; McRae, C. *Tetrahedron Lett.* **2006**, *47*, 5755–5758.

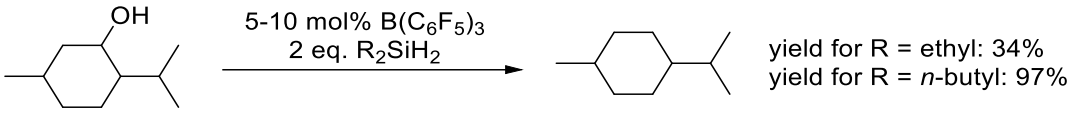

Scheme 1.25: Reduction of secondary alcohols by secondary and primary silanes

Cleavage of allylic ethers in cyclic substrates was also shown using the $B(C_6F_5)_3/Et_3SiH$ system (Scheme 1.26).[72] Under these conditions, catalytic $B(C_6F_5)_3$ in combination with stoichiometric triethylsilane was able to cleave primary, secondary, or tertiary C-O bonds of cyclic allylic ethers. The authors noted the importance of both electronics and sterics for selectivity. Substituted 2,5-dihyrofuran substrates allowed the authors to study the effects of sterics, since reduction on either side of the ring would be allylic ring opening. On the other hand, 3,6-2H-dihydopyrans allowed for the comparison between allylic and non-allylic reductions. Only allylic reductions took place, even when the allylic ether side of the ring was more sterically hindered than the homoallylic ether side (Scheme 1.26). The $B(C_6F_5)_3$ system has also been applied to small molecules that mimic lignin, which has both alkyl and aryl C-O bonds. For these substrates, only alkyl C-O bonds were cleaved.[73]

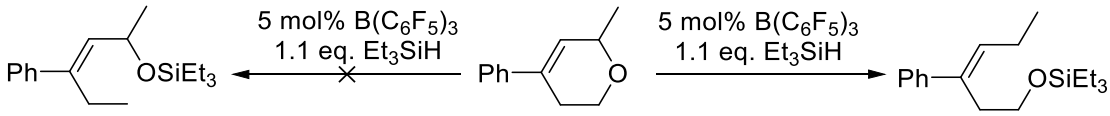

Scheme 1.26: Reduction of allylic ethers in preference to primary ethers

1.3.6 Reduction catalyzed by iridium pincer complexes

In addition to the deoxygenation work using $B(C_6F_5)_3$ as a catalyst, systems have been developed that use Lewis acid iridium complexes to reduce C-X (X = halide or OR) bonds to hydrocarbons and reduce ketones to alcohols (Figure 1.6).[74] The cationic iridium (III) complex,

[72] Mack, D. J.; Guo, B.; Njardarson, J. T. *Chem. Commun.* **2012**, *48*, 7844–7846.

[73] Feghali, E.; Cantat, T. *Chem. Commun.* **2014**, *50*, 862–865.

[74] Yang, J.; White, P. S.; Brookhart, M. *J. Am. Chem. Soc.* **2008**, *130*, 17509–17518.

referred to as (POCOP)IrH^+, has been shown to coordinate silane via the hydride, allowing a substrate to nucleophilically attack the silane to activate the substrate. The resulting (POCOP)IrH_2 complex can then serve as the hydride donor, giving substrate reduction. In the case of ether reductions, extensive mechanistic work indicates that the turnover-limiting step is reduction of the activated substrate (disilyl oxonium) by the (POCOP)IrH_2 complex. For one substrate, diethyl ether, the activated disilyloxonium compound $Et_3SiOEt_2^+$ has been isolated and characterized by NMR and single-crystal X-ray crystallography. In addition, comparison of Et_3SiH and (POCOP)IrH_2 as hydride donors for ether reduction suggests that (POCOP)IrH_2 is approximately 30,000 times more active than Et_3SiH.

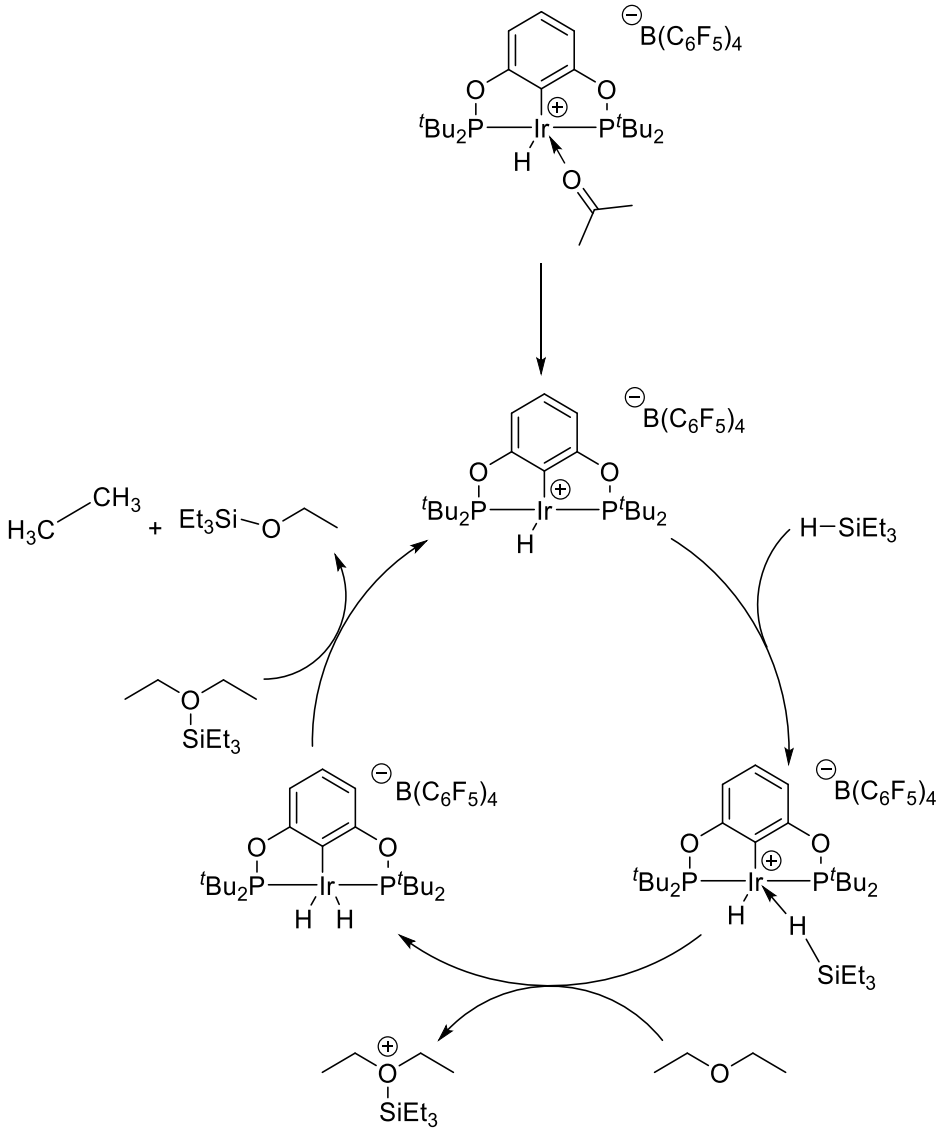

Figure 1.6: Hydrosilylative reduction of alcohols catalyzed by (POCOP)IrH$^+$

In contrast, for the reduction of silyl-protected alcohols, Et_3SiH is determined to be the hydride donor. The Brookhart group attributes this difference to the large size of the iridium species, which likely interacts with the bulky silane groups, and the low concentration of (POCOP)IrH_2 relative to Et_3SiH. The lowered concentration of (POCOP)IrH_2 in the case of alcohol reductions compared to ether reductions results from a change in the catalyst resting state. Instead of (POCOP)IrH_2 as the resting state, the resting state is thought to be the iridium-silane

complex (POCOP)IrH(H-$SiEt_3$)$^+$. A rational for this is based on the reduced basicity and increased steric size of $EtOSiEt_3^+$ compared to Et_2O, which Brookhart and coworkers point out would tend to disfavor transfer of Et_3Si^+ from the iridium center to the protected alcohol substrate.

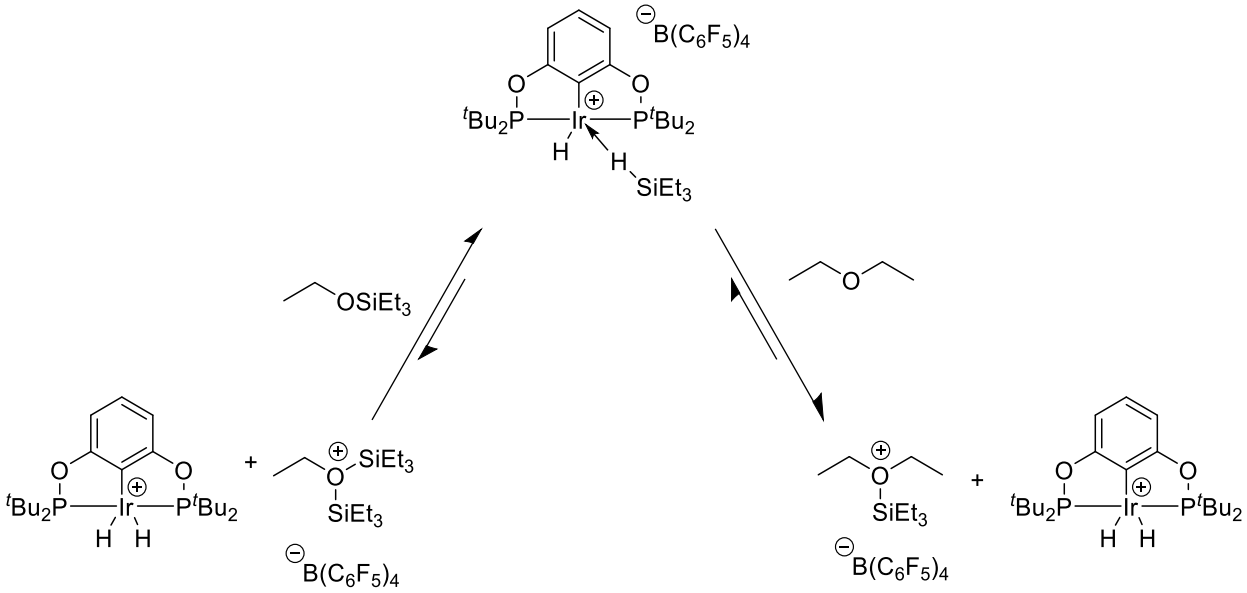

Figure 1.7: Differences in preference for transfer of Et_3Si^+ from iridium complex to substrate

The Brookhart group also compares the relative catalytic competencies of (POCOP)IrH^+ and [Ph_3C][$B(Ar^F)_4$]. In the latter case, the reaction would be initiated by the abstraction of a hydride from Et_3SiH by [Ph_3C]$^+$, providing silyl cation to activate the substrate. A second Et_3SiH would then donate its hydride to the substrate to perform the reduction, yielding another Et_3Si^+ that could activate another substrate, thus turning over the catalytic cycle. Brookhart found that the [Ph_3C][BAr^F_4] catalyst is faster for less electron-rich substrates, whereas the iridium catalyst is faster for more electron-rich substrates. This difference likely occurs because the less electron rich substrates have a reduced propensity for abstracting silyl cation from the iridium center, resulting in lower concentrations of activated substrate (silyl oxonium), which is involved in the rate determining step of the Ir/Et_3SiH cycle. For the Et_3SiH/Ph_3C^+ system, disilyloxonium is the resting state for both electron rich and electron poor substrates, meaning that for electron poor

substrates, there is more disilyloxonium present in the Et_3SiH/Ph_3C^+ system than in the Ir/Et_3SiH system.

1.4 *Research Objectives*

Sugars represent an attractive feedstock for generating value-added compounds. The research reported herein aims to take advantage of these readily available substrates by either functionalization or defunctionalization. Anomeric activation of carbon-bromide and carbon-iodide bonds by palladium(0) is shown to be possible with the appropriate choice of phosphine ligands on the palladium center (chapter 2). In an effort to activate C-O bonds in addition to C-X bonds, an iridium-catalyzed hydrosilylative reduction of ethers was applied to sugars, leading to reduction of all the C-O bonds (chapter 3). The ratio of isomeric hexane products was studied as a function of different starting materials. A switch to a metal-free hydrosilylative deoxygenation systems was enabled by $B(C_6F_5)_3$ (chapter 4). While both the $(POCOP)IrH^+$ system and the $B(C_6F_5)_3$ system were able to effect complete deoxygenation using diethylsilane as the reductant, utilization of tertiary silanes such as dimethylethylsilane and triethylsilane under $B(C_6F_5)_3$ catalysis allowed for controlled, selective deoxygenation (chapter 5).

Chapter 2 Oxidative Addition of Glycosyl Halides to Palladium(0)

This chapter is adapted with permission from Munro-Leighton, C.; Adduci, L. L.; Becker, J. J.; Gagné, M. R. *Organometallics* **2011**, *30*, 2646–2649.

The work in this chapter resulted from collaboration with Dr. Colleen Munro-Leighton, who contributed significantly to sections 2.2 and 2.3.

2.1 *Oxidative addition of secondary alkyl halides*

The S_N2-like oxidative addition of secondary alkyl halides is kinetically difficult[33] and continues to hold back the universal adoption of Pd-based methods for secondary C-C, C-N, and C-O bond-forming catalysis.[28,29,75,76] While developments in the cross coupling of primary alkyl electrophiles using Pd catalysts have progressed smoothly,[31,37-45,77-81] secondary electrophiles have thus far required methodologies wherein the catalyst readily adopts radical mechanisms for oxidative addition.[26,34-36] A noteworthy recent addition is a (Xantphos)Pd catalyst for the cross coupling of 2°-benzyl bromide (with inversion) with aryl and vinyl Grignard reagents.[47] An

[75] Wasa, M.; Engle, K. M.; Yu, J.-Q. *Isr. J. Chem.* **2010**, *50*, 605-616.

[76] Luh, T.-Y.; Leung, M.-k.; Wong, K.-T. *Chem. Rev.* **2000**, *100*, 3187-3204.

[77] Netherton, M. R.; Fu, G. C. *Adv. Synth. Catal.* **2004**, *346*, 1525-1532.

[78] Netherton, M. R.; Fu, G. C. In *Palladium in Organic Synthesis*, 2005; Vol. 14; pp 124-134.

[79] Powell, D. A.; Fu, G. C. *J. Am. Chem. Soc.* **2004**, *126*, 7788-7789.

[80] Manolikakes, G.; Muñoz Hernandez, C.; Schade, M. A.; Metzger, A.; Knochel, P. *J. Org. Chem.* **2008**, *73*, 8422-8436.

[81] Vechorkin, O.; Proust, V.; Hu, X. *J. Am. Chem. Soc.* **2009**, *131*, 9756-9766.

additional well-recognized problem with alkyl halide electrophiles is the facility with which intermediate organometallic complexes undergo β-hydride elimination reactions. Several elegant solutions based on di- and triamine ligands (Ni)[82,83] or carefully tuned phosphines (Pd, primary alkyl-X)[89-91] and broad bite angle diphosphines (Pd, secondary alkyl-Br)[97] have inhibited this tendency and significantly improved the viability of such methods.

Lemieux reported more than 50 years ago that the glycosyl bromide class of secondary electrophiles were remarkable in that they could, with Br^- catalysis, react with nucleophiles as weak as secondary alcohols (Scheme 2.1).[84,85] The outcome of these studies was the development of methods for the synthesis of complex α-disaccharides, which rely on a low but steady state concentration of a reactive (lacking anomeric stabilization) β-bromo glycoside.

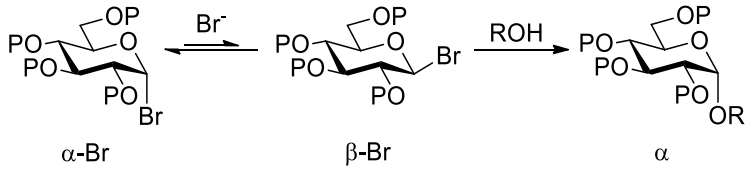

Scheme 2.1 Reactivity of α and β glucosyl bromides

Since anomeric effects play such a dramatic role in the invertive substitution chemistry of glycosyl halides, we questioned whether such effects could be harnessed to kinetically facilitate an S_N2-like oxidative addition of Pd(0). The feasibility of this transformation was supported by results from Scott, who showed that $Pd(PPh_3)_4$ (1-5 mol%, 50°C) catalyzes the conversion of benzyl-protected C_1-mesylates into oxyglycals via a process proposed to require C–O oxidative addition and β-hydride elimination (Scheme 2.2).[52] The goal of nucleophilic C-X activation was

[82] Lu, Z.; Fu, G. C. *Angew. Chem. Int. Ed.* **2010**, *49*, 6676-6678.

[83] Joshi-Pangu, A.; Ganesh, M.; Biscoe, M. R. *Org. Lett.* **2011**, *13*, 1218-1221.

[84] Lemieux, R. U.; Huber, G. *Can. J. Chem.* **1955**, *33*, 128-133.

[85] Lemieux, R. U.; Hendriks, K. B.; Stick, R. V.; James, K. *J. Am. Chem. Soc.* **1975**, *97*, 4056-4062.

attractive in the context of a broader research theme targeting the conversion of poly-saccharides into value added chemical feedstocks. Since the leaving group in the C-O oxidative addition of a polysaccharide would necessarily be oxygen based, the focus was on non-radical methods of activating glycosyl electrophiles.[18,19,21,22,24]

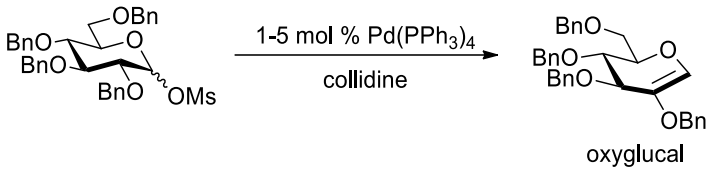

Scheme 2.2 Pd-catalyzed elimination to give oxyglucal[52]

2.2 *Oxidative addition of acetobromo-α-D-glucose*

As expected, no reaction occurred between $Pd(PEt_3)_3$ (**1**)[75] and secondary electrophiles like cyclohexyl bromide (Scheme 2.3a). In contrast, ^{31}P NMR spectroscopy showed that over 8 h, acetobromo-α-D-glucose (**2**) reacted at room temperature with **1** to give a single isomer of $Pd(PEt_3)_2(Br)$(AcO-β-glu) (**3**), the product of invertive bromide displacement (Scheme 2.3b).[86] Purification of the reaction mixture by column chromatography allowed for isolation of **3**, although decomposition on the column limited the isolated yield (34%). The source of the comparative stability of **2** vs. the Scott putative intermediate is not known. Possible candidates include the effect of phosphine, temperature, or the protecting group (Bn vs. Ac)

[86] DeShong, P.; Slough, G. A.; Elango, V.; Trainor, G. L. *J. Am. Chem. Soc.* **1985**, *107*, 7788-7790.

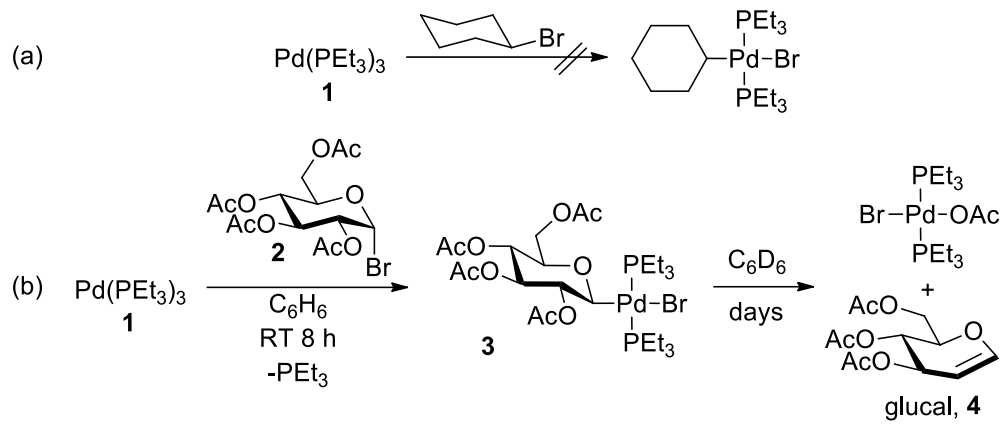

Scheme 2.3: Oxidative addition of acetobromo-α-D-glucose to $Pd(PEt_3)_3$

2.3 *Characterization of glucosyl-palladium complex*

Isolated **3** has been characterized by ^{1}H, ^{31}P and ^{13}C NMR spectroscopy, and all data are consistent with formation of a single "β-glucosyl" isomer. The ^{1}H NMR spectrum is highlighted by seven resonances in the pyranose region (3 – 6 ppm), including a signal at 4.19 ppm, corresponding to C_1H with $^{3}J_{P\text{-}H}$ = 3 and 14 Hz; the diastereotopic nature of the phosphorus nuclei was also evident in the ^{31}P NMR spectrum (AB quartet, $^{2}J_{PP'}$ = 404 Hz).[87] The formation of the β-anomer was additionally implied by the vicinal H_1-H_2 coupling constant ($^{3}J_{H1\text{-}H2}$ = 11 Hz), suggestive of a diaxial arrangement.[88] Single crystals of **3** were grown by slow evaporation of a hexanes solution, and X-ray diffraction confirmed the β-stereoisomer assignment and showed the pyranosyl moiety to adopt a chair conformation (Figure 2.1). To our knowledge, this represents the first reported crystal structure of a pyranosyl palladium complex, and only the second C_1-organometallic complex[24] of a fully oxygenated sugar.

[87] Hoffman, R. A.; Forsen, S.; Gestblom, B. In *N.M.R. Basic Principles and Progress*, 1971; Vol. 71.

[88] Lambert, J. B.; Shurvell, H. F.; Lightner, D. A.; Cooks, R. G. *Organic Structural Spectroscopy*; Simon & Schuster, 1998.

Under the same conditions that produced **3**, $Pd(PEt_3)_3$ reacts even faster (2 h) with acetoiodo-α-D-glucose to give $Pd(PEt_3)_2(I)(OAc\text{-}\beta\text{-}glu)$ (**5**). Glycosyl chloride analogs were unreactive, establishing the reactivity trend: Cl << Br < I.[75] Oxidative addition of a C-O bond proved unsuccessful, as **1** and glucopyranose pentabenzoate do not react. Reaction rates were also sensitive to ligand basicity with less electron-rich metal centers being slower to react. For example, the modestly less basic[89] $Pd(PMePh_2)_3$ required three days to react with acetobromo-α-D-glucose (*c.f.* 8 h for $Pd(PEt_3)_3$), affording $Pd(PMePh_2)_2(Br)(AcO\text{-}\beta\text{-}glu)$ (**6**).

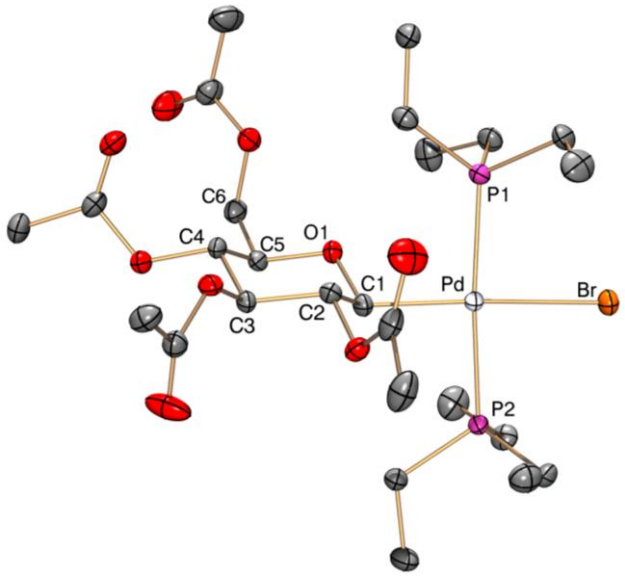

Figure 2.1: ORTEP of acetate-protected glucosyl palladium bromide complex

2.4 *Further reactivity of $Pd(PEt_3)_2(Br)(OAc\text{-}\beta\text{-}glu)$*

In contrast to the reactivity observed by Scott wherein C_1-organometallic complexes generated from oxidative addition of $Pd(PPh_3)_4$ and glucosyl mesylate rapidly β-hydride eliminate,[52] benzene solutions of **3** slowly react via a β-acetoxy elimination process to give tri-*O*-acetylglucal (**4**) and *trans*-$Pd(PEt_3)_2(Br)(OAc)$ (Scheme 2.3). In light of this divergent behavior,

[89] Tolman, C. A. *Chem. Rev.* **1977**, *77*, 313-348.

we initiated mechanistic studies. Suggestive of a pre-equilibrium PEt_3-dissociation pathway were experiments showing that added phosphine, but not added bromide, significantly inhibited the β-elimination. After 14 days at room temperature, 40% conversion of **3** to **4** was observed; 5 equivalents of PEt_3 and 5 equivalents of Br^- led to 1-5% and 35% conversion, respectively. Noting that the stereochemistry of the sugar prevents the complex from adopting the conformation necessary for synperiplanar elimination of OAc (but not hydride) and that the Pd-C_1-C_2-OAc dihedral angle (58.1° in the crystal structure of **3**) was unsuitable for antiperiplanar elimination, we considered two possible elimination transition states: one in which the pyranosyl ring has undergone complete ring inversion to orient all substituents axially (including the monophosphine –Pd(PEt_3)(I) unit), and one in which the ring has partially inverted to adopt a boat structure (Scheme 2.4). To distinguish between these two possibilities, a derivative of **5** was synthesized in which full ring inversion was inhibited by tethering of the C_4 and C_6 positions with a benzylidene group (Pd(PEt_3)$_2$(I)(3-AcO-4,6-benzylidene glucopyranose) (**7**). The failure of this modification to reduce the rate of elimination (50% of **7** had undergone elimination after 1.5 days at 40°C vs. 2 days for **5**) indicated that a mechanism requiring full ring inversion was not necessary, and thus suggested the likelihood of the pathway involving a boat transition state (Scheme 2.4).

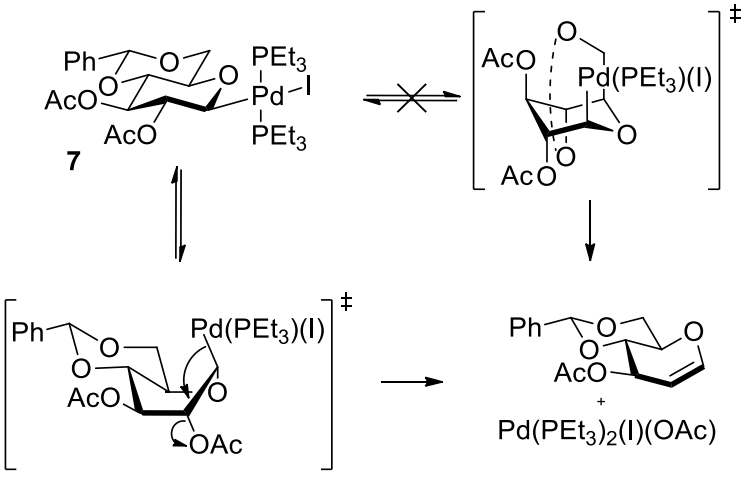

Scheme 2.4: Boat vs chair transition state for β-acetoxy elimination

To examine how the stereochemistry of the C_2-substituent affected the stability of the C_1-organopalladium species, we carried out a reaction of α-D-mannopyranosyl bromide tetrabenzoate with **1**. In contrast to the glucose-based electrophile, this reaction immediately yielded tri-*O*-benzoylglucal and $Pd(PEt_3)_2(Br)(OBz)$ (Scheme 2.5, confirmed by ^1H NMR spectroscopy).

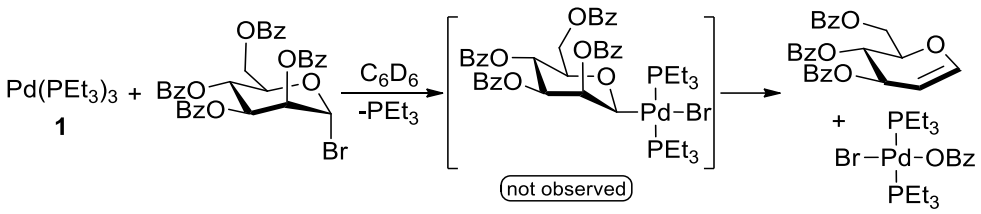

Scheme 2.5: β-elimination from palladium(II) to give glucal

The sensitivity of the reaction to variation in the phosphine ligand was next investigated. For example, commercially available bis(tricyclohexylphosphine)palladium(0) (cone angle PCy_3 = 170° vs 132° for PEt_3) reacts with **2** to directly produce **4** and *trans*-$Pd(PCy_3)_2(Br)(OAc)$ (**8**) within 5 minutes at room temperature (Figure 2.2). In fact, for phosphine ligands both larger and smaller than triethylphosphine, conversion to glucal (not oxyglucal) was facile (Scheme 2.6). Though the target organometallic complex was not detected for PCy_3, its intermediacy and rapid β-acetoxy elimination is implied. Even in the presence of excess PCy_3, direct conversion of **2** to **4** is observed upon treatment with $Pd(PCy_3)_2$. Since the elimination is involves initial phosphine dissociation, we envision sterically bulky ligands being crowded out of the coordination sphere by a bulky pyranosyl moiety and thus accelerating the elimination; smaller ligands likely lack sufficient bulk to inhibit elimination.

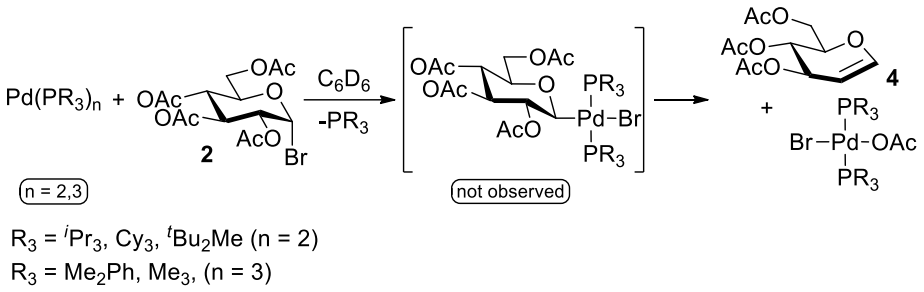

Scheme 2.6: β-acetoxy elimination with different phosphine ligands

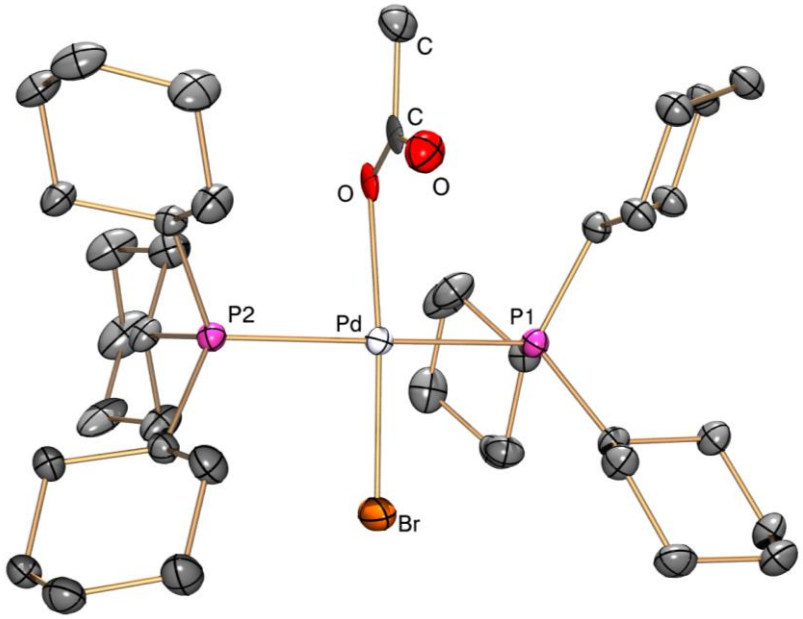

Figure 2.2: ORTEP of elimination product

While glucosyl bromide and glucosyl iodide were readily activated by $Pd(PEt_3)_3$, glucose pentaacetate was not, indicating that, as expected, anomeric C-O bond activation presents a greater challenge than C-X bond activation. As a first step towards C-O activation, a glucose with an anomeric oxygen-based pseudo-halide was employed (acetate-protected glucosyl mesylate). However, no reaction was observed upon treatment of glucosyl mesylate with $Pd(PEt_3)_3$.

Under the described reaction conditions, $Pd(PEt_3)_3$ demonstrated a propensity toward oxidative addition of pyranosyl halides that leads to stable $Pd(PEt_3)_2(Br)$(AcO-β-glu) (**3**), the product of invertive oxidative addition. The reaction is efficient under ambient conditions and represents a rare palladium-based C2°alkyl-X activation and the first isolated pyranosyl palladium complex. Thermolysis has additionally shown this product to be susceptible to β-acetoxy elimination rather than β-hydride elimination.

The susceptibility of **3** and related compounds to β-elimination processes presented a problem for our efforts towards the development of a system for the cross-coupling of carbohydrates with other carbon-based groups. To encourage transmetallation, we performed a ligand exchange to replace the two phosphine groups with a chelating phosphine, orienting the glucosyl ligand and the bromide *syn* to each other in the square planar coordination geometry of the palladium(II) center. This ligand replacement was achieved by exposing **3** in solution to a chelating ligand, and then removing the solvent and uncoordinated $P(Et_3)_3$ ligand under reduced pressure. Three repetitions of this chelating phosphine addition/vacuum cycle were sufficient to drive all of the material to **3** when 1,2-bis(diphenylphosphino)ethane (dppe) was used. Other chelating ligands were less successful and either failed to replace PEt_3 (1,2-bis(diphenylphosphino)methane, 1,2-bis(diphenylphosphino)propane, 1,2-bis(diphenylphosphino)butane and Xantphos) or allowed β-acetoxy elimination to occur (1,2-bis(dicyclohexylphosphino)ethane and 1,2-bis(diethylphosphino)ethane). Although Pd(dppe)(Br)(AcO-β-glu) was treated with various cross-coupling agents, cross-coupling was not observed. Instead, there was either no reaction (with phenyl zinc iodide) or elimination to give glucal was observed (with ethynyltributylstannane, tetramethylstannane).

Overall, our investigations indicated that the properties that make some glucosyl-palladium complexes stable to observation and isolation, namely phosphine, protecting group, and carbohydrate stereochemistry combination, also render them resistant to transmetallation. Alterations of the structure leads only to elimination. While the oxidative addition of glucosyl halides to palladium (0) is an interesting example of secondary alkyl activation and of a carbohydrate-metal complex, it seems that this system is not suited for cross-coupling reactions of carbohydrates.

2.5 *Experimental section*

General Methods. All reactions were conducted under a nitrogen atmosphere using either standard Schlenk techniques or a MBraun Labmaster 100 glovebox. Benzene was purchased as anhydrous from Aldrich, degassed via three freeze-pump-thaw cycles and stored under a dinitrogen atmosphere over 4Å molecular sieves. Benzene-d_6 and methylene chloride-d_2 were degassed via three freeze-pump-thaw cycles and stored under a dinitrogen atmosphere over 4Å molecular sieves. Methylene chloride was purged with argon, passed over a column of activated alumina, degassed via three freeze-pump-thaw cycles, and stored under a dinitrogen atmosphere over 4Å molecular sieves. Other solvents were used without further purification. Acetobromo-α-D-glucose was purchased from Aldrich and purified by dissolution in diethyl ether and passage through a short plug of silica. Acetoiodo-α-D-glucose,[90] acetochloro-α-D-glucose,[91] glucopyranose pentabenzoate,[92] α-D-mannopyranosyl bromide tetrabenzoate[93] , acetate-protected

[90] Mukhopadhyay, B.; Kartha, K. P. R.; Russell, D. A.; Field, R. A. *J. Org. Chem.* **2004**, *69*, 7758-7760.

[91] Lemieux, R. U.; Hayami, J. I. *Can J Chem* **1965**, *43*, 2162-2173.

[92] Maurer, K.; Bohme, R. *Ber. Dtsch. Chem. Ges.* **1936**, *69B*, 1399-1410.

[93] Fletcher, H. G., In: *Methods Carbohydr. Chem.*, 1962, Vol. 2; 1962, pp. 226-228.

glucosyl mesylate[94] and CpPd(allyl)[95] were synthesized according to literature procedures. NMR spectra were recorded using Bruker DRX spectrometers operating at 400, 500, or 600 MHz (^{1}H), 150 MHz (^{13}C), and 243 MHz (^{31}P). NMR chemical shifts are reported in ppm and referenced using the residual proton peaks (^{1}H) or the ^{13}C resonances of the deuterated solvent (^{13}C); ^{31}P NMR signals were calibrated with an external capillary tube standard of 0.18 mM PPh_3 in C_6D_6 (-6 ppm). Coupling constants for AB quartets are calculated according to a published method.[87]

Pd(PEt$_3$)$_2$(Br)(aceto-β-glucopyranose) (3). A vial was charged with CpPd(allyl) (72 mg, 0.34 mmol) and sealed with a septum cap. After dissolution in benzene, PEt_3 (150 μL, 1.0 mmol) was added via microsyringe. The solution turned from deep red to yellow and was then transferred to a septum-capped vial charged with acetobromo-α-D-glucose (117 mg, 0.28 mmol). After 8 h at room temperature, reaction completion was confirmed by TLC. The reaction mixture was transferred directly onto a silica gel column and purified by flash column chromatography (25% EtOAc in hexanes). The resulting colorless oil was triturated with hexanes, and a white solid was collected by filtration and washed with hexanes (73 mg, 0.097 mmol, 34% yield). Crystals suitable for X-ray diffraction were grown by slow evaporation of a hexane solution. ^{1}H NMR (C_6D_6, δ): 5.66 (t, $^{3}J_{HH}$ = 10 Hz, 1H, H_2), 5.44 (t, $^{3}J_{HH}$ = 10 Hz, 1H, H_4), 5.22 (t, $^{3}J_{HH}$ = 9 Hz, 1H, H_3), 4.39 (dd, $^{3}J_{H5\text{-}H6}$ = 4 Hz, $^{3}J_{H6\text{-}H6'}$ = 12 Hz, 1H, H_6), 4.19 (ddd, $^{3}J_{H1\text{-}H2}$ = 11 Hz, $^{3}J_{P\text{-}H1}$ = 14 Hz, $^{3}J_{P'\text{-}H1}$ = 3 Hz, 1H, H_1), 3.85 (dd, $^{3}J_{H5\text{-}H6'}$ = 2 Hz, $^{3}J_{H6\text{-}H6'}$ = 12 Hz, 1H, $H_{6'}$), 3.19 (ddd/m, $^{3}J_{H4\text{-}H5}$ = 10 Hz, $^{3}J_{H6\text{-}H5}$ = 4 Hz, $^{3}J_{H6'\text{-}H5}$ = 2 Hz, 1H, H_5), 2.18, 1.92 (both dddq, $^{3}J_{HH}$ = 8 Hz, $^{2}J_{HH}$ = 14 Hz, $^{2}J_{PH}$ = 14 Hz,

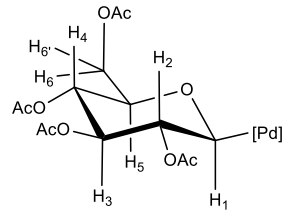

[94] Leroux, J.; Perlin, A. S. *Carbohydr. Res.* **1978**, *67*, 163–178.

[95] Tatsuno, Y.; Yoshida, T.; Otsuka, S. *Inorg. Synth.* **1990**, *28*, 342-5.

$^4J_{P'H}$ = 4 Hz, 3H, PC*H*$_2$CH$_3$), 1.68 - 1.83 (m, 18H, OAc and PC*H'*$_2$CH$_3$), 1.03 and 0.94 (m, $^3J_{HH}$ = 8 Hz, $^3J_{HH}$ = 8 Hz, $^3J_{PH}$ = 12 Hz, $^5J_{PH}$ = 4 Hz, 9H, PCH$_2$C*H*$_3$). ^{13}C {^{1}H} NMR (C_6D_6, δ): 170.1, 169.8, 169.3, 169.0 (each a s, *C*(O)CH$_3$), 79.0 (s, C_5), 76.7 (s, C_3), 75.4 (s, C_2), 72.3 (s, C_1), 68.8 (s, C_4), 62.0 (s, C_6), 20.8, 20.4, 20.3, 20.2 (each a s, C(O)*C*H$_3$), 15.4 (dd, $^2J_{PC}$ = 12 Hz, $^3J_{PC}$ = 7 Hz, P*C*H$_2$CH$_3$), 15.3 (dd, $^2J_{PC}$ = 13 Hz, $^3J_{PC}$ = 7 Hz, P*C*H$_2$CH$_3$), 8.4 and 8.2 (each a s, PCH$_2$*C*H$_3$). ^{31}P {^{1}H} NMR (C_6D_6, δ): 14.8 and 13.5 (AB quartet, $^2J_{PP}$ = 404 Hz). HRMS (ESI): *m/z* [M-Br-PEt$_3$]$^+$ found 555.0981, calcd 555.0975 for $C_{20}H_{34}O_9PPd$, [M-Br]$^+$ found 673.1969, calcd 673.1887 for $C_{26}H_{49}O_9P_2Pd$.

Pd(PEt$_3$)$_2$(I)(aceto-β-glucopyranose) (5). A vial was charged with CpPd(allyl) (66 mg, 0.31 mmol) and sealed with a septum cap. After dissolution in benzene, PEt$_3$ (138 μL, 0.93 mmol) was added via microsyringe. The solution turned from deep red to yellow and was then transferred to a septum-capped vial charged with acetoiodo-α-D-glucose (115 mg, 0.25 mmol). After 2 h at room temperature, reaction completion was confirmed by TLC. The reaction mixture was transferred directly onto a silica gel column and purified by flash column chromatography (30% EtOAc in hexanes). The resulting pale yellow oil was triturated with hexanes, and a white solid was collected by filtration and washed with hexanes (33.1 mg, 0.041 mmol, 16 % yield). ^{1}H NMR (C_6D_6, δ): 5.69 (t, $^3J_{HH}$ = 10 Hz, 1H, H_2), 5.45 (t, $^3J_{HH}$ = 10 Hz, 1H, H_4), 5.22 (t, $^3J_{HH}$ = 9 Hz, 1H, H_3), 4.37 (dd, $^3J_{H5\text{-}H6}$ = 4 Hz, $^3J_{H6\text{-}H6'}$ = 12 Hz, 1H, H_6), 4.29 (m, $^3J_{H1\text{-}H2}$ = 10 Hz, $^3J_{P\text{-}H1}$ = 17 Hz, 1H, H_1), 3.83 (dd, $^3J_{H5\text{-}H6'}$ = 2 Hz, $^3J_{H6\text{-}H6'}$ = 12 Hz, 1H, $H_{6'}$), 3.18 (m, $^3J_{H4\text{-}H5}$ = 10 Hz, $^3J_{H6\text{-}H5}$ = 4 Hz, $^3J_{H6'\text{-}H5}$ = 2 Hz, 1H, H_5), 2.28, 2.04 (both ddq, $^3J_{HH}$ = 8 Hz, $^2J_{HH}$ = 14 Hz, $^2J_{PH}$ = 14 Hz, 3H, PC*H*$_2$CH$_3$), 1.78 - 1.94 (m, 6H, PC*H'*$_2$CH$_3$), 1.78, 1.75, 1.74, 1.71 (s, 3H, C(O)C*H*$_3$), 0.99 and 0.91 (m, $^3J_{HH}$ = 8 Hz, $^3J_{HH}$ = 8 Hz, $^3J_{PH}$ = 12 Hz, $^5J_{PH}$ = 4 Hz, 9H, PCH$_2$C*H*$_3$). ^{13}C {^{1}H} NMR (C_6D_6, δ): 170.1, 169.8, 169.3, 168.9

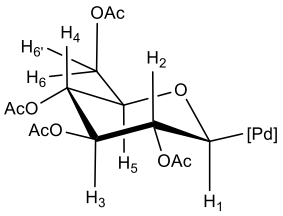

(each a s, *C*(O)CH$_3$), 79.1 (s, C$_5$), 76.7 (s, C$_3$), 75.4 (s, C$_2$), 73.3 (s, C$_1$), 68.7 (s, C$_4$), 62.0 (s, C$_6$), 20.8, 20.4, 20.3, 20.2 (each a s, C(O)*C*H$_3$), 16.8 (d, $^2J_{PC}$ = 6 Hz, P*C*H$_2$CH$_3$), 16.7 (dd, $^2J_{PC}$ = 6 Hz, $^3J_{PC}$ = 2 Hz, P*C*H$_2$CH$_3$), 8.4 and 8.2 (each a s, PCH$_2$*C*H$_3$). ^{31}P {^{1}H} NMR (C$_6$D$_6$, δ): 13.1 and 11.46 (AB quartet, $^2J_{PP}$ = 398 Hz). HRMS (ESI): *m/z* [M - I - PEt$_3$]$^+$ found 555.0941, calcd 555.0975 for C$_{20}$H$_{34}$O$_9$PPd, [M - I]$^+$ found 673.1876, calcd 673.1887 for C$_{26}$H$_{49}$O$_9$P$_2$Pd.

Pd(PMePh$_2$)$_2$(Br)(aceto-β-glucopyranose) (6). A vial was charged with CpPd(allyl) (41 mg, 0.19 mmol) and sealed with a septum cap. After dissolution in C$_6$D$_6$, PMePh$_2$ (108 μL, 0.58 mmol) was added via microsyringe. The solution turned from deep red to orange and was then transferred to a septum sealed NMR tube charged with acetobromo-α-D-glucose (64 mg, 0.16 mmol). The reaction was monitored at room temperature by ^{1}H and ^{31}P spectroscopy; reaction completion was observed after 3 days at room temperature. The product was purified by preparatory TLC; a colorless oil was triturated with hexanes and the resulting white solid was collected by filtration. ^{1}H NMR (C$_6$D$_6$, δ): 8.0-7.0 (m, 20H, Ph), 5.27 (t, $^3J_{HH}$ = 10 Hz, 1H, H$_2$), 4.69 (t, $^3J_{HH}$ = 10 Hz, 1H, H$_3$), 4.43 (t, $^3J_{HH}$ = 9 Hz, 1H, H$_4$), 4.16 (dd, $^3J_{H5\text{-}H6}$ = 6 Hz, $^3J_{H6\text{-}H6'}$ = 12 Hz, 1H, H$_6$), 3.83 (33, $^3J_{H6\text{-}H6'}$ = 12 Hz, $^3J_{H5\text{-}H6'}$ = 3 Hz, 1H, H$_{6'}$), 3.78 (dd, $^3J_{H2\text{-}H1}$ = 10 Hz, $^3J_{HP}$ = 20 Hz, 1H, H$_1$), 2.89 (ddd, $^3J_{H6'\text{-}H5}$ = 3 Hz, $^3J_{H6\text{-}H5}$ = 6 Hz, $^3J_{H4\text{-}H5}$ = 10 Hz, 1H, H$_5$), 2.40, 2.14 (both a d, $^3J_{PH}$ = 8 Hz, 3H, PC*H*$_3$), 1.70, 1.62, 1.56, 1.51 (s, 3H, C(O)C*H*$_3$). ^{13}C {^{1}H} NMR (C$_6$D$_6$, δ): 169.8, 169.7, 169.6, 169.0 (each a s, *C*(O)CH$_3$), 134.7, 134.4, 134.0, 133.6 (each a d, J_{PC} = 10 Hz, Ph), 130.5, 130.2, 130.0, 129.9, 128.6, 128.5 (each a s, Ph), 79.0 (s, C$_5$), 78.0 (s, C$_1$), 75.5 (s, C$_3$), 74.5 (s, C$_2$), 69.6 (s, C$_4$), 63.0 (s, C$_6$), 21.0, 20.4, 20.3, 20.1 (each a s, C(O)*C*H$_3$), 16.1, 14,6 (d, $^1J_{PC}$ = 30 Hz, P*C*H$_3$). ^{31}P {^{1}H} NMR (C$_6$D$_6$, δ): 13.5 and 8.6 (AB quartet, $^2J_{PP}$ = 422 Hz). HRMS (ESI): *m/z* [M - Br -

$PMePh_2]^+$ found 637.0908, calcd 637.0819 for $C_{27}H_{32}O_9PPd$, $[M - Br]^+$ found 837.1616, calcd 837.1574 for $C_{40}H_{45}O_9P_2Pd$.

α-iodo-2,3-aceto-4,6-benzylidene glucopyranose. 4,6-benzylidene-α-D-glucose was prepared

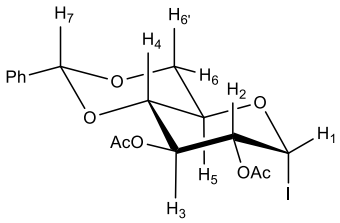

from anhydrous α-D-glucose according to a published procedure.[96] This material was then used to prepare 4,6-benzylidene-aceto glucopyranose according to a published procedure.[97] Product identity and purity was confirmed by comparison to published spectral data.[97] A vial was charged with 4,6-benzylidene-aceto glucopyranose (101 mg, 0.25 mmol) and capped with a septum. After dissolution in 1.0 mL CH_2Cl_2, trimethylsilyl iodide (44 μL, 0.31 mmol) was added via microsyringe and the solution became yellow. After 14 h at room temperature, crude ^1H NMR spectroscopy showed the desired product. The solvent was blown off under a stream of nitrogen to give a brown residue, and the compound was used without further purification. Crude ^1H NMR (CD_2Cl_2, δ): 7.46-7.37 (m, 5H, Ph), 7.04 (d, $^3J_{HH}$ = 4 Hz, 1H, H_1), 5.54 (s, 1H, H_7), 5.54 (t, $^3J_{HH}$ = 9 Hz, 1H, H_3), 4.33 (dd, $^3J_{HH}$ = 5 Hz, $^3J_{HH}$ = H_6, 1H, H_6), 4.25 (dd, $^3J_{HH}$ = 10 Hz, $^3J_{HH}$ = 4 Hz, 1H, H_2), 4.03 (dt, $^3J_{HH}$ = 10 Hz, $^3J_{HH}$ = 5 Hz, 1H, H_5), 4.00-3.89 (m, 2H, H_4 and $H_{6'}$).

$Pd(PEt_3)_2$(I)(2,3-aceto-4,6-benzylidene glucopyranose) (**7**). A vial was charged with

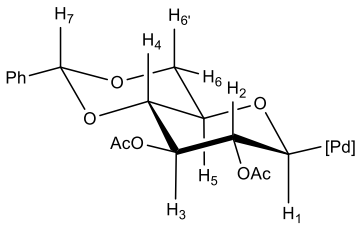

CpPd(allyl) (67 mg, 0.32 mmol) and capped with a septum. After dissolution in benzene, PEt_3 (140 μL, 0.95 mmol) was added at room temperature, and the color changed from deep red to yellow. The solution was added to the brown residue of α-iodo-2,3-aceto-4,6-benzylidene glucopyranose to give an orange solution. After 2 h at room temperature, the reaction

[96] Wood, H. B.; Diehl, H. W.; Fletcher, H. G. *J. Am. Chem. Soc.* **1957**, *79*, 1986-1988.

[97] Barili, P. L.; Berti, G.; Catelani, G.; Cini, C.; D'Andrea, F.; Mastrorilli, E. *Carbohyd. Res.* **1995**, *278*, 43-57.

mixture was transferred directly onto a silica gel column and purified by column chromatography (20% EtOAC in hexanes). The resulting yellow oil was triturated with hexamethyldisiloxane and a yellow powder was collected by filtration (33.1 mg, 0.041 mmol, 16% yield). ^{1}H NMR (C_6D_6, δ): 5.69 (t, $^{3}J_{HH}$ = 10 Hz, 1H, H_2), 5.46 (t, $^{3}J_{HH}$ = 10 Hz, 1H, H_3), 5.30 (s, 1H, H_7), 5.42 (dd, $^{3}J_{H2\text{-}H1}$ = 11 Hz, $^{3}J_{P\text{-}H1}$ = 19 Hz, 1H, H_1), 4.08 (dd, $^{3}J_{H5\text{-}H6}$ = 5 Hz, $^{3}J_{H6'\text{-}H6}$ = 10 Hz, 1H, H_6), 3.79 (t, $^{3}J_{HH}$ = 10 Hz, H_4), 3.31 (dt, $^{3}J_{H6\text{-}H5}$ = 5 Hz, $^{3}J_{H4\text{-}H5}$ = 10 Hz, $^{3}J_{H6'\text{-}H5}$ = 10 Hz, 1H, H_5), 2.20, 2.11, 1.87, 1.82 (each a ddq, $^{3}J_{HH}$ = 7 Hz, $^{2}J_{HH}$ = 14 Hz, $^{2}J_{PH}$ = 14, 3H, PCH_2CH$_3$), 1.79, 1.76 (each a s, 3H, C(O)CH_3), 1.09 and 0.90 (each dt, $^{3}J_{PH}$ = 15 Hz, $^{3}J_{HH}$ = 7 Hz, 9H, PCH$_2$CH_3). ^{13}C {^{1}H} NMR (C_6D_6, δ): 169.7, 168.93 (each a s, *C*(O)CH$_3$), 137.7, 128.9, 128.1, 126.4 (each a s, Ph), 101.8 (s, C_7), 79.7 (s, C_4), 76.1 (s, C_2), 75.4 (s, C_3), 74.2 (s, C_5), 73.6 (s, C_1), 68.8 (s, C_6), 20.6, 20.2 (each a s, C(O)*C*H$_3$), 16.6 (m, P*C*H$_2$CH$_3$), 8.1, 8.0 (each a s, PCH$_2$*C*H$_3$). ^{31}P {^{1}H} NMR (C_6D_6, δ): 13.3 and 10.3 (AB quartet, $^{2}J_{PP}$ = 400 Hz). HRMS (ESI): *m/z* [M - I - PEt$_3$]$^+$ found 559.1094, calcd 559.1077 for $C_{23}H_{34}O_7PPd$, [M - I]$^+$ found 677.2105, calcd 677.1988 for $C_{29}H_{49}O_7P_2Pd$.

Pd(dppe)(Br)(aceto-β-glucopyranose). A vial was charged with Pd(PEt$_3$)$_2$(Br)(aceto-β-glucopyranose) (11 mg, 0.015 mmol) and 1,2-bis(diphenylphosphino)ethane (5.9 mg, 0.015 mmol). Dry toluene (0.5 mL) was added to dissolve all materials. After stirring for 10 minutes, volatiles were removed under reduced pressure. An additional 0.5 mL dry toluene was added, and volatiles were removed again. After a third addition of 0.5 mL toluene, volatiles were removed and the powder that remained was analyzed by NMR. This product was used without further purification. ^{1}H NMR (400 MHz, C_6D_6): δ 8.04 (m 1H), 7.83 – 7.68 (m, 2H), 7.67 – 7.55 (m, 1H), 7.50 – 6.86 (m, 26H), 5.55 – 5.28 (m, 1H), 4.71 (t, J = 9.8 Hz, 1H), 4.43 – 4.26 (m, 1H), 4.00 (dd, J = 12.2, 3.7 Hz, 1H), 3.56 (dd, J = 12.1, 2.4 Hz, 1H), 2.91 (ddd, J = 10.2, 3.9, 2.5 Hz, 1H), 2.16 (s, 3H), 2.10 (s, 3H), 1.62 (s, 3H), 1.61 (s, 3H).

Reaction of $Pd(PEt_3)_2(Br)$(aceto-β-glucopyranose) with other chelating phosphine ligands: $Pd(PEt_3)_2(Br)$(aceto-β-glucopyranose) (11 mg, 0.015 mmol) and 0.015 mmol of a chelating phosphine ligand were dissolved in dry toluene-d_8, and a ^1H NMR spectrum was acquired. No reaction was observed for 1,2-bis(diphenylphosphino)methane, 1,2-bis(diphenylphosphino)propane, 1,2-bis(diphenylphosphino)butane and Xantphos. Tri-acetoxy glucal was observed for 1,2-bis(dicyclohexylphosphino)ethane and 1,2-bis(diethylphosphino)ethane.

Reaction of $Pd(PEt_3)_3$ (1) with bromocyclohexane. A vial was charged with CpPd(allyl) (8.7 mg, 0.038 mmol) and sealed with a septum cap. After dissolution in C_6D_6, PEt_3 (19 μL, 0.13 mmol) was added via microsyringe. The solution turned from deep red to yellow and was then transferred to a septum sealed NMR tube charged with bromocyclohexane (4.1 μL, 0.033 mmol). The reaction was monitored at room temperature by ^1H and ^{31}P NMR spectroscopy; no reaction was observed after three days.

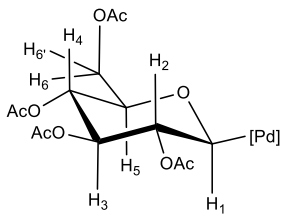

Reaction of $Pd(PEt_3)_3$ (1) with acetochloro-α-D-glucose. A vial was charged with CpPd(allyl) (10 mg, 0.047 mmol) and sealed with a septum cap. After dissolution in C_6D_6, PEt_3 (21 μL, 0.14 mmol) was added via microsyringe. The solution turned from deep red to yellow and was then transferred to a septum sealed NMR tube charged with acetochloro-α-D-glucose (14 mg, 0.038 mmol). The reaction was monitored at 40 °C; no reaction was observed after one day.

Reaction of $Pd(PEt_3)_3$ (1) with α-D-mannopyranosyl bromide tetrabenzoate. A vial was charged with CpPd(allyl) (7.0 m g, 0.033 mmol) and sealed with a septum cap. After dissolution in C_6D_6, PEt_3 (15 μL, 0.10 mmol) was added via microsyringe. The solution turned from deep red to yellow and was then transferred to a septum sealed NMR tube charged with α-D-

mannopyranosyl bromide tetrabenzoate (18 mg, 0.027 mmol). The reaction was monitored at room temperature by ^{1}H and ^{31}P NMR spectroscopy; complete conversion to tri-*O*-benzoylglucal was observed over the course of nine hours.

Reaction of $Pd(PCy_3)_2$ with acetobromo-α-D-glucose. A vial was charged with acetobromo-α-D-glucose (6.5 mg, 0.016 mmol) and sealed with a septum. After dissolution in C_6D_6, the solution was transferred to NMR tube charged with $Pd(PCy_3)_2$ (11 mg, 0.016 mmol) and a color change to yellow was observed immediately; complete conversion to tri-*O*-acetylglucal was observed by ^{1}H NMR spectroscopy after five minutes. Single crystals of $Pd(PCy_3)_2(Br)(OAc)$ (**8**) suitable for X-ray diffraction were grown by slow evaporation from pentane.

Reaction of $Pd(PCy_3)_2$ with acetobromo-α-D-glucose with added PCy_3. 8.0 mg (0.012 mmol) of $Pd(PCy_3)_2$ was massed into a vial, dissolved in C_6D_6, and transferred to a vial containing PCy_3 (17 mg, 0.061 mmol). The solution was then transferred to an NMR tube charged with acetobromo-α-D-glucose (5.0 mg, 0.012 mmol) and turned from light brown to yellow. Within 5 minutes, conversion to tri-*O*-acetylglucal was observed by ^{1}H NMR spectroscopy.

Reaction of $Pd(PEt_3)_3$ (1) with glucopyranose pentabenzoate. A vial was charged with CpPd(allyl) (13 mg, 0.062 mmol) and sealed with a septum cap. After dissolution in C_6D_6, PEt_3 (28 μL, 0.19 mmol) was added via microsyringe. The solution turned from deep red to yellow and was then transferred to a septum sealed NMR tube charged with glucopyranose pentabenzoate (46 mg, 0.066 mmol). The reaction was monitored at room temperature by ^{1}H and ^{31}P NMR spectroscopy; no reaction was observed after three days.

β-acetoxy elimination of $Pd(PEt_3)_2(Br)$(AcO-β-glu) (3). 9.0 mg (0.012 mmol) of **2** was massed into an NMR tube and sealed with a septum. After dissolution in C_6D_6, an initial ^{1}H NMR

spectrum was acquired and the β-acetoxy elimination of **2** was monitored at room temperature by ^{1}H spectroscopy; 40% of **2** had converted to tri-*O*-acetylglucal after 14 days.

β-acetoxy elimination of $Pd(PEt_3)_2(Br)(AcO\text{-}\beta\text{-}glu)$ (3) with added PEt_3. 5.4 mg (0.0072 mmol) of **2** was massed into an NMR tube and sealed with a septum. After dissolution in C_6D_6, PEt_3 (4.6 μL, 0.031 mmol) was added via microsyringe. An initial ^{1}H spectrum was acquired and the β-acetoxy elimination of **2** was monitored at room temperature by ^{1}H NMR spectroscopy; 1-5% of **2** had converted to tri-*O*-acetylglucal after 14 days.

β-acetoxy elimination of $Pd(PEt_3)_2(Br)(AcO\text{-}\beta\text{-}glu)$ (3) with added Br^-. 8.2 mg (0.011 mmol) of **2** and $[P(oct)_4][Br]$ (32 mg, 0.057 mmol) was massed into an NMR tube and sealed with a septum. After dissolution in C_6D_6, an initial ^{1}H NMR spectrum was acquired. The β-acetoxy elimination of **2** was monitored at room temperature by ^{1}H NMR spectroscopy; 35% of **2** had converted to tri-*O*-acetylglucal after 14 days.

β-acetoxy elimination of $Pd(PEt_3)_2(I)(AcO\text{-}\beta\text{-}glu)$ (5). 12.6 mg (0.059 mmol) of **4** was massed into an NMR tube. An external integration standard (0.18 mM PPh_3 in C_6D_6 sealed in a capillary tube) was inserted and the NMR tube was sealed with a septum . After dissolution in C_6D_6, initial ^{1}H and $^{31}P\{^{1}H\}$ NMR spectra were acquired and the β-acetoxy elimination of **4** was monitored at 40°C by ^{1}H and ^{31}P NMR spectroscopy; 50% of **4** had converted to tri-*O*-acetyl glucal after 2 days.

β-acetoxy elimination of $Pd(PEt_3)_2(I)$(2,3-aceto-4,6-benzylidene glucopyranose) (7). 5.6 mg (0.0070 mmol) of **5** was massed into an NMR tube. An external integration standard (0.18 mM PPh_3 in C_6D_6 sealed in a capillary tube) was inserted and the NMR tube was sealed with a septum. After dissolution in C_6D_6, initial ^{1}H and $^{31}P\{^{1}H\}$ NMR spectra were acquired and the β-acetoxy elimination of **5** was monitored at 40°C by ^{1}H and ^{31}P NMR spectroscopy; 50% of **5** had converted to 3-*O*-acetyl-4,6-*O*-benzylideneglucal and a second species after 1.5 days.

Crystallographic Data.

$Pd(PEt_3)_2(Br)$(aceto-β-glucopyranose), 3. A suitable single crystal of **3** was selected, covered in oil, and mounted on the end of a fiber. Intensity data were collected on a Bruker-AXS SMART 1D diffractometer with CCD detector using Cu Kα radiation. Structure solution was carried out using direct methods[98] and refined by least-squares techniques on F^2 using the Oxford University *Crystals for Windows* software.[99] Figures were prepared using ORTEP.[100]

Empirical formula	$C_{26}H_{49}BrO_9P_2Pd$
Formula weight	753.93
Temperature	100(2) K
Crystal system	Monoclinic
Space group	P 2_1
Unit cell dimensions	a = 10.4902(1) Å α = 90°
	b = 28.3899(4) Å β = 96.4119(5)°
Unit cell volume	3426.17(8) $Å^3$
Z	4
Density (calculated)	1.46 mg/m^3
Absorption coefficient	6.99 mm^{-1}
Crystal size	$0.193 \times 0.288 \times 0.334$ mm^3
Theta range for data collection	3.11 - 70.0°
Reflections collected	24791
Independent reflections	11140
Completeness	98%
Absorption correction	Numerical
Refinement method	Full-matrix least-squares on F^2

[98] Altomare, A.; Cascarano, G.; Giacovazzo, C.; Guagliardi, A.; Burla, M. C.; Polidori, G.; Camalli, M. *J. Appl. Cryst.* **1994**, *27*, 435.

[99] Betteridge, P. W.; Carruthers, J. R.; Cooper, R. I.; Prout, K.; Watkin, D. J. *J. Appl. Cryst.* **2003**, *36*, 1487.

[100] Farrugia, L. *J. Appl. Cryst.* **1997**, *30*, 565.

Data / restraints / parameters	11099 / 0 / 704
Flack parameter	0.009(4)
Goodness-of-fit on F^2	0.949
Final R-indices [I>2σ (I)]	R1 = 0.0255, wR2 = 0.0555
R indices (all data)	R1 =0.0265, wR2 = 0.0559

$Pd(PCy_3)_2(Br)(OAc)$ (8). A suitable single crystal of **8** was selected, covered in oil, and mounted on the end of a fiber. Intensity data were collected on a Bruker-AXS SMART 1D diffractometer with CCD detector using Mo Kα radiation. The structures were solved by direct methods[1019] and refined by least-squares techniques on F^2. The acetate ligand displayed disorder by a 180° rotation, which was modeled successfully by two ligands each with 50% occupancy and forced to have the same geometry. Figures were prepared using ORTEP.[11]

Empirical formula	$C_{38}H_{69}BrO_2P_2Pd$
Formula weight	806.18
Temperature	100(2) K
Crystal system	Monoclinic
Space group	P $2_1/c$
Unit cell dimensions	a = 12.4843(8) Å α = 90°
	b = 26.1392(17) Å β = 113.351(5)°
Unit cell volume	3892.3(5) $Å^3$
Z	4
Density (calculated)	1.376 mg/m^3
Absorption coefficient	6.046 mm^{-1}
Crystal size	0.09 × 0.13 × 0.34 mm^3
Theta range for data collection	3.38-68.14

Reflections collected	43319
Independent reflections	7053
Completeness	99.3%
Absorption correction	Multi-scan
Refinement method	Full-matrix least-squares on F^2
Data / restraints / parameters	7053 / 93 / 417
Goodness-of-fit on F^2	1.124
Final R-indices [I>2σ (I)]	R1 = 0.0462, wR2 = 0.1094
R indices (all data)	R1 =0.0501, wR2 = 0.1113

Chapter 3 **Iridium-catalyzed Hydrosilylative Reduction of Glucose to Hexane(s)**

This is chapter adapted with permission from McLaughlin, M. P.; Adduci, L. L.; Becker, J. J.; Gagné, M. R. *J. Am. Chem. Soc.* **2013**, *135*, 1225–1227.

The work in this chapter resulted from collaboration with Dr. Matthew McLaughlin, who contributed significantly to sections 3.2 and 3.6.

3.1 ***Reductive deoxygenation of biomass***

The dwindling of petroleum resources has made carbohydrates attractive targets for renewable energy and chemical feedstocks.[102,103] Chemists have sought to defunctionalize sugars to simpler chemical feedstocks, which are compatible with modern chemical processes and infrastructure.[54] Despite significant effort, most systems relevant to carbohydrate defunctionalization utilize harsh conditions (high temperatures, pressures, and strong acids) and

[102] Ragauskas, A. J.; Williams, C. K.; Davison, B. H.; Britovsek, G.; Cairney, J.; Eckert, C. A.; Jr, W. J. F.; Jason, P. H.; Leak, D. J.; Liotta, C. L.; Mielenz, J. R.; Murphy, R.; Templer, R.; Tschaplinski, T. *Science* **2006**, *311*, 484-489.

[103] Kerr, R. A.; Service, R. F. *Science* **2005**, *309*, 101.

are generally low yielding for defunctionalized products.[53,55,56,62,63,104-117] To date, the mildest systems for the reduction of carbon-oxygen bonds are hydrosilylative, but for sugars these methods

[104] Barrett, C. J.; Dumesic, J. A.; Liu, Z. Y.; Roman-Leshkov, Y. *Nature* **2007**, *447*, 982-985.

[105] Yang, W.; Grochowski, M. R.; Sen, A. *ChemSusChem* **2012**, *5*, 1218-1222.

[106] Gallezot, P. *Chem. Soc. Rev.* **2012**, *41*, 1538-1558.

[107] Huber, G. W.; Iborra, S.; Corma, A. *Chem. Rev.* **2006**, *106*, 4044-4098.

[108] Mascal, M.; Nikitin, E. B. *Angew. Chem. Int. Ed.* **2008**, *47*, 7924-7926.

[109] Zhao, H.; Holladay, J. E.; Brown, H.; Zhang, Z. C. *Science* **2007**, *316*, 1597-1600.

[110] Ahmed Foskey, T. J.; Heinekey, D. M.; Goldberg, K. I. *ACS Catal.* **2012**, *2*, 1285-1289.

[111] Ewing, G. J.; Robins, M. J. *Org. Lett.* **1999**, *1*, 635-636.

[112] In Hwan, O.; Gray, G. R. *Carbohydr. Res.* **1995**, *278*, 329-338.

[113] Taher, D.; Thibault, M. E.; Di Mondo, D.; Jennings, M.; Schlaf, M. *Chem. Eur. J.* **2009**, *15*, 10132-10143.

[114] Ghosh, P.; Fagan, P. J.; Marshall, W. J.; Hauptman, E.; Bullock, R. M. *Inorg. Chem.* **2009**, *48*, 6490-6500.

[115] Ziegler, J. E.; Zdilla, M. J.; Evans, A. J.; Abu-Omar, M. M. *Inorg. Chem.* **2009**, *48*, 9998-10000.

[116] Arceo, E.; Marsden, P.; Bergman, R. G.; Ellman, J. A. *Chem. Commun.* **2009**, 3357-3359.

[117] Rosen, B. M.; Quasdorf, K. W.; Wilson, D. A.; Zhang, N.; Resmerita, A.-M.; Garg, N. K; Percec, V. *Chem. Rev.* **2011**, *111*, 1346–1416.

have been limited to defunctionalization at the activated C_1 position and take many hours.[51,67,71] 118-127

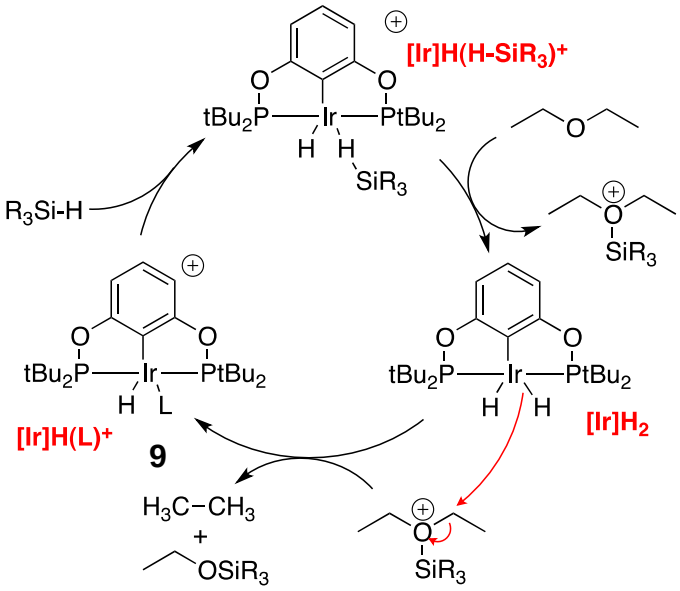

Scheme 3.1: Catalytic cycle for hydrosilylative reduction

Brookhart has reported a cationic iridium pincer complex, **9**, which acts as a potent catalyst (<1 mol%) for the hydrosilylative reduction of alkyl ethers to alkanes (e.g. Scheme 3.1).[74] In combination with triethylsilane, **9** mediates the complete reduction of primary and methyl ethers

[118] Chatani, N.; Shinohara, M.; Ikeda, S.-i.; Murai, S. *J. Am. Chem. Soc.* **1997**, *119*, 4303-4304.

[119] Murai, T.; Furuta, K.; Kato, S.; Murai, S.; Sonoda, N. *J. Organomet. Chem.* **1986**, *302*, 249-254.

[120] Gevorgyan, V.; Liu, J.-X.; Rubin, M.; Benson, S.; Yamamoto, Y. *Tetrahedron Lett.* **1999**, *40*, 8919-8922.

[121] Gutsulyak, D. V.; Vyboishchikov, S. F.; Nikonov, G. I. *J. Am. Chem. Soc.* **2010**, *132*, 5950-5951.

[122] Rolf, D.; Bennek, J. A.; Gray, G. R. *Carbohydr. Res.* **1985**, *137*, 183-196.

[123] Guo, Z.-W.; Hui, Y.-Z. *Synth. Commun.* **1996**, *26*, 2067-2073.

[124] Sergeev, A. G.; Hartwig, H.F. *Science* **2011**, *332*, 439-442.

[125] Nichols, J. M.; Bishop, L. M.; Bergman, R. G.; Ellman, J. A. *J. Am. Chem. Soc.* **2010**, *132*, 12554-12555.

[126] Scott, V. J.; Çelenligil-Çetin, R.; Ozerov, O. V. *J. Am. Chem. Soc.* **2005**, *127*, 2852-2853.

[127] Douvris, C.; Ozerov, O. V. *Science* **2008**, *321*, 1188-1190.

to the hydrocarbon. In the case of secondary ethers, only a single C-O cleavage occurs and the secondary silyl ether is obtained. Despite these potential limitations, we surmised that the enhanced stability of the C_1-carbocation of a sugar might support an alternative, Murai-like[118-119] mechanism for the reduction of at least one secondary C-O bond in glucose (Scheme 3.2). In this scenario we anticipated C_1 reduction to be especially rapid.

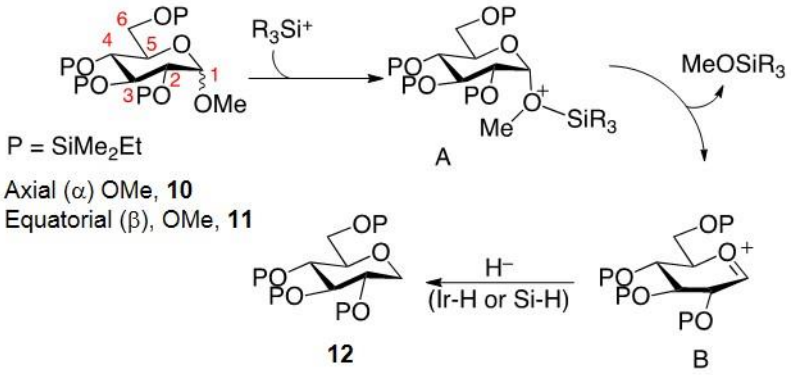

Scheme 3.2: Proposed mechanism of C_1 reduction

3.2 *C_1 Reduction*

Initial experiments with 1% catalyst, 1.2 equiv of $SiMe_2EtH$, and the α and β anomers of silylated MeO-glucose (**10** and **11**), showed that reduction to **12** was rapid and complete within minutes (over 90% by NMR)**.** Although both the α and β anomers reacted too fast to monitor rates, a competition between 1 equiv each of **10** and **11**, with 1 equiv of $SiMe_2EtH$ (1% catalyst), established (by NMR) the near exclusive consumption of the equatorial (β) OMe isomer. The reduction of **13**, on the other hand, was substantially slower, requiring hours of reduction time and either many equivalents $SiMe_2EtH$ or the more reactive $SiEt_2H_2$[8] for complete conversion. In addition to a slower rate, the selectivity for C_1 deoxygenation was compromised (Eq 1). Although reduction of **13** still yielded **12** through cleavage site "a", a number of other products were also formed, including D-glucitol (**14**), which would require cleavage at site "b." In situ monitoring by NMR spectroscopy of the reduction of **13** indicated that like the C_1-OMe case, the β-anomer reacts

faster (greater than 10x the rate), leading to the following comparative C-O hydrosilylation rates: $C_{1\ equatorial,\ OMe} > C_{1\ axial,\ OMe} >> C_{1\ equatorial,\ OSiR3} > C_{1\ axial,\ OSiR3} > C_{n,\ OSiR3\ (n = 2,3,4,6)}$. This trend can be rationalized by noting the importance of a basic ether in forming the key silyloxonium ion, **A**, and the enhanced stability of the C_1-oxocarbenium ions (B, Scheme 3.2)

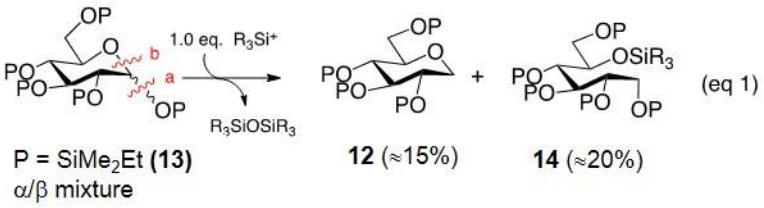

3.3 *Complete Deoxygenation*

Increasing the catalyst loadings, silane concentration, and using the more reactive diethylsilane[71] revealed that **10** could be completely reduced to hexane isomers (i.e. "hexanes", Eq 2). Unprotected glucose also yielded hexanes under the reaction conditions. Preferable were pre-protected carbohydrates that avoided excessive H_2 evolution during the reaction. ^{13}C NMR and the spiking of reaction mixtures with authentic products verified the formation of the indicated hexane isomers: n-hexane (**15**), 2- and 3-methylpentane (**16** and **17**), and trace amounts of 2,3-dimethylbutane (**18**). Using $^{13}C_6$ and $^{13}C_1$ labeled **13** to follow the reaction showed that both ^{13}C-labeled sugars converged on a similar mixture of hexanes, with one enhanced signal for **15** and **18** and two for **16** and **17**. Over the course of the reduction of ^{13}C-**13**, hexanes were observable within 12 hours but the signal continued to develop for weeks. Over the course of 2 weeks, all the ^{13}C NMR peaks associated with C-O bonds (50-100 ppm) diminished below the detection limit, accompanied by continual growth of peaks in the alkyl region (10-50 ppm).

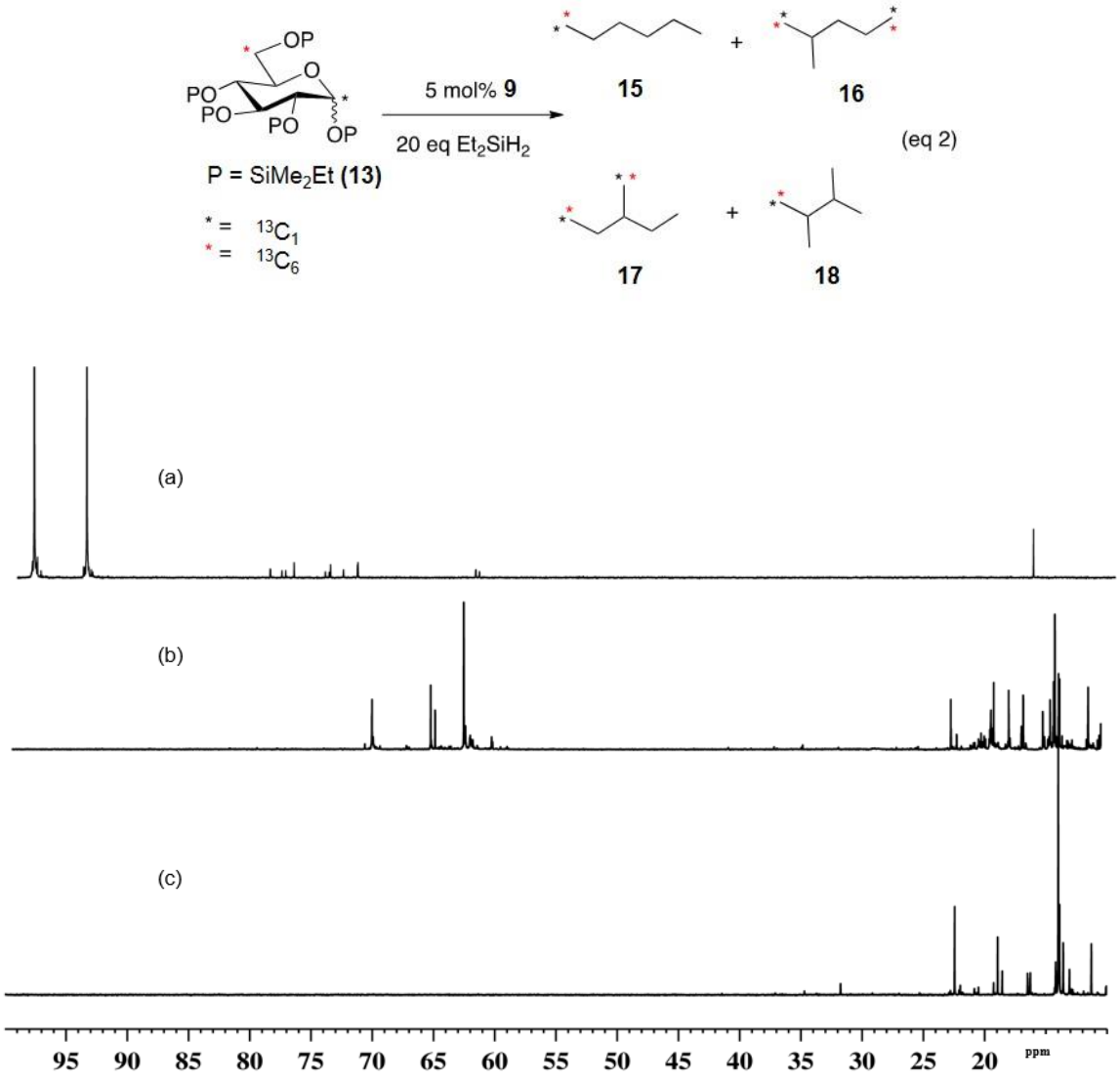

Figure 3.1: In situ $^{13}C\{_1H\}$ NMR spectra of the hydrosilylation of $^{13}C_1$-13 at various time points: (a) starting material (b) 14 hours (c) 7 days. Peaks upfield of 10 ppm are silane related.

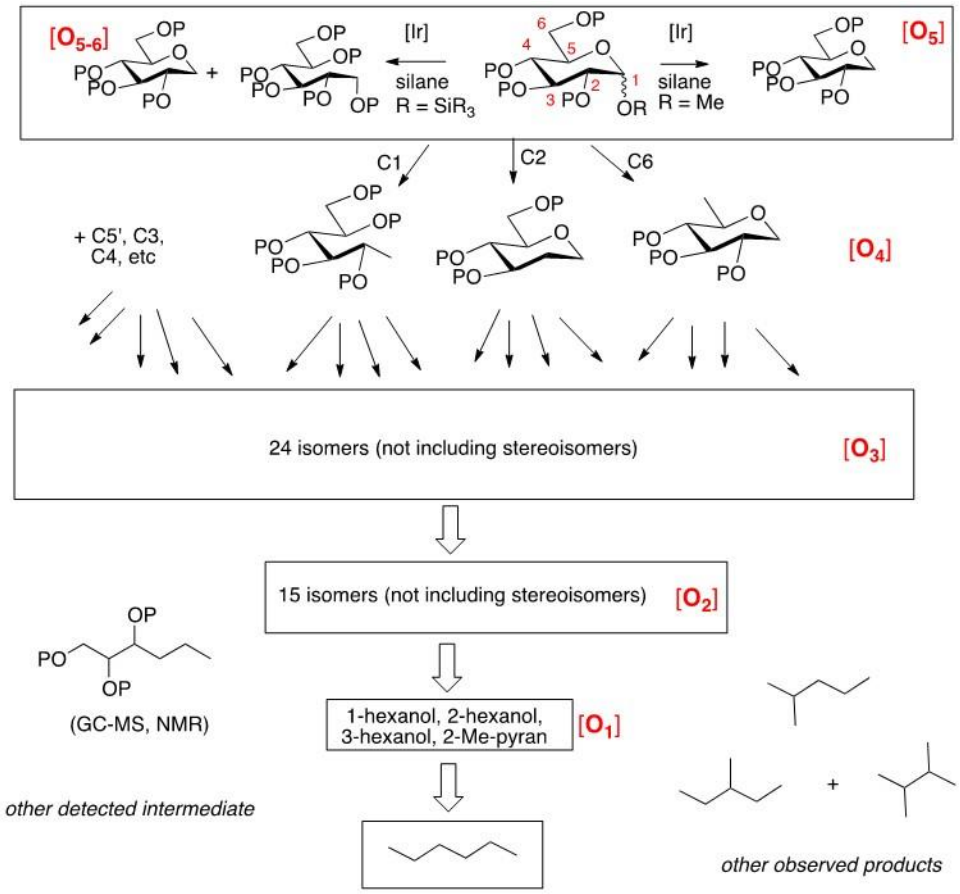

Scheme 3.3: Intermediates of glucose reduction

3.4 *Diversity of intermediates*

The in situ monitoring of the non-labeled sugars proved fascinating. As discussed above **10** and **11** quickly convert to **12**, but as the signals of this C_1-deoxy product diminish they are not replaced with new signals until much later when hexane begins appearing. For compound **13**, a dramatic loss of signal intensity occurs immediately upon its consumption. As shown in Scheme 3.3, we surmised that a non-selective C-O reduction would lead to a large increase in the number of components, and a concomitant decrease in spectral intensity. This hypothesis was verified by monitoring the reduction of ^{13}C-labeled **5** by ^{13}C NMR spectroscopy. As shown in Figure 3.1, numerous intermediates are observed both in the C-O region (50-100 ppm) and in the upfield alkane region. Contributing to this diversity of intermediates are traces of unsaturated compounds

(100-150 ppm, not shown), which appear transiently, including a match for 1-hexene. Such an observation not unreasonably suggests that elimination is also a competitive process.

3.5 *Degree of rearrangement*

To overcome the technical challenges of quantifying the volatile hexane products, the yields were estimated by an in situ ^{13}C NMR spectroscopy experiment utilizing internal standard and a calibrated 90-degree pulse sequence (see experimental section for details).[128] Both the α and β anomers of MeO-glu, **10** and **11**, consistently yielded a higher proportion of the rearranged products than **5** (Figure 3.2). A possible source for this surprising divergence in hexane isomer production was suggested by the comparative deoxygenation of **12** and 14 (glucitol). Like **10**, the C_1-deoxy **12** gives significant rearrangement, consistent with rapid conversion of **10** to **12** during the reaction. Reduction of **14**, however, gives predominantly n-hexane suggesting that **10** and **13** may bifurcate at the first reaction steps. It thus seems likely that pyranose **12** is the species most likely to initiate branching, presumably through carbocation(s)[129,130] that may or may not involve neighboring group participation.

[128] Pieters, L. A. C.; Vlietinck, A. J. *J. Pharm. Biomed. Anal.* **1989**, *7*, 1405-1417

[129] Olah, G. A.; White, A. M. *J. Am. Chem. Soc.* **1969**, *91*, 5801-5810

[130] Olah, G. A. In *Carbonium Ions*, Olah, G. A. Ed. Wiley: New York, 1970; Vol. 2, pp 655-782

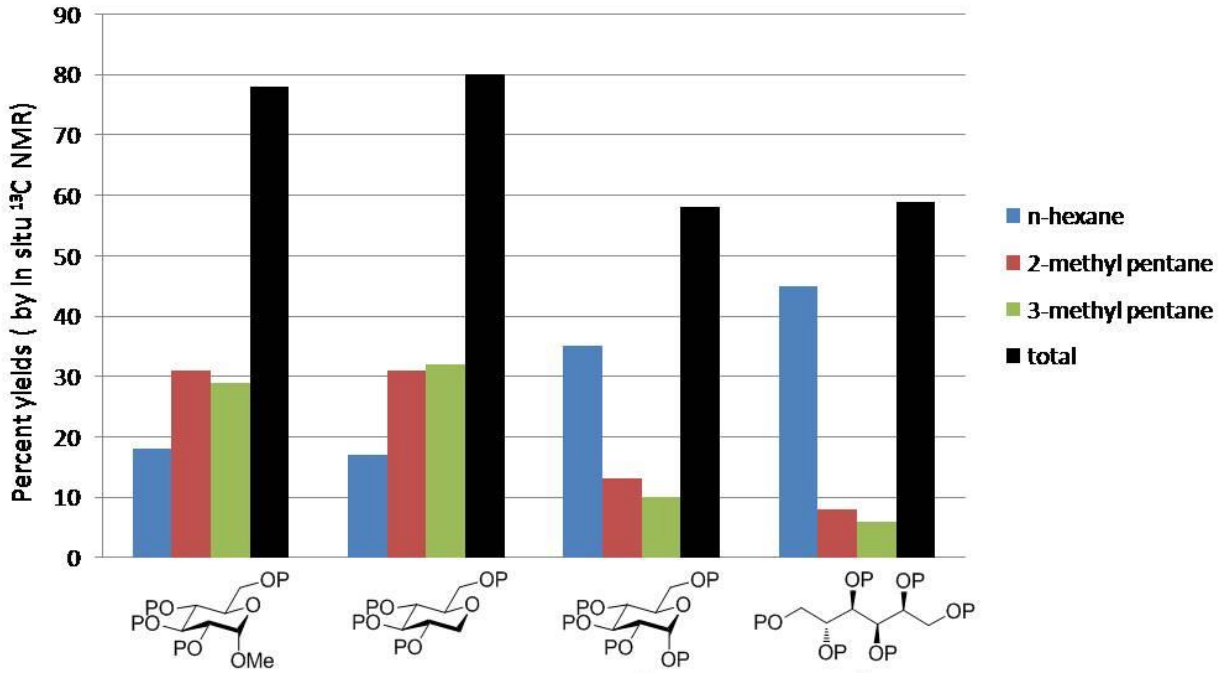

Figure 3.2: Absolute yields (%) of the hexane isomers 15-17 for the hydrosilylation of 10 and 12 as determined by semi-quantitative ^{13}C NMR spectroscopy. General reaction conditions: 5% catalyst 9 and 20 equivalents of $SiEt_2H_2$ (see experimental section for details).

3.6 *Control experiments*

The nature of the catalytic species responsible for the deoxygenative behavior is not fully understood. As expected, hydride resonances between -8 and -12 ppm were observed. While these resonances are similar to those previously reported by Brookhart, they eventually drop below the detection limit even as catalysis continues. Attempts to utilize simple iridium precursors ($[Ir(COE)Cl]_2$,[131] $[Ir(COD)Cl]_2$,[132] and Vaska's complex (both PPh_3 and PMe_3),[24]) both with and without added $LiB(C_6F_5)_4 \bullet Et_2O$ were unsuccessful. The Lewis acid $B(C_6F_5)_3$, a known deoxygenative hydrosilylation catalyst,[118-127] was considered as a potential active impurity. In-situ ^{19}F NMR spectroscopy of iridium-catalyzed reaction mixtures revealed only trace $[B(C_6F_5)_4]^-$

[131] Cheng, C.; Brookhart, M. *J. Am. Chem. Soc.* **2012**, *134*, 11304-11307

[132] Apple, D. C.; Brady, K. A.; Chance, J. M.; Heard, N. E.; Nile, T. A. *J. Mol. Catal. A* **1985**, *29*, 55-64

decomposition and no observable borane; spiking completed reactions with borane show it to be readily detectable at 0.1 mol%. Since reactions containing 0.1 mol% borane do not proceed in the absence of iridium catalyst, and significantly higher concentrations of borane give a different product distribution, we conclude that the iridium complex predominately catalyzes the reaction.

3.7 *Conclusion*

In summary, we have identified a system that catalyzes the full reduction of silyl protected sugars to a mixture of hexane isomers. MeO- sugars **10** and **11** proceed by selective C_1 reduction to **12** whereas the persilyl glucose, **13**, is reduced to a mixture that includes **12** and the ring opened sugar **14**. The hexane isomer distribution is sensitive to the C_1-substituent, with the 1-OMe protected sugars **10** and **11** yielding mostly 2- and 3-methylpentane, whereas the C_1-$OSiR_3$, **13**, yielded mostly n-hexane. The reaction rate is affected by the silane, with the less hindered Et_2SiH_2 giving the fastest rates. Studies on the role of sugar, catalyst, and silane on the efficiency and hexane selectivity of this reaction are ongoing.

3.8 *Experimental section*

General Methods: Unless otherwise stated, all reactions were conducted under an argon atmosphere using a Vacuum Atmospheres glovebox. Chlorobenzene-d_5, $^{13}C_1$ glucose, and $^{13}C_6$ glucose were purchased from Cambridge Isotope labs; chlorobenzene-d_5 was degassed via three freeze-pump-thaw cycles and dried over 4Å molecular sieves prior to use. Diethyl silane and dimethyl ethyl silane were purchased from Aldrich and stored in the glovebox. 1-deoxy-glucopyranose was purchased from Carbosynth. Chlorodimethylethylsilane was purchased from TCI America. $[(POCOP)Ir(H)(acetone)]^+[B(C_6F_5)_4]^-$ (POCOP = 2,6-$[OP(t\text{Bu})_2]_2C_6H_3$) (**1**) was prepared according to a published procedure.[133]

[133] Yang, J.; Brookhart, M. *J. Am. Chem. Soc.* **2007**, *129*, 12656–12657.

NMR spectra were recorded using Bruker DRX spectrometers operating at 400 or 600 MHz (^{1}H), and 100 or 150 MHz (^{13}C). NMR chemical shifts are reported in ppm and referenced using the residual proton peaks (^{1}H) or the ^{13}C resonances of the deuterated solvent (^{13}C). Where necessary, 2D COSY, HSQC, HMBC, and APT data were used for peak assignment.

GC-MS data was obtained using an Agilent G2570A GC/MSD system containing a 6850 GC equipped with an HP-5MS column (length 30 m; I.D. 0.250 mm) connected to an Agilent 5983N MSD. GC-MS was obtained with the following parameters: *Initial*: 125°C (3 min); *Ramp 1*: 20 °C/min to 250°C (8 min); *Injection Port T* = 300 °C; *Column Flow*: 1 mL/min; *Column Pressure*: 11.9 psi helium.

General Procedure **A**: silyl protection of carbohydrates

Silyl protected carbohydrates were prepared by analogy to published procedure:[134]

A scintillation vial was charged with 2 mmol of a carbohydrate. 8 mL anhydrous pyridine was added to give a suspension, and chlorodimethylethylsilane (1.3 eq. per –OH group) was added via syringe while stirring. The reaction mixture was stirred at room temperature for 2 days (an inert atmosphere was not necessary). Subsequently, 10 mL water was added to the vial to quench excess silane. The reaction mixture was diluted with additional water in a separatory funnel. The aqueous phase was extracted three times with diethyl ether; the combined ether layers were then washed three times with water and three times with brine. After drying over magnesium sulfate, the organic layer was concentrated under vacuum. Co-evaporation with toluene removed residual

[134] Bourdreux, Y.; Lemetais, A.; Urban, D.; Beau, J.-M. *Chem. Comm.* **2011**, *47*, 2146–2148.

pyridine. The resulting oils were dried under high vacuum at 40°C overnight, transferred into the glovebox, and used without further purification.

General Procedure **B**: catalytic hydrosilylative reduction of carbohydrates

In an argon-filled glovebox, a 1-dram vial was charged with $[(POCOP)IrH(acetone)]^+[B(C_6F_5)_4]^-$ catalyst (**9**) (5 mol%). The silyl-protected carbohydrate (1 eq.) was massed into the same vial. Enough C_6D_5Cl was added to ensure a total volume of 500 μL after addition of the standard solution and silane. A standard solution of hexamethylbenzene in C_6D_5Cl was added, followed by silane (20 eq). The reaction mixture was then transferred to a J-Young tube or a septum-capped NMR tube. Samples were periodically removed from the glovebox for carbon NMR monitoring using a standard proton-decoupled experiment. After two weeks, a $^{13}C\{^1H\}$ NMR spectrum was acquired using a 90° pulse procedure (described below). To estimate absolute yields, integrations of the product peaks were compared to the integration of the standard peak.

Occasionally, the reaction was set up with catalyst **9** omitted. An initial $^{13}C\{^1H\}$ NMR spectrum was acquired, and the reaction was returned to the glovebox. Catalyst **9** was then added, and the reaction proceeded normally.

$^{13}C\{^1H\}$ NMR using 90° pulse procedure

Determination of parameters for 90° degree pulse procedure:

The 90° pulse was calibrated by varying the pulse width (p1) until a 360° pulse was identified (i.e. a weak mixture of positive and negative peaks were observed). The pulse width needed for a 360° pulse was divided by 4 to obtain a 90° pulse. Using the calibrated 90° pulse width (p1 = 10.45 microseconds) a sufficient relaxation time (d1) was identified by varying the delay until a solution

of hexane isomers and hexemethylbenzene had the correct relative integrations (d1 = 100 seconds). Shown below is a solution containing 80 μmol of each hexane isomer and 13 μmol of hexamethylbenzene; the peak integrations demonstrate that each species has effectively relaxed fully (Figure 3.3).

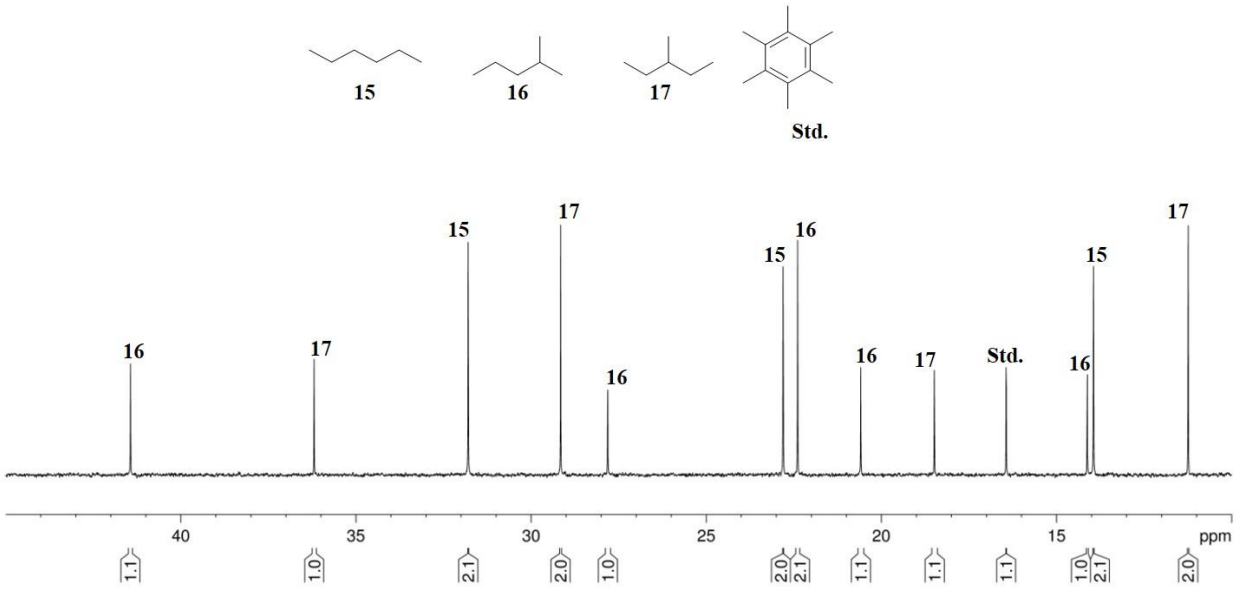

Figure 3.3: Relative integrations for $^{13}C\{^{1}H\}$ NMR peaks of different hexane isomers

Spectra of reaction mixtures taken using this 90° pulse procedure were obtained by setting the pulse width (p1) to 10.5 microseconds, the delay time (d1) to 100 seconds, and the probe temperature to 283K. The spectra were centered (o1p) at 30 ppm, and 300-400 scans were acquired.

α-1-OMe-2,3,4,6-OSiMe$_2$Et-glucopyranose (10) was prepared from α-1-OMe-glucopyranose according to General Procedure A. ^{1}H NMR ($CDCl_3$, 600 MHz): 4.60 (d, $^{3}J_{H1,H2}$ = 3.6 Hz, 1H, H_1), 3.76 (dd, $^{3}J_{H6,H5}$ = 1.8 Hz, $^{2}J_{H6,H6'}$ = 11.4 Hz, 1H, H_6), 3.74 (t, $^{3}J_{H,H}$ = 9.0 Hz, 1H, H_3), 3.66 (dd, $^{2}J_{H6',H6}$ = 11.4 Hz, $^{3}J_{H6',H5}$ = 6.0 Hz, 1H, $H_{6'}$), 3.48 (ddd, $^{3}J_{H5,H4}$ = 9.6 Hz, $^{3}J_{H5,H6'}$ = 5.4

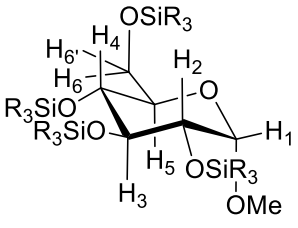

$R_3 = Me_2Et$

Hz, $^{3}J_{H5,H6}$ = 1.8 Hz, 1H, H_5), 3.44 (dd, $^{3}J_{H1,H2}$ = 3.6 Hz, $^{3}J_{H2,H3}$ = 9.6 Hz, 1H, H_2), 3.40 (dd, $^{3}J_{H4,H5}$ = 9.6 Hz, $^{3}J_{H4,H3}$ = 8.4 Hz, 1H, H_4), 3.33 (s, 3H, -OCH_3), 0.96-0.90 (m, 12 H, –SiCH_2CH$_3$), 0.65-0.57 (m, 8H, –SiCH_2CH$_3$), 0.14-0.09 (m, 18H, –SiCH_3). ^{13}C{^{1}H} NMR (C_6D_5Cl, 125 MHz): 100.0 (s, C_1), 75.5 (s), 74.2 (s), 72.5 (s), 71.9 (s), 61.9 (s), 54.2 (s, -OCH_3), 9.3, 9.0, 8.8, 8.4, 7.1, 7.0, 6.8, 6.7 (each a s, –SiCH_2CH$_3$, –SiCH$_2$CH_3, and –SiCH_3).

β-1-OMe-2,3,4,6-OSiMe$_2$Et-glucopyranose (11) was prepared from β-1-OMe-glucopyranose according to General Procedure A. ^{1}H NMR (CD_2Cl_2, 600 MHz): 4.05 (d, $^{3}J_{H1,H2}$ = 7.2 Hz, 1H, H_1), 3.80 (dd, $^{3}J_{H5,H6}$ = 1.8 Hz, $^{2}J_{H6,H6'}$ = 11.4 Hz, 1H, H_6), 3.70 (dd, $^{2}J_{H6,H6'}$ = 4.8 Hz, $^{3}J_{H1,H2}$ = 11.4 Hz, 1H, $H_{6'}$), 3.46 (t, $^{3}J_{H,H}$ = 8.4 Hz, 1H, H_4), 3.42 (t, $^{3}J_{H,H}$ = 8.1 Hz, 1H, H_3), 3.43 (s, 3H, –OCH_3), 3.24 (t, $^{3}J_{H,H}$ = 7.8 Hz, 1H, H_2), 0.97-0.92 (m, 12H, SiCH$_2$CH_3), 0.67-0.58 (m, 8H, SiCH_2CH$_3$), 0.14-0.09 (m, 24H, SiCH_3). ^{13}C{^{1}H} NMR (C_6D_5Cl, 125 MHz): 114.2 (s, C_1), 79.6 (s, C_3), 76.8, 76.7 (each a s, C_2 and C_5), 71.5 (s, C_4), 62.0 (s, C_6), 55.9 (s, –OCH_3), 9.4, 9.3, 9.1, 8.6, 7.3, 7.2, 6.9, -0.7, -0.8, -0.9, -1.1, -1.3, -1.4, -2.2, -2.4 (each a s, –SiCH$_2$CH_3, –SiCH_2CH$_3$, and –SiCH_3).

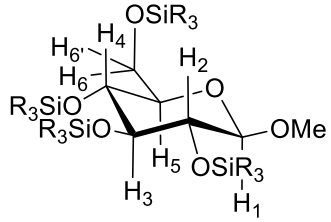

R$_3$ = Me$_2$Et

1-deoxy-2,3,4,6-OSiMe$_2$Et-glucopyranose (12) was prepared from 1-deoxy-glucopyranose according to General Procedure A. ^{1}H NMR ($CDCl_3$, 600 MHz): 3.88 (dd, $^{3}J_{H,H}$ = 11.4 Hz, 5.4 Hz, 1H), 3.79 (dd, $^{3}J_{H,H}$ = 11.4 Hz, 1.8 Hz, 1H), 3.60 (dd, $^{3}J_{H,H}$ = 11.4 Hz, 6.0 Hz, 1H), 3.51-3.47 (1H, m), 3.39-3.33 (m, 2H), 3.13-3.10 (2H, m), 0.99-0.94 (m, 12H), 0.70-0.58 (m, 8H), 0.16-0.11 (m, 18H). ^{13}C{^{1}H} NMR (C_6D_5Cl, 125 MHz): 81.8 (s, C_5), 80.9 (s, C_3), 72.4(s, C_2), 71.7 (s, C_4), 70.5 (s, C_1), 62.5 (s, C_6), 9.4, 9.1, 9.0, 8.6, 7.3, 7.3, 1.0, 6.9, -0.7, -1.2, -1.4, -1.7, -1.8, -2.2, -2.4 (each a s, –SiCH_2CH$_3$, –SiCH$_2$CH_3, and –SiCH_3).

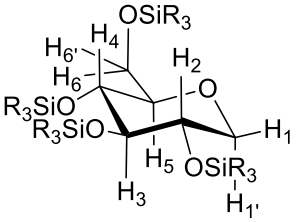

R$_3$ = Me$_2$Et

1,2,3,4,6-OSiMe$_2$Et-glucopyranose (13) was prepared from glucopyranose according to General Procedure A. NMR analysis revealed a mixture of α and β anomers. ^{1}H NMR ($CDCl_3$, 600 MHz): 4.98 (d, $^3J_{H1,H2}$ = 3.0 Hz, 1H, α-H_1), 4.44 (d, $^3J_{H1,H2}$ = 7.2 Hz, 1H, β-H_1), 3.79 (t, $^3J_{H,H}$ = 9.0 Hz, 1H), 3.77 (dd, $^3J_{H,H}$ = 10.8 Hz, 2.4 Hz, 1H), 3.72 (m, 1H), 3.64 (m, 2H), 3.59 (dd, $^3J_{H,H}$ = 10.8 Hz, 6.6 Hz, 1H), 3.40-3.34 (m, 3H), 3.31 (dd, $^3J_{H,H}$ = 9.6 Hz, 3.6 Hz, 1H), 3.23-3.19 (m, 2H), 0.95-0.90 (m, 15H, –SiCH$_2$C*H*$_3$), 0.64-0.54 (m, 10H, –SiC*H*$_2$CH$_3$), 0.14 - 0.07 (m, 30H, –SiC*H*$_3$). ^{13}C{^{1}H} NMR (C_6D_5Cl, 125 MHz): 98.4 (s, β-C_1), 94.2 (s, α-C_1), 79.1 (s, β-C_3), 78.1 (s, β-C_2), 77.2 (s, β-C_5), 74.5 (s, α-C_2), 74.3 (s, α-C_3), 73.2 (s, α-C_5), 72.0 (s, α-C_4), 71.0 (s, β-C_4), 62.3 (s, β-C_6), 62.0 (s, α-C_6), 9.4-8.2, 7.2-6.6, (-0.9) - (-2.8) (–Si*C*H$_2$CH$_3$, –SiCH$_2$*C*H$_3$, and –Si*C*H$_3$).

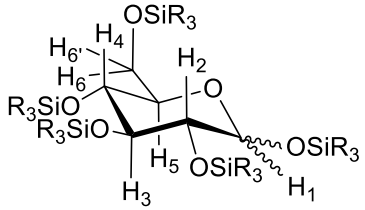

R$_3$ = Me$_2$Et

1,2,3,4,5,6-OSiMe$_2$Et-glucitol (14) was prepared from glucitol according to General Procedure A. ^{1}H NMR (CD_2Cl_2, 600 MHz): 3.92 (dt, *J* = 2.4, *J* = 8.4 Hz), 3.81-3.74 (m, 4H), 3.61-3.60 (m, 1H), 3.52-3.47 (m, 2H), 0.97-0.95 (m, 18H, SiCH$_2$C*H*$_3$), 0.66-0.56 (m, 12H, SiC*H*$_2$CH$_3$), 0.12-0.10 (m, 36H, SiC*H*$_3$). ^{13}C{^{1}H} NMR (C_6D_5Cl, 125 MHz): 77.1, 77.0, 76.1, 74.9, 64.3, 64.0 (each a s, carbohydrate backbone), 9.18, 9.11, 9.08, 8.97, 8.16, 7.13, 7.10, 7.07, 6.98, 6.91, 6.87 (each a s, –SiCH$_2$*C*H$_3$, –Si*C*H$_2$CH$_3$, and –Si*C*H$_3$).

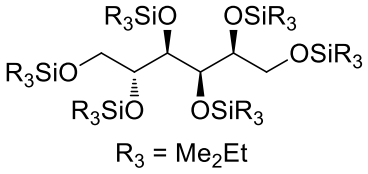

R$_3$ = Me$_2$Et

1,2,3-OSiMe$_2$Et-hexanetriol was prepared from 1,2,3-hexanetriol according to General Procedure A. ^{1}H NMR (CD_2Cl_2, 600 MHz): 3.66-3.62 (m, 2H), 3.57-3.55 (m, 1H), 3.48-3.45 (m, 1H), 1.47-1.39 (m, 3H), 1.30-1.25 (m, 1H), 0.96-0.89 (m, 12H), 0.60-0.55 (m, 6H), 0.09-0.07 (m, 18H) ^{13}C{^{1}H} NMR (CD_2Cl_2,

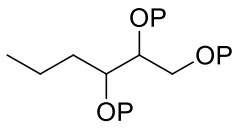

P = SiMe$_2$Et

125 MHz): 77.1, 74.1, 64.2, 35.2, 18.9, 14.1 (each a s, hexane backbone), 8.8, 8.7, 7.9, 6.7, 6.6, -2.1, -2.2, -3.1 (each a s, –SiCH$_2$*C*H$_3$, –Si*C*H$_2$CH$_3$, and –Si*C*H$_3$).

Single reduction of α-1-OMe-2,3,4,6-OSiMe$_2$Et-glucopyranose (10):

In an argon-filled glovebox, a 1-dram vial was charged with 52 mg (0.097 mmol) α-1-OMe-2,3,4,6-OSiMe$_2$Et-glucopyranose (**10**), 14 μL (0.11 mmol) dimethylethylsilane, 1.2 mg (9.0×10^{-4} mmol) catalyst **9**, 5.0 mg (0.031 mmol) hexamethylbenzene, and 300 μL of C_6D_5Cl. Proton and carbon NMR spectra showed nearly quantitative conversion to 1-deoxy-2,3,4,6-OSiMe$_2$Et-glucopyranose (**12**) within 20 minutes of mixing and no further changes thereafter. An in situ yield determination showed 0.095 mmol (98%) **12**.

Single reduction of β-1-OMe-2,3,4,6-OSiMe$_2$Et-glucopyranose (11):

In an argon-filled glovebox, a 1-dram vial was charged with 52 mg (0.097 mmol) β-1-OMe-2,3,4,6-OSiMe$_2$Et-glucopyranose **11**), 14 μL (0.11 mmol) dimethylethylsilane, 1.2 mg (9.0×10^{-4} mmol) catalyst **9**, 5.0 mg (0.031 mmol) hexamethylbenzene, and 300 μL of C_6D_5Cl. Proton and carbon NMR spectra showed nearly quantitative conversion to 1-deoxy-2,3,4,6-OSiMe$_2$Et-glucopyranose (**12**) within 20 minutes of mixing and no further changes thereafter. An in situ yield determination showed 0.092 mmol (95%) **12**.

α vs. β competition experiment between 1-OMe glucoses 10 and 11:

In an argon-filled glovebox, a 1-dram vial was charged with 30 mg (0.056 mmol) each of α- and β-1-OMe-2,3,4,6-OSiMe$_2$Et-glucopyranose (**10** and **11**), 2.3 mg (0.015 mmol) hexamethylbenzene, 300 μL C_6D_5Cl, 1.2 mg catalyst **9** (9.0×10^{-4} mmol), and 8 μL (0.062 mmol)

Me_2EtSiH. A standard proton-decoupled ^{13}C NMR spectrum was acquired within 20 minutes of mixing, showing complete consumption of **3** to yield a mixture of unreacted **10** and 1-deoxy-2,3,4,6-$OSiMe_2Et$-glucopyranose (**12**), which indicated that the β anomer **12** is more reactive than the α anomer **10**.

Reduction of 1,2,3,4,6-$OSiMe_2Et$-glucopyranose (13) with dimethylethylsilane:

In an argon-filled glovebox, a 1-dram vial was charged with 50.4 mg (0.082 mmol) 1,2,3,4,6-$OSiMe_2Et$-glucopyranose (**13**), 109 μL (0.82 mmol) dimethylethylsilane, 3.0 mg (2.3×10^{-3} mmol) catalyst **9**, and 300 μL of C_6D_5Cl. NMR spectra were recorded periodically using standard proton-decoupled ^{13}C experiments, which showed conversion to a complex mixture of products including 1-deoxy-2,3,4,6-$OSiMe_2Et$-glucopyranose (**12**) and 1,2,3,4,5,6-$OSiMe_2Et$-glucitol (**14**) after 12 hours.

Reduction of 1,2,3,4,6-$OSiMe_2Et$-glucopyranose 13) with diethylsilane:

In an argon-filled glovebox, a 1-dram vial was charged with 104 mg (0.17 mmol) 1,2,3,4,6-$OSiMe_2Et$-glucopyranose (**13**), 22 μL (0.17 mmol) diethylsilane, 1.2 mg (9.0×10^{-4} mmol) catalyst **9**, 5.0 mg (0.031 mmol) hexamethylbenzene, and 350 μL of C_6D_5Cl. NMR spectra were recorded periodically using standard proton-decoupled ^{13}C experiments, which showed conversion to a mixture of products including 1-deoxy-2,3,4,6-$OSiMe_2Et$-glucopyranose (**12**) and 1,2,3,4,6-$OSiMe_2Et$-glucitol (**14**). After 12 hours of reaction, a spectrum was acquired using the 90° pulse procedure. At this time, the approximate in situ yields (by (90° $^{13}C\{^1H\}$ NMR) were 0.026 mmol (15%) **12** and 0.034 mmol (20%) **14.** Multiple other products were observed.).

α vs. β competition experiment between per-silylated glucoses α-$^{13}C_1$-13 and β-$^{13}C_1$-13:

In an argon-filled glovebox, a 1-dram vial was charged with 53 mg (0.087 mmol) of an α/β mixture of $^{13}C_1$-1,2,3,4,6-OSiMe$_2$Et-glucopyranose (**$^{13}C_1$-13**), 5.3 mg (0.03 mmol) hexamethylbenzene, 350 μL C_6D_5Cl, and 14 μL (0.24 mmol) Me_2EtSiH. A ^{1}H NMR spectrum was acquired, indicating a 1.0:1.4 α/β ratio of starting material. The sample was returned to the glovebox and transferred into a vial that had been charged with 1.0 mg (7.5×10^{-4} mmol) catalyst **9**, resulting in dissolution of **9**. The reaction mixture was transferred back into the NMR tube. A ^{1}H NMR spectrum acquired 10 minutes after addition of catalyst **9** revealed that the concentration of β anomer was less than α-anomer, indicating that the β anomer is more reactive than the α anomer. After 75 minutes, the concentration of β anomer had decreased even further relative to α anomer (Figure 3.4).

Reduction of α-1-OMe-2,3,4,6-OSiMe$_2$Et-glucopyranose (10) to hexanes:

According to General Procedure B, α-1-OMe-2,3,4,6-OSiMe$_2$Et-glucopyranose (**10**) (49 mg, 0.091 mmol) was treated with 250 μL (1.9 mmol) diethylsilane and 6.1 mg (4.6×10^{-3} mmol) catalyst **9**. 200 μL of 0.051 M hexamethylbenzene in C_6D_5Cl was included in the reaction mixture, along with an additional 100 μL of C_6D_5Cl. NMR spectra were recorded periodically using standard proton-decoupled ^{13}C experiments (Figure 3.5), and after two weeks, a spectrum was acquired using the 90° pulse procedure. This reaction was repeated three times, and the in situ (by 90° $^{13}C\{^1H\}$ NMR) product yields were averaged to give 0.016 mmol (18%) *n*-hexane, 0.028 mmol (31%) 2-methylpentane, and 0.026 mmol (29%) 3-methylpentane (Figure 3.6). In addition, spiking the reaction mixture with authentic samples confirmed the presence of *n*-hexane, 2-methylpentane, and 3-methylpentane.

Reduction of 1,2,3,4,6-OSiMe$_2$Et-glucopyranose (13) to hexanes:

According to General Procedure B, 1,2,3,4,6-OSiMe$_2$Et-glucopyranose (**5**) (56 mg, 0.092 mmol) was treated with 250 μL (1.9 mmol) diethylsilane and 6.6 mg (5.0×10^{-3} mmol) catalyst **9**. 200 μL of 0.051 M hexamethylbenzene in C_6D_5Cl was included in the reaction mixture, along with an additional 100 μL of C_6D_5Cl. NMR spectra were recorded periodically using standard proton-decoupled ^{13}C experiments (Figure 3.7), and after two weeks, a spectrum was acquired using the 90° pulse procedure. This reaction was repeated three times, and the in situ product yields (by 90° $^{13}C\{^1H\}$ NMR) were averaged to give 0.032 mmol (35%) *n*-hexane, 0.012 mmol (13%) 2-methylpentane, and 0.0092 mmol (10%) 3-methylpentane (Figure 3.8). Comparison to the $^{13}C\{^1H\}$ spectrum of reduced α-1-OMe-2,3,4,6-glucopyranose (**10**) revealed that the mixture of hexane isomers given by 1,2,3,4,6-OSiMe$_2$Et-glucopyranose contained a greater proportion of *n*-hexane (Figure 3.9).

Reduction of α-1-OMe-2,3,4,6-OSiMe$_2$Et-glucopyranose (10) showing an intermediate:

According to General Procedure B, α-1-OMe-2,3,4,6-OSiMe$_2$Et-glucopyranose (**10**) (49 mg,0.091 mmol) was treated with 247 μL (1.9 mmol) dimethylethylsilane and 6.1 mg (4.6×10^{-3} mmol) catalyst **9**. 5 μL of 0.20 M hexamethylbenzene in C_6D_5Cl was included in the reaction mixture, along with an additional 200 μL of C_6D_5Cl. The reaction mixture was heated to 50 °C and NMR spectra were taken periodically, revealing after two weeks a reaction intermediate that has been ascribed to 1,2,3-OSiMe$_2$Et-hexanetriol. One peak in the GC-MS trace of the sample matched authentic sample of this compound with a retention time of 7.96 min and a matching MS pattern.

Reduction of $^{13}C_1$-1,2,3,4,6-OSiMe$_2$Et-glucopyranose ($^{13}C_1$-13):

According to General Procedure B, $^{13}C_1$-1,2,3,4,6-OSiMe$_2$Et-glucopyranose (**$^{13}C_1$-5**) (50 mg, 0.082 mmol) was treated with 240 μL (1.9 mmol) diethylsilane and 6.0 mg (4.6×10^{-3} mmol) catalyst **9**. 5.3 mg (0.033 mmol) hexamethylbenzene was included in the reaction mixture, along with 200 μL of C_6D_5Cl. NMR spectra were recorded periodically using standard proton-decoupled ^{13}C experiments (Figure 3.10). After 3 weeks, the reaction mixture was spiked with authentic hexane isomers, confirming the presence of *n*-hexane, 2-methylpentane, 3-methylpentane, and 2,3-dimethylbutane.

Reduction of $^{13}C_6$-1,2,3,4,6-OSiMe$_2$Et-glucopyranose ($^{13}C_6$**-13)**:

According to General Procedure B, $^{13}C_6$-1,2,3,4,6-OSiMe$_2$Et-glucopyranose (**$^{13}C_6$-13**) (50 mg, 0.082 mmol) was treated with 240 μL (1.9 mmol) diethylsilane and 6.0 mg (4.6×10^{-3} mmol) catalyst **9**. 50 μL of 0.12 M hexamethylbenzene in C_6D_5Cl was included in the reaction mixture, along with an additional 250 μL of C_6D_5Cl. NMR spectra were recorded periodically using standard proton-decoupled ^{13}C experiments (Figure 3.11). A peak matching the chemical shift of the C_1 peak of 1-hexene (114 ppm) was observed after 30 min; this peak persisted for at least 18 h but was absent after three days. The spectra of fully reduced **$^{13}C_1$-13**, **$^{13}C_6$-13**, and unlabeled **13** were compared (Figure 3.12) and the signal intensity for the terminal carbons of hexane isomers was found to be enhanced by C_1 and C_6 labeling.

Reduction of β-1-OMe-2,3,4,6-OSiMe$_2$Et-glucopyranose (11) to hexanes:

According to General Procedure B, β-1-OMe-2,3,4,6- OSiMe$_2$Et-glucopyranose (**11**) (55 mg, 0.10 mmol) was treated with 240 μL (1.9 mmol) diethylsilane and 6.2 mg (4.7×10^{-3} mmol) catalyst **9**. 2 mg hexamethylbenzene was included in the reaction mixture, along with 250 μL of C_6D_5Cl.

NMR spectra were recorded periodically using standard proton-decoupled ^{13}C experiments. Comparison to the $^{13}C\{^{1}H\}$ spectrum of reduced α-1-OMe-2,3,4,6-glucopyranose (**10**) revealed that the α and β anomers give similar distributions of hexane isomers (Figure 3.13).

Reduction of 1-deoxy-2,3,4,6-OSiMe$_2$Et-glucopyranose (12) to hexanes:

According to General Procedure B, 1-deoxy-2,3,4,6- OSiMe$_2$Et-glucopyranose (**12**) (50 mg, 0.098 mmol) was treated with 240 μL (1.9 mmol) diethylsilane and 6.2 mg (4.7×10^{-3} mmol) catalyst **9**. 170 μL of 0.063 M hexamethylbenzene in C_6D_5Cl was included, along with an additional 100 μL of C_6D_5Cl. NMR spectra were recorded periodically using standard proton-decoupled ^{13}C experiments, and after two weeks, a spectrum was acquired using the 90° pulse procedure. The in situ product yields (by 90° $^{13}C\{^{1}H\}$ NMR) were 0.016 mmol (17%) *n*-hexane, 0.030 mmol (31%) 2-methylpentane, and 0.032 mmol (32%) 3-methylpentane. Comparison to the $^{13}C\{^{1}H\}$ spectrum of reduced α-1-OMe-2,3,4,6-glucopyranose (**10**) revealed that reductions of these two starting materials give similar distributions of hexane isomers (Figure 3.14).

Reduction of 1,2,3,4,6-OSiMe$_2$Et-glucitol (14) to hexanes:

According to General Procedure B, α-1-OMe-2,3,4,6-glucopyranose (**14**) (64 mg, 0.92 mmol) was treated with 240 μL (1.9 mmol) diethylsilane and 6.2 mg (4.7×10^{-3} mmol) catalyst **9**. 170 μL of a 0.063 M hexamethylbenzene in C_6D_5Cl was included, along with an additional 100 μL of C_6D_5Cl. NMR spectra were recorded periodically using standard proton-decoupled ^{13}C experiments after two weeks, a spectrum was acquired using the 90° pulse procedure. The in situ product yields (by 90° $^{13}C\{^{1}H\}$ NMR) were 0.041 mmol (45%) *n*-hexane, 0.0072 mmol (8%) 2-methylpentane, and 0.0055 mmol (6%) 3-methylpentane. Comparison to the $^{13}C\{^{1}H\}$ spectrum of reduced 1,2,3,4,6-

OSiMe$_2$Et-glucopyranose (**13**) revealed that the mixture of hexane isomers given by 1,2,3,4,6-OSiMe$_2$Et-glucitol contained a greater proportion of *n*-hexane (Figure 3.15).

Reduction of unprotected glucose to hexanes:

In an argon-filled glovebox, a 20 mL scintillation vial was charged with 17 mg (0.094 mmol) unprotected glucose, 6.0 mg (4.5×10^{-3} mmol mmol) [(POCOP)IrH(acetone)]$^+$[B(C$_6$F$_5$)$_4$]$^-$ catalyst (**9**) and 1.5 mg (9.2×10^{-3} mmol) hexamethylbenzene standard. 300 µL C$_6$H$_5$Cl was added, followed by 375 µL (2.9 mmol) Et$_2$SiH$_2$. The vial was capped, and the reaction was stirred at room temperature in the glovebox for two days. After the reaction mixture was transferred to an NMR tube, a ^{13}C NMR spectrum was acquired that showed full consumption of starting material and generation of hexane isomers (Figure 3.16).

Unsuccessful reduction with 0.1 mol% B(C$_6$F$_5$)$_3$ loading:

In an argon-filled glovebox, a stock solution of B(C$_6$F$_5$)$_3$ in C$_6$H$_5$Cl was prepared by serial dilution: 11 mg (0.021 mmol) B(C$_6$F$_5$)$_3$ was diluted in 4 mL C$_6$H$_5$Cl, and 0.5 mL of this solution was diluted to a volume of 5 mL C$_6$H$_5$Cl for a final concentration of 5.2×10^{-4} M. 0.2 mL of this solution (0.0011 mmol B(C$_6$F$_5$)$_3$) was used to dissolve 51 mg (0.094 mmol) α-1-OMe-2,3,4,6-OSiMe$_2$Et-glucopyranose (**10**), to give a B(C$_6$F$_5$)$_3$ loading of 0.1 mol%. 0.270 mL (2.1 mmol) Et$_2$SiH$_2$ was added, and the reaction mixture was transferred to an NMR tube. The reaction was monitored by ^{13}C{^{1}H} NMR, and no consumption of starting material was observed.

Screening iridium salts for hydrosilylative reduction of carbohydrates

In an argon-filled glovebox, a 1-dram vial was charged with 5 mol% of an iridium complex. The

silyl-protected carbohydrate (1 eq.) was massed into the same vial. Enough C_6D_5Cl was added to ensure a total volume of 500 µL after addition of the standard solution and silane. A standard solution of hexamethylbenzene in C_6D_5Cl was added, followed by the silane $SiEt_2H_2$ (20 eq). The reaction mixture was then transferred to a J-Young tube or a septum capped NMR tube. Samples were periodically removed from the glovebox for carbon NMR monitoring using a standard proton-decoupled experiment. Each sample showed no measurable activity after at least 3 days of monitoring. The protocol was repeated with 5 mol% of lithium tetrakis(pentafluorophenyl)borate ethyl etherate with each iridium salt, which also yielded no detectable activity. The complexes screened by this protocol included: chlorobis(cyclooctene)iridium(I)dimer ($[Ir(COE)Cl]_2$), chloro(1,5-cyclooctadiene)iridium(I) dimer ($[Ir(COD)Cl]_2$), trans-chlorocarbonylbis(triphenylphosphine)iridium(I) (Vaska's complex), and trans-chlorocarbonylbis(trimethylphosphine)iridium(I) (PMe_3 Vaska's complex).

O_3 species:

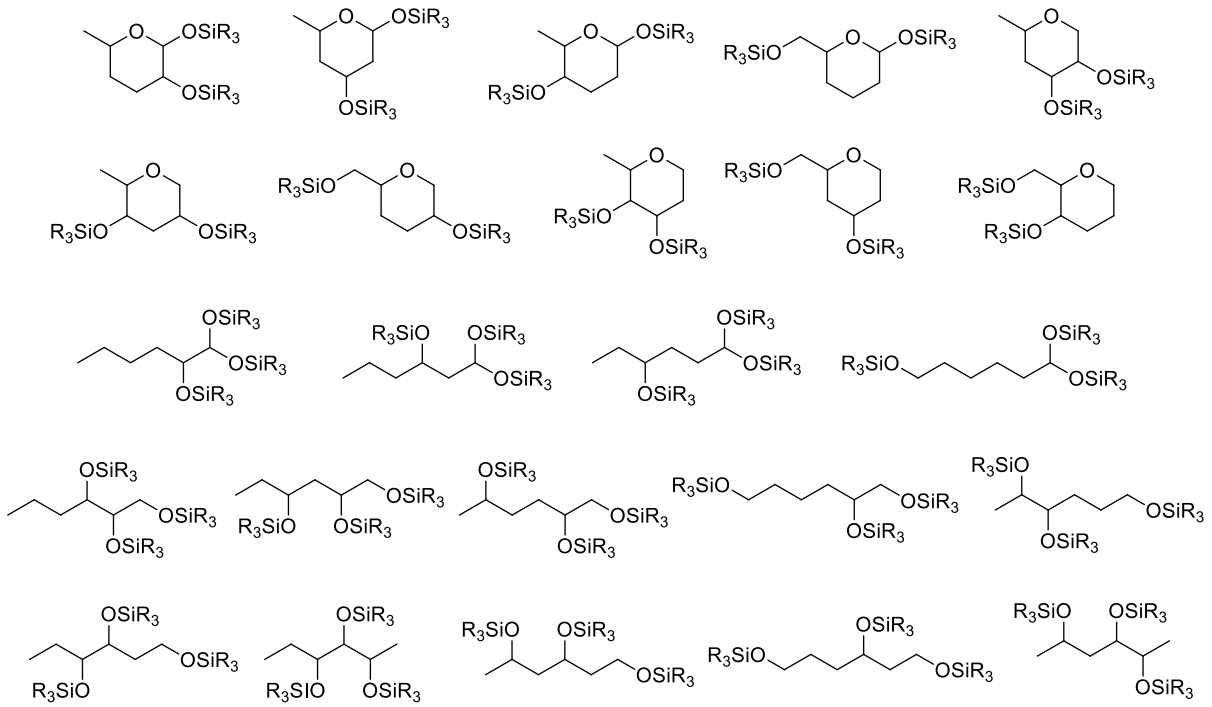

O_2 species:

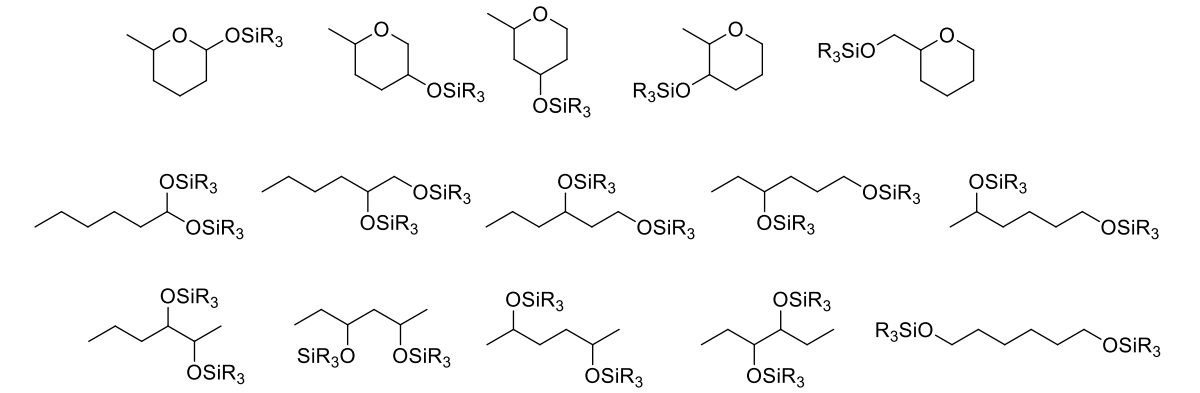

O_1 species:

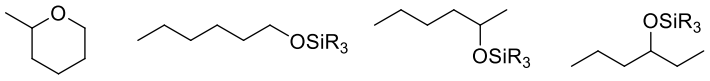

Scheme 3.4: Isomers of potential partially deoxygenated species (i.e. potential reaction intermediates)

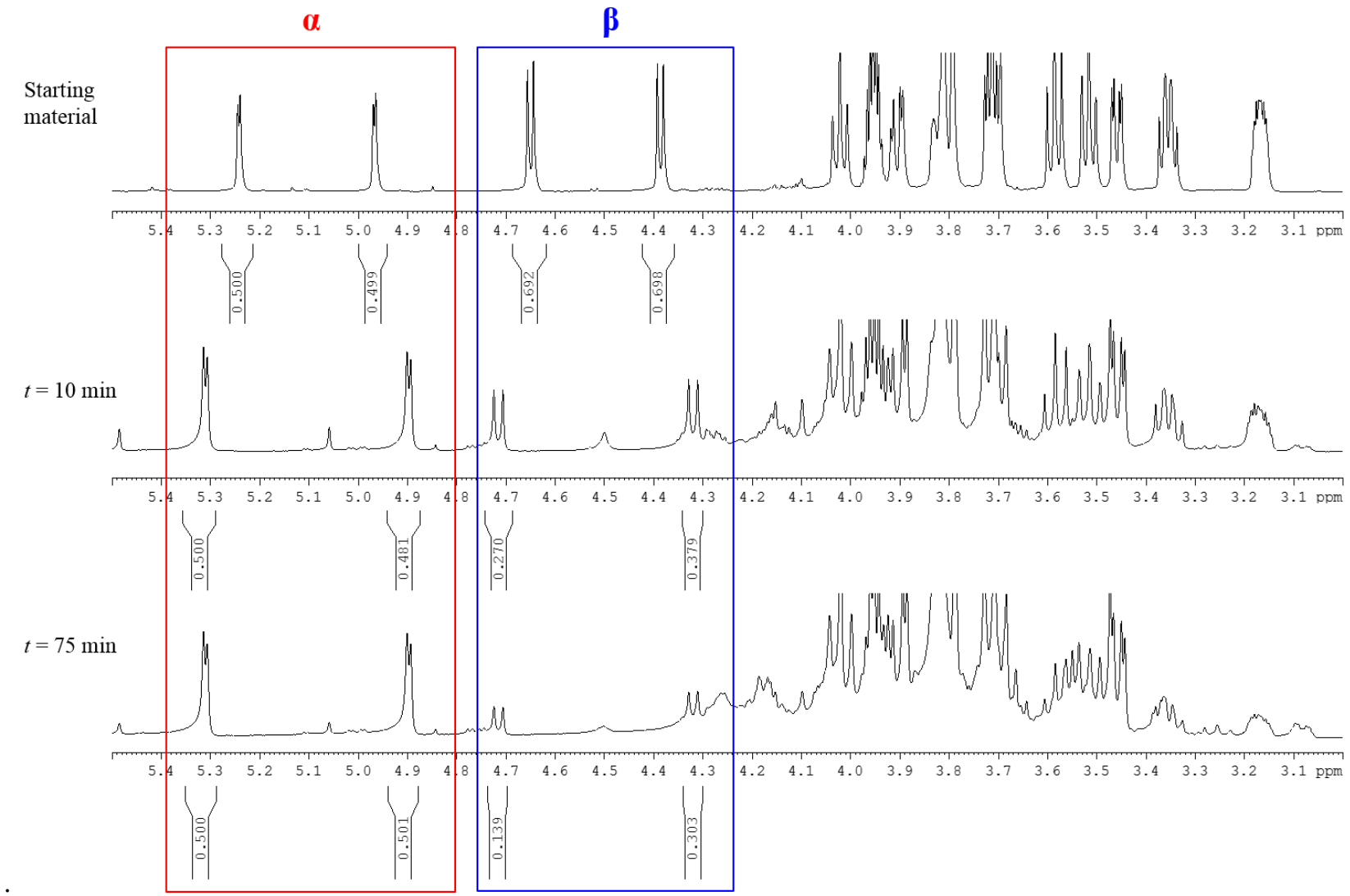

Figure 3.4: α vs. β competition experiment with C_1-labeled per-silylated glucose $^{13}C_1$-13.

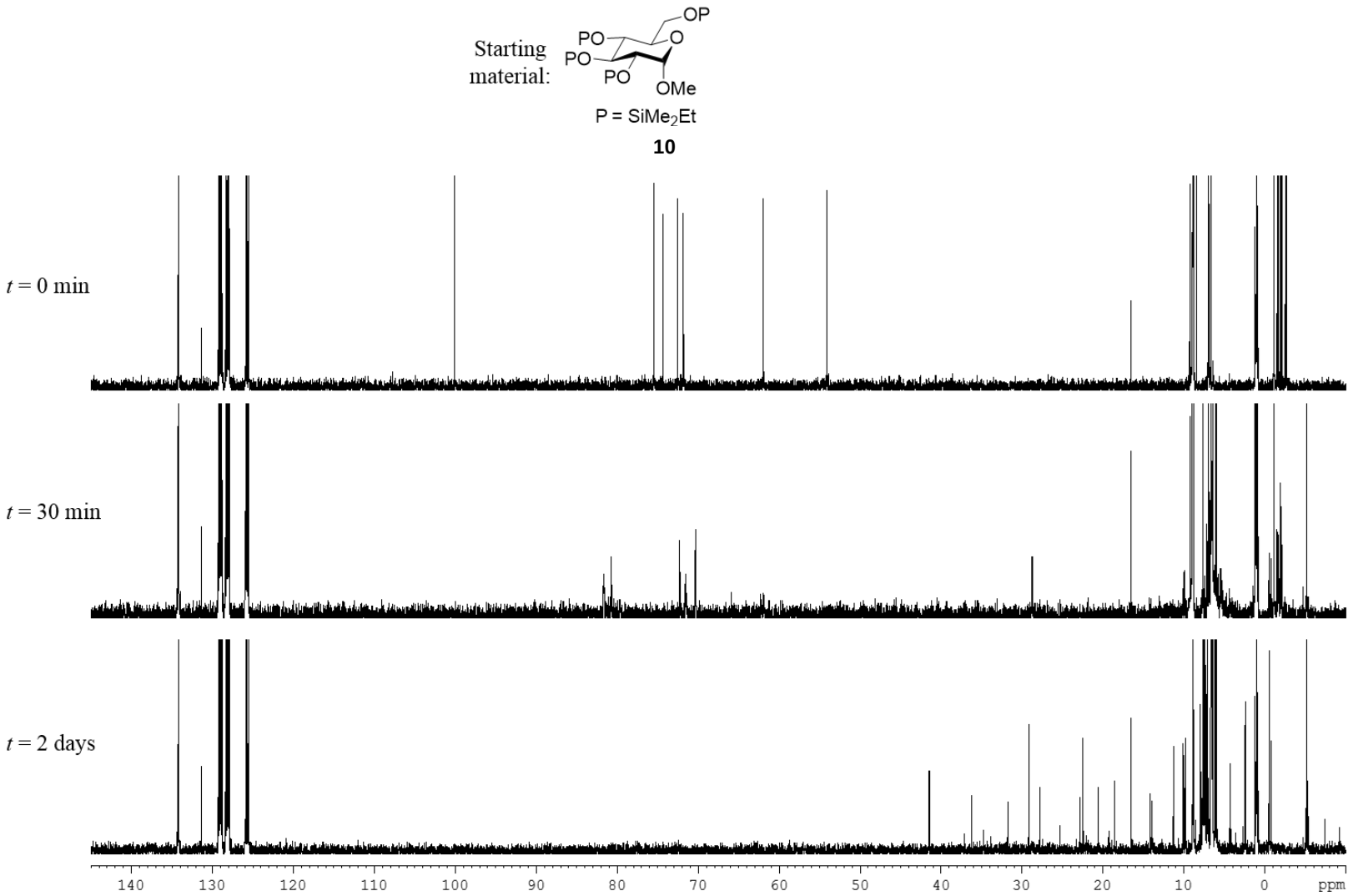

Figure 3.5: Convergence of material to hexane isomers in the reduction of 10 (standard $^{13}C\{^{1}H\}$ spectra).

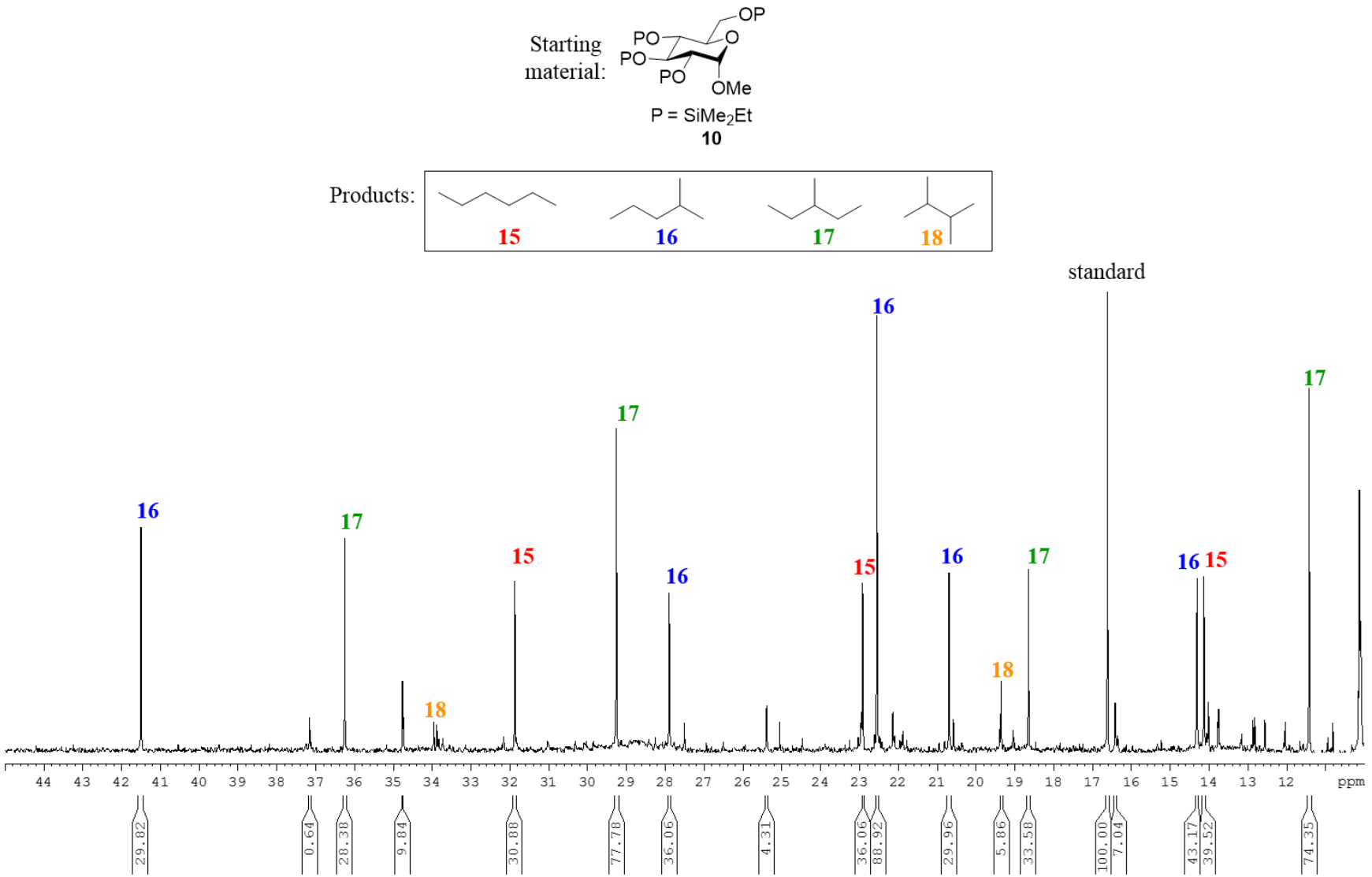

Figure 3.6. Hexane isomers resulting from reduction of methyl glucoside.

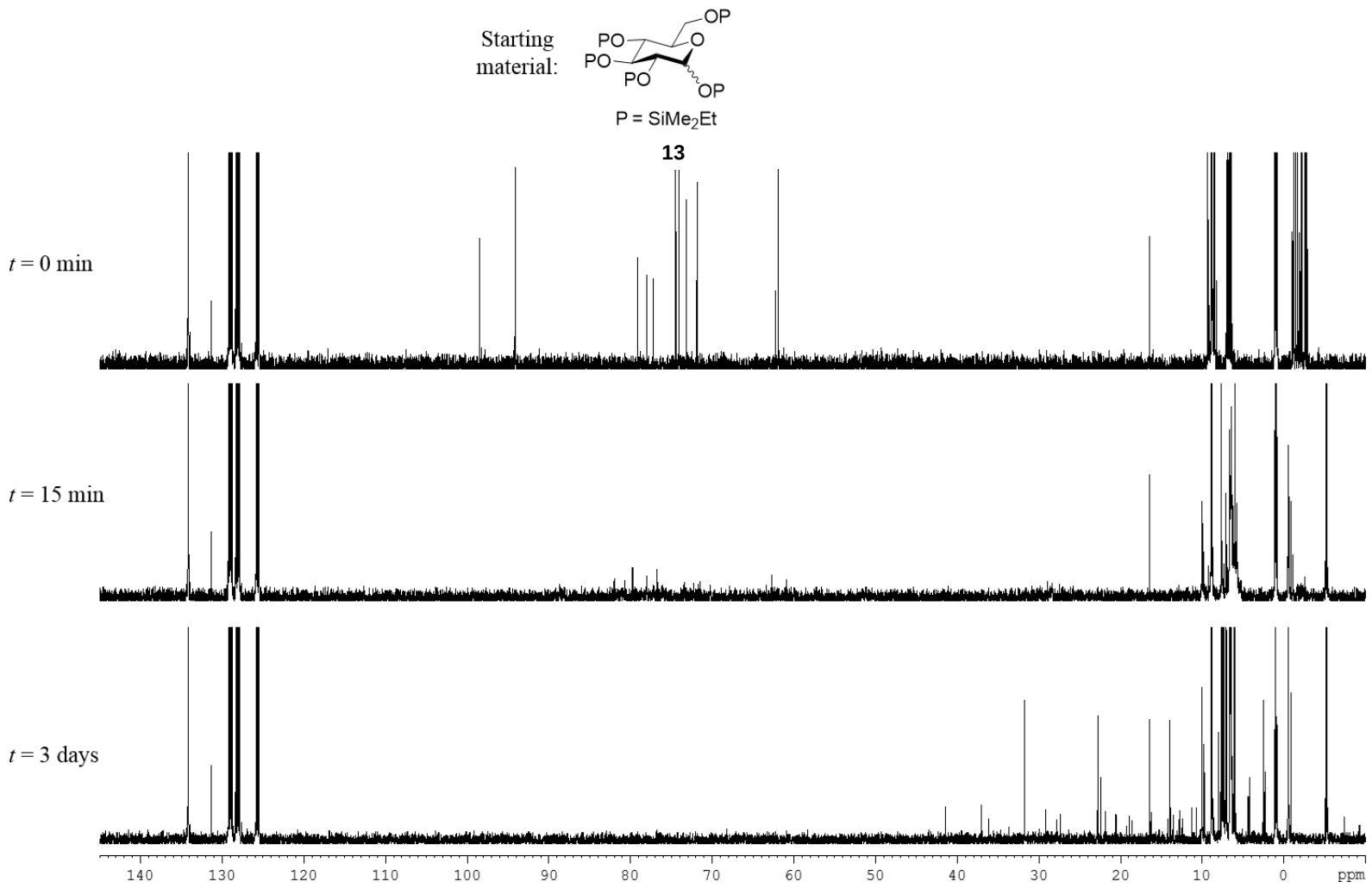

Figure 3.7: Convergence of material to hexane isomers in the reduction of 13 (standard $^{13}C\{^{1}H\}$ spectra).

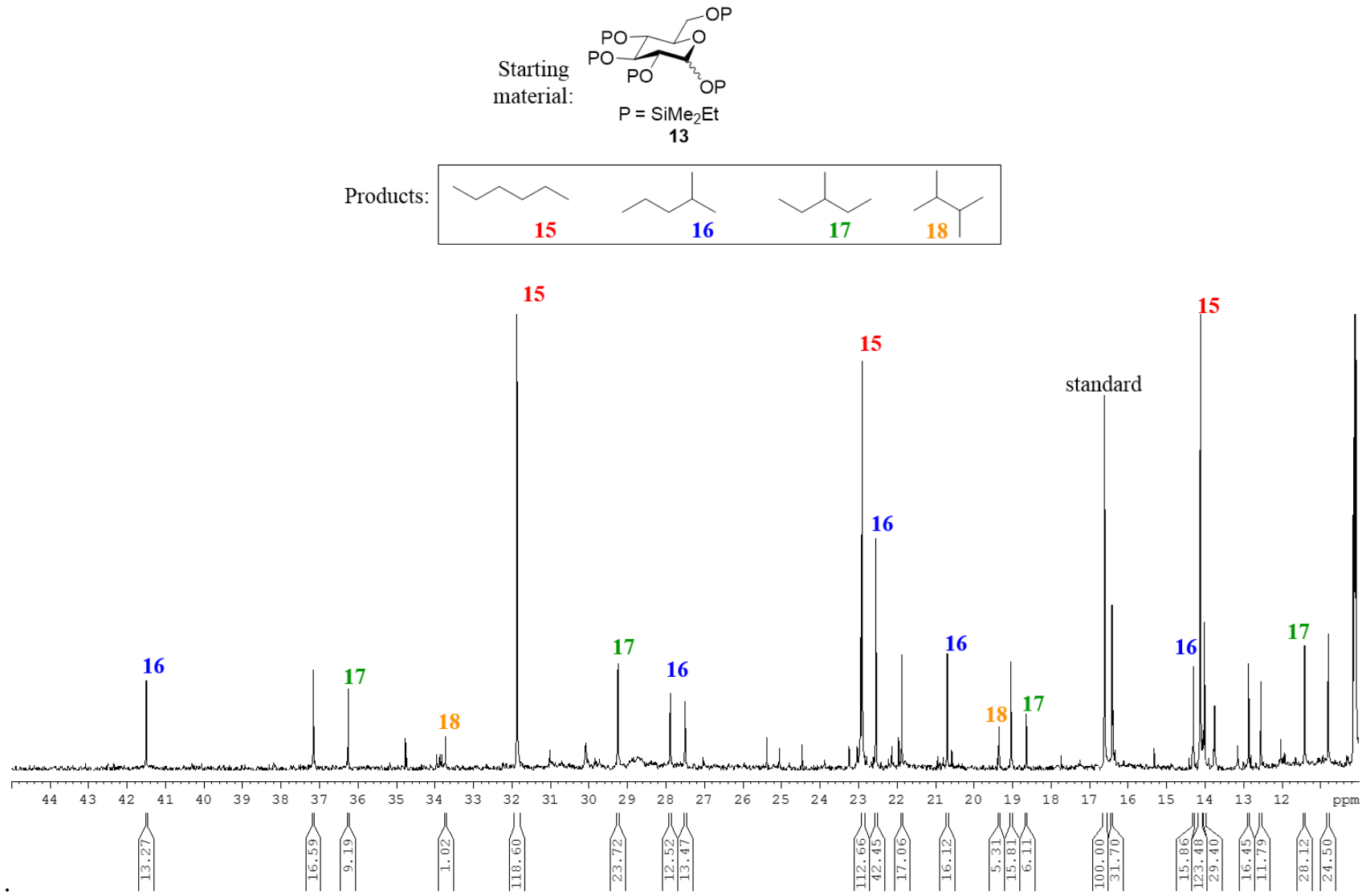

Figure 3.8: Hexane isomer distribution from reduction of 13 (90° pulse spectrum).

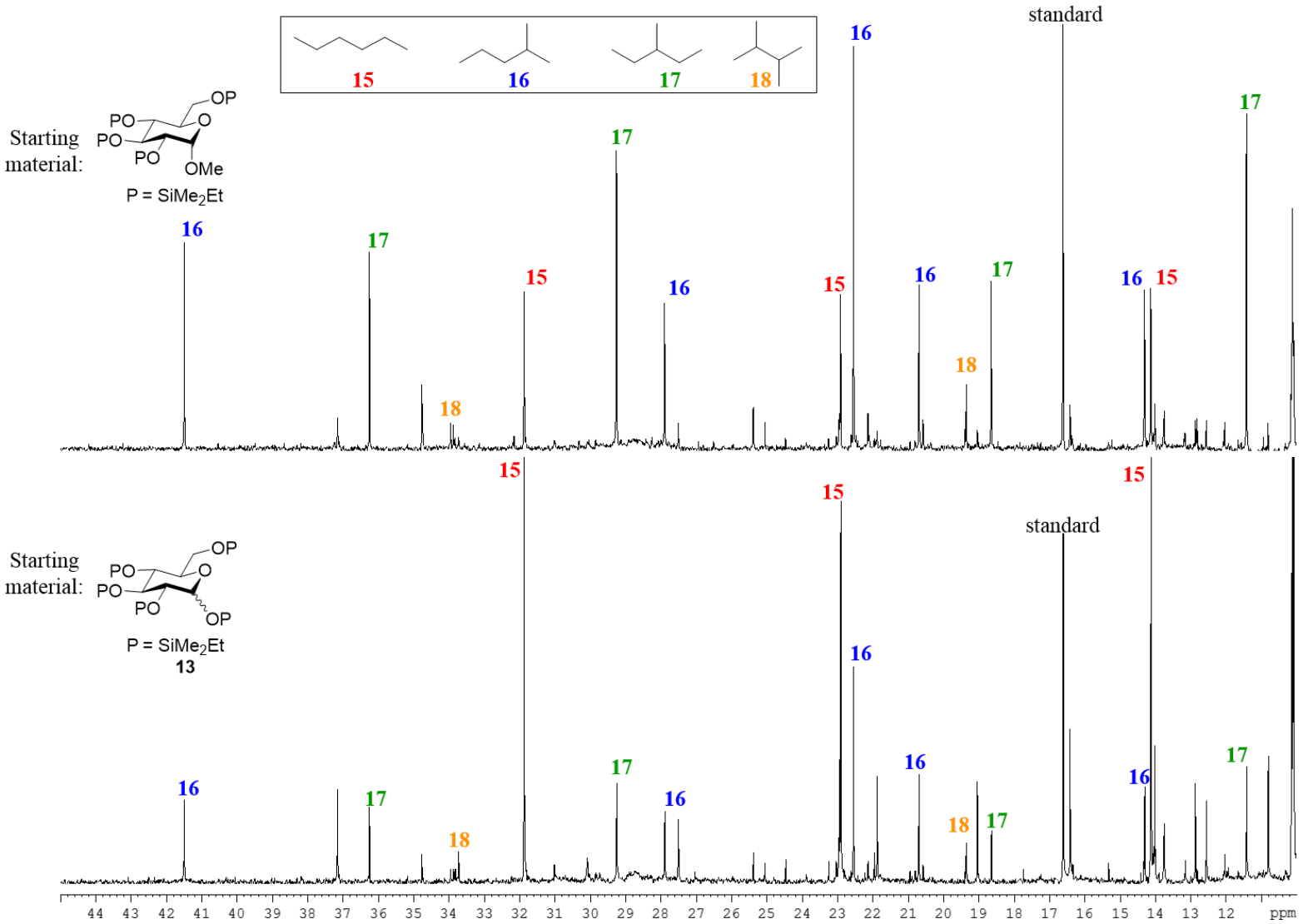

Figure 3.9: Different hexane isomer distributions from the reductions of 10 **and** 13 **(90° pulse spectra).**

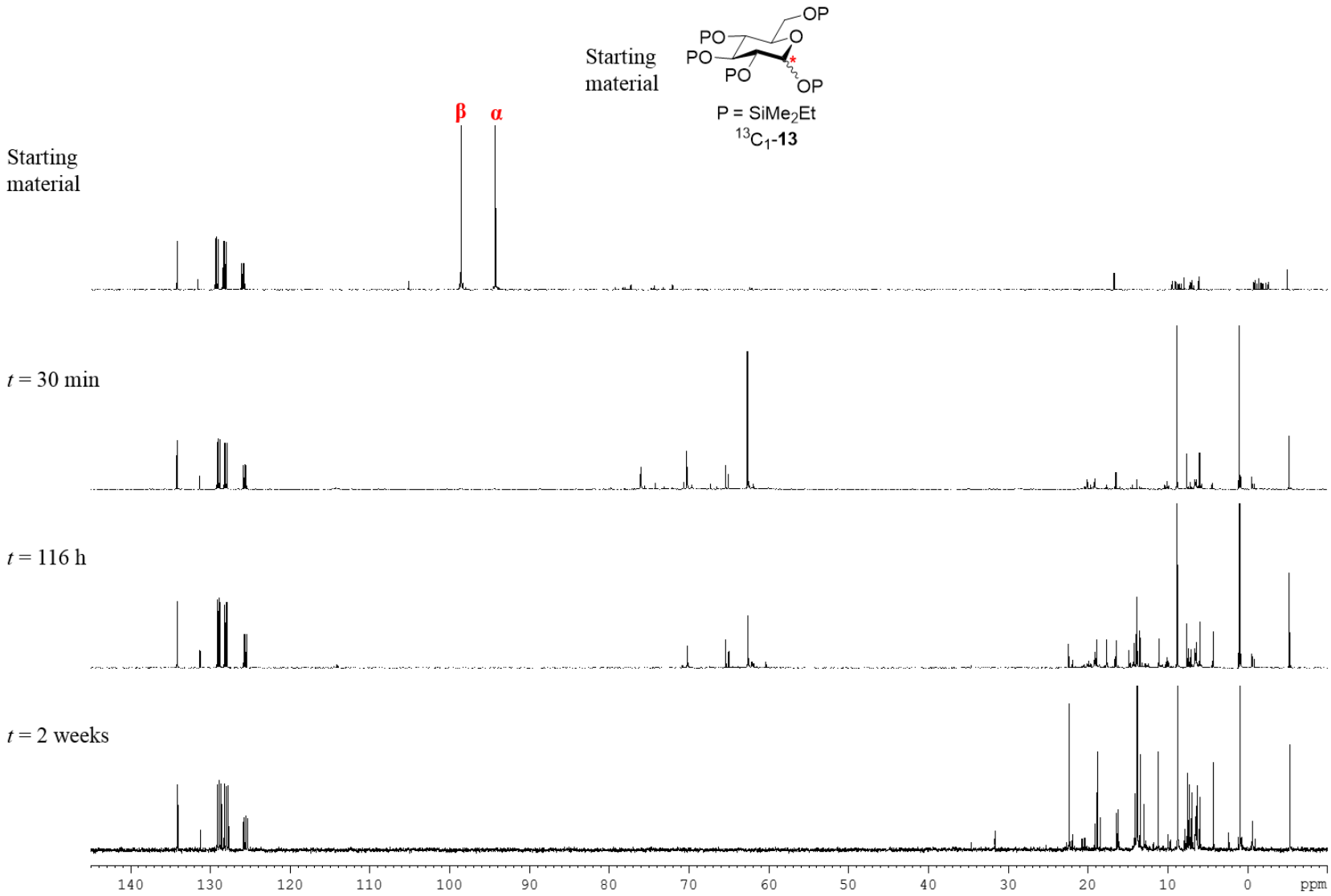

Figure 3.10: Convergence of material to hexane isomers in the reduction of $^{13}C_1$-13 (standard $^{13}C\{^1H\}$ spectra).

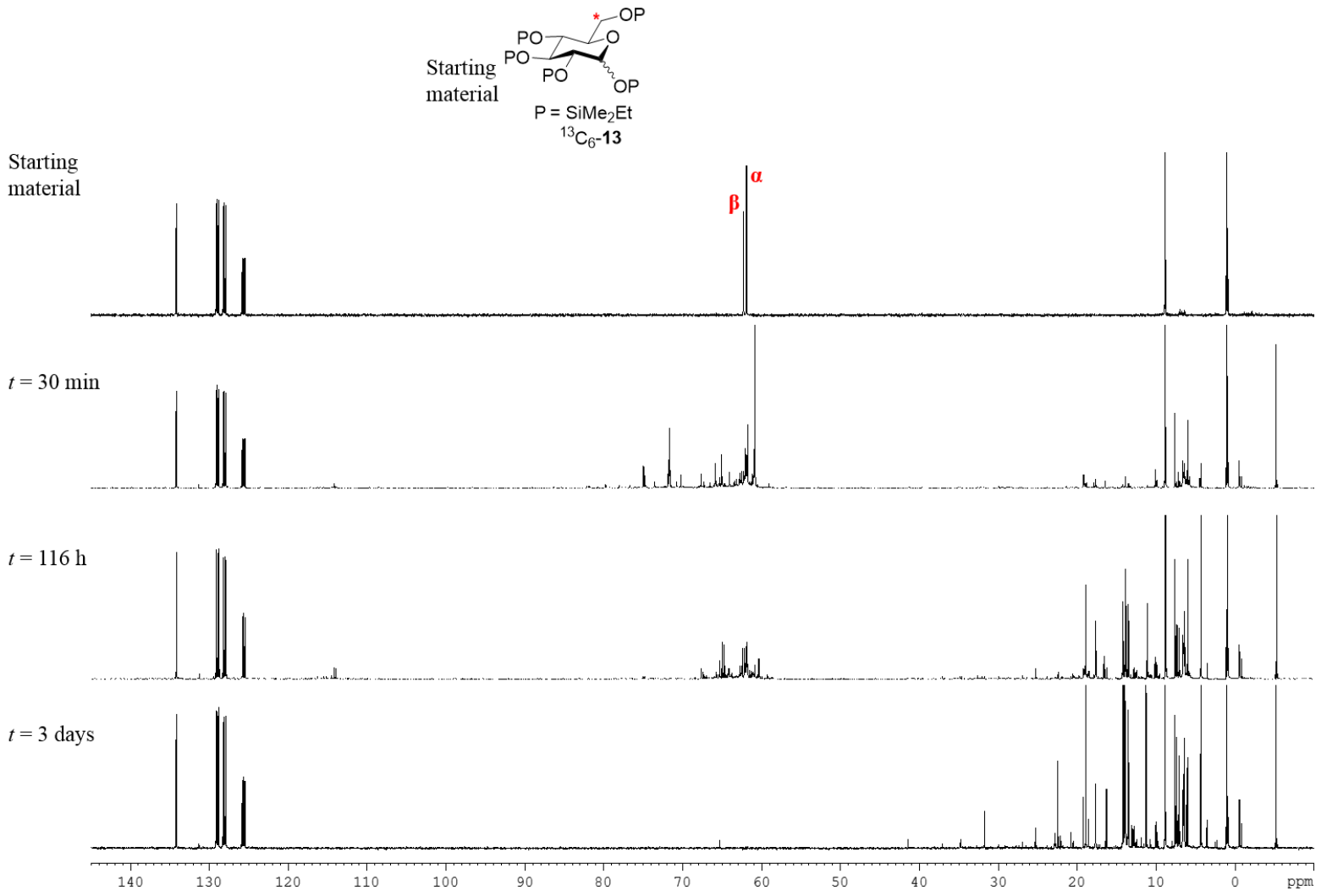

Figure 3.11: Convergence of material to hexane isomers in the reduction of $^{13}C_6$-13 (standard $^{13}C\{^1H\}$ spectra).

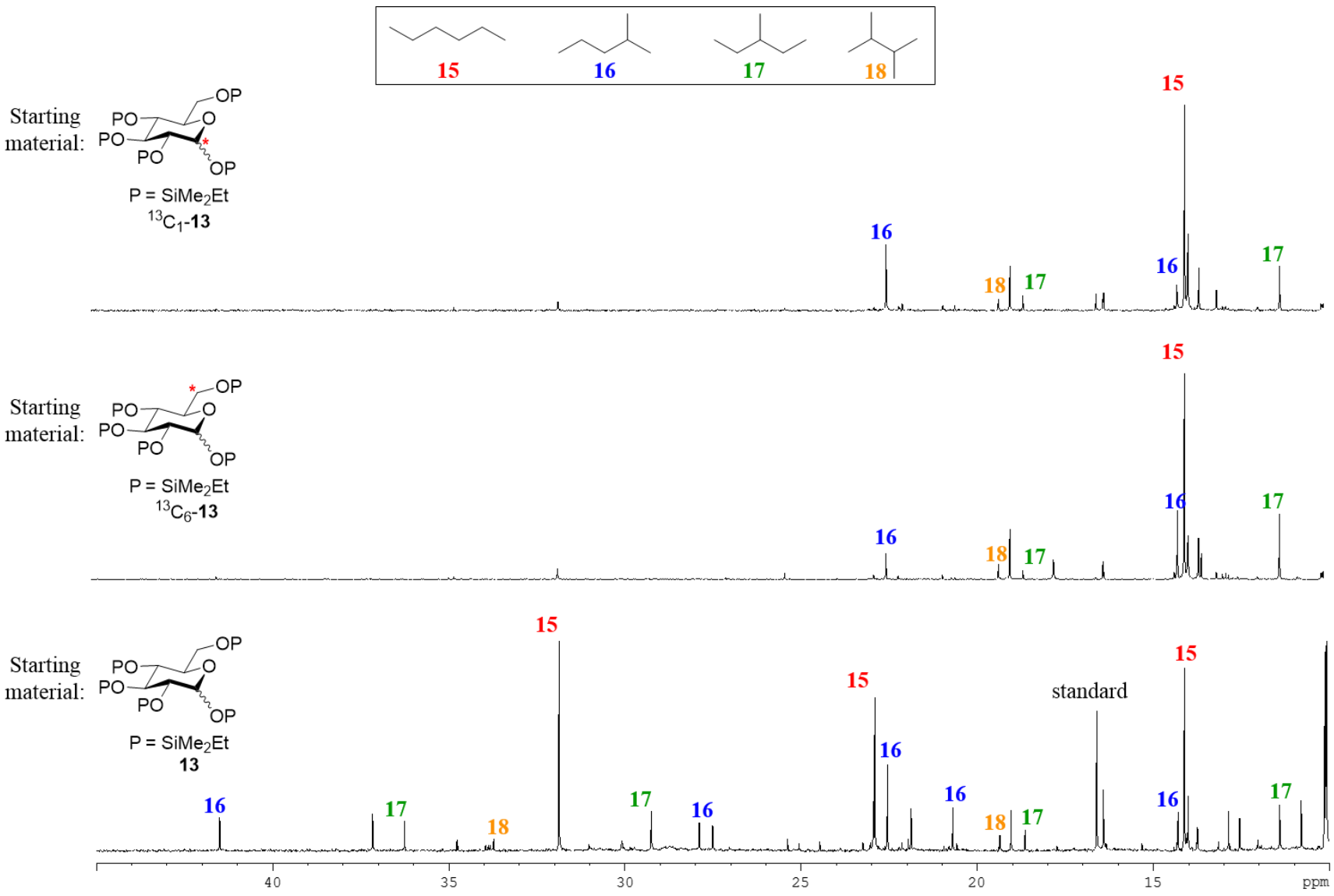

Figure 3.12: Comparison of products resulting from the reductions of $^{13}C_1$-13, $^{13}C_6$-13, and unlabeled 13.

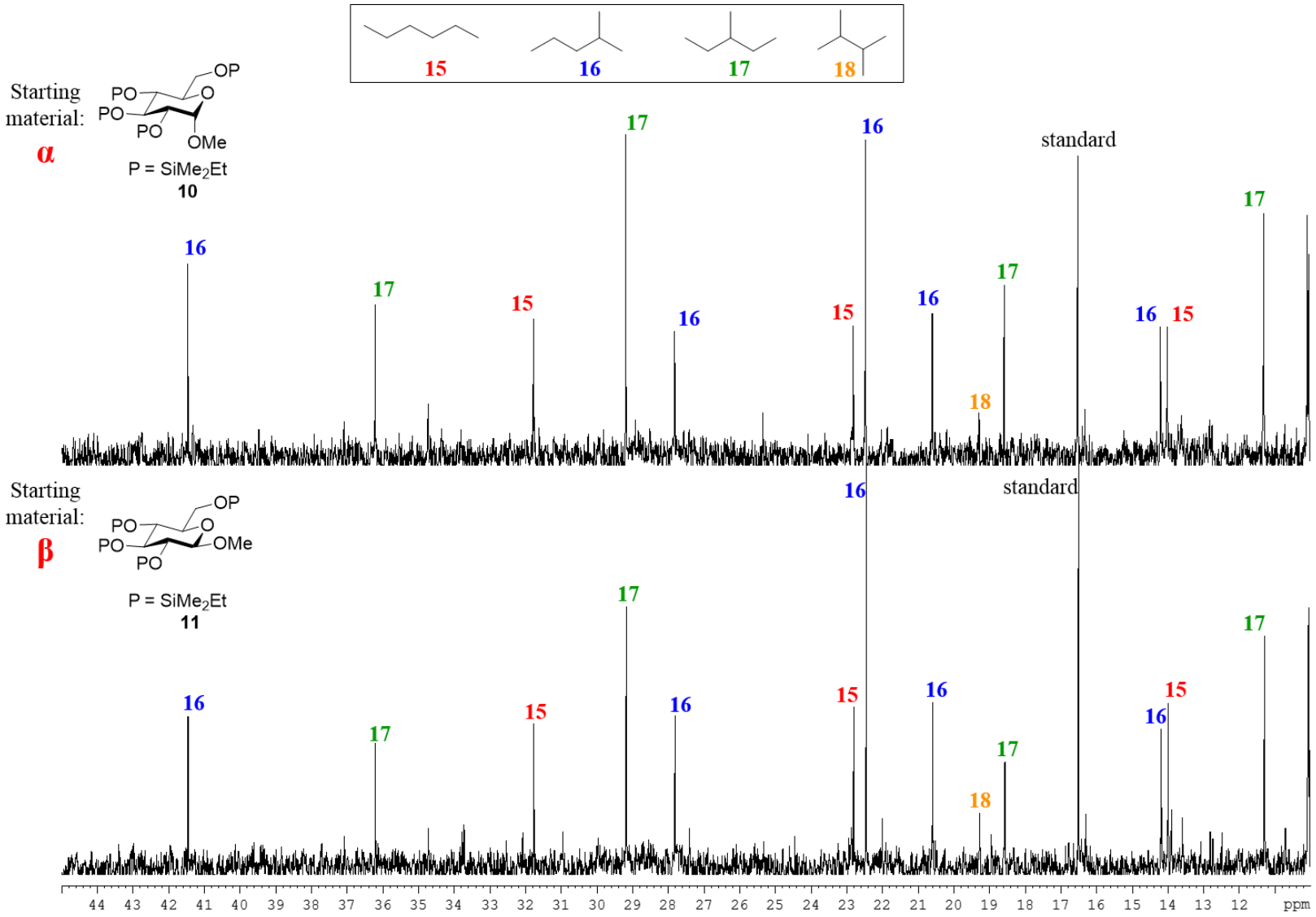

Figure 3.13: Similar hexane isomer distributions from the reductions of 10 and 11 (standard $^{13}C\{^{1}H\}$ spectra).

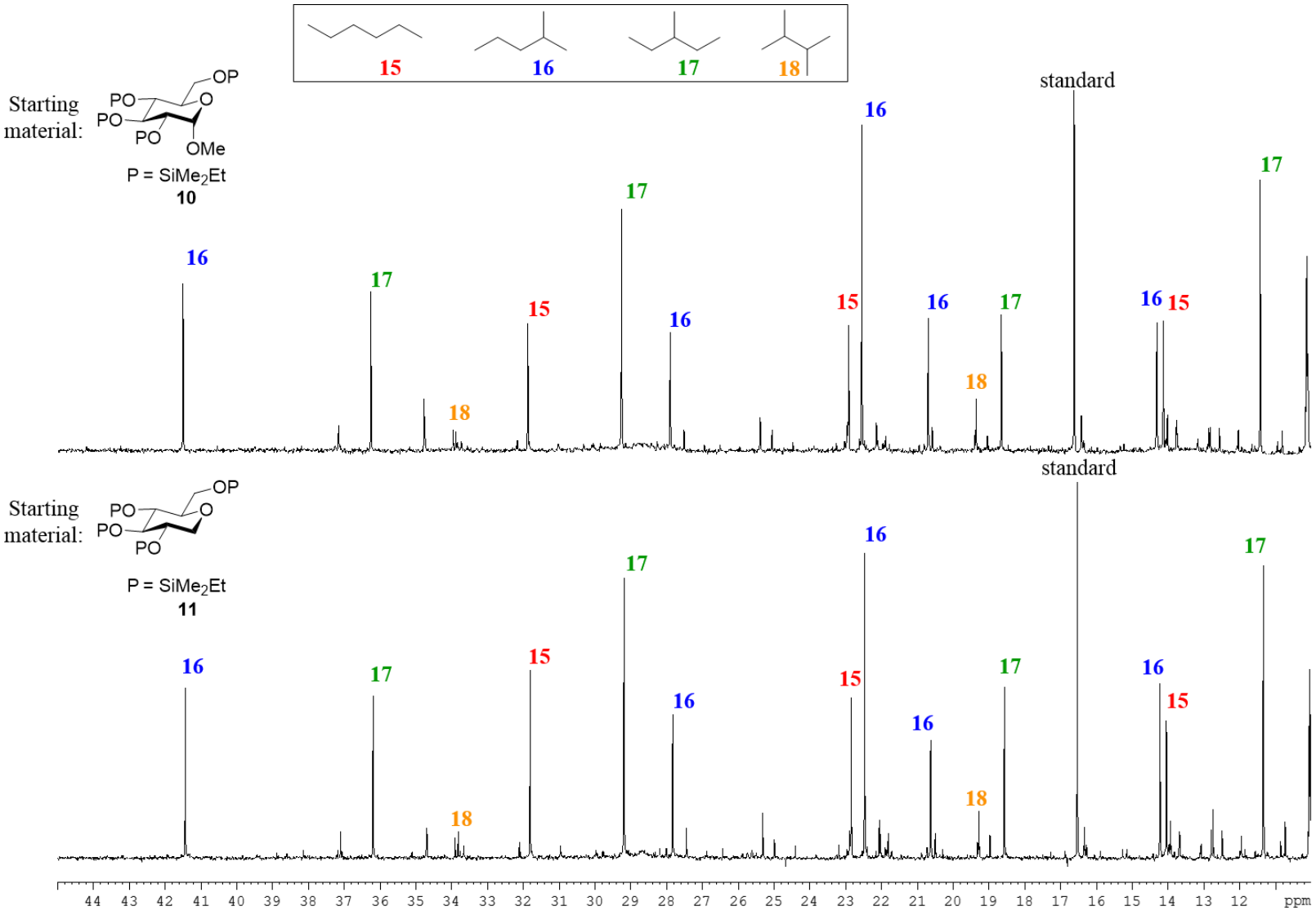

Figure 3.14: Similar hexane isomer distributions from the reductions of 10 and 12 (90° pulse spectrum).

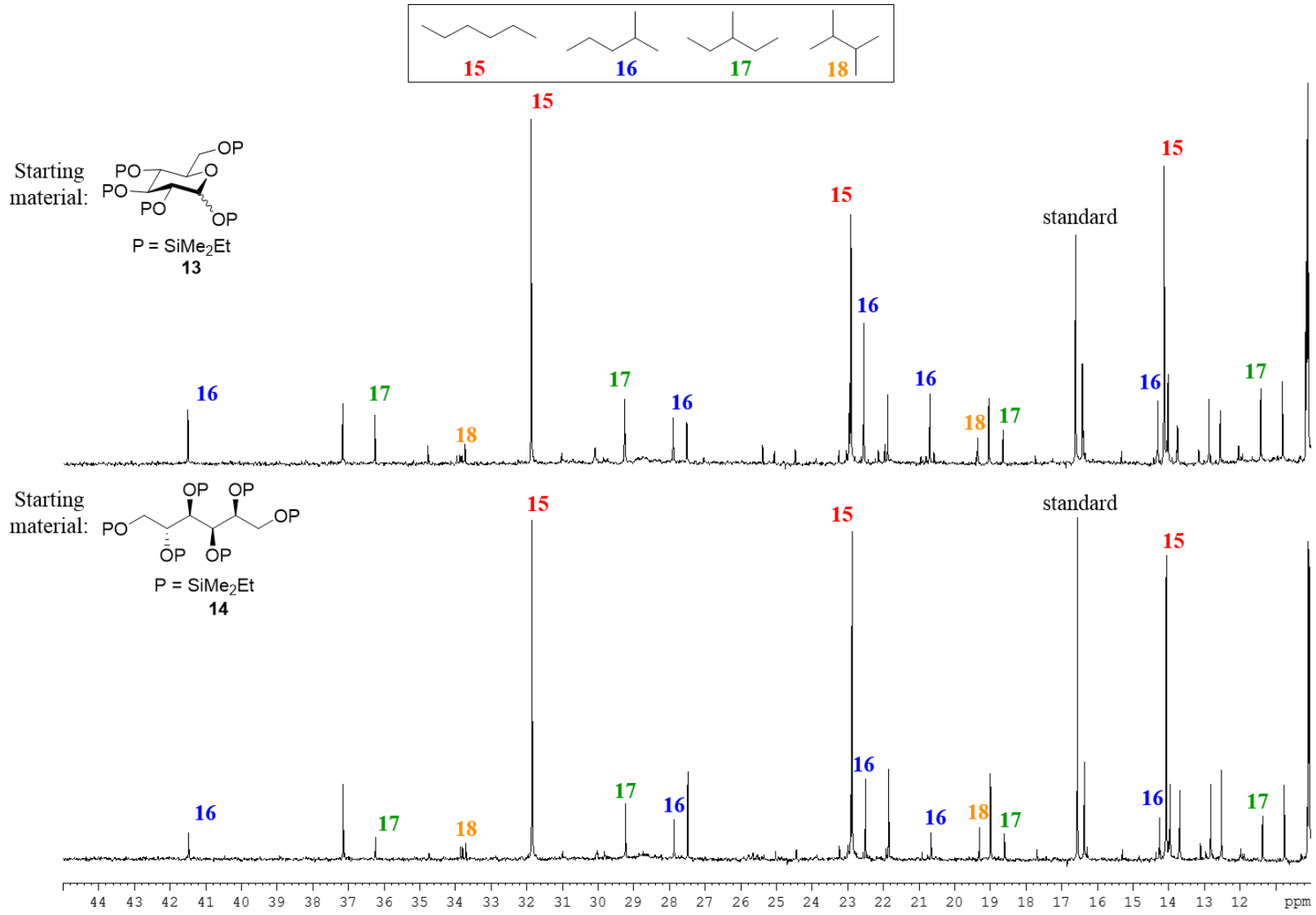

Figure 3.15: Hexane isomer distributions from the reductions of 13 and 14 (90° pulse spectra).

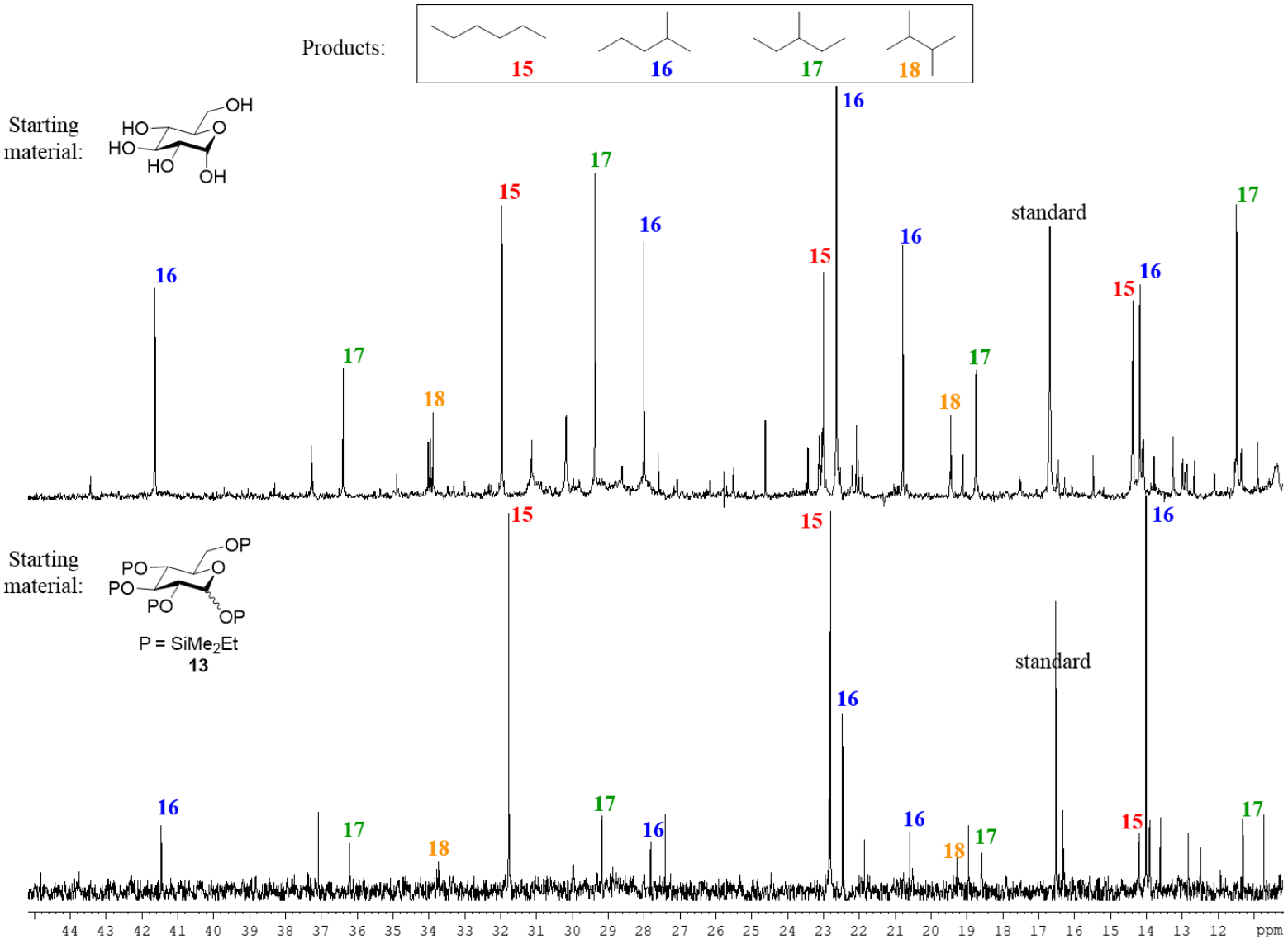

Figure 3.16: Reduction of unprotected glucose to a mixture of hexane isomers.

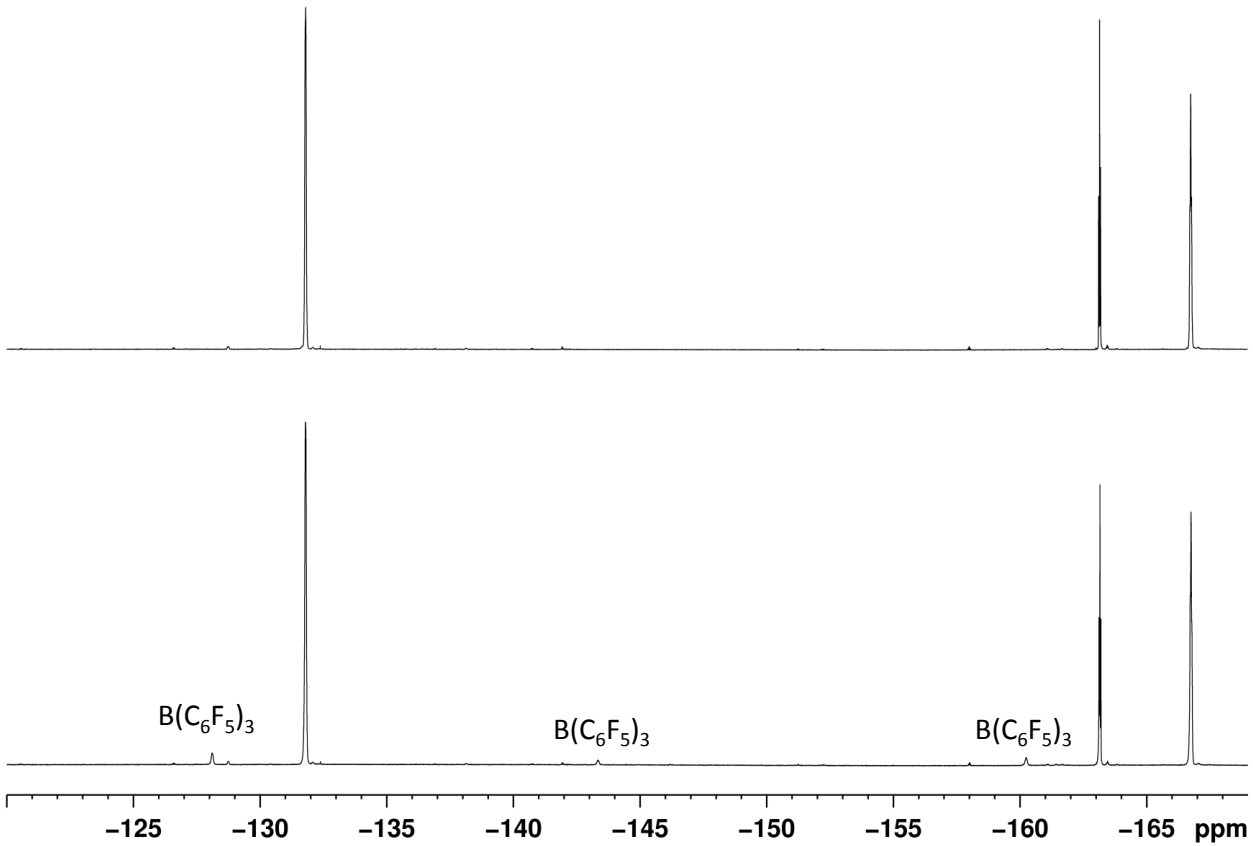

Figure 3.17: ^{19}F NMR of a standard catalytic mixture at 4 weeks, with 4.7 µmol catalyst 9, before (above) and after (below) the addition of 0.19 µmol $B(C_6F_5)_3$. It is clear from the spectra that the detection limit for $B(C_6F_5)_3$ is below 0.19 µmol and that there is no detectable $B(C_6F_5)_3$ in the reaction mixture. Control experiments with $B(C_6F_5)_3$ in place of 9 as the catalyst have shown no detectable activity at this concentration.

Chapter 4 **Metal-free Deoxygenation of Carbohydrates**

This chapter resulted from a collaboration with Dr. Matthew McLaughlin, who contributed significantly to sections 4.3 and 4.7.

4.1 *Biomass deoxygenation*

The ubiquity of petroleum-based materials in everyday products has driven a growing interest in developing renewable sources for important feedstocks and fuels.[53,135,136] As many feedstocks and fuels are composed of hydrocarbons or partially oxygenated hydrocarbons, one natural source for their production might be cellulosic biomass, which is readily available but requires deoxygenation for further use,[102,137] a need with significant inherent challenges.[63,104-117,138,139]

[135] Geilen F. M. A., Engendahl, B., Harwardt, A., Marquardt, W., Klankermayer, J., Leitner, W. *Angew. Chem. Int. Ed.* **2010**, *149*, 5642-5646

[136] Besson, M., Gallezot,P., Pinel, C. *Chem. Rev.* **2014**, *114*, 1827-1870.

[137] Werpy, T. and Petersen G., Top Value Added Chemicals from Biomass, Volume I, Results of Screening for Potential Candidates from Sugar and Synthesis Gas, US Department of Energy DOE/GO-102004-1992, August 2004

[138] Román-Leshkov, Y.; Chheda, J. N.; Dumesic, J. A. *Science* **2006**, *312*, 1933–1937.Y. Román-Leshkov, J. N. Chheda, J. A. Dumesic, *Science* **2006**, *312*, 1933-1937

[139] Zhao, H.; Holladay, J. E.; Brown, H.; Zhang, Z. C. *Science* **2007**, *316*, 1597–1600.

Chapter 3 reported that the hydrosilylative reduction of glucose to a mixture of hexane isomers can be catalyzed by a (POCOP)IrH$^+$ species ([(POCOP)IrH(acetone)]$^+$[B(C_6F_5)$_4$]$^-$, **9**), with Et_2SiH_2, serving as the terminal hydride source. Reported in Chapter 4 are investigations showing that the commercially available Lewis acid trispentafluorophenylborane ($_{B(C6F5)3}$ **19**), a known catalyst for the hydrosilylative reduction of primary and secondary alcohols,[67,69,71,120] can also catalyze the complete hydrosilylative reduction of carbohydrates (Scheme 4.1),[140] and moreover that it can be tuned to selectively deoxygenate glucose to value-added products.

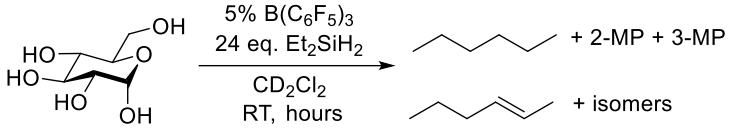

Scheme 4.1: Example of B(C_6F_5)$_3$-catalyzed hydrosilylative carbohydrate deoxygenation.

4.2 *Complete deoxygenation catalyzed by B(C_6F_5)$_3$*

When unprotected carbohydrates are utilized, the deoxygenation is preceded by an in situ conversion of the alcohols to silyl ethers (with concomitant H_2 evolution). For this reason experiments to contrast the deoxygenation activity of catalysts **9** and BCF used sugars that were preprotected (Figure 4.1), while experiments to gauge the breadth of the substrate scope of **19** used unprotected sugars for convenience. ^{13}C NMR, which proved the most useful method for monitoring C-O bond cleavage, indicated that the metal-free borane-catalyzed reaction proceeds faster at the 5 mol % catalyst level than does the iridium-catalyzed version. For example, after one hour at room temperature, the B(C_6F_5)$_3$-catalyzed deoxygenation of per-TMS-protected glucose (**TMS-13**) displayed exclusively deoxygenated products by ^{13}C NMR, while oxygenates persisted in the iridium-catalyzed reaction (Figure 4.1).

[140] Robert, M. Oestreich, *Angew. Chem. Int. Ed.* **2013**, *52*, 5216-5218

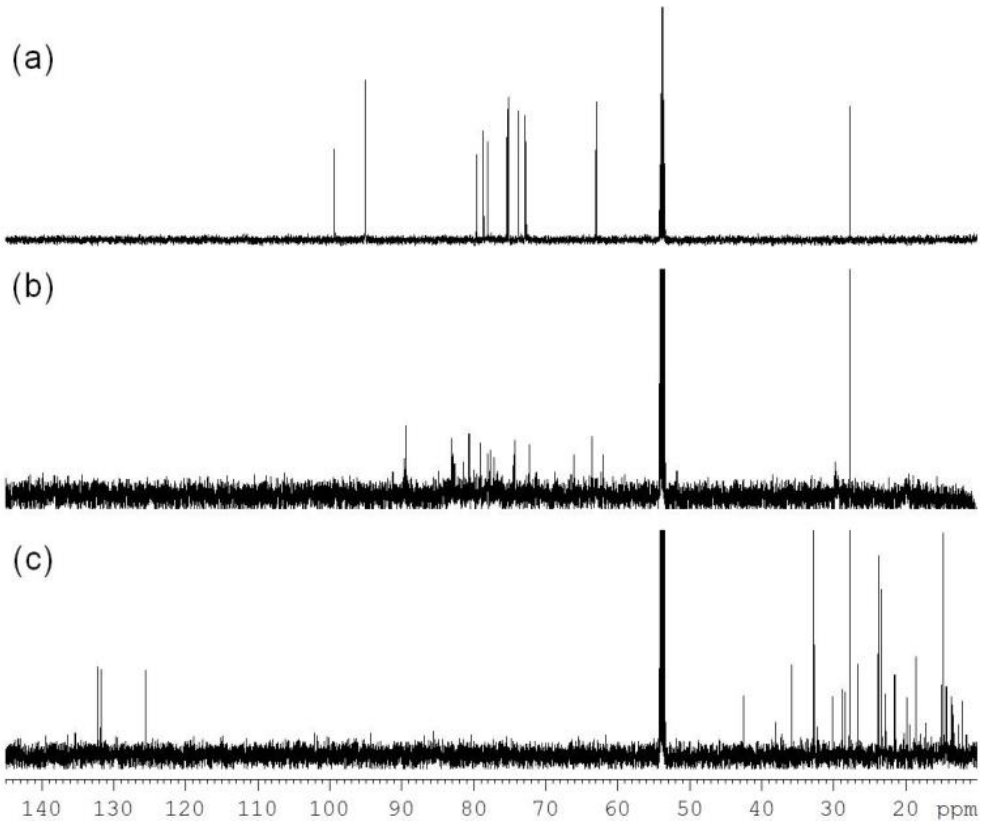

Figure 4.1: 150 MHz $^{13}C\{^1H\}$ NMR spectra showing (a) TMS-13 starting material with cyclooctane standard, (b) 5 mol % (POCOP)IrH$^+$-catalyzed hydrosilylative reduction of TMS-13 with 20 eq of Et_2SiH_2 after 1 hour, (c) 5 mol % $B(C_6F_5)_3$-catalyzed hydrosilylative deoxygenation of TMS-13 with 20 eq. Et_2SiH_2 after 1 hour.

In both cases, however, the reactions eventually proceeded to a point where all observable C-O bonds had been cleaved. Like the (POCOP)IrH$^+$-catalyzed deoxygenation, the $B(C_6F_5)_3$-catalyzed deoxygenation yields a product mixture that is dominated by hexane isomers, namely n-hexane, 2-methylpentane (2-MP), and 3-methylpentane (3-MP). The observation of 2-MP and 3-MP points to the likelihood of alkyl shifts and carbenium ions at some point in the deoxygenation sequence.[127]

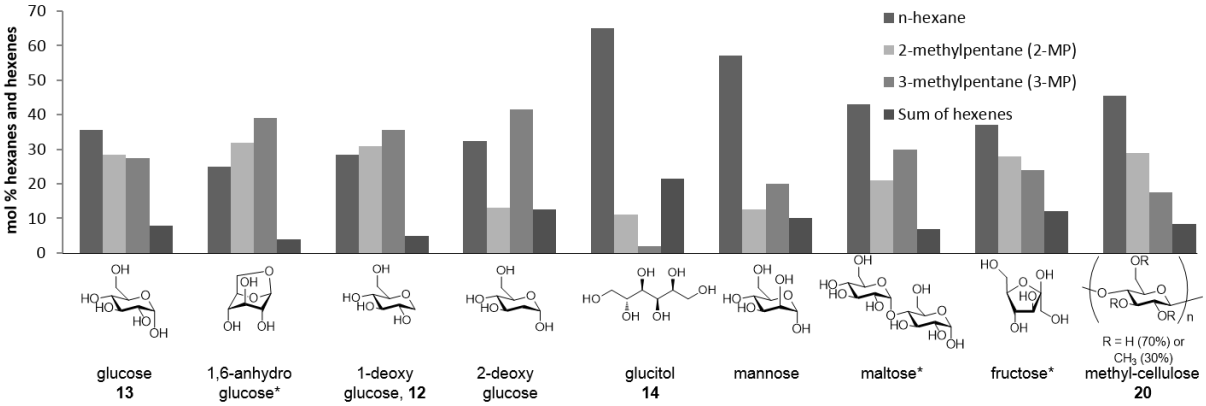

Figure 4.2: Hydrosilylative defunctionalization of representative carbohydrates. The proportions of each of the hexanes and hexenes are reported as a percentage of the total. Alkane and alkene yields were determined by semiquantitative $^{13}C\{^1H\}$ NMR spectroscopy, corroborated in select cases by GC analysis (see experimental section for details and absolute yields). General reaction conditions: 5% catalyst 2, 24 equiv of Et_2SiH_2, RT, 18 hours. Data are average of two trials, except where * denotes result of one trial.

4.3 *Substrate Scope*

While catalysts **9** and **19** were able to effect complete deoxygenation, the hydrocarbon product distribution was different in several cases. For example, the $B(C_6F_5)_3$-catalyzed deoxygenation of **TMS-13** affords a significant quantity of hexene isomers in addition to the alkanes observed in the iridium-catalyzed hydrosilylation. Additionally, for TMS-protected methyl glucoside (**TMS-10**), the iridium-catalyzed product distribution favored the alkyl shifted 2-MP and 3-MP isomers, while the major deoxygenation product of **TMS-10** deoxygenation under $B(C_6F_5)_3$ catalysis was n-hexane (Scheme 4.2 and Figure 4.5). The buildup of hexene isomers for **19** but not for **9** is also a point of differentiation (Figure 4.1). As recently discussed,[140]studies by Brookhart for **9**[74] and Piers/McRae/Gevorgyan for **19**[66,67,69,70,71] indicate that there are numerous similarities and some differences between these two catalysts. The commercial availability and ease of handling **19** was considered a major benefit, prompting an exploration of its reactivity with a range of carbohydrates.

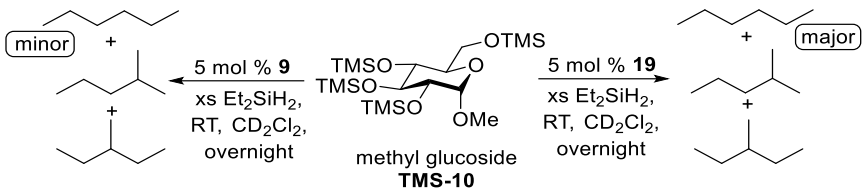

Scheme 4.2: Iridium vs $B(C_6F_5)_3$-catalyzed deoxygenation of methy glucoside.

Employment of $B(C_6F_5)_3$ in combination with diethylsilane allowed us to hydrosilylatively deoxygenate a wide range of glycosidic substrates. While complete deoxygenation was observed by ^{13}C NMR in all cases, the relative yields of alkane and alkene products were dependent on the substrate, catalyst, and protecting group (Figure 4.2). The proportion of alkyl shifted C_6-products was greatest for 1-deoxyglucose (**12**) and smallest for the ring-opened glucitol (**14**) (Figure 4.2). Intriguingly, the relative proportions of 2-MP and 3-MP were also substrate dependent, with 2-deoxyglucose showing a disproportionately high amount of 3-MP. In all cases, other C_6 hydrocarbons including methylcyclopentane, cyclohexane, 2,2-dimethylbutane, and 2,3-dimethylbutane were either not observed or present in quantities too trace to be reliably quantified by NMR spectroscopy.

4.4 *Comparison of iridium and $B(C_6F_5)_3$*

As noted above, the iridium catalyst **9** gave little detectable elimination whereas the borane catalyst **19** gave significant elimination (up to 20% overall yield). Spiking product mixtures with authentic samples revealed that alkenes observed in the ^{13}C NMR spectra of $B(C_6F_5)_3$-catalyzed reactions included *trans*-2-hexene > *trans*-3-hexene > *cis*-2-hexene, with *cis*-3-hexene not being observed in any appreciable quantity. Because the absolute yield of alkenes was small, not exceeding a sum of 25%, a correlation between the quantity of hexenes and experimental parameters was challenging. However, a rough inverse relationship between the yield of alkenes and alkyl shifted products was apparent. For example, 1-deoxyglucose (**12**), which gave the highest relative yields of alkyl shifted products, was also observed to give the least elimination.

These data may suggest a common branch point or intermediate in the mechanism, though this has yet to be adequately explained.

A full accounting for the mass balance of the completely deoxygenated products was hampered both by the volatility of the products and the complexity of the mixture. Looking at only the aforementioned hexane and hexene isomers, a sum of the products consistently gave an estimated total yield between 60 and 90% for various sugar substrates, although the absolute yield of each hydrocarbon typically varied 5-10% between trials. This variability also characterized the product ratios in most of the runs. ^{13}C NMR spectra revealed the wide variety of species contributing to the total mass balance, and although several products including C2-C4 hydrocarbons were identified by GC/MS analysis, many remain unidentified. Additionally, while ^{19}F NMR spectroscopy revealed minor catalyst decomposition during the experiment, the addition of a second portion of carbohydrate and silane after the first portion had been fully consumed showed the second portion of carbohydrate to be reduced in good yield (80%). Catalysis also continued in the presence of small amounts of added water (6 eq. relative to $B(C_6F_5)_3$), which was quickly hydrosilylated to provide dry reaction conditions, indicating that rigorous drying of catalyst, substrate, or solvent is not necessary. Polymethylhydrosiloxane, $(-(OSiMe(H))_n-)$, an inexpensive waste product of the silicone industry, also reduces carbohydrates under $B(C_6F_5)_3$ catalysis to give hexane and hexene isomers in 80% yield.

4.5 *Partial deoxygenation*

Reactions in chlorobenzene and methylene chloride both gave facile reduction of glucose and a good yield of the fully deoxygenated products in similar proportions. Although the reaction mixture appeared homogeneous when pentane was used as the solvent, the rate and yield of the reaction was dramatically reduced, perhaps speaking to the importance of generating reactive ion

pairs during silane activation and/or oxygen abstraction. The rate and yield of the reaction was also reduced with the tertiary silane Me_2EtSiH, indicating a significant steric effect. This difference is evident in the reduction of Me_2EtSi-protected glucitol (**Me_2EtSi-14**) with Me_2EtSi-H, which only proceeds to partial consumption of C-O bonds after 1 week (eq. 4.1). Under these conditions it is evident that primary C-O bond reduction is kinetically favored, though other minor products are also observed. In contrast, complete reduction of **Me_2EtSi-14** occurs with Et_2SiH_2 after only 2 hours. It is worth noting that silyl-exchange does occur at a sufficient rate to cause doubling of ^{13}C resonances. This phenomenon is avoided by matching the protecting group (-$SiMe_2Et$ or --$SiEt_3$) with the silane (Me_2EtSi-H or Et_3Si-H) (see Figure 4.17).

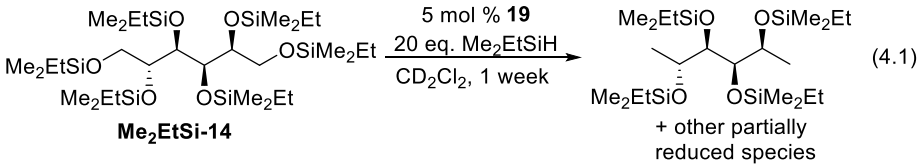

(4.1)

Under silane limited conditions (2 eq), we observed that Me_2EtSi-H converted **Me_2EtSi-14** to 1,6-deoxy glucitol as the major product (eq. 4.2). On a preparative scale (0.8 mmol), treating unprotected **14** with 9 eq. Me_2EtSi-H in the presence of $B(C_6F_5)_3$ gave 1,6-deoxy glucitol in 70% yield (by in situ ^1H NMR spectroscopy). The tetraol was isolated in 62% yield, with 2,3,4-hexanetriol (6:1 *d.r.*, the product of one additional reduction) also contributing to the mass balance (~7%). With 2 eq of Et_2SiH_2, the product mixture was considerably more complex, but 1,6-deoxy glucitol was also identified as the major observed product by ^{13}C NMR spectroscopy (>50%, see Figure 4.9). These data suggest that Et_2SiH_2 may be less inherently selective or that O-$SiEt_2$(H) groups generated via silyl exchange may participate in further, presumably intramolecular, reductions. The primary over secondary selectivity parallels that observed for simple alcohols.[66-70]

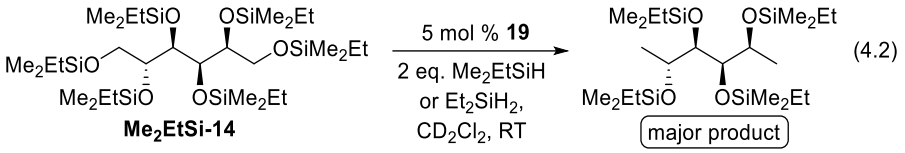

(4.2)

4.6 *Initial steps of reaction*

Slowing the reaction further by using Et_3Si-protected glucose (**Et_3Si-13**) with Me_2EtSiH allowed us to observe the initial steps of the reaction for a ring-closed sugar. Curiously, the first step causes ring opening over the course of minutes to give spectroscopically identified glucitol as the major product (**14**), and not reduction of the primary C_6 or anomeric C_1 positions. Ring opening was followed by a considerably slower (hours) reduction of the primary sites to give 1,6-deoxy glucitol (Scheme 4.3). The preference for ring opening is likely the result of a comparatively increased Lewis basicity and steric accessibility of the pyranose oxygen.

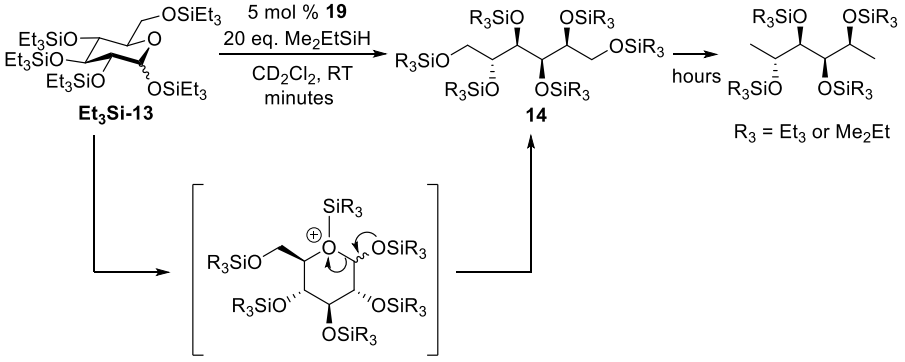

Scheme 4.3: Et_3Si-13 is reduced first to glucitol (14) and then to 1,6-deoxy glucitol.

4.7 *Reduction of cellulose*

Finally, the direct deoxygenation of cellulose has historically been limited by its low solubility and steric congestion, therefore often requiring pre-treatment to separate the chains or cleave the glycosidic linkages before defunctionalization.[141,142] Not surprisingly then, cellulose

[141] Petzold, K., Koschella, A., Klemm, D., Heublein, B., *Cellulose* **2003**, *10*, 251-269

[142] Fan, J.; De bruyn, M.; Budarin, V. L.; Gronnow, M. J.; Shuttleworth, P. S.; Breeden, S.; Macquarrie, D. J.; Clark, J. H. *J. Am. Chem. Soc.* **2013**, *135*, 11728–11731.

itself was completely insoluble and unreactive to our conditions, even at elevated temperatures. Commercially available 30% methylated cellulose (**20**), however, was significantly more soluble. While displaying no apparent solubility in CH_2Cl_2, this material is rapidly solubilized by the addition of $B(C_6F_5)_3$ and Et_2SiH_2, which presumably silylates at least some of the unprotected alcohols and allows for complete dissolution under reaction conditions. Although the degree of silyl vs. methyl protection at the time of reduction is unknown, fully deoxygenated products are observable within 20 minutes (Scheme 4.4 and Figure 4.2), with yields reaching 80% after our 18 h assay. This suggests both that the method is exceptionally active and can consequently activate congested, minimally soluble substrates, and that the cellulose problem may be exclusively one of solubility.

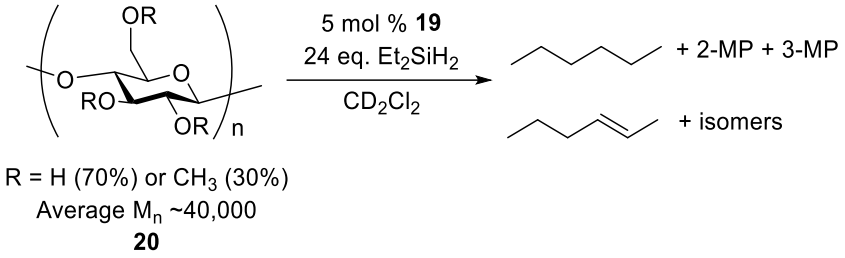

Scheme 4.4: .$B(C_6F_5)_3$-catalyzed hydrosilylative deoxygenation of 30% methylcellulose (20). Major products observed by $^{13}C\{^1H\}$ NMR.

4.8 *Conclusion*

In summary, we have demonstrated a new mild method for the metal free deoxygenation of carbohydrates to mixtures of alkane and alkene hydrocarbons. The product distribution and rate of reduction are sensitive to substrate, solvent, silane, protecting group, and catalyst. This feature enables conditions for the selective deoxygenation of glucose to more valuable products like 1,6-deoxy glucitol to be realized. The mechanism of deoxygenation is currently under investigation.

4.9 *Experimental section*

General Methods: Unless otherwise stated, all reactions were conducted under an argon atmosphere using a Vacuum Atmospheres glovebox. Chlorobenzene-d_5 and methylene chloride-d_2 were purchased from Cambridge Isotope labs. Both were degassed via three freeze-pump-thaw cycles and dried over 4Å molecular sieves prior to use. Diethyl silane, dimethyl ethyl silane, and polymethylhydrosiloxane (average M_n 1,700-3,200) were purchased from Aldrich and dried over 4Å molecular sieves prior to use. 1-deoxyglucopyranose was purchased from Carbosynth. Glucose, α-D-methylglucoside, fructose, maltose, 2-deoxyglucose, glucitol, α-D-mannose, methylcellulose (30% methylated, M_n~40,000), and hydrogen fluoride pyridine (~30% pyridine, 70% hydrogen fluoride) were all purchased from Aldrich. $^{13}C_{1\text{-}6}$ glucose, $^{13}C_1$ glucose, and $^{13}C_6$ glucose were purchased from Cambridge Isotope Labs. Chlorodimethylethylsilane, trimethylchlorosilane, and triethylchlorosilane were purchased from TCI America. $[(POCOP)Ir(H)(acetone)]^+[B(C_6F_5)_4]^-$ (**9**) was prepared according to a published procedure.[133] Trispentafluorophenylborane ($B(C_6F_5)_3$), catalyst **19**) was purchased from Strem and TCI and used as received. A comparison of the activity and selectivity from each source showed nearly indistinguishable results.

NMR spectra were recorded using a Bruker Avance III spectrometer equipped with a cryoprobe operating at 600 MHz (^{1}H), 565 MHz (^{19}F), 150 MHz (^{13}C). NMR chemical shifts are reported in ppm and referenced using the residual proton peaks (^{1}H) or the ^{13}C resonances of the deuterated solvent (^{13}C).

GC analysis was performed on an Agilent 6890 using an HP PLOT-Q column (30m x 0.32mm x 20.0 μm) with the following parameters: inlet temperature 250℃, 19.99 psi of helium; oven temperature held at 100℃ for 0 min then ramped to 150 ℃ at 30 ℃/min and held 8 min; then

ramped to 240 ℃ at 30 ℃/min and held 4 min. The column with was run using 17.1 psi at 4.0 mL/min helium; the FID detector was held at 250℃ with a flow rate of 40 mL/min H_2, 450 mL/min air and makeup flow of 45 mL/min helium. A 15:1 split ratio was applied.

GC/MS analysis of reaction solutions was performed with an Agilent G4350A GC/MSD system containing a 7820A GC with an HP-5MS column (length 30m; I. D. 0.250 mm) connected to an Agilent 5975 MSD. A 100:1 split ratio was applied. The GC method consisted of the following parameters: inlet temperature 250°C; inlet and column pressure of 11.9 psi He; column flow rate 1 mL/min; oven temperature held at 125 ˚C for 3 min then ramped 20 ˚C/min to 250 ˚C. The temperature was then held at 250 ˚C for 5 minutes. The detector temperature was set to 280 ˚C. GC/MS analysis of reaction headspace was performed using a Varian 450-CG gas chromatograph connected to a Varian 220-MS mass spectrometer, which utilized a Varian FactorFour column (60m x 0.32 mm x 1.8 µm). The GC method consisted of the following parameters: inlet temperature 225°C, column flow rate 1 mL/min, oven temperature held at 40°C for 3 minutes, then ramped 15°/minute to 220°C, then held for 10 minutes. This research made use of instrumentation (gas inject GC/MS spectrometer) funded by the UNC EFRC: Center for Solar Fuels, an Energy Frontier Research Center supported by the U.S. Department of Energy, Office of Science, Office of Basic Energy Sciences, under award number DE-SC0001011.

Reaction conditions for protected and unprotected sugars.

Catalytic hydrosilylative reduction of carbohydrates:

In an argon-filled glovebox, a 1-dram vial was charged with $[(POCOP)IrH(acetone)]^+[B(C_6F_5)_4]^-$ catalyst (**9**) or $B(C_6F_5)_3$-catalyst (**19**) (5 mol%, 5 µmol). The silyl-protected or unprotected carbohydrate (100 µmol, 1 eq.) was massed into the same vial. Enough solvent was added to ensure a total volume of 500 µL after addition of the silane. Cyclooctane (10 µL, 74 µmol) was added as

an internal standard, followed by silane (2.40 mmol, 24 eq). After gas evolution subsided, the reaction mixture was transferred to a J-Young tube or a septum capped NMR tube and removed from the glovebox. After the reaction time (1 day to 2 weeks), a $^{13}C\{^{1}H\}$ NMR spectrum was acquired using a standard proton-decoupled experiment (delay time = 2 s, pulse width = 10.75 μsec, sweep width = 36058 Hz, transmitter offset = 100 ppm, decoupling scheme = waltz16). To estimate absolute yields, integration of the product peaks was compared to the integral of the standard peak (cyclooctane at 27.5 ppm) and a calibration plot described below. The same procedure was applied to defunctionalizations with polymethylhydrosiloxane and catalyst **19**, but because of limited solubility of the polysilane products in methylene chloride, a 3:1 solvent mixture of toluene:methylene chloride was used to make product analysis easier.

Calibration plots for semi-quantitative ^{13}C yield determination

Known amounts of cyclooctane and various hexane and hexane isomers were mixed in a 1:1 combination of methylene chloride-d_2 and Et_2SiH_2 and analyzed by $^{13}C\{^{1}H\}$ NMR. This mixture mimicked the solvent composition of a typical catalytic run. The integration for an isolated peak for each alkane and alkene isomer was recorded relative to the integration of cyclooctane standard. The calibration plot for each hexane and hexene was prepared by plotting [mol product]/[mol standard] versus [integration product]/[integration standard] and fitting with a least squares fit. The calibration plot fit was solved for moles of product. For example, for n-hexane, moles of n-hexane was determined with the equation: (4.69([integration product at 31 ppm]/[integration standard])+0.2)*mol standard]. The moles of product were determined by inputting the measured integrations and moles of standard used. The product yield was determined by dividing the moles of starting material and multiplying by 100. As described in the text, this approach gave run-to-run variations of <10% in both total mass balance and the individual components. This approach

was found to not differ appreciably with the more rigorous approach previously utilized but was consistently more rapid.

Corroboration of NMR yields with GC data in select cases:

GC calibration plot for n-hexane yield determination: The calibration plot for n-hexane was prepared by plotting [mol n-hexane]/[mol cycloocatane] versus [integration n-hexane]/[integration cyclooctane] and fitting with a least squares fit. The calibration plot fit was solved for moles of product. For n-hexane, moles of n-hexane was determined with the equation: (1.86([integration n-hexane]/[integration cyclooctane])-0.005)*mol cyclooctane]. The moles of n-hexane were determined by inputting the measured integrations and moles of cyclooctane used. Using the described GC method, the n-hexane was completely resolved from other the other hexane/hexene isomers and the silane byproducts of the reaction. The n-hexane yield was determined by dividing the moles of starting material and multiplying by 100. This approach gave results in good agreement with the NMR quantitation method, with variations of less than 2%, further validating the NMR approach used.

Table 4.1: Total yields (%) of hexane and hexene isomers from deoxygenation of carbohydrates

Substrate[a]	n-hexane	2-methyl pentane	3-methyl pentane	*trans*-2-hexene	*trans*-3-hexene	*cis*-2-hexene	total
glucose	25	20	19	3	3	0	70
1,6-anhydro glucose[b]	23	29	35	3	0	0	91
1-deoxyglucose	19	21	24	3	1	0	67
2-deoxyglucose	31	12	39	6	3	3	94
glucitol	52	9	2	8	7	2	80
mannose	48	11	17	5	3	0	85
maltose[b]	31	15	21	3	2	0	72
fructose[b]	24	18	15	4	4	0	65
cellulose (30% methylated)	35	23	14	5	1	0	78
TMS-MeO-glucose	22	26	15	8	2	2	75
TMS-glucose	32	15	11	8	2	3	70
TMS glucitol[b]	39	14	15	2	0	0	70
TMS-MeO-glucose[b,c]	17	31	18	0	0	0	66
TMS-glucose[b,c]	30	6	5	0	0	0	41

[a] standard reaction conditions: 5 mol% $B(C_6F_5)_3$, 24 eq Et_2SiH_2, CD_2Cl_2, >18 h of reaction time. Average of two runs unless indicated. Yields estimated with a ^{13}C NMR calibration plot

versus an internal standard. Utilizing C_6D_5Cl as a solvent gave an insignificant variation in the products whereas when pentane was used as a solvent, products were observed but were too trace to quantify.

[b] results from a single trial.

[c] (POCOP)IrH^+ catalyst (5 mol%), reaction time of three weeks.

Table 4.2: Yields (%) of hexane and hexene isomers relative to the total amount of observed hydrocarbon deoxygenation products

Substrate[a]	n-hexane	2-methyl pentane	3-methyl pentane	sum of 2-methylpentane and 3-methylpentane	Sum of hexenes
glucose	36	28	28	56	8
1,6-anhydroglucose[b]	25	32	39	71	4
1-deoxyglucose	28	31	36	66	5
2-deoxyglucose	33	13	42	55	12
glucitol	65	11	2	13	22
mannose	57	13	20	33	10
maltose[b]	43	21	30	51	7
fructose[b]	37	28	24	51	12
cellulose(30% methylated)	45	29	17	46	9
TMS-MeO-glucose	29	34	20	54	17
TMS-glucose	45	21	15	36	19
TMS glucitol[b]	56	20	22	42	2
TMS-MeO-glucose[b,c]	26	47	28	74	0
TMS-glucose[b,c]	73	15	12	27	0

[a] standard reaction conditions: 5 mol% $B(C_6F_5)_3$, 24 eq Et_2SiH_2, CD_2Cl_2, >18 h of reaction time. Average of two runs unless indicated. Yields estimated with a ^{13}C NMR calibration plot versus an internal standard.

[b] results from a single trial.

[c] (POCOP)IrH^+ catalyst (5 mol%), reaction time of three weeks.

Reduction of TMS-protected glucose: [(POCOP)IrH(acetone)][$B(C_6F_5)_4$] vs. $B(C_6F_5)_3$

In an argon-filled glovebox, TMS-protected glucose (**TMS-13**, 202 mg, 0.37 mmol, 4 eq.) was dissolved in 0.9 mL CD_2Cl_2. Cyclooctane (5 µL, 0.036 mmol, 0.1 eq.) was added as a standard. A new vial was charged with (POCOP)IrH^+ catalyst **9** (7 mg, 0.005 mmol, 5 mol%), and a different vial was charged with $B(C_6F_5)_3$ catalyst **19** (2.1 mg, 0.004 mmol, 4 mol%). 0.25 mL of the glucose solution was added to each catalyst-charged vial. Subsequently, Et_2SiH_2 (0.27 mL, 2.1 mmol, 23 eq.) was added to each vial. After bubbling subsided, the reaction mixtures were transferred to J-Young tubes and removed from the glovebox. In addition, 0.25 mL of the glucose solution was transferred to a new NMR tube, followed by the addition of 0.25 mL CD_2Cl_2. Lacking catalyst and silane, this sample was used as a reference to compare the relative concentrations of TMS-glucose starting material and cyclooctane. After 1 hour at room temperature, a $^{13}C\{^1H\}$ NMR spectrum of each sample was acquired. The absence of observable peaks in the C-O region (50-110 ppm)/presence of alkane peaks (10-45 ppm) for the $B(C_6F_5)_3$-catalyzed reaction and the presence of small C-O peaks/absence of alkane peaks for the (POCOP)IrH^+-catalyzed reaction indicated the faster rate of the $B(C_6F_5)_3$ system relative to the (POCOP)IrH^+ system (Figure 4.3). $^{13}C\{^1H\}$ spectra were also acquired after 3 weeks at room temperature, showing the presence of hexene isomers in the $B(C_6F_5)_3$-catalyzed reaction (Figure 4.4).

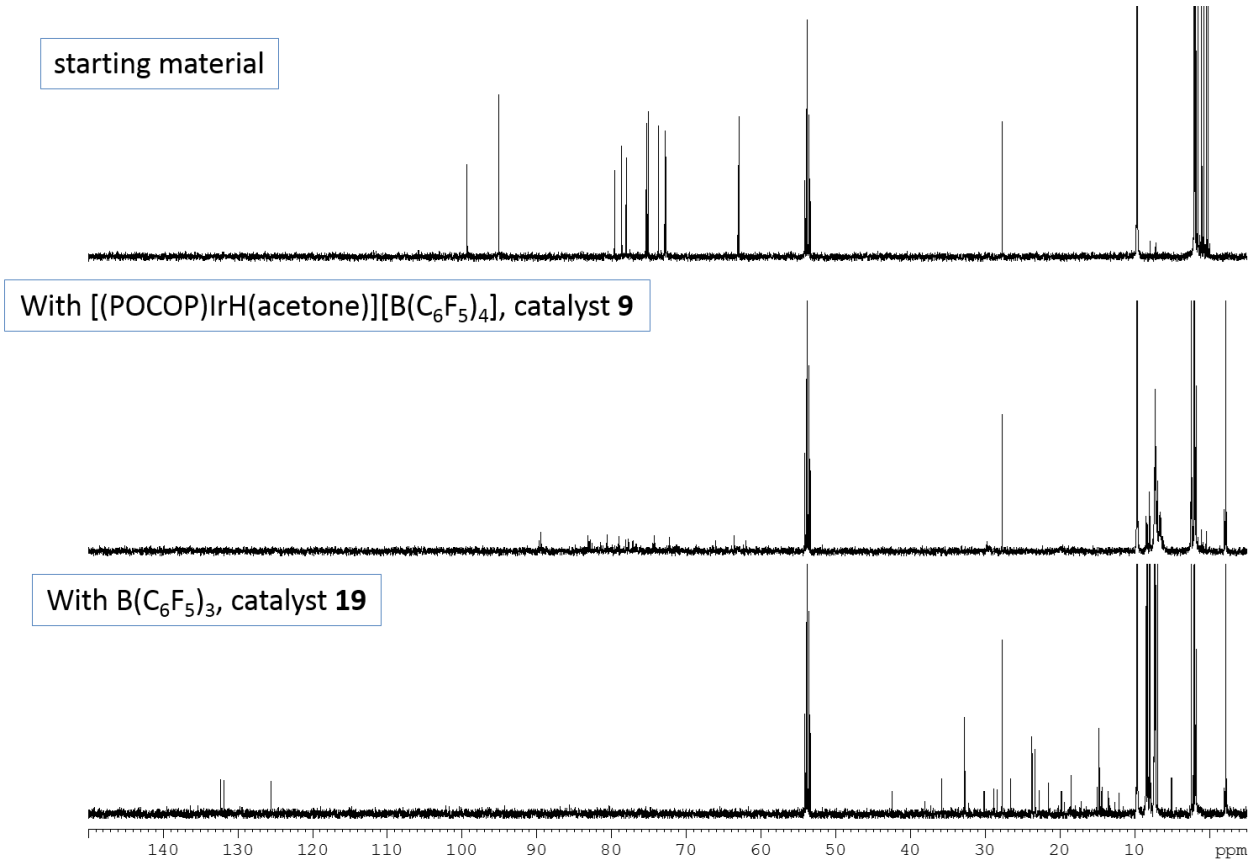

Figure 4.3: A comparison of TMS-protected glucose starting material (TMS-13, top, sample contains cyclooctane standard) with the (POCOP)IrH$^+$-catalyzed deoxygenation (middle) and B(C_6F_5)$_3$-catalyzed deoxygenation (bottom) after 1 hour. (Reproduction of Figure 4.1)

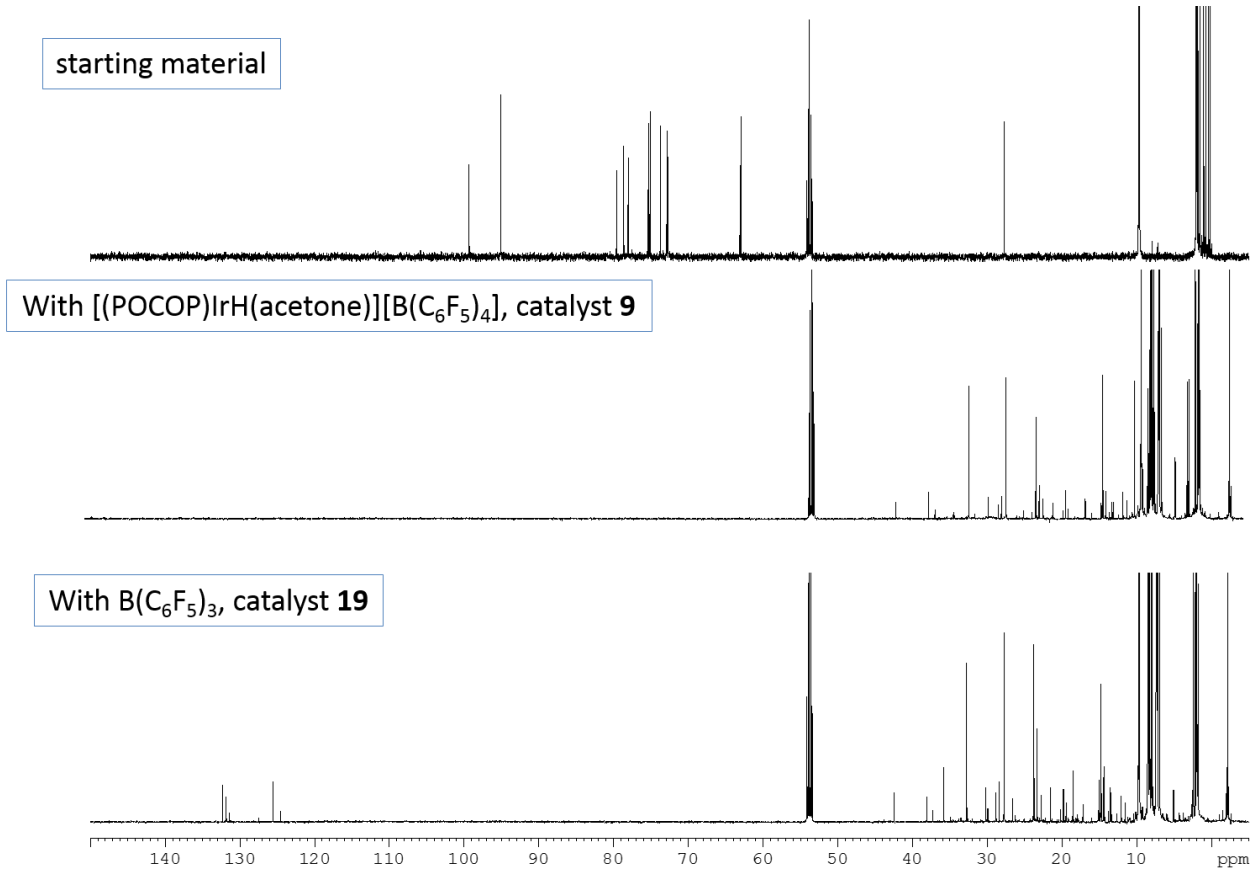

Figure 4.4: Comparison of TMS-glucose starting material (TMS-13, top, sample contains cyclooctane standard) with the (POCOP)IrH$^+$-catalyzed reaction mixture (middle) and B(C_6F_5)$_3$-catalyzed reaction mixture (bottom) after 3 weeks. The (POCOP)IrH$^+$-catalyzed reaction does not give hexene products, while hexenes are observed in the B(C_6F_5)$_3$-catalyzed reaction.

Reduction of TMS-protected methyl glucoside: [(POCOP)IrH(acetone)][B(C_6F_5)$_4$] vs. B(C_6F_5)$_3$

The above procedure was repeated using TMS-protected methyl glucoside (**TMS-10**, 202 mg, 0.42 mmol, 4 eq.) in place of the TMS-glucose. Significantly more 2-methylpentane and 3-methylpentane relative to the amount of n-hexane was observed for the (POCOP)IrH$^+$-catalyzed reaction in comparison to the B(C_6F_5)$_3$-catalyzed reaction (Figure 4.5).

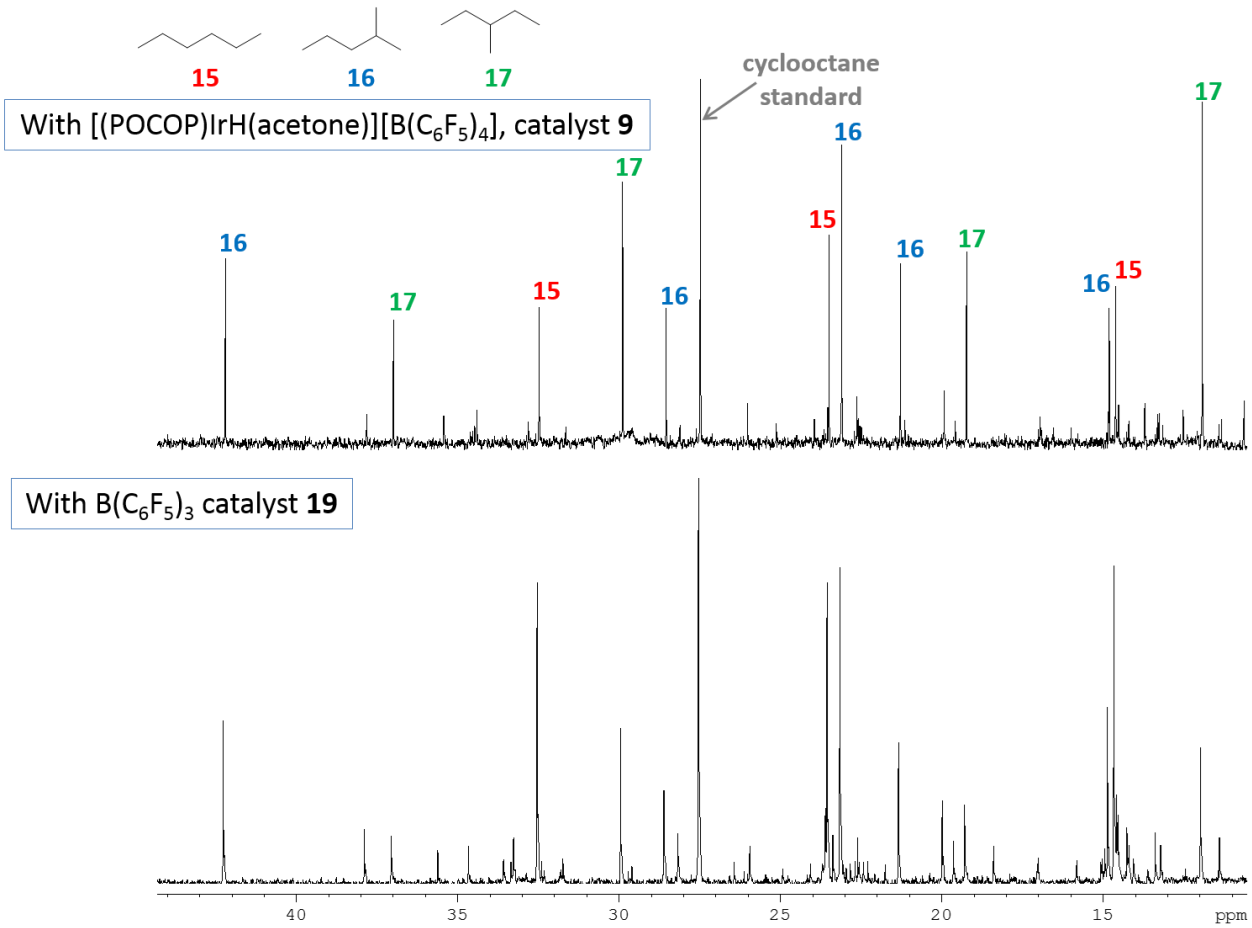

Figure 4.5: Reduction of TMS-protected methyl glucoside (TMS-4) catalyzed by (POCOP)IrH$^+$ (top) and B(C_6F_5)$_3$ (bottom). The product mixture from the (POCOP)IrH$^+$ catalyzed reaction shows more 2-methylpentane and 3-methylpentane relative to the amount of n-hexane than the product mixture from the B(C_6F_5)$_3$-catalyzed reaction.

Catalyst Recyclability Experiments:

In an argon-filled glovebox, a 1-dram vial was charged with B(C_6F_5)$_3$-catalyst (**19**) (5 mol%, 5 µmol). Glucitol (100 µmol, 1 eq.) was massed into the same vial. Enough solvent to ensure a total volume of 500 µL after addition of the silane was added. Cyclooctane (10 µL, 74 µmol) was added as an internal standard, followed by silane SiH_2Et_2 (2.40 mmol, 24 eq). After gas evolution subsided, the reaction mixture was transferred to a J-Young tube or a septum capped NMR tube and removed from the glovebox. After 2 hours a $^{13}C\{^1H\}$ NMR spectrum was acquired using a

standard proton-decoupled experiment (delay time = 2 s, pulse width = 10.75 μsec, sweep width = 36058 Hz, transmitter offset = 150 ppm, decoupling scheme = waltz16). Based on the NMR it was clear that the starting material was fully consumed. Additional glucitol (100 μmol, 1 eq.) and silane (2.40 mmol, 24 eq) were added and reacted for 24 hours. To estimate absolute yields, integration of the product peaks was compared to the integral of the standard peak (cyclooctane at 27.5 ppm) and a calibration plot described below. Despite some catalyst decomposition, hexane and hexene isomers were generated in good yields (80%), indicating some catalyst recyclability.

Analysis of reaction mixture and headspace by GC/MS:

A hydrosilylative reduction was performed using glucose (1**3**) as a substrate, as described previously. A septum-capped NMR tube was used as the reaction vessel. NMR analysis after 1 day indicated complete consumption of starting material and the appearance of hydrocarbon products. At this point, an aliquot of the headspace from this reaction mixture was removed via gas-tight syringe and analyzed using a GC/MS spectrometer equipped with a gas-tight inlet. Ethylene, propene, and butene were detected. To verify that these hydrocarbons were reaction products, the experiment was repeated using glucose in which every carbon atom was labeled with ^{13}C (**$^{13}C_{1\text{-}6}$-13**). GC/MS analysis of the headspace from this reaction indicated the presence of ^{13}C-labeled ethylene, propene, and butene. Although the concentration of these products was not quantified, it is clear that they contribute to the mass balance of the reaction products. An aliquot of each reaction solution was also diluted and analyzed by GC/MS to look for heavier or coupled products. In this case, there were no differences in the MS traces for peaks at the same retention times in the labeled and unlabeled reactions, indicating that heavier products were not formed during the reaction.

Hydrosilylative reductions of mono-^{13}C-labeled glucose:

Using the previously described standard protocol, a hydrosilylative reduction was performed using glucose that was ^{13}C-labeled exclusively at the C_1 position (**$^{13}C_1$-13**). Separately, glucose that was ^{13}C-labeled exclusively at the C_6 position (**$^{13}C_6$-13**) was reduced. In both cases, NMR analysis after 1 day showed consumption of starting material and generation of hydrocarbon products. Figure 4.6 shows the 10-25 ppm region of both reaction mixtures. While the identified alkane and alkene products make up the majority of the product mixture as indicated in Table 4.1 and Table 4.2, it is evident that the rest of the mass balance is made up of a wide variety of species; these species remain uncharacterized at this point.

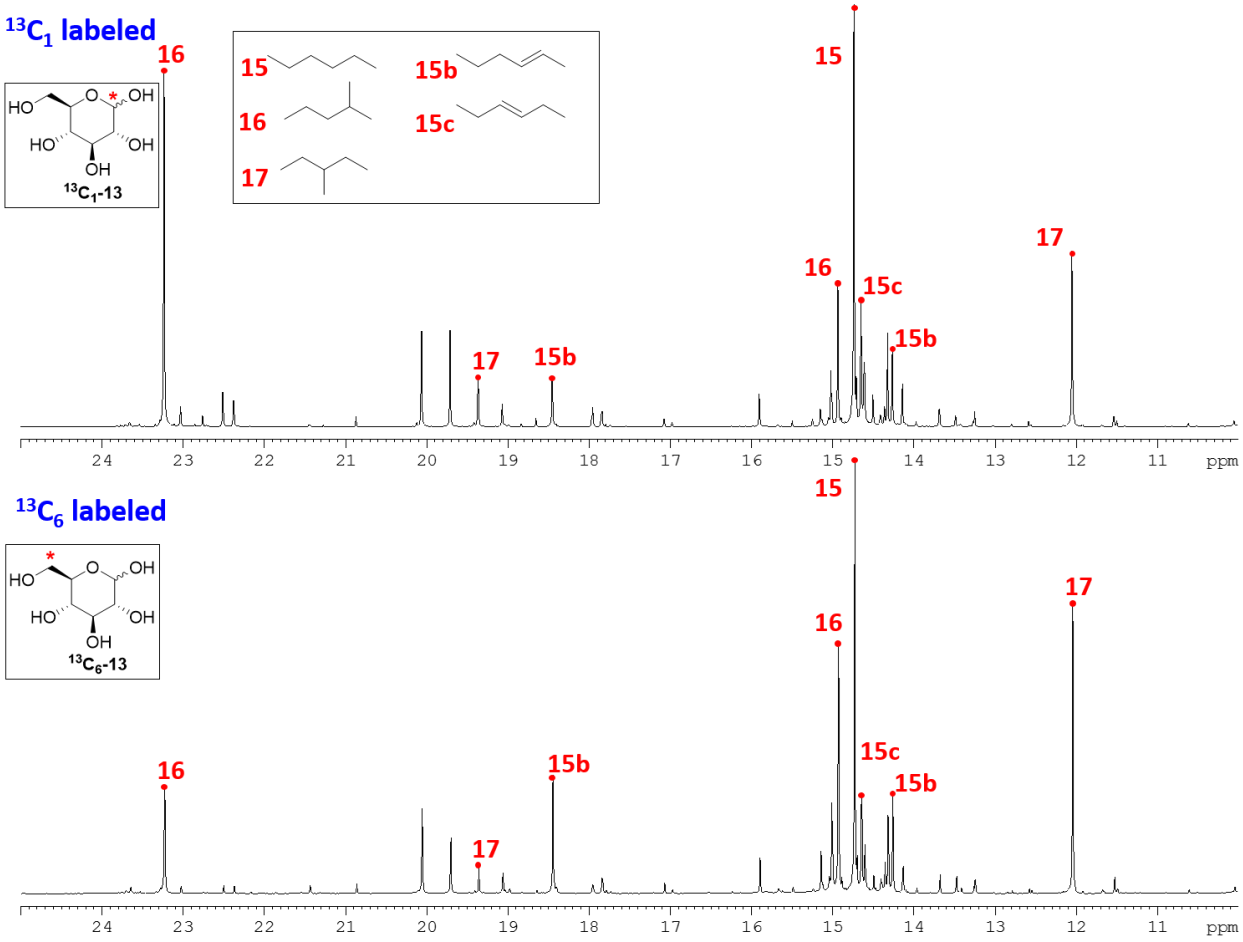

Figure 4.6: 10-25 ppm region of $^{13}C\{^{1}H\}$ NMR spectra of the product mixtures from the hydrosilylative reduction of $^{13}C_1$-labeled glucose ($^{13}C_1$-13) and $^{13}C_6$-labeled glucose ($^{13}C_6$-13). The unlabeled peaks are products that, while currently unidentified, contribute to the total mass balance of these reactions.

Carbohydrate reduction in the presence of water:

$B(C_6F_5)_3$ (4.5 mg, 8.7 µmol) was dissolved in 0.5 mL CD_2Cl_2 and transferred to a septum-capped NMR tube. A ^{19}F NMR spectrum was acquired, showing three broad peaks for $B(C_6F_5)_3$ as the major species present. Argon-sparged water (1 µL, 6 eq. relative to $B(C_6F_5)_3$) was added through the septum using a µL-syringe. A ^{19}F NMR spectrum acquired at this time showed conversion to a new product with three peaks, likely the borane-water adduct. Et_2SiH_2 (35 µL, 5 eq. relative to water) was added. ^{19}F NMR spectroscopy revealed conversion back to $B(C_6F_5)_3$, with the resonances now visible as sharp peaks, indicating that the $B(C_6F_5)_3/Et_2SiH_2$ system can give rise

to "self-drying" conditions. The addition of Me_2EtSi-protected glucose (54 mg) and additional Et_2SiH_2 (250 µL) at this point produced hexane and hexene isomers as usual, also pointing to the robustness of this reaction. The $^{19}F\{^1H\}$ NMR spectra are shown in Figure 4.7.

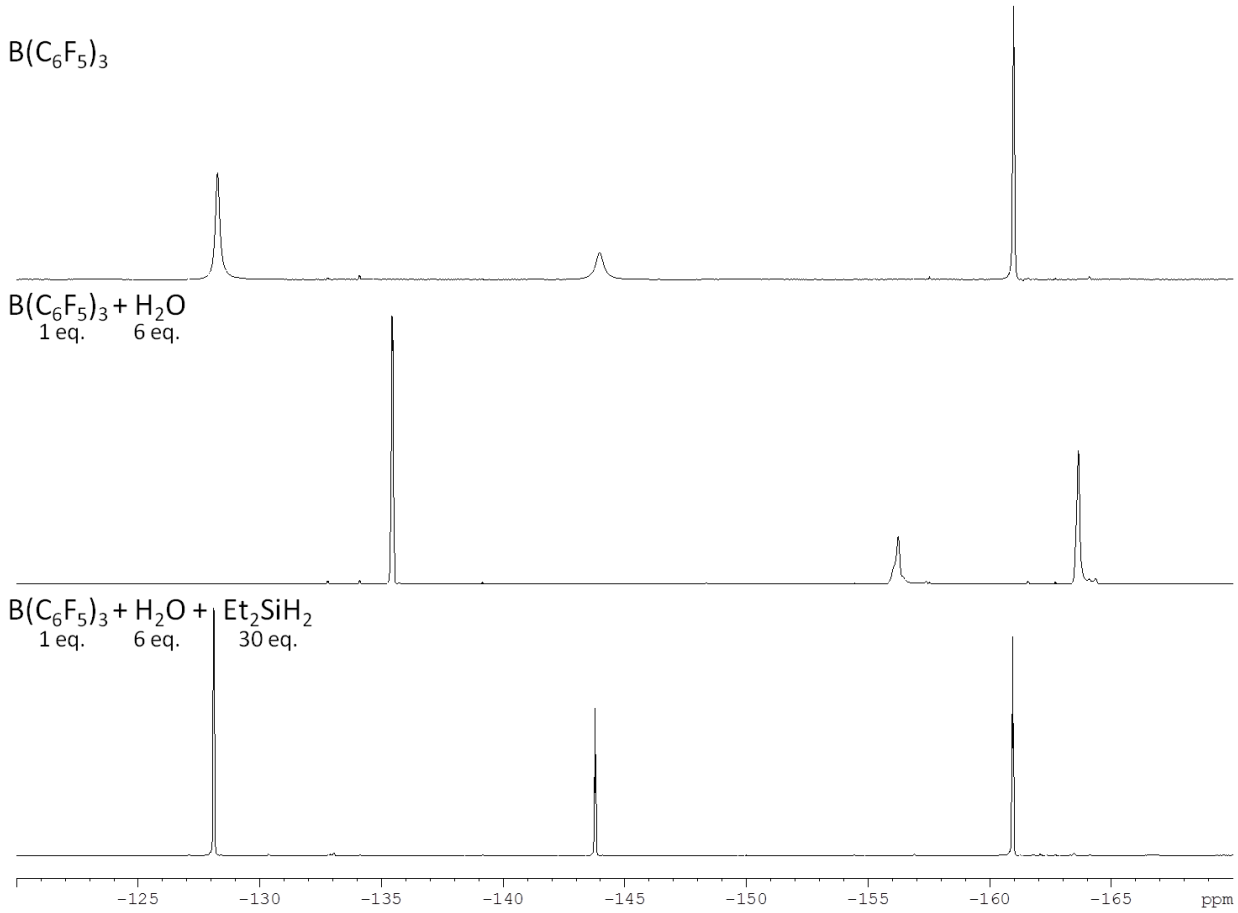

Figure 4.7: $^{19}F\{^1H\}$ NMR spectra of $B(C_6F_5)_3$ before the addition of water, after the addition of water, and after the addition of water and Et_2SiH_2 showing that the a new species forms in the presence of water but that the addition of Et_2SiH_2 consumes water, reverting the fluorine-containing species back to $B(C_6F)_3$

$B(C_6F_5)_3$-catalyzed reduction of Me_2EtSi-protected glucitol with Et_2SiH_2 and Me_2EtSiH

In an argon-filled glovebox, a 1-dram vial was charged with $B(C_6F_5)_3$ (2.9 mg, 0.006 mmol, 6 mol %) and Me_2EtSi-protected glucitol (**Me_2EtSi-14**, 69 mg, 0.10 mmol, 1 eq.). 0.25 mL CD_2Cl_2 was added, followed by cyclooctane (2.5 µL, 0.018 mmol, 0.18 eq.). This mixture was transferred to a J-Young tube, and Me_2EtSiH was added (0.26 mL, 2.0 mmol, 20 eq.). The tube was capped and

removed from the glovebox. A $^{13}C\{^{1}H\}$ NMR spectrum taken after two hours showed large peaks in both the carbohydrate region and the alkane region; C-O peaks persisted for over a week (Figure 4.8, bottom).

The above procedure was repeated using 2.5 mg (0.005 mmol, 5 mol %) $B(C_6F_5)_3$, 73 mg Me_2EtSi-protected glucitol (0.10 mmol, 1 eq.), 0.25 mL CD_2Cl_2, 2.5 µL (0.018 mmol, 0.18 eq.) cyclooctane, and Et_2SiH_2 (0.26 mL, 2.0 mmol, 20 eq.). In this case, a $^{13}C\{^{1}H\}$ spectrum taken after 2 hours showed no observable C-O bonds and a significant quantity of alkanes, indicating that the reaction with Et_2SiH_2 proceeds faster than the reaction with Me_2EtSiH (Figure 4.8, top).

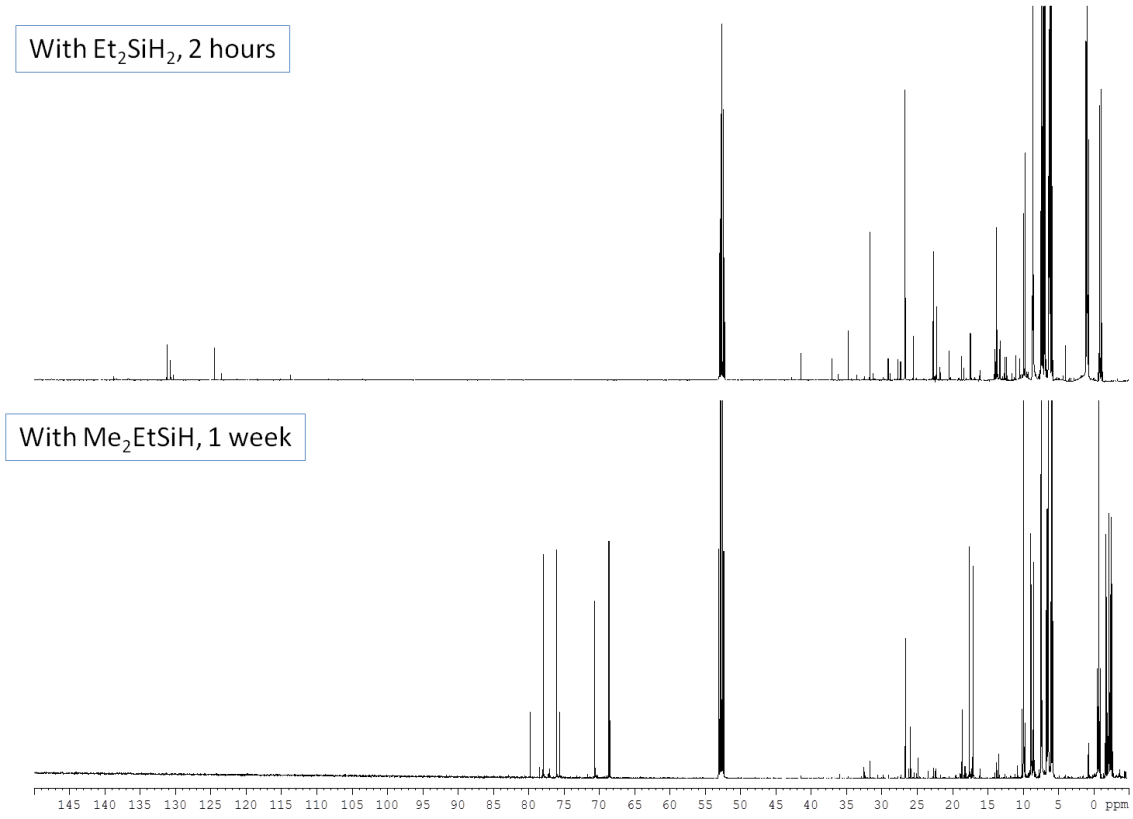

Figure 4.8: Treatment of Me_2EtSi-protected glucitol (Me_2EtSi-14) with $B(C_6F_5)_3$ and Et_2SiH_2 (top, 2 hours) or Me_2EtSiH (bottom, 1 week) showing that deoxygenation is faster with Et_2SiH_2.

Primary vs. Secondary Selectivity

In an argon-filled glovebox, a 1-dram vial was charged with $B(C_6F_5)_3$ (2 mg, 0.004 mmol, 5 mol %) and Me_2EtSi-protected glucitol (**Me_2EtSi-14**, 50 mg, 0.072 mmol, 1 eq.) CH_2Cl_2 (0.5 mL) was added, followed by Me_2EtSiH (25 µL, 0.15 mmol, 2.5 eq.), and the reaction was transferred to an NMR tube. A $^{13}C\{^1H\}$ APT spectrum taken the next day showed methyl resonances in the 10-40 region and methyne resonances in the 50-100 region, indicating that the primary sites on the substrate had been reduced (Figure 4.11). The product was characterized by ^1H and $^{13}C\{1H\}$ NMR in situ and identified as Me_2EtSi-protected 1,6-deoxy glucitol (Figure 4.10 and Figure 4.11). ^1H NMR (600 MHz, CD_2Cl_2): 4.08 (dq, $^3J_{H,H}$ = 2.0 Hz, $^3J_{H,H}$ = 6.1 Hz, 1H), 3.84-3.79 (m, 1H), 3.69 (dd, $^3J_{H,H}$ = 2.0 Hz, $^3J_{H,H}$ = 7.3 Hz, 1H), 3.34 (dd, $^3J_{H,H}$ = 7.3 Hz, $^3J_{H,H}$ = 4.5 Hz, 1H), 1.14 (d, $^3J_{H,H}$ = 6.5 Hz, 3H), 1.05 (d, $^3J_{H,H}$ = 6.1, 3H). $^{13}C\{^1H\}$ NMR (150 MHz, CD_2Cl_2): 78.3 (s), 76.6 (s), 71.0 (s), 69.2 (s), 18.3 (s), 17.8 (s).

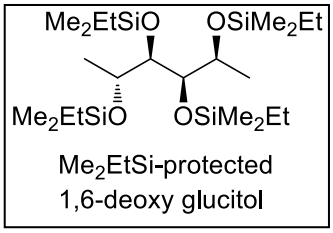

The above procedure was repeated using Et_2SiH_2 (19 µL, 0.15 mmol, 2 eq.) in place of the Me_2EtSiH. The product mixture was considerably more complex, but the major observable species was also 1,6-deoxy glucitol (Figure 4.9).

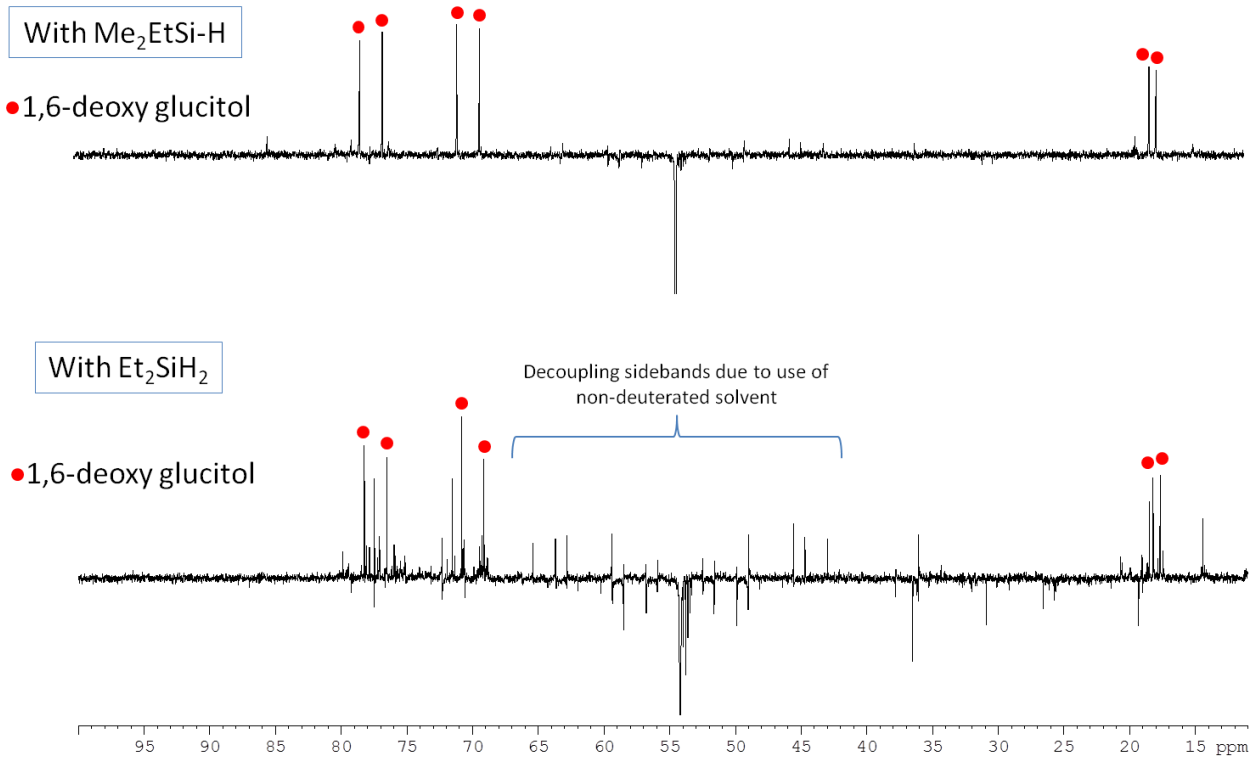

Figure 4.9: $^{13}C\{^1H\}$ APT NMR spectra from treatment of Me_2EtSi-protected glucitol (Me_2EtSi-14) with 5 mol % $B(C_6F_5)_3$ and 2 eq. Me_2EtSiH (top) and 2 eq. Et_2SiH_2 (bottom).

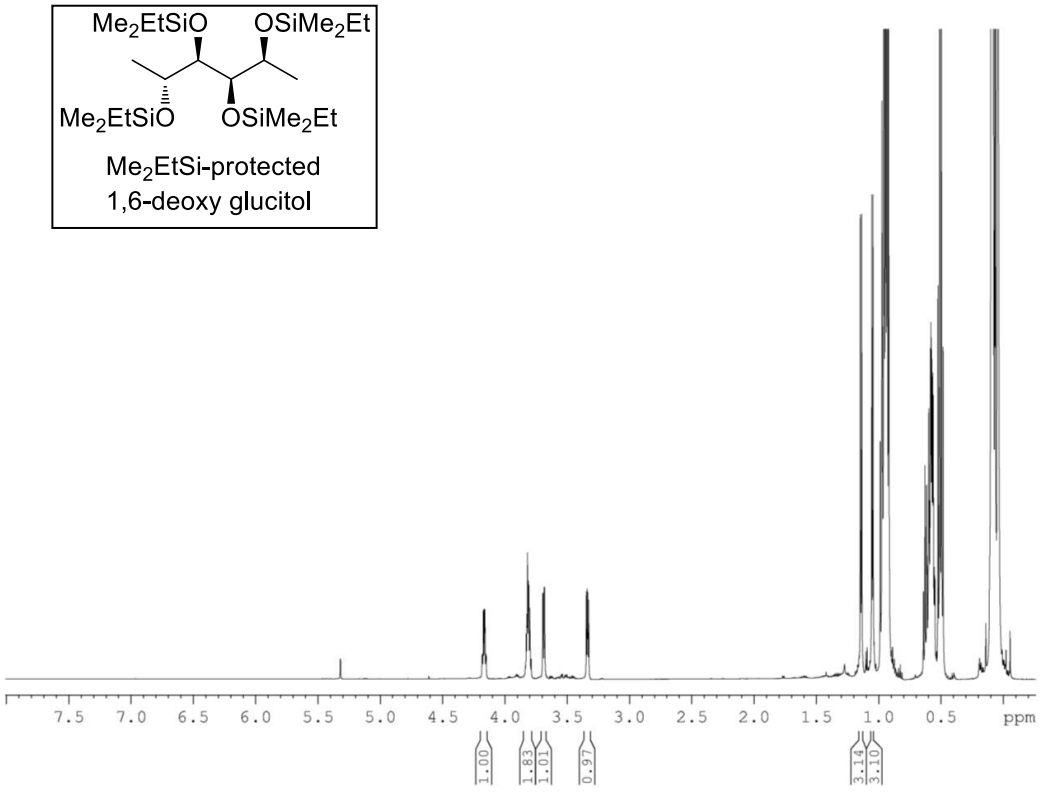

Figure 4.10: In situ ^{1}H NMR of Me_2EtSi-protected 1,6-deoxy glucitol. Increased integration at 3.8 ppm is due to the slight excess of Me_2EtSiH. Resonances upfield of 1 ppm are silane related.

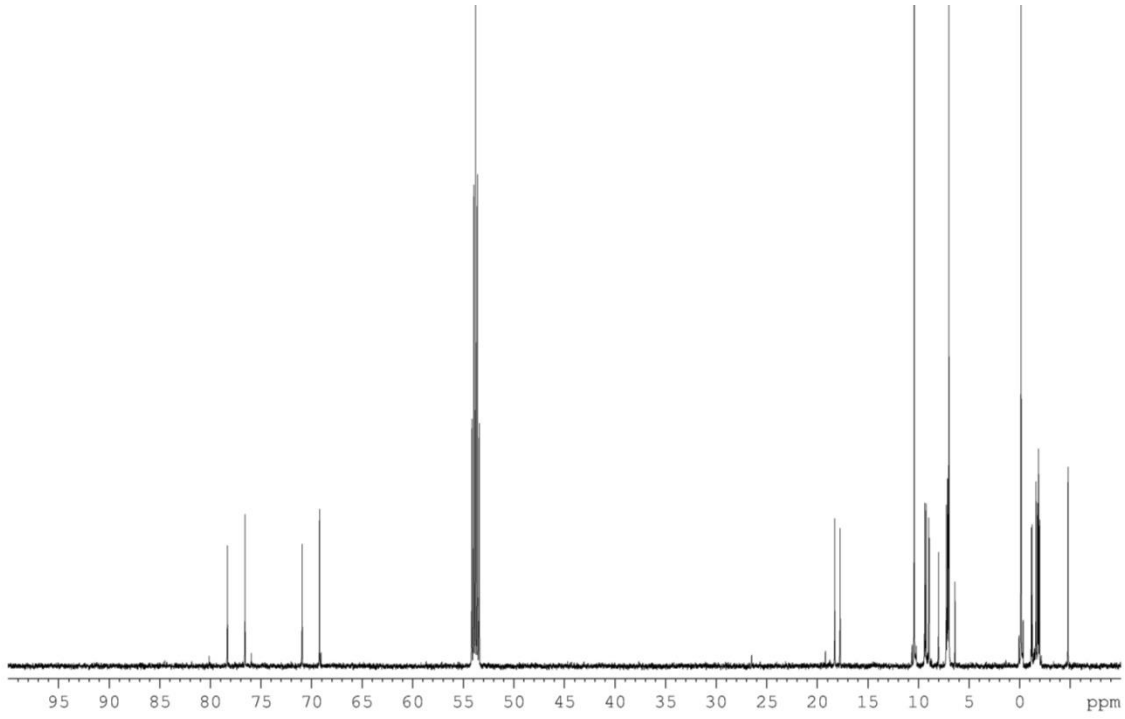

Figure 4.11: In situ $^{13}C\{^{1}H\}$ NMR of Me_2EtSi-protected 1,6-deoxyglucitol. Resonances upfield of 12 ppm are silane related.

Scale-up and isolation of 1,6-deoxy glucitol

In an argon-filled glovebox, a pressure tube was charged with $B(C_6F_5)_3$ (21 mg, 0.041 mmol, 5 mol %) and glucitol (**14**, 150 mg, 0.82 mmol, 1 eq). CH_2Cl_2 (4 mL) was added to give a heterogeneous mixture, followed by the addition of Me_2EtSi-H (1 mL, 7.5 mmol, 9 eq). Vigorous bubbling was observed. The pressure tube was capped, removed from the glovebox, and stirred for 4 h at ambient temperature (caution: hydrogen evolution as a result of alcohol protection resulted in elevated pressure). Volatiles were then removed on a rotovap and the resulting oil was taken up in CD_2Cl_2. 20 µL of benzene was added to use as an integration standard, and ^{1}H and $^{13}C\{^1H\}$ NMR spectra were acquired to calculate an in situ yield. Volatiles were then evaporated from this sample, and the material was transferred to a polypropylene tube using dry THF (although this reaction was not carried out under an inert atmosphere). Additional dry THF was added to give a total volume of 10 mL, and then 0.7 mL pyridine-HF (~30% pyridine, ~70% HF) was added. The reaction vessel was vented to an oil bubbler and stirred overnight. Subsequently, 5 g of dry silica was added to the reaction mixture. The resulting slurry was transferred to the top of a silica plug and flushed with additional THF until TLC (10:90 MeOH/CH_2Cl_2) revealed that no additional material with $R_f \approx 0.3$ was eluting. Volatiles were removed under reduced pressure. Flash column chromatography (10:90 MeOH/CH_2Cl_2) provided 76 mg (62%) of the desired product, 1,6-deoxy glucitol. Separate fractions contained the minor products, which were identified as epimers of 2,3,4-hexanetriol (6:1 *d.r.*) ^{1}H NMR of 1,6-deoxy glucitol (D_2O): 3.71-3.65 (m, 2H), 3.37 (dd, $^3J_{HH}$ = 2.5 Hz, $^3J_{HH}$ = 6.5 Hz, 1H), 3.25 (dd, $^3J_{HH}$ = 2.5 Hz, $^3J_{HH}$ = 9.8 Hz, 1H), 1.04 (d, $^3J_{HH}$ = 6.5 Hz, 3H), $^3J_{HH}$ = (d, $^3J_{HH}$ = 6.5 Hz, 3H) (Figure 4.12). $^{13}C\{^1H\}$ NMR (D_2O): 74.7 (s), 73.7 (s), 68.6 (s), 67.0 (s), 18.3 (s), 18.1 (s) (Figure 4.13). HRMS: *m/z* $[M + Na]^+$

found 173.0748, calcd 173.0784 for $C_6H_{14}NaO_4$. ^{1}H NMR of major epimer of 2,3,4-hexanetriol (D_2O): 3.71 (quintet, $^3J_{HH}$ = 6.4 Hz, 1H), 3.51 (ddd, $^3J_{HH}$ = 3.7 Hz, $^3J_{HH}$ = 5.5 Hz, $^3J_{HH}$ = 8.0 Hz, 1H), 3.20 (dd, $^3J_{HH}$ = 3.7 Hz, $^3J_{HH}$ = 6.4 Hz, 1H), 1.41-1.35 (m, 2H), 1.06 (d, $^3J_{HH}$ = 6.4 Hz, 3H), 0.78 (t, $^3J_{HH}$ = 7.2 Hz, 3H) (Figure 4.14). ^{13}C{^{1}H} NMR of major epimer of 2,3,4-hexanetriol (D_2O): 76.5 (s), 71.9 (s), 67.2 (s), 25.5 (s), 17.7 (s), 9.3 (s) (Figure 4.15).

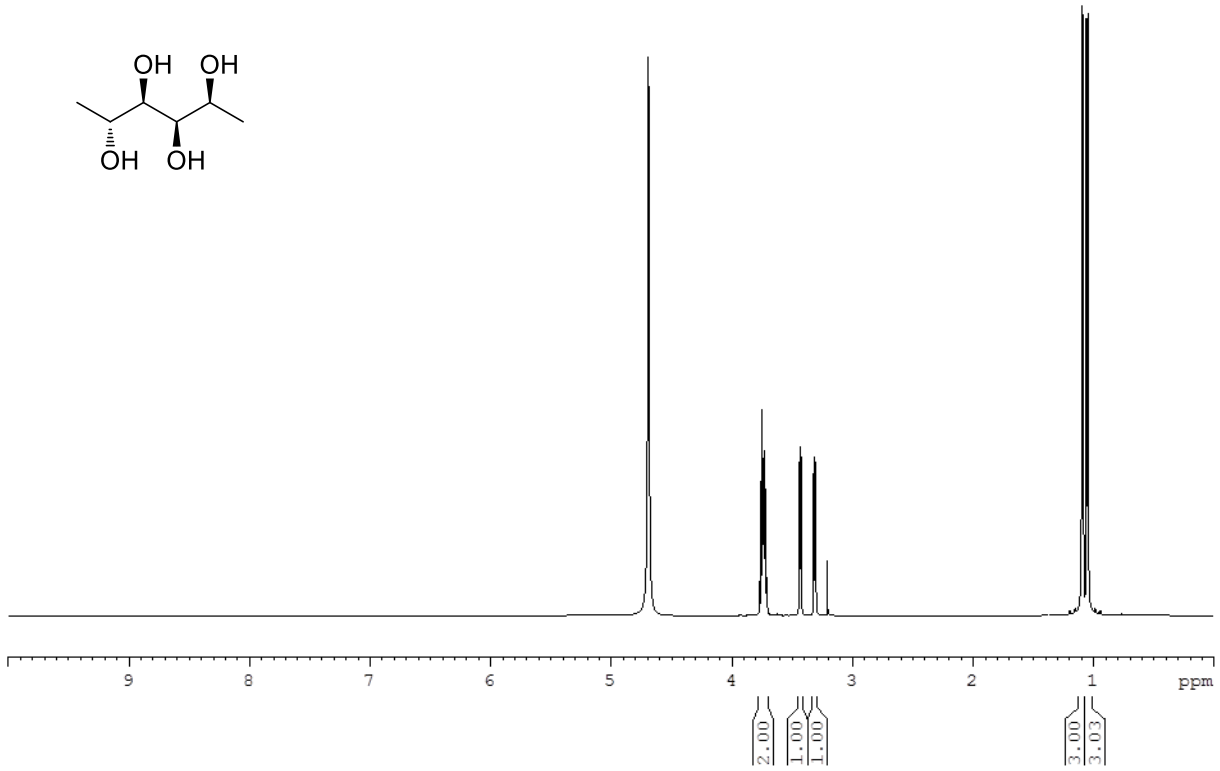

Figure 4.12: ^{1}H NMR spectrum of unprotected 1,6-deoxyglucitol.

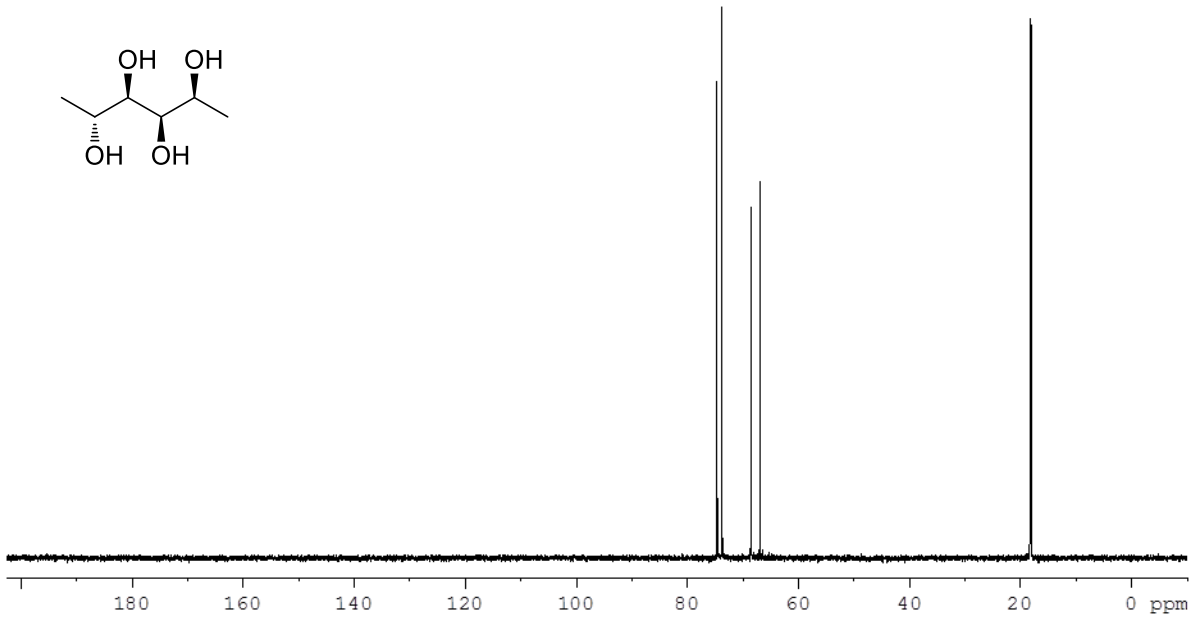

Figure 4.13: $^{13}C\{^{1}H\}$ NMR spectrum of unprotected 1,6-deoxyglucitol.

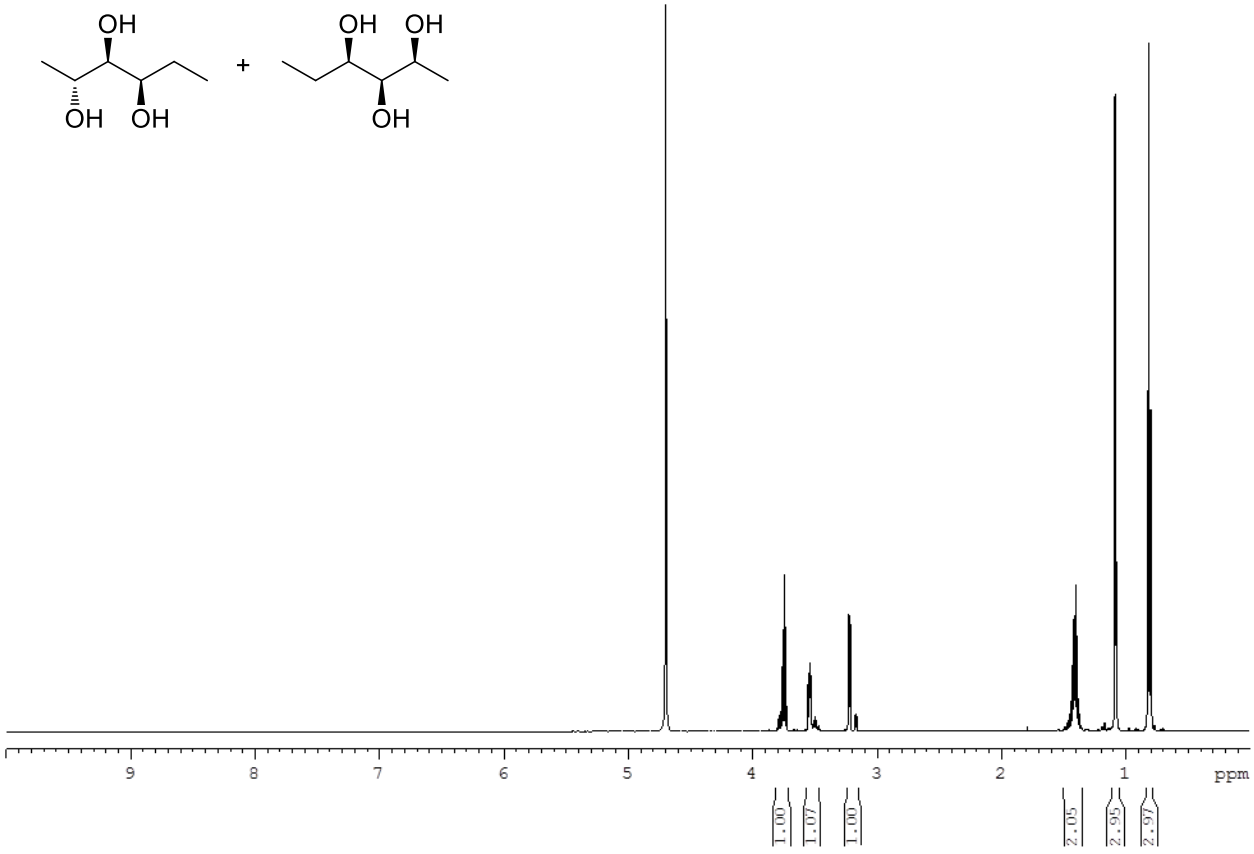

Figure 4.14: ^{1}H NMR spectrum of unprotected 2,3,4-hexanetriol epimers

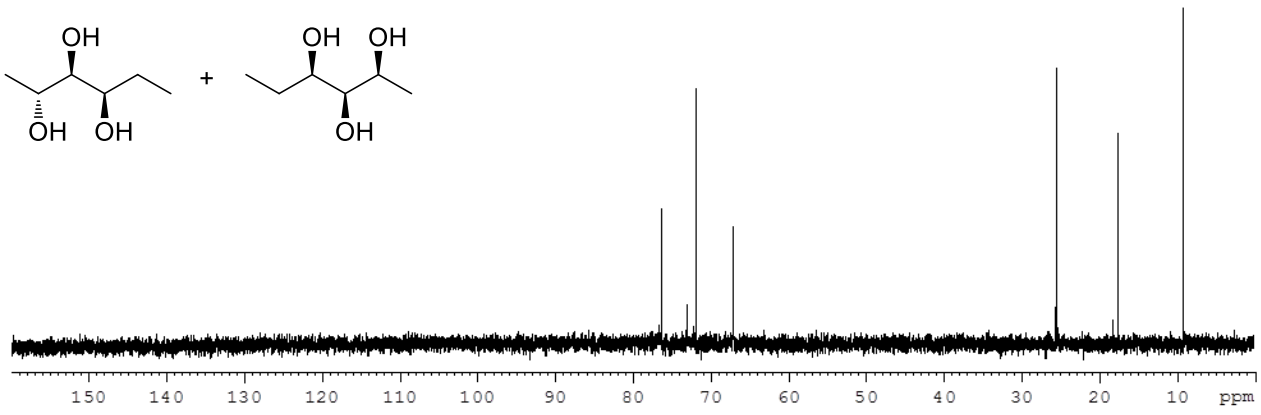

Figure 4.15: $^{13}C\{^{1}H\}$ NMR spectrum of unprotected 2,3,4-hexanetriol epimers.

Stepwise reduction of Et_3Si-protected glucose

In an argon-filled glovebox, a vial was charged with $B(C_6F_5)_3$ (2 mg, 0.004 mmol, 10 mol %) and Et_3Si-protected glucose (**Et_3Si-13**, 30 mg, 0.04 mmol, 1 eq.). CD_2Cl_2 (0.25 mL) was added, followed by Me_2EtSi-H (0.25 mL, 1.8 mmol, 45 eq.). The reaction mixture was transferred to a J-Young tube and removed from the glovebox. After 2 hours at room temperature, $^{13}C\{^{1}H\}$ NMR showed, glucitol as the major product. After 16 hours at room temperature, the major observed product was 1,6-deoxy glucitol (Figure 4.16). Doubling of peaks is presumed to be caused by protecting group exchange between -$SiMe_2Et$ and -$SiEt_3$ (see Figure 4.17).

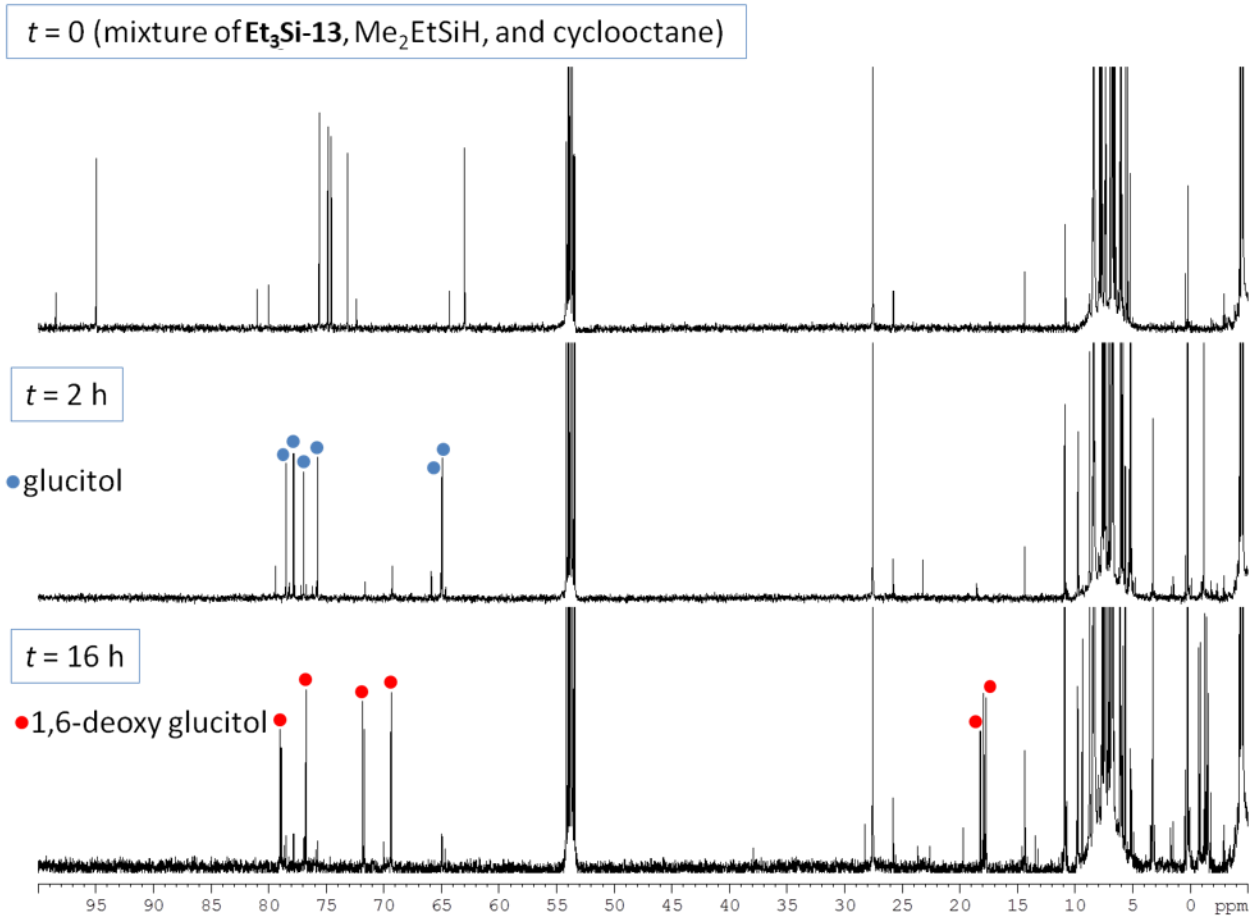

Figure 4.16: Et_3Si-protected glucose (Et_3Si-13, top), 2 hours (middle) and 16 hours (bottom) after the addition of $B(C_6F_5)_3$ and Me_2EtSi-H.

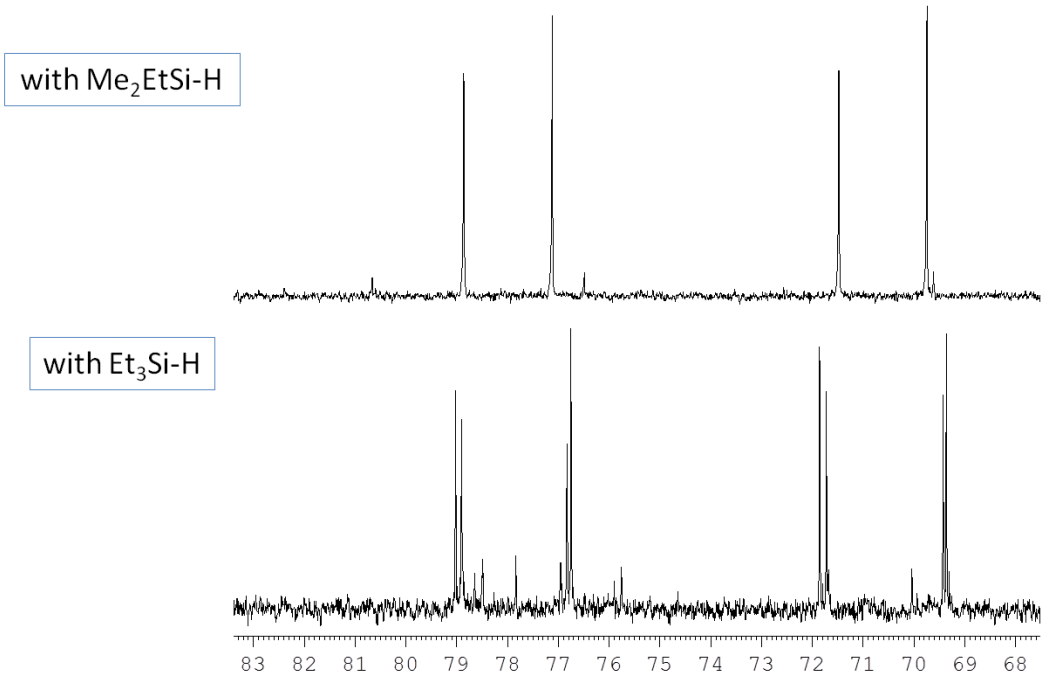

Figure 4.17: $B(C_6F_5)_3$-catalyzed reduction of Me_2EtSi-protected glucitol with Me_2EtSiH (top) and Et_3SiH (bottom). When R is different for the R_3Si-protecting group and R_3Si-H, a doubling of peaks is observed, likely due to silyl protecting group exchange. This doubling is avoided by matching the silane with the protecting group.

Chapter 5 **Selective Deoxygenation of Monosaccharides**

5.1 ***Synthesis of chiral feedstocks***

The synthesis of small molecule building blocks has been the focus of much effort in recent years.[135-137] Particularly desirable are compounds with well-defined stereochemistry.[143] The synthesis of chiral compounds from achiral starting materials is challenging and has been the subject of extensive research, often focusing on stereoselective catalysts.[144] An alternative approach involves staring with chiral substrates and ensuring that their chirality is preserved throughout their catalytic transformations.[145] In this scenario, carbohydrates represent an attractive source of chirality as they naturally occur with well-defined stereochemistry. In addition, the availability of sugars with a wide variety of stereochemical frameworks suggests that the development of protocols for their reactions would allow access to building blocks with a similarly wide variety of stereochemistry.

Chapters 3 and 4 reported hydrosilylative reductions of carbohydrates using metal and non-metal catalysts. In these cases, the use of the very active secondary silane Et_2SiH_2 effected the complete deoxygenation of cellulosic biomass, resulting in the production of hexanes. In addition, our group and others have reported that alcohols and ethers can be reduced by the combination of $B(C_6F_5)_3$ and a tertiary silane, with primary alcohols and ethers typically being more susceptible

[143] Xia, Q.-H.; Ge, H.-Q.; Ye, C.-P.; Liu, Z.-M.; Su, K.-X. *Chem. Rev.* **2005**, *105*, 1603–1662.

[144] Mikami, K.; Lautens, M. *New Frontiers in Asymmetric Catalysis*; Wiley-Interscience, Inc.: Hoboken, N.J, 2007.

[145] Blaser, H. U. *Chem. Rev.* **1992**, *92*, 935–952.

to reduction than secondary or tertiary alcohols. Reported in Chapter 5 is the exploitation and further development of this methodology, enabling the transformation of inexpensive and readily available carbohydrates into difficult-to-access small molecule building blocks with multiple chiral centers.

5.2 *Selective hydrosilylative reduction of glucitol and mannitol*

Initial experiments with linear monosaccharides such as glucitol, **14**, revealed that a combination of $B(C_6F_5)_3$ and Me_2EtSiH was able to hydrosilylatively reduce the primary alcohol positions, giving tetraol **14c** as the major product (Scheme 5.1). Deprotection with HF/pyridine and purification via column chromatography gave unprotected **14c** and, when mannitol **21a** was utilized, **21c.**

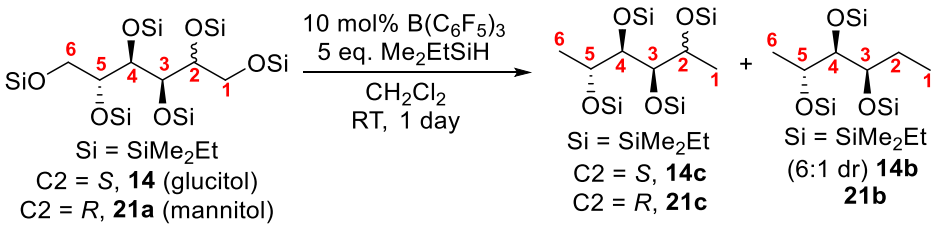

Scheme 5.1: Reduction of glucitol and mannitol to tetraol and triol products

Available mechanistic data[67,71] would suggest that these primary reductions take place by borane catalyzed generation of a silylium ion equivalent, transient generation of a primary disilyloxonium followed by S_N2 displacement with either the $HB(C_6F_5)_3^-$ counterion or excess R_3Si-H. In the discussion here we consider the borohydride to be the most likely reductant, though this has not been rigorously established with the tested substrate classes (Figure 5.1).

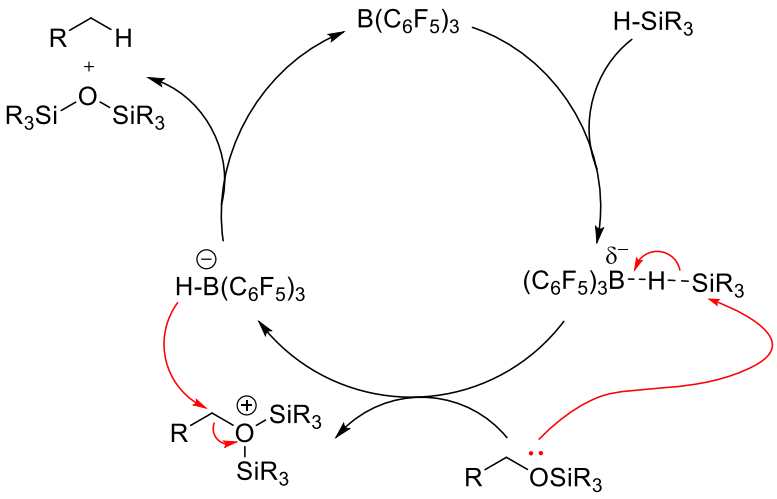

Figure 5.1: Proposed catalytic cycle for hydrosilylative reduction and silyl-protected alcohol substrates

Starting with unprotected glucitol and allowing both the protection and reduction to take place in situ (with concomitant generation of H_2) gives similar results to reducing pre-protected **14.** When beginning with unprotected carbohydrates, an appropriate amount of additional silane was required to account for both the protection and the reduction. As in chapters 3 and 4, pre-protected sugars were often used to avoid extensive off-gassing of H_2.

In addition to **14c**, a small quantity (5%) of triol **14b** was observed as a 6:1 mixture o5f diastereomers. The predominant diastereomer was determined by applying the same experimental conditions to mannitol, **21a**, which should provide a single triol that matches one possible diastereomer of the 1,2,6-deoxy gluco-triol. Similar to the glucitol case after one day, the product mixture contained symmetric tetraol **21c** and a single triol (**21b)** in a 10:1 ratio. ^{1}H and ^{13}C NMR spectroscopy indicated that **21b** matched the major diastereomer of **14b**. The major triol derived from glucitol therefore results from the preferential reduction of the C_2 over the C_5 position in the non-symmetric **14c**.

This suggestion was additionally confirmed by the reduction of 1,2-dideoxy glucose**, 22a**. Since **22a** is not oxygenated at the C_2 position, its stepwise reduction provides the 1,2,6-deoxy

compound **22b** (Scheme 5.2). When cyclic glucose or mannose is similarly reduced instead of the acyclic **14** and **22a,** the same compounds products ensue.

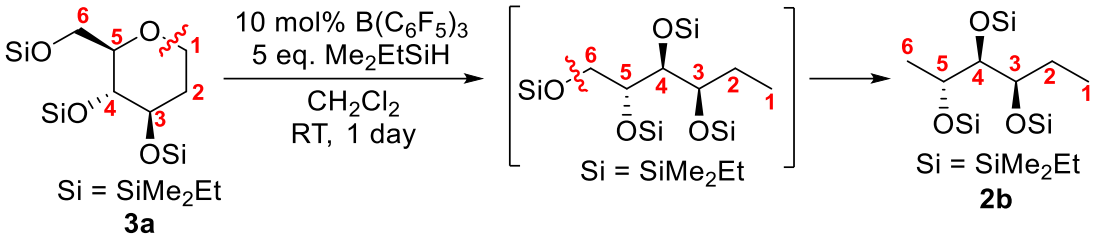

Scheme 5.2: Reduction of 1,2-dideoxy glucose

5.3 *Selective hydrosilylative reduction of galactitol*

In contrast to the gluco- and manno- series, the same reaction conditions convert galactitol **23a** directly to a single diastereomer of a triol (Scheme 5.3A). That is, galactitol is more reactive. Unlike the above cases, however, the ^{1}H and ^{13}C NMR spectra of this triol did not match those of the triol (**24b**) that results from reduction of 1,2-dideoxy galactose **24a** (Scheme 5.3C). In addition to 2**3a**, galactose (**25a**) and methyl galactoside (**26a**) also proceeded to triol **23b** (distinct from **24b**) and did not stop at tetraol **23c** (Scheme 5.3B). This mismatch suggested that one of the reduction sequences (**23a** to **23b** or **24a** to **24b**) causes the inversion of one or more stereocenters.

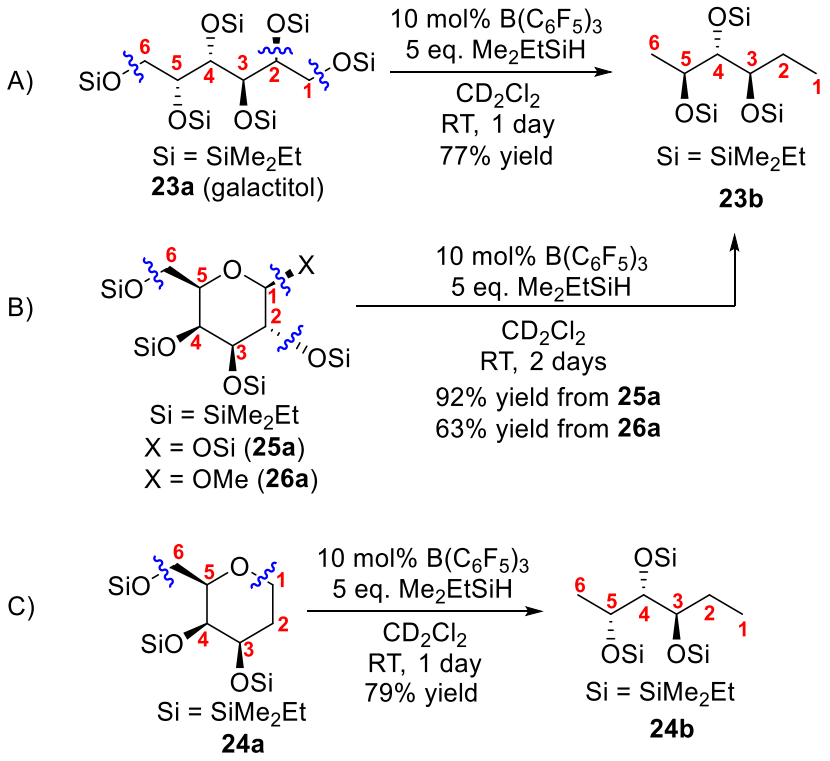

Scheme 5.3: Reduction of galactitol, galactose, C_1-methoxy galactose, and 1,2-dideoxy galactose to triols

A stereochemical analysis of the polyols by the method of Kishi[146] enabled the source of this discrepancy to be determined (Figure 5.2). This spectroscopic method relies on patterns of vicinal H/H coupling constants to characterize the relative stereochemistry of adjacent carbinol centers. First, reduction of **23a** using only two equivalents of Me_2EtSi-H provided tetraol **23c** as the major product **(**Scheme 5.4**)**. Comparison of **23c** to Kishi's polyol library[146] confirmed that the stereochemistry of the secondary carbinol centers in **23c** matched those of the fully oxygenated **23a**. That is, primary reductions (C_1 and C_6) do not affect the secondary centers. The Kishi analysis on the two different triol products indicated that 1,6-reduction of **24a** proceeds without compromising any of the secondary centers to form the expected product **24b**, while 1,2,6-reduction of galactitol **23a** provides a product that has been epimerized at C_5. Since 1,6-reduction

[146] Higashibayashi, S.; Czechtizky, W.; Kobayashi, Y.; Kishi, Y. *J. Am. Chem. Soc.* **2003**, *125*, 14379–14393.

does not cause this, it is clear that monoreduction of tetraol **23c** to triol **23b** proceeds with C_5 inversion.

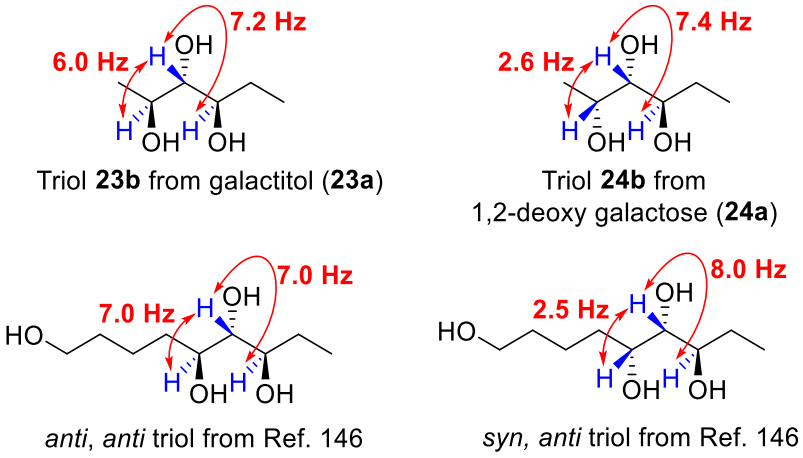

Figure 5.2: Coupling constants used to determine stereochemistry of triol products from reduction of 23a and 24a

5.4 *Proposed cyclic intermediates*

To account for this behavior, we suggest that C_2 reduction occurs via the intermediacy of a cyclic silyl-oxonium ion that results from intramolecular attack of the C_2-OSi group onto a putative doubly silylated C_5 oxygen (**I**) as shown in Scheme 5.4. Of course, given the inversion symmetry of **23c**, the O5 attack onto the activated C_2-O center is equally likely to give the enantiomeric intermediate. Analysis of **II** suggests that nucleophilic hydride attack by either $(C_6F_5)_3B\text{-}H^-$ or $Me_2EtSi\text{-}H$ along a trajectory that minimizes steric congestion with the adjacent $OSiR_3$ group (red path) provides the observed triol **23b** wherein the stereochemistry at C_5 has been inverted relative to tetraol **23c**, and with retention of the C3 and C4 stereochemistry (Scheme 5.4).

Stereochemical control of nucleophile addition to related cyclic oxonium compounds has been demonstrated in several similar systems.[147-149]

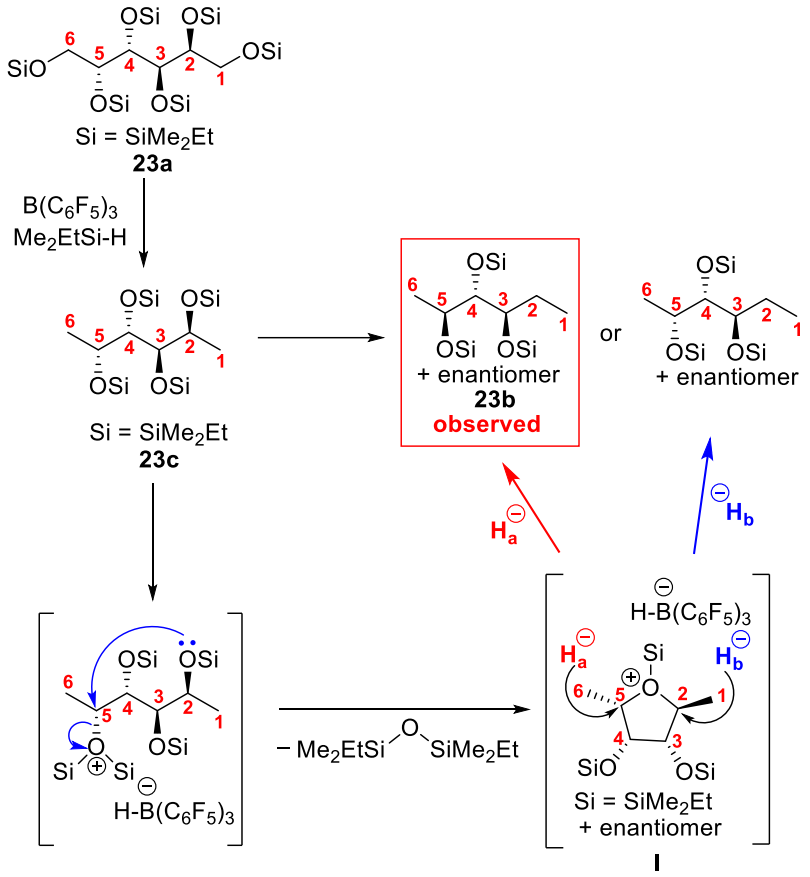

Scheme 5.4: Reduction of galactitol via a cyclic intermediate that results in C_5 epimerization

Additional evidence supporting the notion that cyclic intermediates may be common in such reductions was obtained from the reduction of iditol **27a** (Scheme 5.5). Although the reduction is sluggish and provides a complex product mixture at intermediate times, reacting for a day leads to full conversion of **27c** to **27b**. Like **23b,** a stereochemical analysis of **27b** indicated that one stereocenter had been inverted. This outcome is also predicted by invoking an O2 to C_5

[147] Smith, D. M.; Tran, M. B.; Woerpel, K. A. *J. Am. Chem. Soc.* **2003**, *125*, 14149–14152.

[148] Smith, D. M.; Woerpel, K. A. *Org. Lett.* **2004**, *6*, 2063–2066.

[149] Larsen, C. H.; Ridgway, B. H.; Shaw, J. T.; Smith, D. M.; Woerpel, K. A. *J. Am. Chem. Soc.* **2005**, *127*, 10879–10884.

or a symmetry equivalent O5 to C_2 cyclization event to yield the cyclic **III**, C_2 reduction of which yields **27b**. In analogy to the analysis of **II**, reduction at the least congested center (C_2), which brings the nucleophile along a path that is *anti* to the C3-OSi substituent, leads to the observed product.

The generation of a cyclic intermediate does not necessarily lead to a product with a center inverted. Take the case of allitol **28a**, which would lead to a silyl oxonium (**IV**) with the stereochemistry shown in Scheme 5.6. In this situation, reduction of the least congested site (C_5) leads to a product where the inverted center is the one excised from the structure. That is, the C_2 vs. C_5 reduction preference occurs at, and is predicted by, the structure of the silyl oxonium intermediate. This same situation applies to mannitol **21a**, which should generate silyl oxonium **V** en route to **21b** (Scheme 5.7). Although an invertive process occurs to form the cyclic intermediate, the diastereoselectivity of its reduction leads to a non-invertive product.

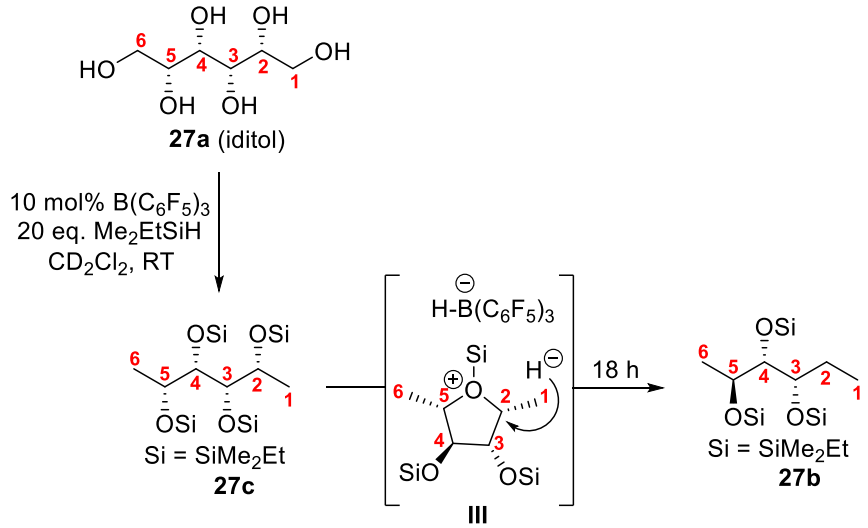

Scheme 5.5: Reduction of iditol via a cyclic intermediate that results in C_5 epimerization

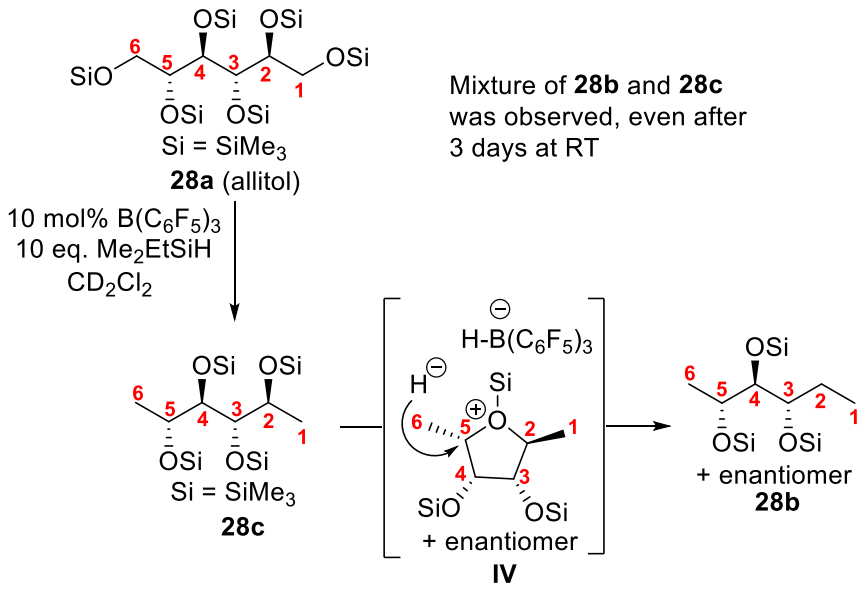

Scheme 5.6: Reduction of allitol via a cyclic intermediate does not result in the inversion of stereocenters

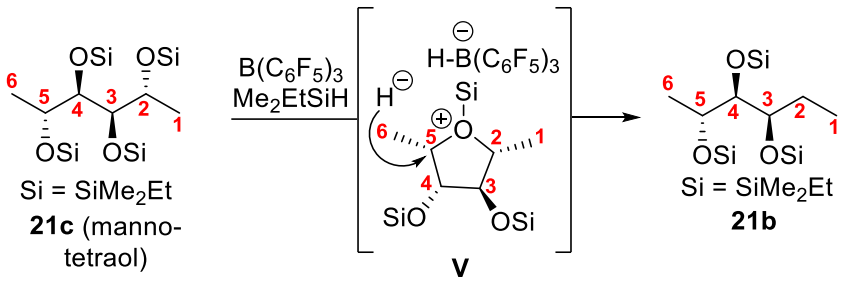

Scheme 5.7: Reduction of mannitol via a cyclic intermediate does not result in the inversion of stereocenters

This same model also provides a rational explanation for the observation of two triols in the reduction of glucitol. Glucitol **14** is unique among the tested substrates in that it displays neither C_2 nor inversion symmetry. As such, it can produce diastereomeric cyclic silyl oxonium ions from either C_2-O to C_5 or C_5-O to C_2 attack (Scheme 5.8). Since both intermediates have C_2 symmetry, they should each lead to a single (but different) triol product. We propose that the observed diasteroselectivity results from different rates of cyclizing to intermediates **VI** and **VII** from **14c**. While it is tempting to ascribe a detrimental cost of generating a species with two pairs

of *syn* substituents on the central tetrahydrofuran ring (**VI**) versus **VII**, with an all anti relationship of ring substituents, the real reason may be more complex.

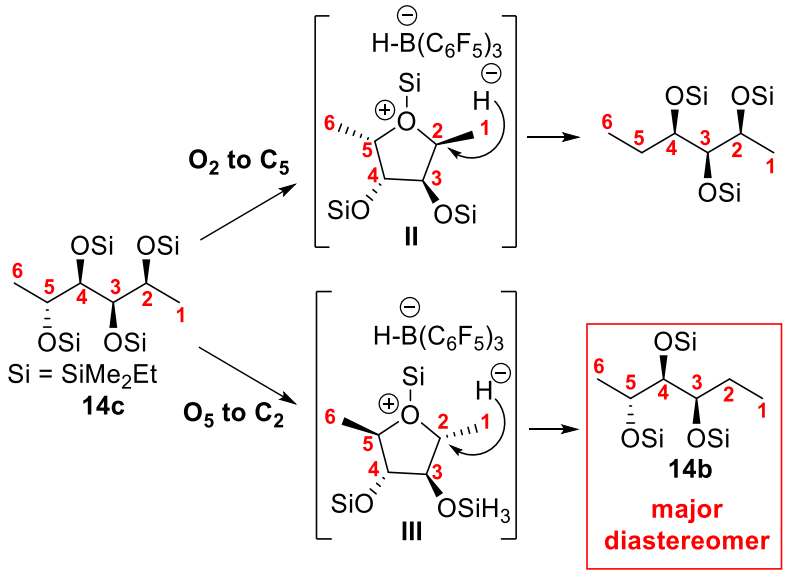

Scheme 5.8: Two cyclic intermediates are possible in the reduction of glucitol; reduction of II leads to the minor diastereomer of triol while reduction of III leads to the major observed diastereomer of triol

5.5 *Independent generation and characterization of proposed cyclic intermediates*

The cyclic intermediates **II-VII** proposed for the conversion of tetraol to triol were of particular interest, as they account for the observed stereochemistry of the triol products and apparently also influence the reactivity of the tetraol. In situ spectroscopic studies show no sign of an intermediate during the tetraol to triol conversion, suggesting that the rate of reduction of cyclic intermeidates is faster than the rate of tetraol reduction. Evidence for a cyclic silyl-oxonium intermediate was thus gathered by generating a silylium ion equivalent that was free of a reducing counterion or excess silane. This was accomplished using a combination of Me_2EtSiH and $[Ph_3C][BAr^F{}_4]$ ($BAr^F{}_4$ = tetrakis(pentafluorophenyl)borane) to generate a stoichiometric quantity of the $[Me_2EtSi][BAr^F{}_4]$ equivalent in situ, analogous to methods used by Brookhart,[74] and

Lambert.[150] This method provides an equivalent of silyl cation to activate the substrate, without an available hydride to complete the reduction.

After Me_2EtSiH is added at -78^{0}C to a mixture of $[Ph_3C][BAr^F{}_4]$ and isolated **23c**, the yellow color of the trityl cation fades quickly on warming to room temperature, yielding a solution of a new species, which we attribute to the silyl oxonium ion **II′** (Scheme 5.9A). Intermediate **II′** differs from **II** in that its counterion is the noncoordinating $B(Ar^F)_4^-$ instead of the reactive $H\text{-}B(C_6F_5)_3^-$. **II′** was sufficiently stable for full characterization by NMR spectroscopy, but decomposes over the course of hours at ambient temperatures. $^{13}C\{^1H\}$ NMR spectroscopy revealed that the symmetric **23c** was converted to an asymmetric species with two methyl groups (17 and 19 ppm) and four trisubstituted carbon centers (70, 77, 92, and 98 ppm) (Figure 5.3). The chemical shift of two of these trisubstituted carbon centers (at 92 and 98 ppm) move significantly downfield from where one typically observes secondary alcohols (68-83 ppm), consistent with the electron deficient nature of the silyl oxonium ion. 2D NMR experiments indicated that the carbons with peaks at 92 and 98 ppm are adjacent to methyl groups. Although the relative stereochemistry was not readily discernable, the data are consistent with an invertive cyclization process that converts a symmetric tetraol precursor to an asymmetric cyclic species capable of reacting as described in Scheme 5.

[150] Lambert, J. B.; Zhao, Y.; Wu, H. *J. Org. Chem.* **1999**, *64*, 2729–2736.

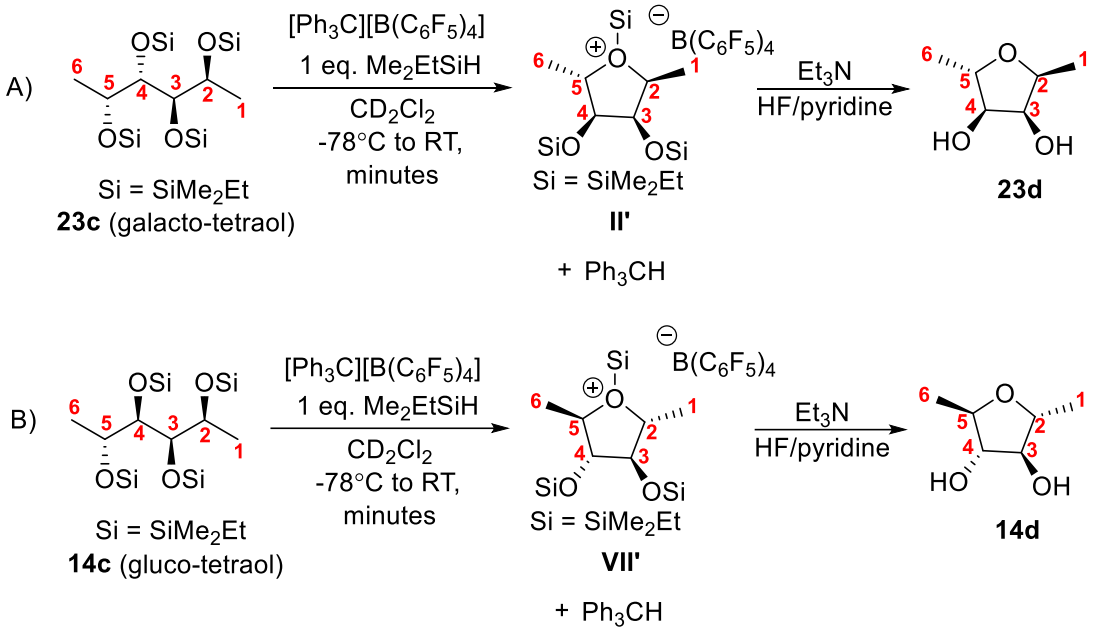

Scheme 5.9: Trapping of proposed cationic cyclic intermediates and isolation of neutral tetrahydrofuran species

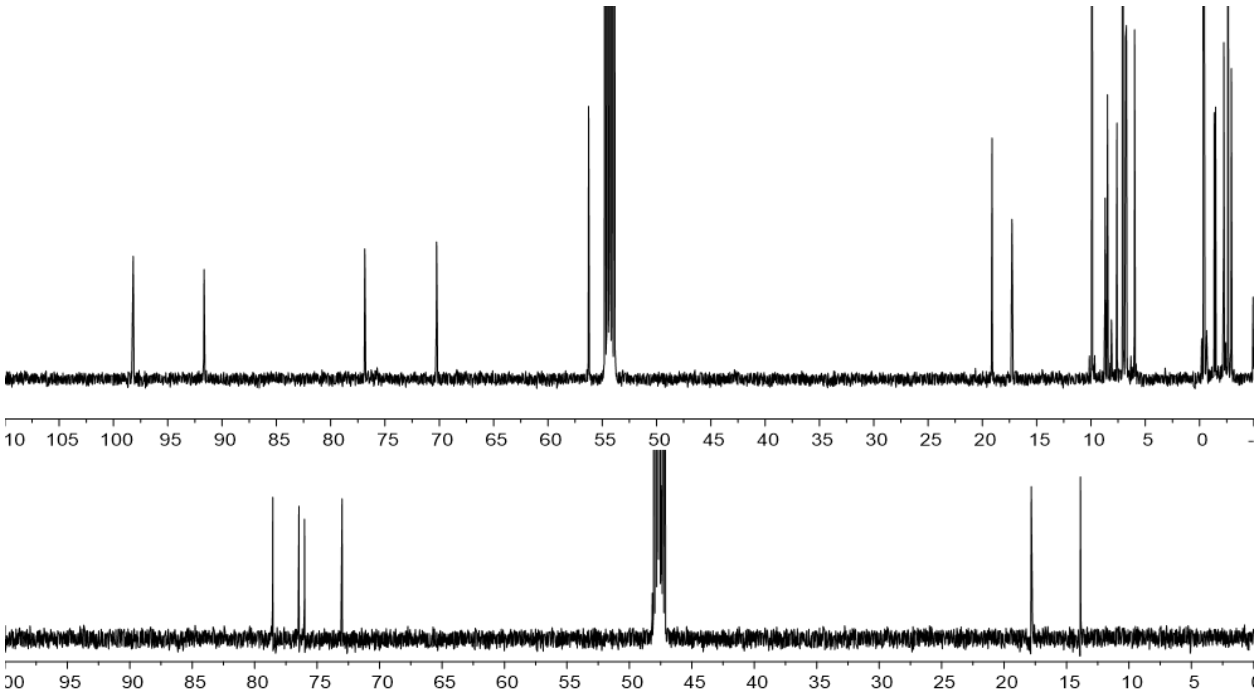

Figure 5.3: Room temperature $^{13}C\{^{1}H\}$ NMR spectra of species generated from treatment of Me_2EtSi-protected galacto-tetraol with 1 eq. Me_2EtSiH in the presence of 1 eq. $[Ph_3C][BAr^F_4]$, before (top, in CD_2Cl_2) and after (bottom, in CD_3OD) silyl deprotection and isolation

The analogous experiment with the gluco-tetraol **14c** was similarly informative. Adding Me_2EtSiH to a mixture of isolated **14c** and $[Ph_3C][B(Ar^F)_4]$ at -78°C, followed by warming to room temperature, led to a quenching of the trityl cation color and a conversion of the asymmetric **1c** to a symmetric species that we attribute to **VII′** (Scheme 5.9B). NMR analysis of **VII′** was similar to the case of **II′**, although the symmetry of **VII′** reduces the number of apparent peaks in the NMR spectrum (Figure 5.4). 2D data indicates that a methyl group with a ^{13}C chemical shift of 19 ppm is adjacent to a trisubstituted carbon center at 102 ppm, which in turn is adjacent to a trisubstituted carbon at 82 ppm. Again, the significant downfield shift of some of the carbon peaks suggests a cationic compound.[74]

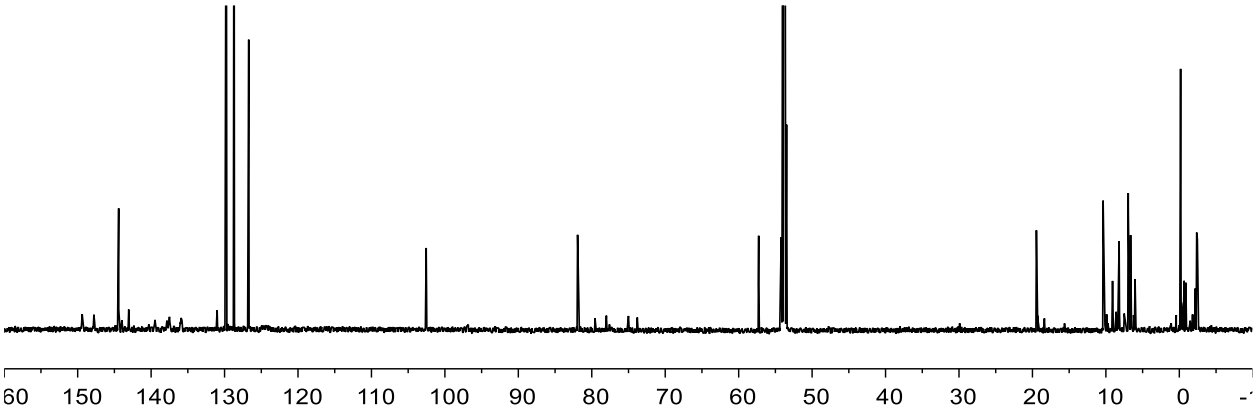

Figure 5.4: Room temperature in situ $^{13}C\{^1H\}$ NMR spectra of species generated from treatment of Me_2EtSi-protected gluco-tetraol with 1 eq. Me_2EtSiH in the presence of 1 eq. $[Ph_3C][BAr^F_4]$.

To confirm our assignment of these putative silyl oxonium species, the reactive SiR_3 group was first removed with Et_3N, followed by silyl ether deprotection with HF/pyridine and isolation by column chromatography to provide the neutral substituted tetrahydrofurans **23d** and **14d** (Scheme 5.9). As expected, NMR spectroscopy indicated that **23d** was asymmetric while **14d** was symmetric. Based on the stereochemistry of the products that they generate under catalytic

conditions, these 3,4-disiloxy tetrahydrofurans are assigned the stereochemistry shown in Scheme 5.9. ^{1}H and ^{13}C NMR spectroscopy were fully consistent with these formations.

5.6 *Alternative syntheses of tetraols and triols*

Although we often matched the silane reducing agent to the silyl protecting group of the substrate (e.g. Me_2EtSiH and Me_2EtSi- protected substrate) or used unprotected alcohols which became protected in situ, occasionally we noted that other protecting group/silane combinations gave the same products. The most cost-effective combination, Me_3Si-protected substrate and Et_3SiH as a reductant, was used when possible, especially if the reactions were to be run on a gram scale. For example, Me_3Si-protected galactitol was reduced to tetraol by 2 equivalents of Et_3SiH.

5.7 *Silyl group exchange*

The importance of silane and protecting group selection was further complicated by the tendency of substrates to undergo silyl group exchange under our reaction conditions in the case of a mismatch between the silane and protecting group. The rate of silyl group exchange was competitive with the rate of reduction, making it difficult to separate the two processes. Since Et_3Si-H appears unable to reduce fully saturated primary or secondary Et_3Si-protected alcohols, replacement of a smaller protecting group by Et_3Si- prevented reactivity at that site. For example, Me_3Si-protected galactitol **23e** could be reduced to a triol by Me_2EtSi-H, but when Et_3Si-H was used as the reductant, exchange of protecting groups installed Et_3Si-groups on two of the secondary alcohols, preventing reduction past the tetraol stage. This was confirmed by isolation of the protected tetraol from the reaction mixture; this product contained two Me_2Si-protecting groups and two Et_3Si-protecting groups (Scheme 5.10).

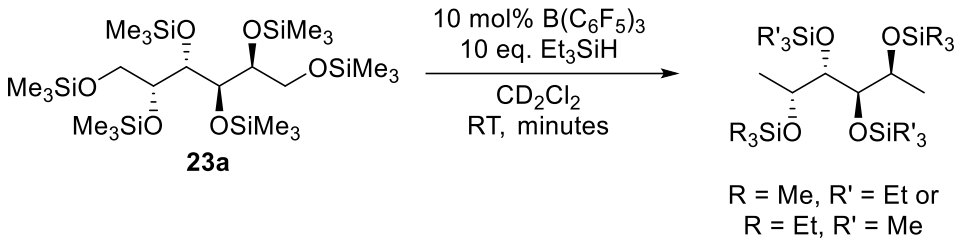

Scheme 5.10: Silyl group exchange upon reduction of Me_3Si-protectd galactitol with Et_3SiH

5.8 *Primary alcohol vs primary ether reduction*

The selective nature of our system allowed us to examine the relative reactivity of primary ethers (CH_2-O-R) and primary alcohols within the same molecule. Although we quickly established that the first reduction of **TES-10a** would cleave the C_1-OMe bond to provide 1-deoxy glucose **12 (**Scheme 5.11**,** step 1), it was unclear whether the next reduction would reduce the C_1-pyranose bond to open the pyranose ring (giving 1-deoxy glucitol **10b**, Scheme 5.11 path *a*) or reduce the C_6 alcohol functionality to provide 1,6-dideoxy glucose **10d** (Scheme 5.11 path *b*). As the first reduction reliably occurs at the C_1 position for this substrate, a deuterium labeling experiment was performed in which Et_3Si-D was used for the first reduction to install a deuterium label at C_1. Subsequent reduction with Et_3Si-H revealed that the deuterium label was located on a methyl group, indicating that the second reduction at C_1 had taken place at the primary ether (Scheme 5.11, path *a*) to afford the ring-opened pentitol product **10b**.

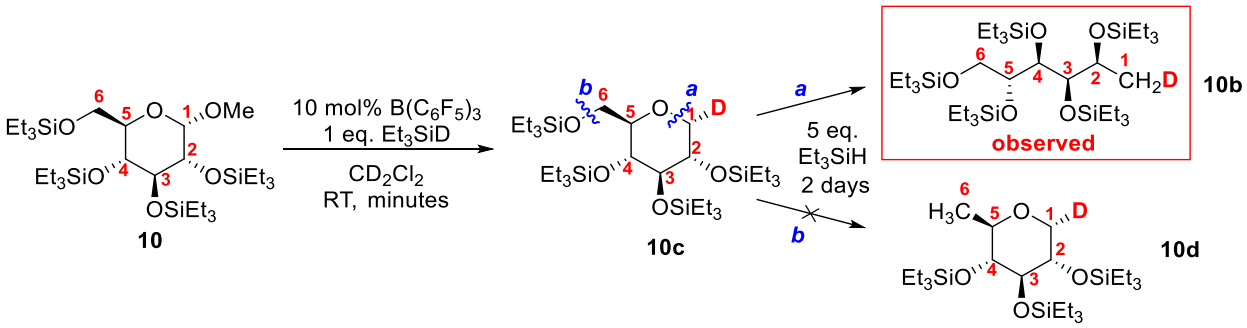

Scheme 5.11: Reduction of C_1 primary ether in preference to C_6 primary alcohol

5.9 *Reduction of simple model compounds*

To aid in our study of selective carbohydrate reduction, simple C_6 model compounds were reduced. For example, a comparison of selectivity for primary vs. secondary ether reduction was performed by treating 2-methyl tetrahydrofuran **29** with 1 eq. of Me_2EtSiH in the presence of catalytic $B(C_6F_5)_3$ (Scheme 5.12). Relative integration of the remaining alcohol peaks in the $^{13}C\{^1H\}$ NMR spectrum revealed roughly a 2.5:1 ratio of primary alcohol (resulting from secondary ether reduction) to secondary alcohol (resulting from primary ether reduction).

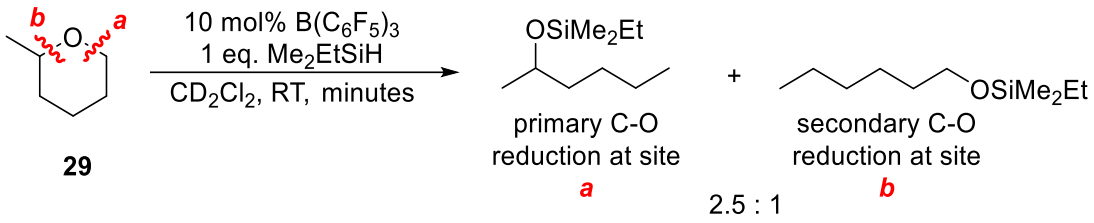

Scheme 5.12: Reduction of primary ethereal C-O bond in preference to secondary ethereal C-O bond

Hexanediol compounds were used to explore the feasibility of in situ intramolecular cyclization enabled by a silylium ion. Me_2EtSi-protected 1,5-hexanediol **30a** and 2,5-hexanediol **31a** were each treated with stoichiometric amounts of $[Ph_3C][BAr^F{}_4]$ and Me_2EtSiH, giving compounds consistent with cationic 2-methyl tetrahydropyran **30b** and 2,5-dimethyl tetrahydrofuran **31b**, respectively (Scheme 5.13). The stereochemistry of the starting materials and cationic products is not known.

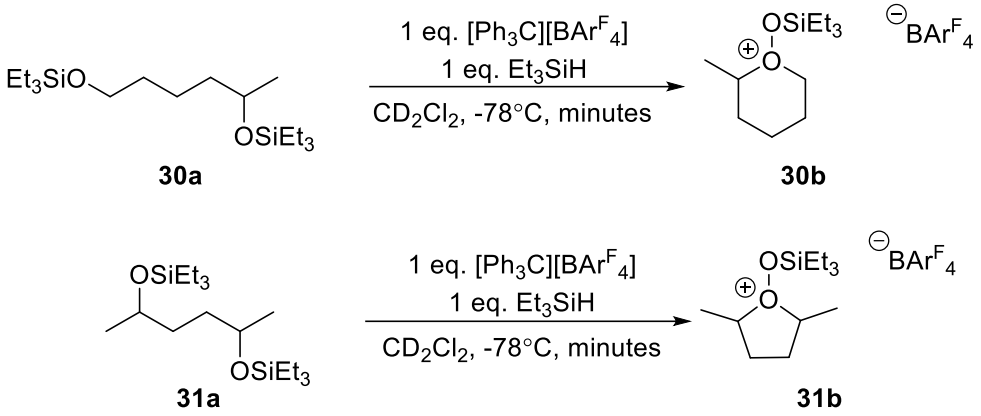

Scheme 5.13: Intramolecular cyclization of model diol compounds

Finally, a noteworthy observation was investigated. Surprisingly, the reduction of 1-deoxy glycoses occurs more slowly than reduction of other substrates such as fully oxygenated glycoses and 1,2-dideoxy glycoses. For example, the reductive ring opening of 1-deoxy glucose **12** to 1-deoxy glucitol takes about a day, versus minutes or hours for other substrates. Nevertheless, ring opening outcompetes even primary alcohol (C_6) reduction, which occurs within minutes for acyclic substrates. This sluggishness suggests that either the catalyst or one of the reagents has been sequestered through interaction with the substrate, further supported by the broadness of peaks observed in both the $^{13}C\{^1H\}$ and the ^1H NMR spectra (Figure 5.5). However, a solution of **12** and $B(C_6F_5)_3$ did not show this broadening of peaks, suggesting involvement of silane. In light of the increased Lewis basicity of ethers relative to silyl-protected alcohols, we proposed coordination of in situ generated silyl cation to the pyranose oxygen (Scheme 5.14).

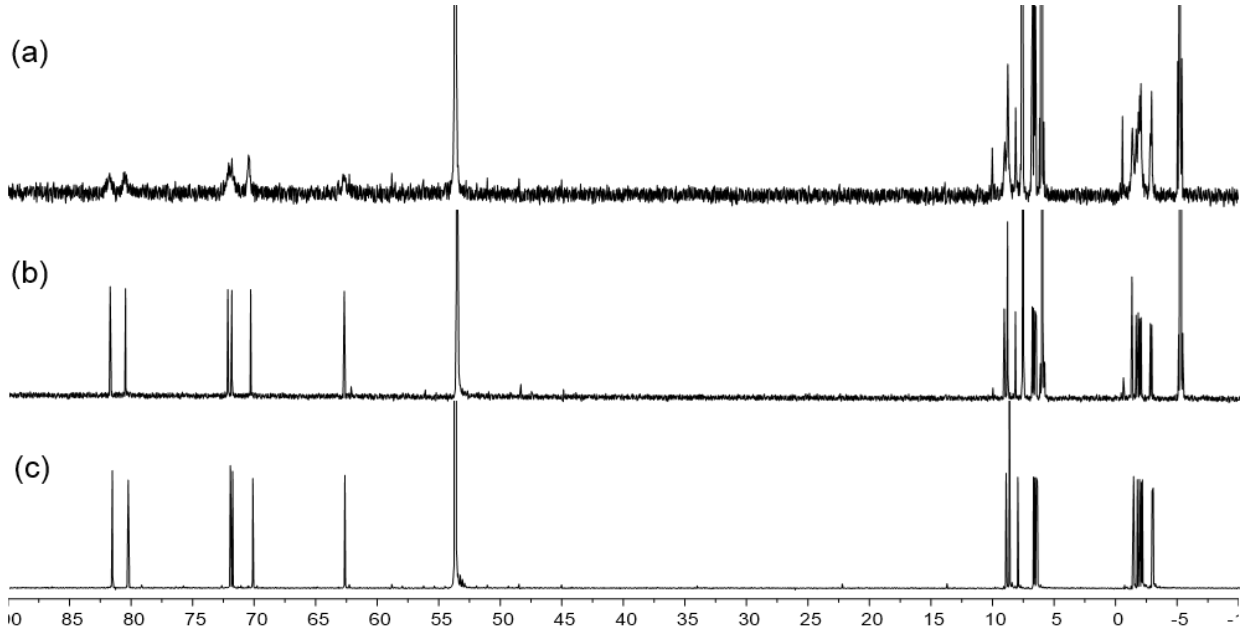

Figure 5.5: Room temperature $^{13}C\{^1H\}$ NMR spectra of Me_2EtSi-protected 1-deoxy glucose 12 in the presence of (a) 10 mol% $B(C_6F_5)_3$ and 10 eq. Me_2EtSiH, (b) 10 eq. Me_2EtSiH, or (c) 10 mol% $B(C_6F_5)_3$.

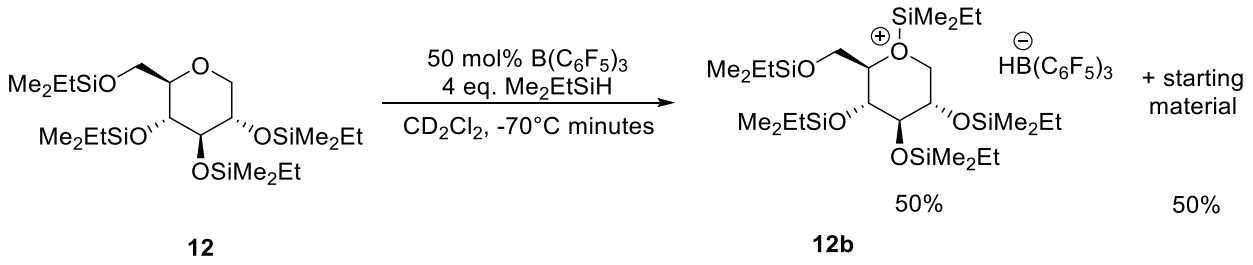

Scheme 5.14: Interaction of silyl cation with 1-deoxy glucose observed by NMR at -70°C.

To investigate this system, we initiated low temperature NMR studies. Observation of the $^{13}C\{^1H\}$ NMR at range of temperatures showed sharper peaks at lower temperatures, along with the presence of new peaks. These peaks are likely small due to the low concentration (0.1 eq.) of $B(C_6F_5)_3$ relative to protected 1-deoxy glucose (1 eq.) and Me_2EtSiH (1 eq.). When the amount of $B(C_6F_5)_3$ was increased to 0.5 eq., the new peaks were larger (Figure 5.6). Relative to regular 1-

deoxy glucose **12**, the new species **12b** contained two peaks that were shifted downfield, while the rest were shifted upfield.

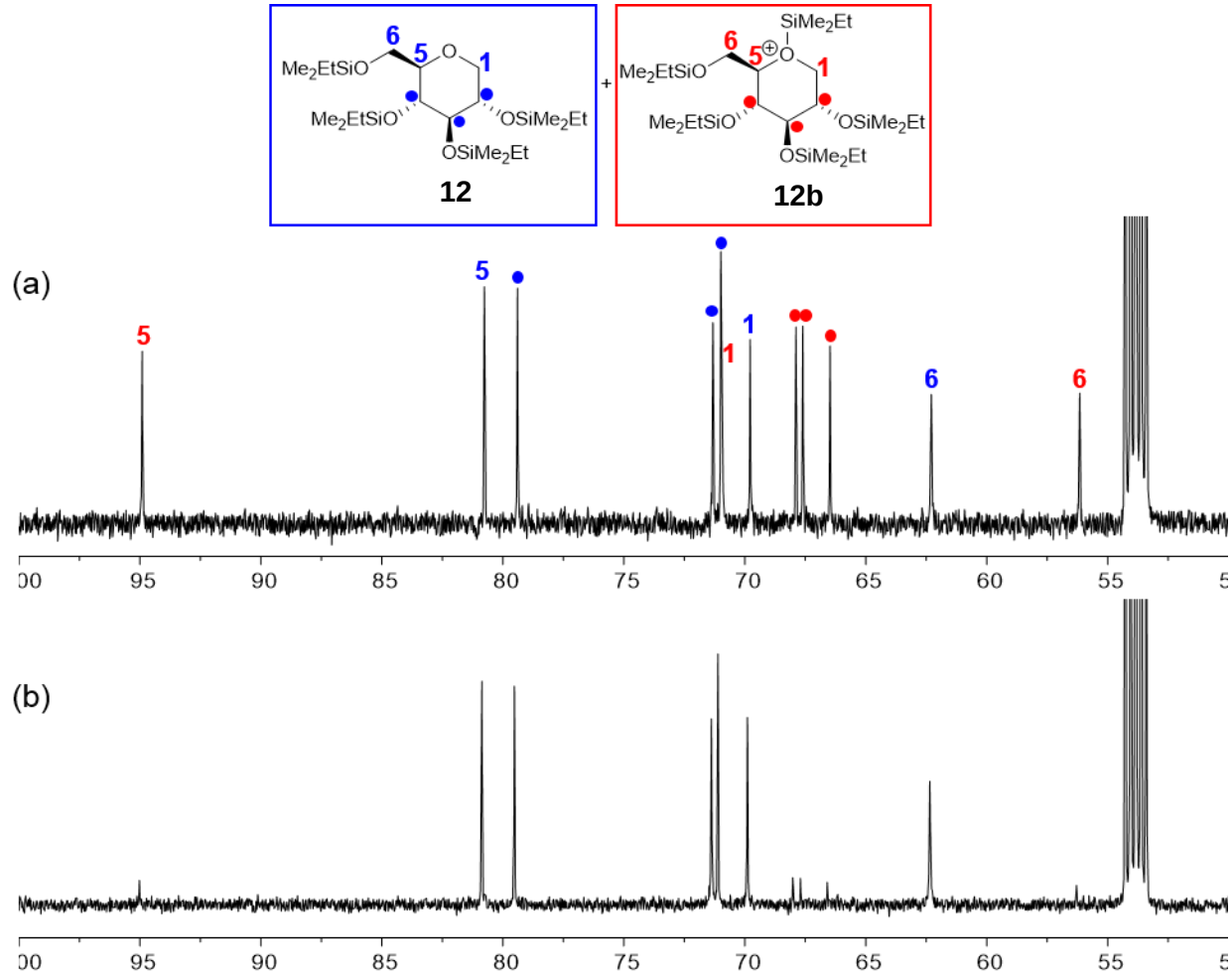

Figure 5.6: $^{13}C\{^1H\}$ NMR spectra at -70°C. Me_2EtSi-protected 1-deoxy glucose in the presence of 4 eq. Me_2EtSiH and (a) 10 mol% $B(C_6F_5)_3$ or (b) 50 mol% $B(C_6F_5)_3$. Blue indicates peaks of 1-deoxy glucose while red indicates peaks of new cationic species.

Partial characterization by 2D NMR indicated that the $^{13}C\{^1H\}$ NMR peaks of C_1 and C_5 have been shifted downfield, while C_2, C3, C4, and C_6 were shifted upfield. This is consistent with literature precedent, such as characterization of silylium coordinated diethyl ether (that is, $Et_3SiOEt_2^+$) from the Brookhart group indicating that the methylene and methine peaks α to the oxonium ion are shifted downfield relative to diethyl ether while the methyl peak of the charged species are shifted upfield. We considered the possibility that the C_6 alcohol was involved in this

interaction, but as 1-methoxy 6-deoxy glucose **32a**, (which is quickly reduced to 1,6-dideoxy glucose **32b** in situ) showed a similar effect, this possibility was discounted. While it is not immediately clear what role this intermediate plays in the reduction chemistry or why is appears to be more stable for 1-deoxy glucose than for other substrates, the investigation of putative intermediates with this methodology will likely prove useful as we continue our detailed study of the selective hydrosilylative reduction of polyoxygenated compounds.

With the experiments described in this chapter, we have initiated a project that leads to the production of value-added chemicals from biomass materials. As we continue to develop a framework for controlling and directing selective reduction, the choice of silane and protecting group will likely be pivotal. The potential for stereochemical inversion is also important to recognize. In particular, the demonstration of intramolecular cyclization as a viable process will plays a key role as we develop pathways to enable the synthesis of target compounds.

5.10 **Experimental section**

General methods:

Unless otherwise stated, all reactions were conducted under a nitrogen atmosphere using a Vacuum Atmospheres glovebox. Methylene chloride-d_2 was purchased from Cambridge Isotope labs. Both CD_2Cl_2 and CH_2Cl_2 were degassed via three freeze-pump-thaw cycles and dried over 4Å molecular sieves prior to use. Triethyl silane and dimethyl ethyl silane, were purchased from Aldrich and dried over 4Å molecular sieves prior to use. 1-deoxyglucopyranose, α-1-methoxy 6-deoxy glucose, β-1-methoxy-galactose, and galactitol were purchased from Carbosynth. D-galactal and D-glucal were purchased from Chemimpex. Glucose, α-D-methylglucoside,, glucitol, α-D-mannose, allitol, iditol, and hydrogen fluoride pyridine (~30% pyridine, 70% hydrogen fluoride), 2-methoxy tetraohydropyran, 2-methyl tetrahydropyrane, and 2-methoxy tetrahydropyran were

purchased from Aldrich. Chlorodimethylethylsilane, trimethylchlorosilane, and triethylchlorosilane were purchased from TCI America. Trispentafluorophenylborane ($B(C_6F_5)_3$), catalyst **19**) and 1,2,3-hexanetriol was purchased from Acros and used as received. Room-temperature NMR spectra were recorded using a Bruker Avance III spectrometer equipped with a cryoprobe operating at 600 MHz (^1H) and 150 MHz (^{13}C). NMR chemical shifts are reported in ppm and referenced using the residual proton peaks (δ $CHCl_3$ = 7.26, δ CH_2Cl_2 = 5.32), ^{13}C resonances of the deuterated solvent (δ $CDCl_3$ = 77.16, δ CD_2Cl_2 = 53.84) or the proteo solvent (δ CH_2Cl_2 = 54.24). Low temperature NMR spectra were recorded using a Bruker Avance III spectrometer equipped with a BBO probe operating at 500 MHz (^1H) and 125 MHz (^{13}C). High resolution mass spectra were obtained on an Agilent Accurate LC-TOF Mass Spectrometer (Agilent Series 6220) operating in positive ion mode with an electrospray ionization source (fragmentor = 175 V). The data were analyzed using an Agilent MassHunter Workstation Software, Qualitative Analysis (V. B.02.00). Occasionally cyclooctane was added to reaction mixtures as a standard. Thin-layer chromatography TLC was conducted on silica gel places and visualized with an acidic cerium ammonium molybdate solution (CAM).

General procedure 5A: Silyl protection of polyol substrates

$Me_2EtSiCl$ or Et_3SiCl (1.2 eq. per alcohol) was added to a solution or suspension of the unprotected substrate in pyridine under a nitrogen atmosphere. After stirring for at least 12 hours, the reaction mixture was diluted with water. The water layer was extracted three times with Et_2O. The combined ether layers were washed three times with water and brine, dried over Na2SO4, filtered, and rotovapped to give a colorless to pale yellow solution. ^1H NMR integration of the silyl groups vs. the carbon backbone was used to ensure complete hydroxyl group protection.

General procedure 5B: Hydrosilylative reduction experiments

In a nitrogen-filled glovebox, $B(C_6F_5)_3$ was massed into a vial. Substrate was massed into the same vial. CD_2Cl_2 or CH_2Cl_2 was added to dissolve all materials. Silane was then added. If bubbling was observed (usually for unprotected polyol substrates), the vial was left uncapped until the bubbling slowed or stopped. The solution was mixed by pipette and transferred to a 5 mm NMR tube. The NMR tube was capped with a septum and removed from the glovebox.

General procedure 5C: Deprotection and isolation of partially reduced substrates

The reaction was quenched by the addition of a few drops of Et_3N, and volatiles were removed using a rotary evaporator. The residue was redissolved in dry THF and the solution was transferred to a polyethylene conical tube. 5 mL of dry THF was added, followed by HF/pyridine was then added (0.1 mL per 0.1 mmol of substrate). The conical tube was capped, vented to an oil bubbler, and stirred for 16 h at room temperature. Dry silica gel was then added. The resulting slurry was transferred to a glass frit and washed with 10% methanol in CH_2Cl_2 until TLC revealed that all CAM-active material had been collected. The products were then isolated by column chromatography using silica gel and methanol/dichloromethane. The ratio used was varied to give $R_f = 0.3$ for the desired product (not exceeding 15%).

General procedure 5D: Cyclization experiments using $[Ph_3C][BAr^F{}_4]$

In a nitrogen-filled glovebox, $[Ph_3C][BAr^F{}_4]$ and substrate were massed into a vial. CD_2Cl_2 was added to give a bright yellow solution. The solution was transferred to an NMR tube, capped with a septum, and removed from the glovebox. The septum was then wrapped in parafilm and the tube

was cooled to -78°C. A needle with flowing nitrogen was then inserted to equalize pressure. Me_2EtSiH or Et_3SiH, which had been removed from the glovebox in a septum-capped vial, was then injected into the NMR tube. All needles were removed, the septum was again wrapped in parafilm, and the NMR tube was momentarily removed from the cold bath, inverted twice to mix, and then replaced in the cold bath. The color remained bright yellow throughout this process. Just before insertion into the NMR magnet, the tube was removed from the cold bath and allowed to warm to room temperature, at which point the yellow color typically lightened. In situ NMR spectra of samples prepared using this method show Ph_3CH (144.4, 129.8, 128.7, 126.7, 57.3 ppm in the $^{13}C\{^1H\}$ NMR spectrum).

Synthesis of 1,2-dideoxy glucose and 1,2-dideoxy galactose:

1,2-dideoxy glucose and 1,2-dideoxy galactose were generated by dissolving 300 mg of commercially available glucal or galactal in ethanol and adding 20 mg of 5% palladium on carbon to the solution. After saturating the solution and atmosphere with hydrogen, the reaction was stirred under hydrogen for 16 hours. The Pd/C catalyst was then removed by filtration over Celite. The filtrate was evaporated to dryness, and the resulting residue was purified by passage through a short column of silica using 10% methanol in CH_2Cl_2.

Reduction of glucitol with Me_2EtSiH

Following Procedure 5B, 151 mg (0.82 mmol) unprotected glucitol was reduced using 1 mL (7.5 mmol, 10 eq.) Me_2EtSiH in the presence of 21 mg (0.041 mmol, 5 mol %) $B(C_6F_5)_3$. In situ NMR spectra were acquired. Tetraol **14c** and triol **14b** were deprotected and separated using Procedure 5C. Tetraol **14c**: ^1H NMR (600 MHz, D_2O) δ 3.87 – 3.80 (m, 2H), 3.53 (dd, J = 6.5, 2.6 Hz, 1H),

1.19 (d, *J* = 6.5 Hz, 3H), 1.15 (d, *J* = 6.7 Hz, 3H). $^{13}C\{^{1}H\}$ NMR (151 MHz, D_2O) δ 74.7, 73.8, 68.6, 66.9, 18.3, 18.1. HRMS (ESI): *m/z* $[M+Na]^+$ found 173.0784, calcd 173.0784 for $C_6H_{14}O_4Na$. Triol **14b**: ^{1}H NMR (600 MHz, CD_3OD) δ 3.78 (dq, *J* = 7.4, 6.4 Hz, 1H) 3.68 (ddd, *J* = 8.0, 5.9, 2.5 Hz, 1H), 3.15 (dd, *J* = 7.3, 2.5 Hz, 1H), 1.56 – 1.54 (m, 2H), 1.22 (d, *J* = 6.3 Hz, 3H), 0.97 (t, *J* = 7.5 Hz, 3H). ^{13}C NMR (151 MHz, D_2O) δ 76.4, 71.9, 67.1, 25.5, 17.6, 9.3. HRMS (ESI): *m/z* $[M+Na]^+$ found 157.0836, calcd 157.0835 for $C_6H_{14}O_3Na$.

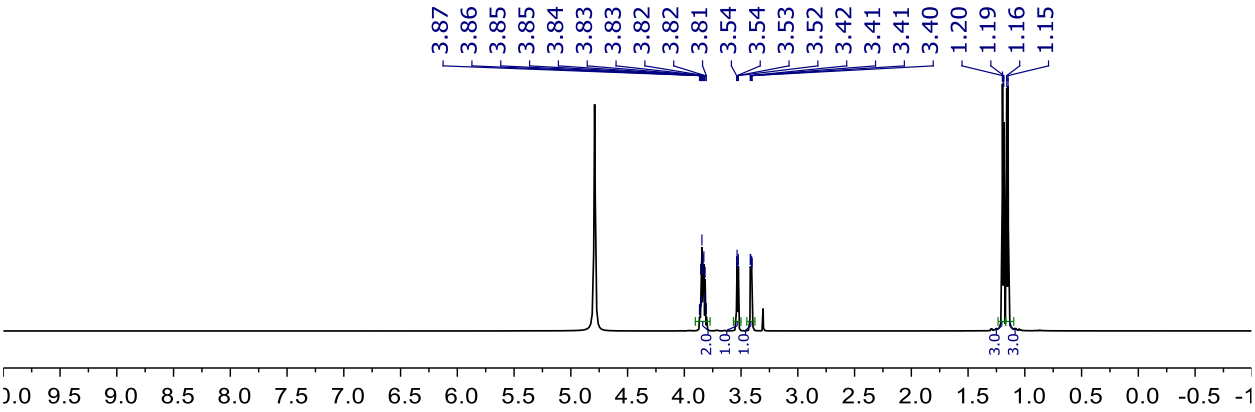

Figure 5.7: ^{1}H NMR spectrum of isolated deprotected gluco-tetraol

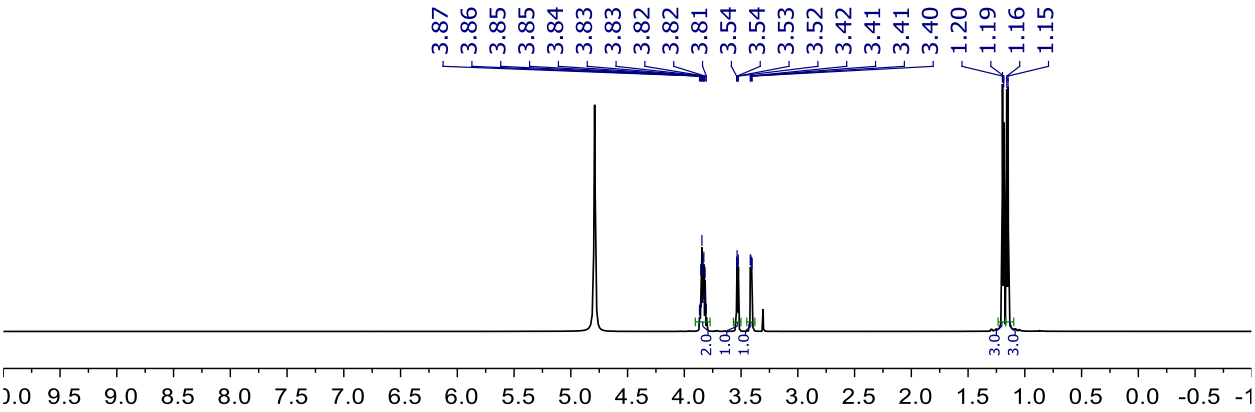

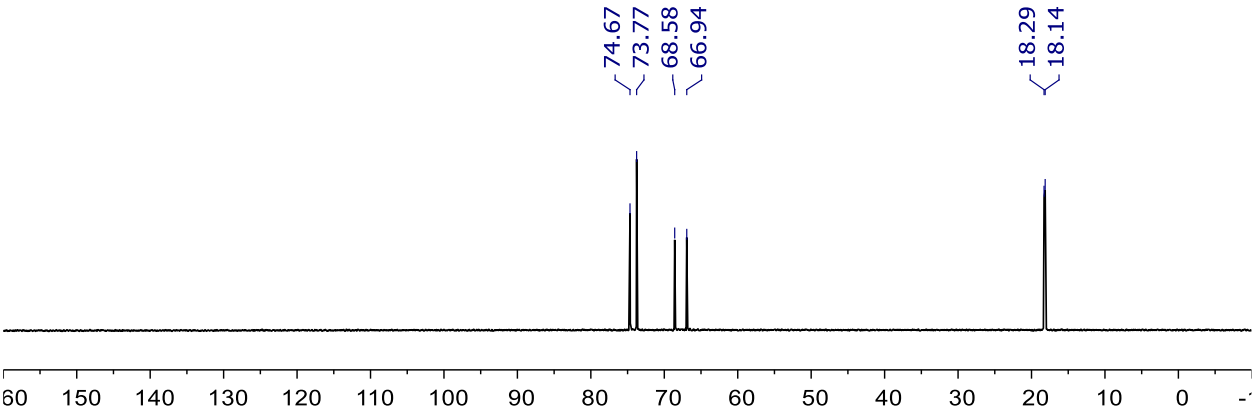

Figure 5.8: $^{13}C\{^{1}H\}$ NMR spectrum of isolated deprotected gluco-tetraol

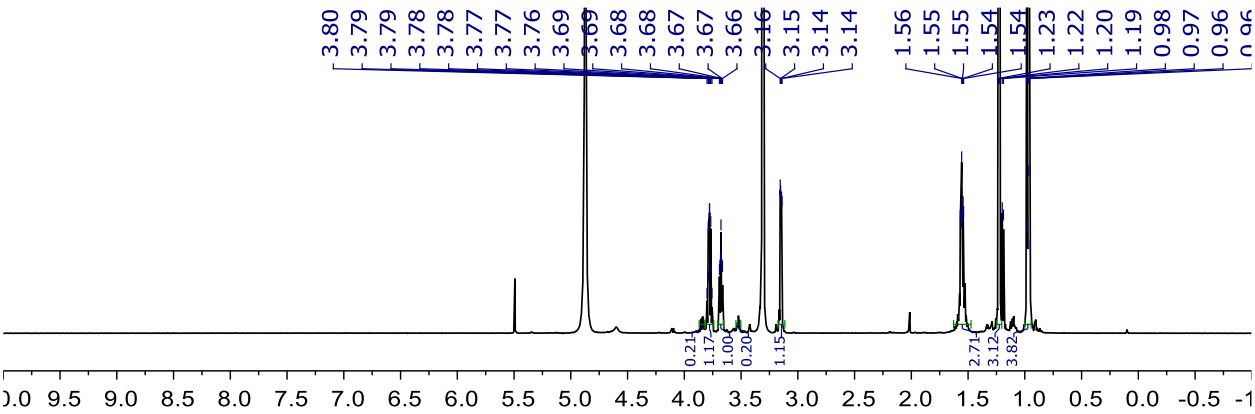

Figure 5.9: ^{1}H NMR spectrum of isolated deprotected gluco-triol

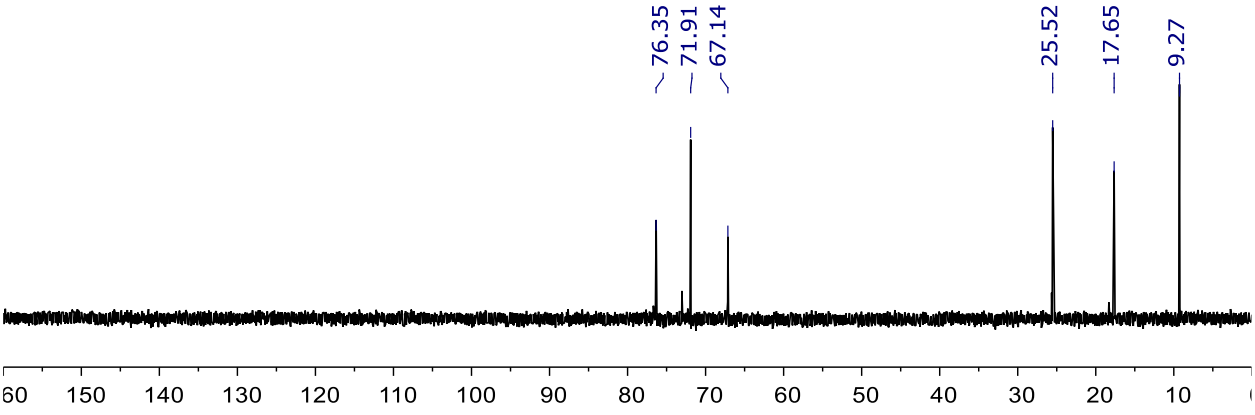

Figure 5.10: $^{13}C\{^{1}H\}$ NMR spectrum of isolated deprotected gluco-triol

Reduction of mannitol with Me_2EtSiH.

Following Procedure 5B, 30 mg (0.16 mmol) unprotected mannitol was reduced using 0.22 mL (1.66 mmol, 10 eq.) Me_2EtSiH in the presence of 4.6 mg (0.0090 mmol, 5 mol %) $B(C_6F_5)_3$. Tetraol **21c** and triol **21b** products were then deprotected and separated using Procedure 5C. The NMR spectra of the triol product were compared to the major diastereomer of the triol resulting from reduction of glucitol and found to be the same compound.

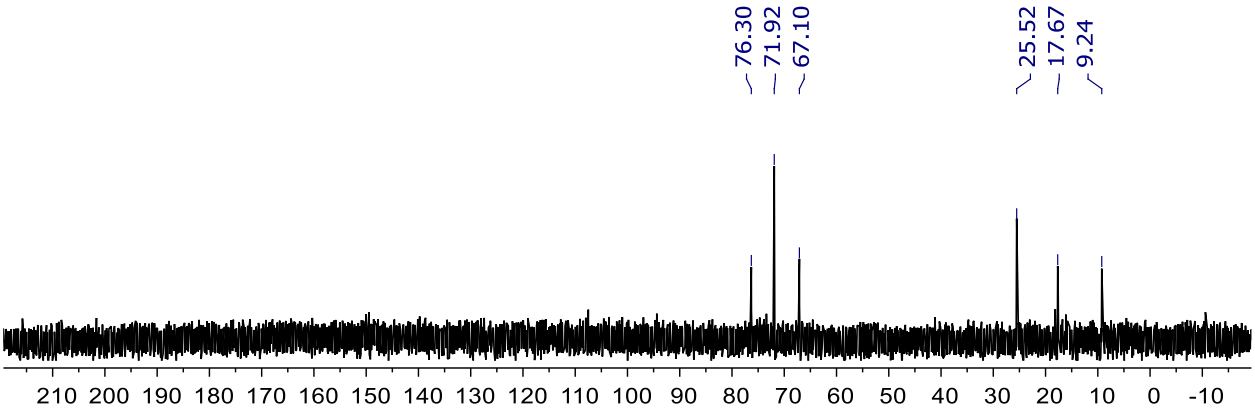

Figure 5.11: $^{13}C\{^1H\}$ NMR spectrum of isolated deprotected manno-triol

Reduction of 1,2-dideoxy glucose 22a with Me_2EtSiH

Following Procedure 5B, 48 mg (0.12 mmol) Me_2EtSi-protected 1,2-didoxyglucose **22a** was reduced with 0.1 mL (0.78 mmol 6 eq.) Me_2EtSiH in the presence of 4 mg (0.0078 mmol, 6.5 mol %) $B(C_6F_5)_3$ and a drop of cyclooctane. After 20 minutes, the a $^{13}C\{^1H\}$ NMR spectrum was acquired, which matched triol **14b** observed from reduction of glucitol **14**.

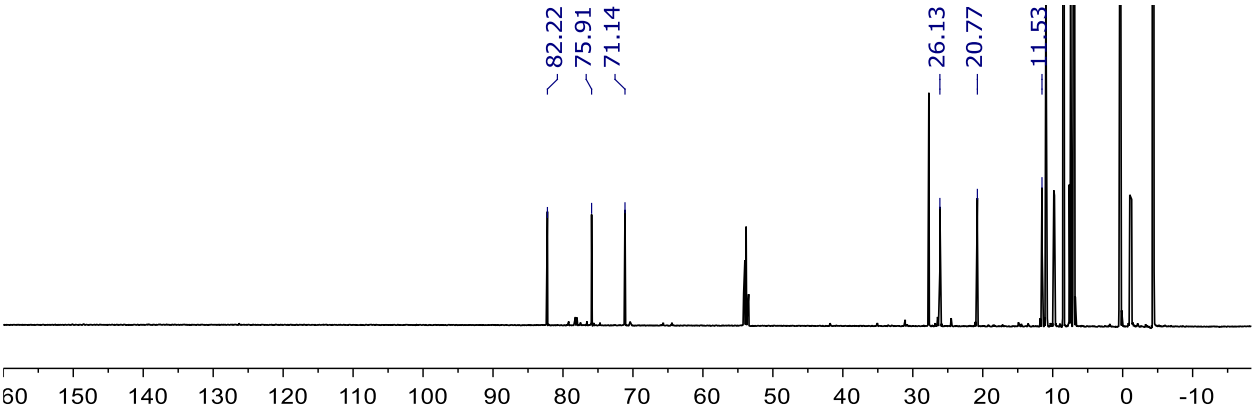

Figure 5.12: In situ $^{13}C\{^{1}H\}$ NMR spectrum of triol observed in reduction of 1,2-dideoxy glucose

Reduction of galactitol 23a with Me_2EtSiH

Following Procedure 5B, 30 mg (0.16 mmol) unprotected galactitol was reduced with 0.3 mL (1.7 mmol, 10 eq.) Me_2EtSiH in the presence of 6 mg (0.011, 7 mol %) $B(C_6F_5)_3$. After 1 hour, $^{13}C\{^{1}H\}$ NMR spectroscopy revealed triol **23b**. This material was isolated using procedure 5C. ^{1}H NMR (600 MHz, CD_3OD) δ 3.85 (quintet, *J* = 6.2 Hz, 1H), 3.44 – 3.41 (m, 1H), 3.28 (dd, *J* = 7.3, 6.0 Hz, 1H), 1.79 – 1.74 (m, 1H), 1.44 – 1.38 (m, 1H), 1.19 (d, *J* = 6.4 Hz, 3H), 0.99 (t, *J* = 7.4 Hz, 3H). ^{13}C NMR (151 MHz, CD_3OD) δ 78.5, 75.5, 70.0, 26.8, 18.4, 10.2. HRMS (ESI): *m/z* $[M+Na]^+$ found 157.0835, calcd 157.0835 for $C_6H_{14}O_3Na$.

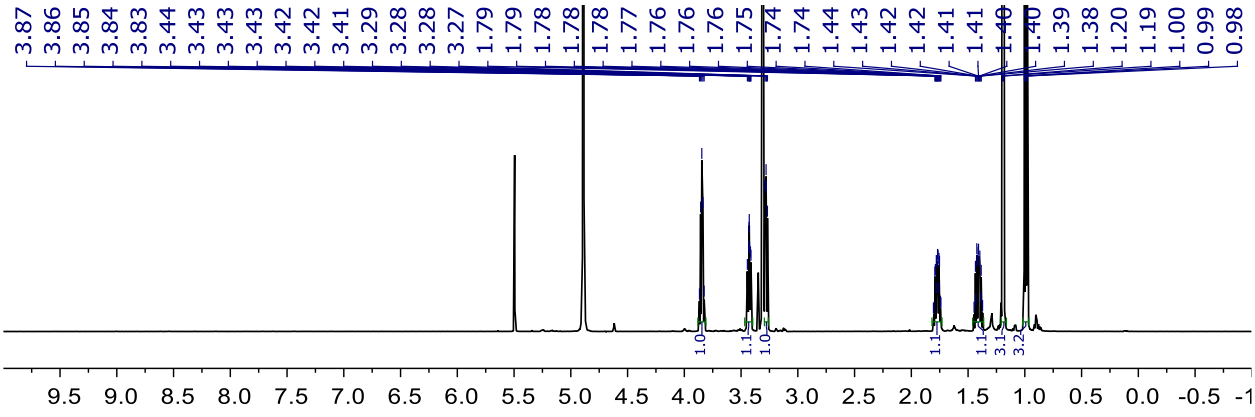

Figure 5.13: ^{1}H NMR spectrum of isolated deprotected triol from reduction of galactitol

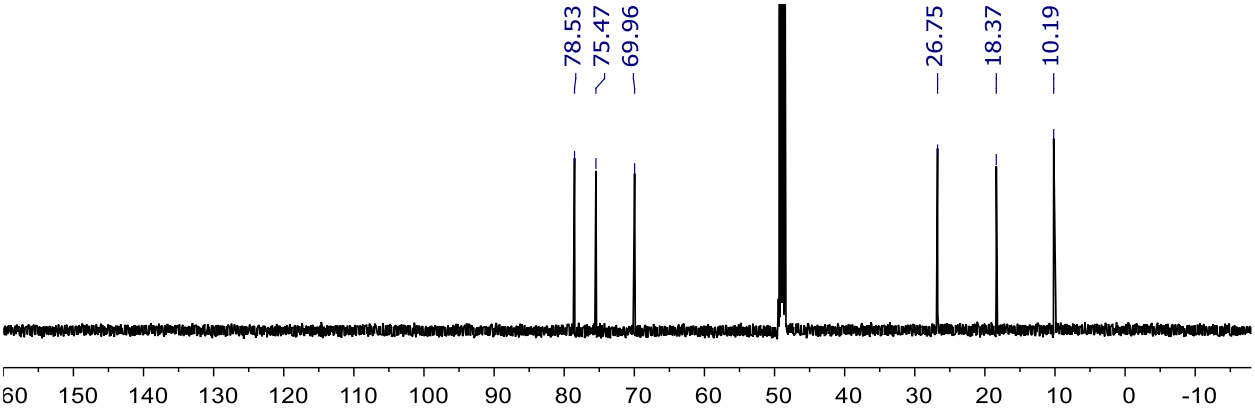

Figure 5.14: ^{13}C{^{1}H} NMR spectrum of isolated deprotected triol from reduction of galactitol

Reduction of 1,2-dideoxy galactose (24a) with Me_2EtSiH

Following Procedure 5B, 30 mg (0.20 mmol) unprotected 1,2-didoxyglucose was reduced with 0.2 mL (1.5 mmol, 7.5 eq.) Me_2EtSiH in the presence of 6 mg (0.012 mmol, 6 mol %)$B(C_6F_5)_3$. ^{13}C{^{1}H} NMR showed triol **24b** which did not match the triol **23b** observed from reduction of other galactose-based substrates. ^{1}H NMR (600 MHz, CD_3OD) δ 4.00 (dq, *J* = 2.6 Hz, 6.5 Hz 1H), 3.51 (ddd, *J* = 8.9, 7.4, 2.9 Hz, 1H), 3.12 (dd, *J* = 7.4, 2.6 Hz, 1H), 1.75-1.73 (m, 1H), 1.42-1.40

(m, 1H), 1.20 (d, *J* = 6.5 Hz, 3H), 0.99 (t, *J* = 7.4 Hz, 3H). ^{13}C NMR (151 MHz, CD_3OD) δ 77.9, 74.3, 67.8, 27.2, 19.9, 10.3.

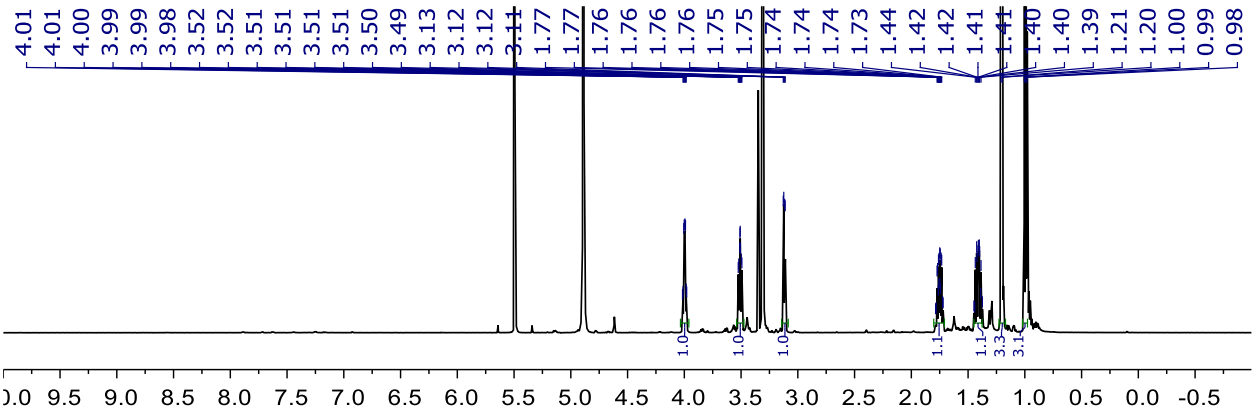

Figure 5.15: ^{1}H NMR spectrum of isolated deprotected triol from reduction of 1,2-dideoxy galactose

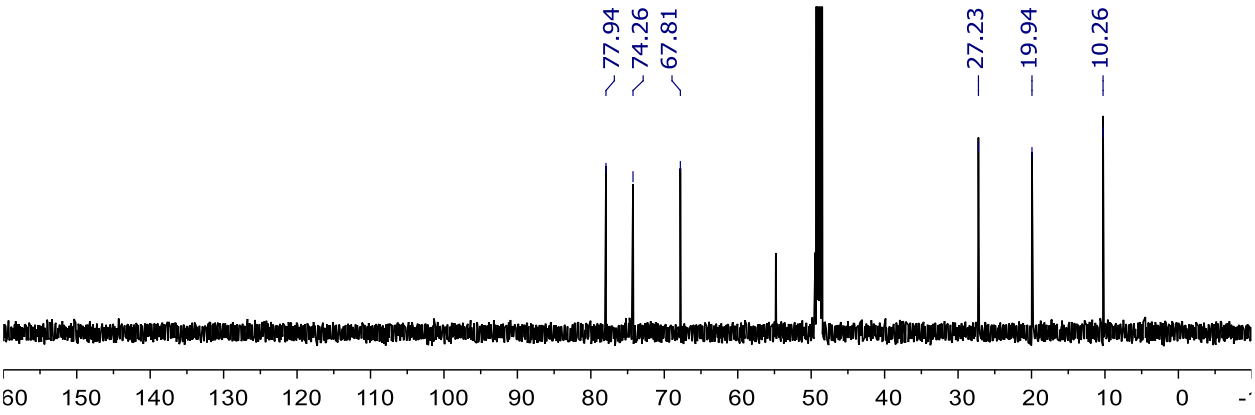

Figure 5.16: ^{13}C{^{1}H} NMR spectrum of isolated deprotected triol from reduction of 1,2-dideoxy galactose

Reduction of galactose 25a

Following Procedure 5B, 155 mg (0.25 mmol) Me_2EtSi-protected galactose **25a** was reduced with 0.2 mL (1.5 mmol, 6 eq.) Me_2EtSiH in the presence of 6 mg (0.011 mmol, 5 mol %) $B(C_6F_5)_3$.

$^{13}C\{^{1}H\}$ NMR spectroscopy revealed triol **23b** observed from reduction of galactitol but not triol **24b** observed from reduction of 1,2-dideoxy galactose.

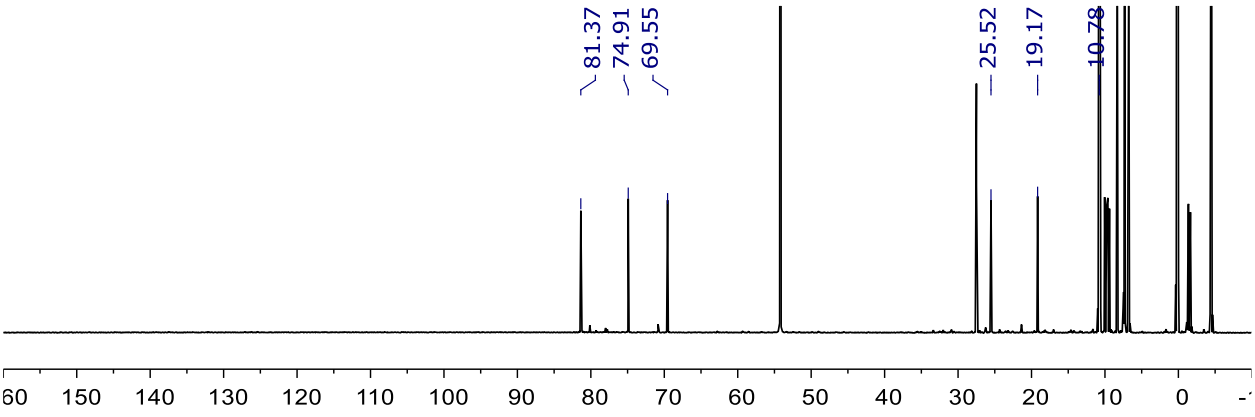

Figure 5.17: In situ $^{13}C\{^{1}H\}$ NMR of triol from reduction of galactose

Reduction of C_1-methoxy galactose 26a

Following Procedure 5B, 16 mg (0.082 mmol) unprotected C_1-methoxy galactose was reduced with 0.2 mL (1.5 mmol, 18 eq.) Me_2EtSiH in the presence of 4 mg (0.0078 mmol, 10 mol%) $B(C_6F_5)_3$. $^{13}C\{^{1}H\}$ NMR spectroscopy revealed a triol, which triol **23b** observed from reduction of galactitol but not triol **24b** observed from reduction of 1,2-dideoxy galactose.

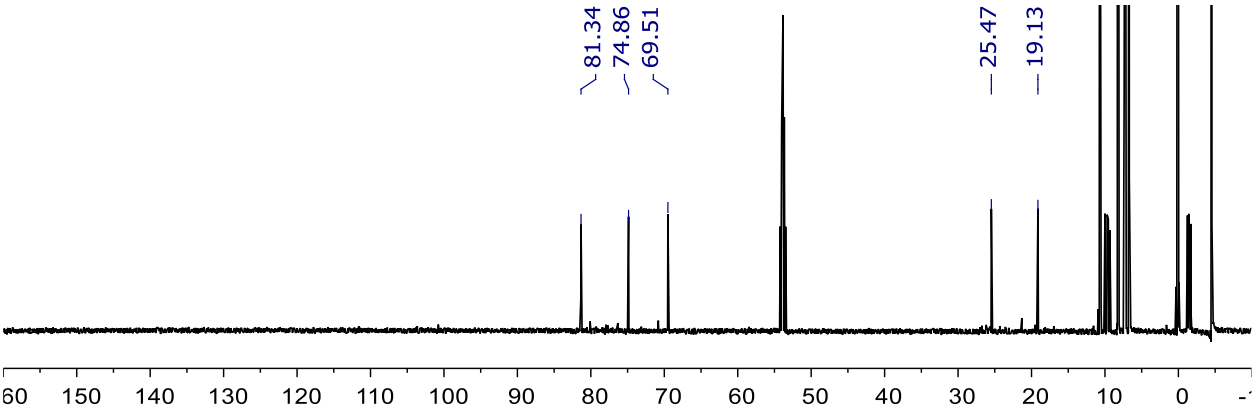

Figure 5.18: In situ $^{13}C\{^{1}H\}$ NMR spectrum of triol from reduction of C_1-methoxy galactose

Reduction of iditol 27a to triol 27b

Following Procedure 5B, 20 mg (0.11 mmol) iditol **27a** was reduced with 0.2 mL (1.5 mmol, 14 eq.) Me_2EtSiH in the presence of 4 mg (0.0078 mmol, 7 mol%) $B(C_6F_5)_3$. The resulting triol **27b** was deprotected following Procedure 5C and isolated via preparatory TLC. NMR data matched the triol isolated from the reduction of mannitol (**21b**) and the major diastereomer of the triol isolated from the reduction of glucitol (**14b**)

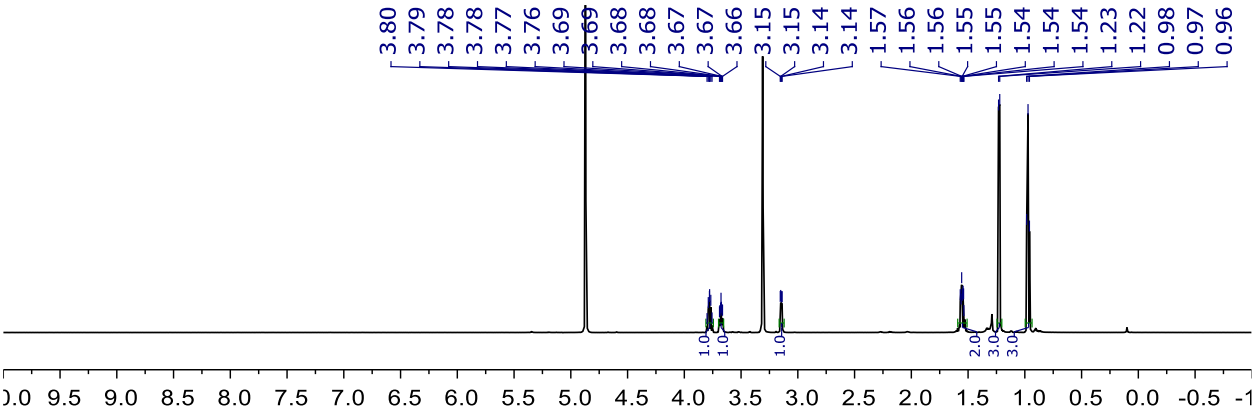

Figure 5.19: ^{1}H NMR spectrum of isolated deprotected triol from reduction of iditol

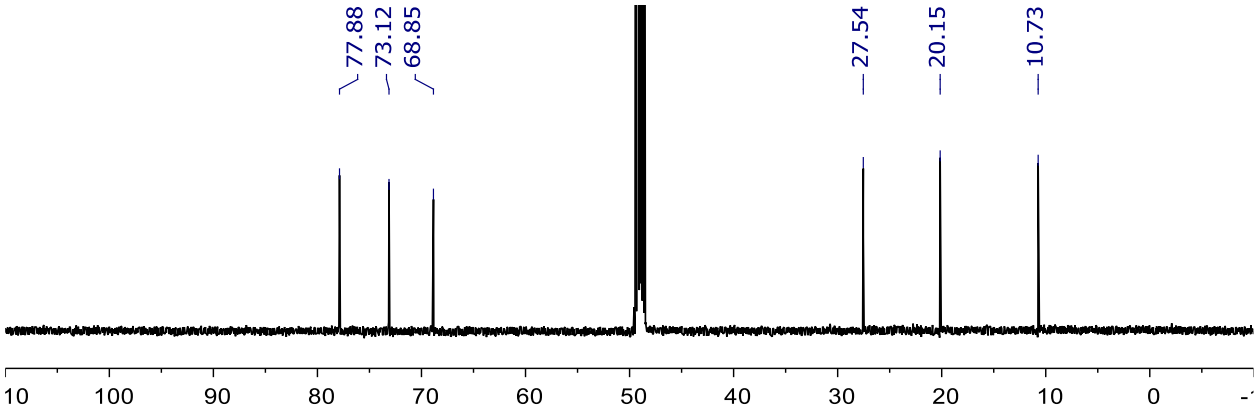

Figure 5.20: $^{13}C\{^{1}H\}$ NMR spectrum of isolated deprotected triol from reduction of iditol

Reduction of allitol 28a

Following Procedure 5B, 50 mg (0.081 mmol) Me_3Si-protected allitol **28a** was reduced with 0.2 mL (1.5 mmol, 19 eq.) Me_3SiH in the presence of 10 mg (0.020 mmol, 25 mol %) $B(C_6F_5)_3$. The in situ NMR spectrum of the minor triol product compared to the minor triol product generated from reduction of mannitol and found to be the same compound.

Generation of cyclic intermediate from galacto-tetraol 23c

Following Procedure 5D, 23 mg (0.046 mmol) Me_2EtSi-protected galacto-tetraol **23c** was reduced by 6 µL (0.046 mmol, 1 eq.) Me_2EtSiH in the presence of 42 mg (0.046 mmol, 1 eq.) $[Ph_3C][BAr^F{}_4]$, giving intermediate **II'**. In situ NMR spectra were then acquired.

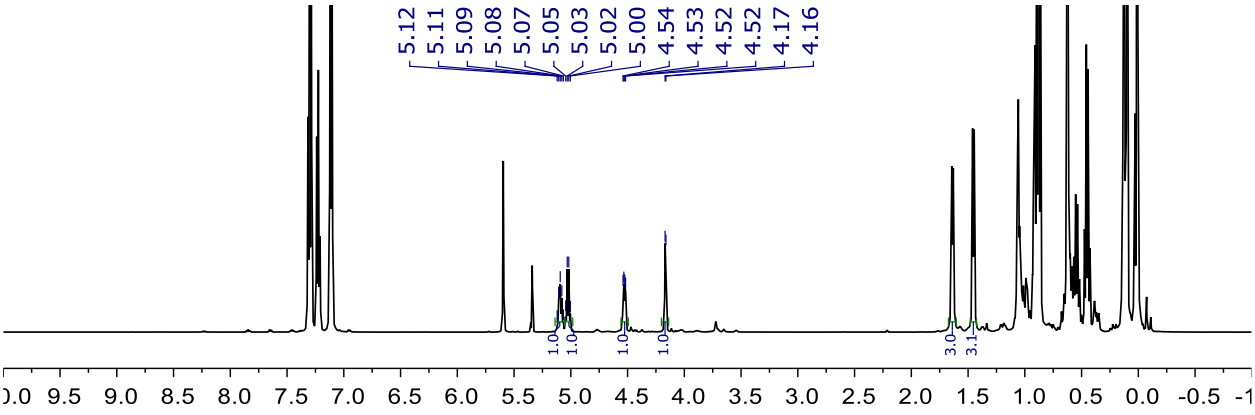

Figure 5.21: In situ ^{1}H NMR spectrum of cyclic intermediate generated from cyclization of galacto-tetraol

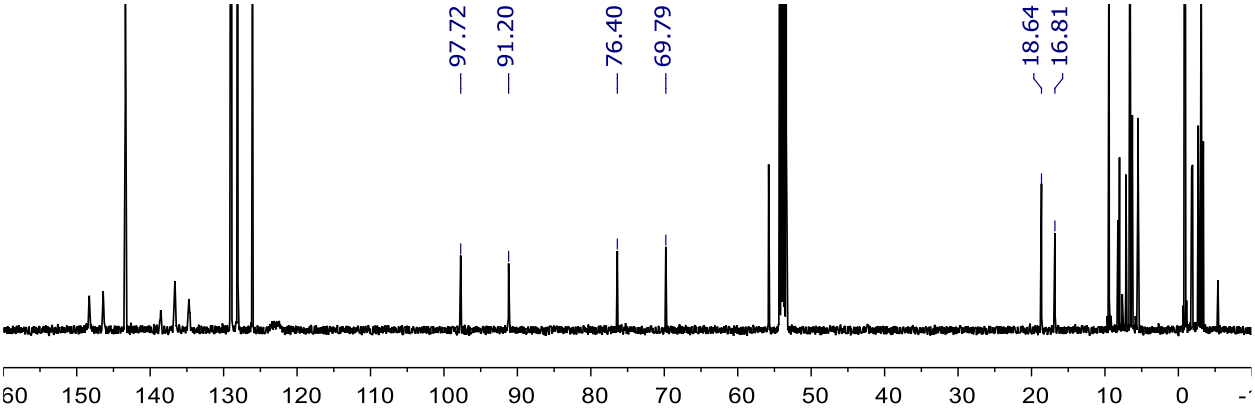

Figure 5.22: In situ ^{13}C{^{1}H} NMR spectrum of cyclic intermediate generated from cyclization of galacto-tetraol

Generation of cyclic intermediate from gluco-tetraol 14c

Following Procedure 5D, 17 mg (0.034 mmol) Me_2EtSi-protected gluco-tetraol **14c** was reduced by 5 µL (0.034 mmol, 1 eq.) Me_2EtSiH in the presence of 32 mg (0.032 mmol, 1 eq.) $[Ph_3C][BAr^F_4]$, giving intermediate **VII'**. A ^{13}C{^{1}H} NMR spectrum was then acquired.

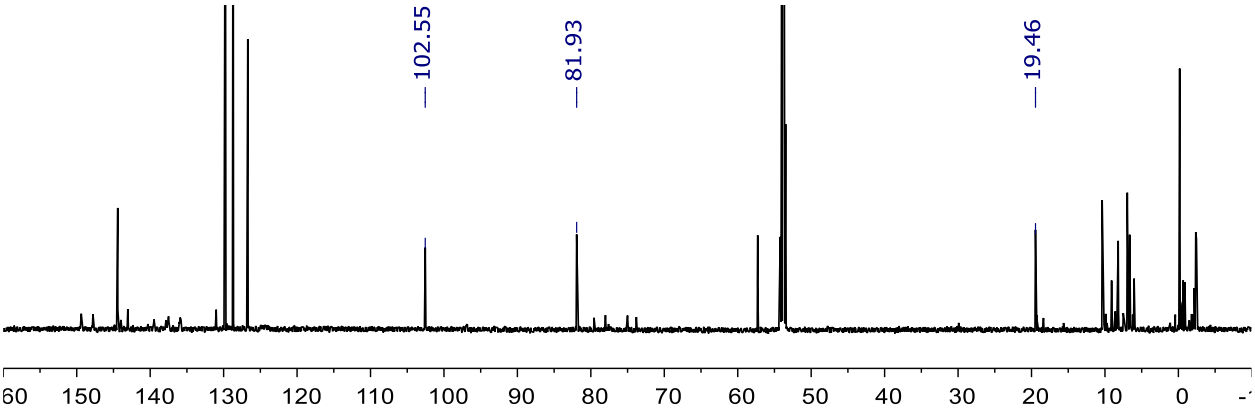

Figure 5.23: In situ $^{13}C\{^{1}H\}$ NMR spectrum of cyclic intermediate generated from cyclization of gluco-tetraol

Isolation of cyclic intermediate from galacto-tetraol 23c and [Ph_3C][BAr^F_4]

Following Procedure 5D, 17 mg (0.034 mmol) Me_2EtSi-protected galacto-tetraol **4c** was reduced by 5 µL (0.034 mmol, 1 eq.) Me_2EtSiH in the presence of 32 mg (0.034 mmol, 1 eq) [Ph_3C][BAr^F_4]. The resulting product was then isolated by Procedure 5C, giving cyclic **23d**. ^{1}H NMR (600 MHz, CD_3OD) δ 4.14 (qd, *J* = 6.5, 3.4 Hz, 1H), 3.92 – 3.89 (m, 1H), 3.86 (dq, *J* = 8.1, 6.2 Hz, 1H), 3.74 (dd, *J* = 8.0, 4.5 Hz, 1H), 1.24 (d, *J* = 6.1 Hz, 3H), 1.20 (d, *J* = 6.5 Hz, 3H). ^{13}C NMR (151 MHz, CD_3OD) δ 80.0, 77.9, 77.4, 74.4, 19.2, 15.3.

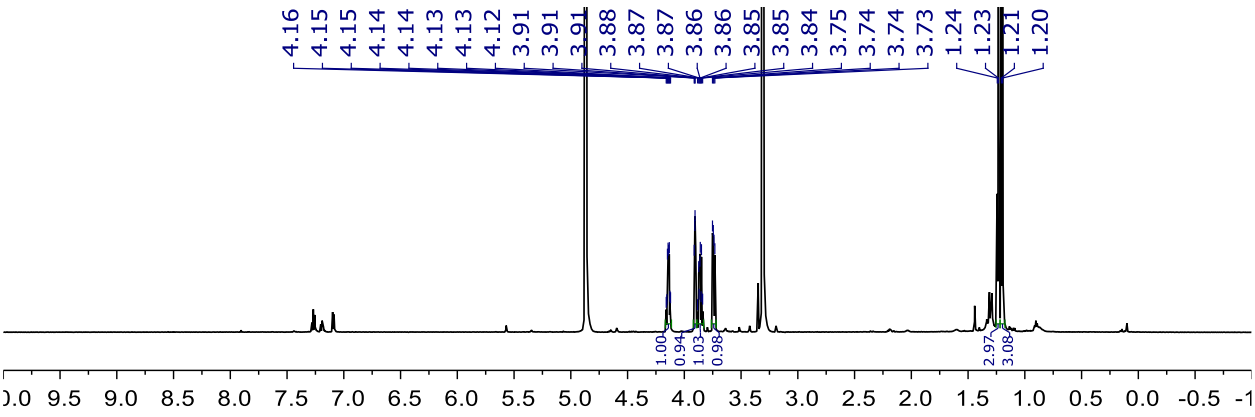

Figure 5.24: ^{1}H NMR spectrum of deprotected cyclized intermediate from gluco-tetraol

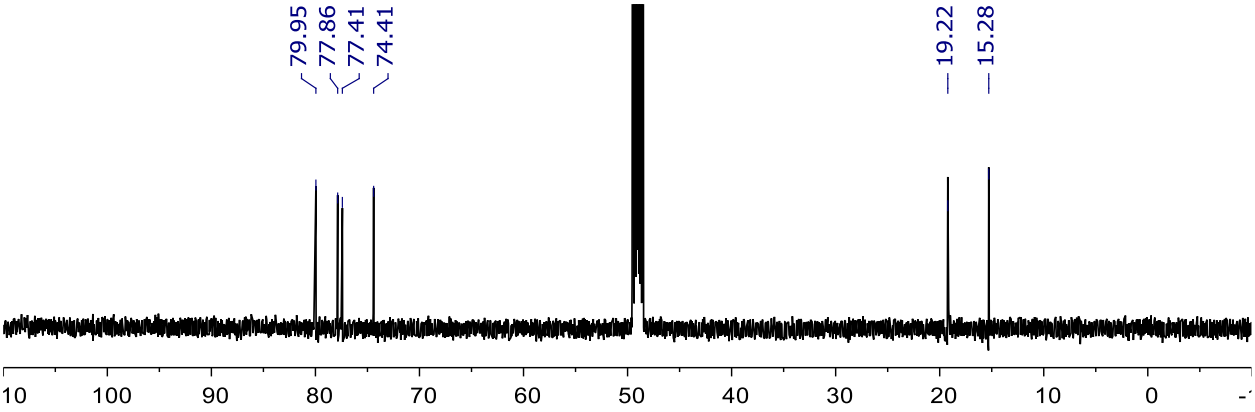

Figure 5.25: ^{13}C{^{1}H} NMR spectrum of deprotected cyclized intermediate from gluco-tetraol

Reduction of TMS-galactitol with Et_3SiH (showing silyl group exchange)

Following Procedure 5B, 8.0g (9.8 mmol) of Me_3Si-protected galactitol was treated with 4.6 mL (29 mmol, 3 eq.) Et_3SiH in the presence of 60 mg (1 mol%) $B(C_6F_5)_3$. A portion of the reaction mixture was passed through a column of alumina. Analysis by NMR spectroscopy indicated two Me_3Si-protecting groups and two Et_3Si-protecting groups. Another portion of this reaction mixture was isolated using Procedure 5C. Some of this isolated material was re-protected with $Me_2EtSiCl$ using Procedure 5A for use in further experiments. Deprotected material: ^{1}H NMR (600 MHz,

CD_3OD) δ 4.05-4.02 (m, 1H), 3.40 (t, *J* = 0.9 Hz, 1H), 1.23 (d, *J* = 6.6 Hz, 3H). ^{13}C NMR (151 MHz, CD_3OD) δ 75.0, 67.8, 19.9. Protected material: ^{1}H NMR (600 MHz, Chloroform-*d*) δ 3.88 (quintet, *J* = 6.5 Hz, 1H), 3.56 (d, *J* = 7.1 Hz, 1H), 1.17 (d, *J* = 6.3 Hz, 3H), 0.96 (t, *J* = 8.0 Hz, 9H), 0.64 (q, *J* = 8.0 Hz, 6H), 0.11 (s, 18H)

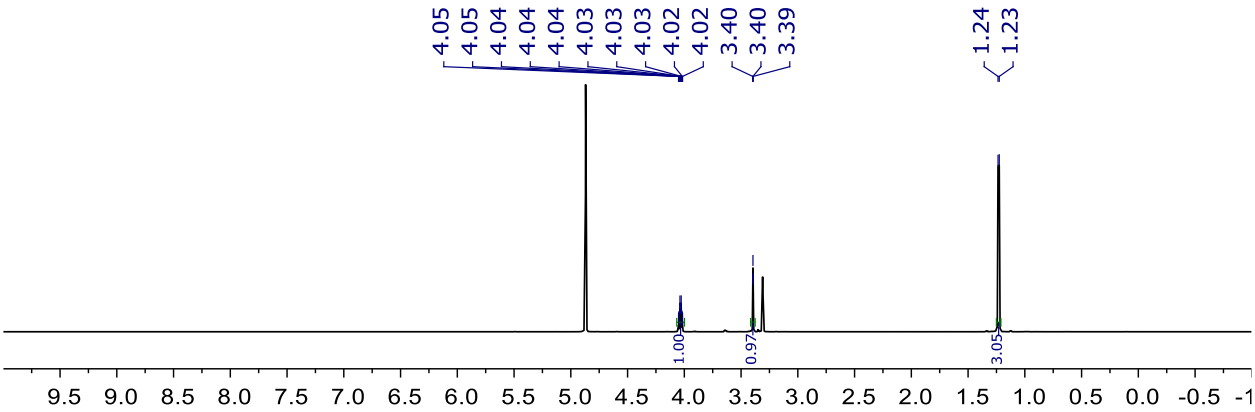

Figure 5.26: ^{1}H NMR spectrum of isolated deprotected galacto-tetraol

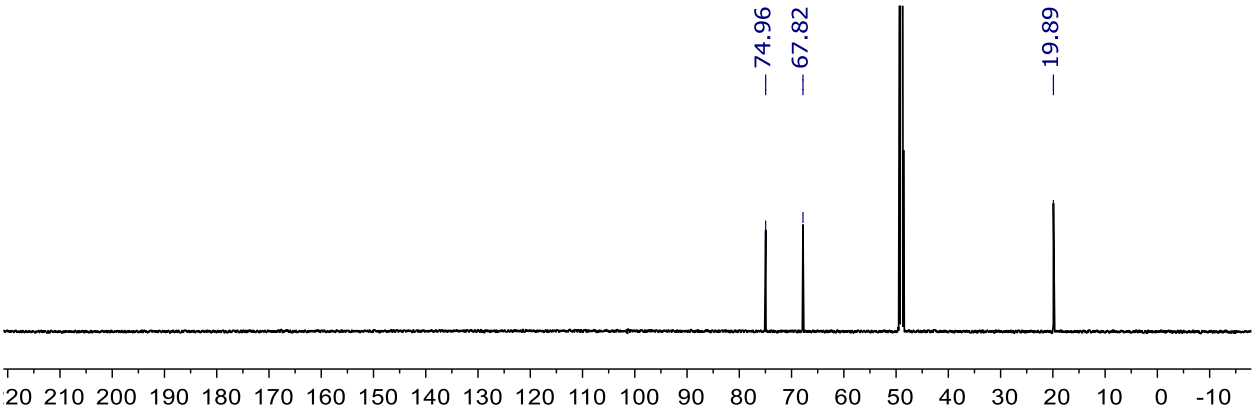

Figure 5.27: $^{13}C\{^{1}H\}$ NMR spectrum of isolated deprotected galacto-tetraol

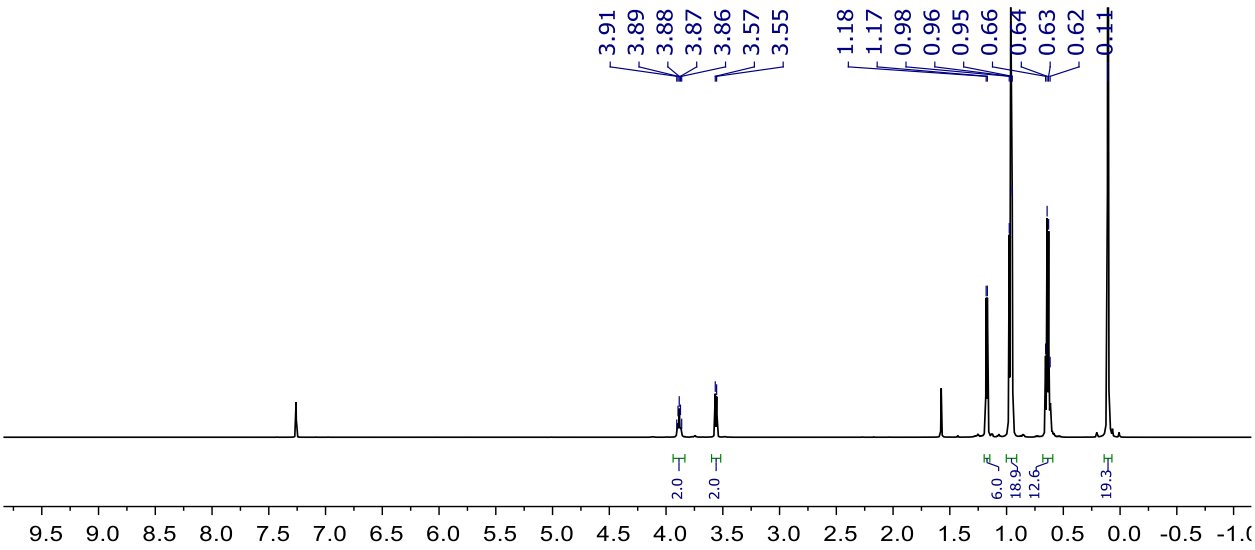

Figure 5.28: ^{1}H NMR spectrum of isolated protected galacto-tetraol showing two Et_3Si-groups and two Me_2EtSi-groups

Reduction of C_1-methoxy glucose 12 to pentitol without deuterium

Following Procedure 5B, 98 mg (0.15 mmol) Et_3Si-protected C_1-methoxy glucose **12** was reduced with 0.3 mL (1.8 mmol, 13 eq.) Et_3SiH in the presence of 4 mg (0.008 mmol, 5 mol %)$B(C_6F_5)_3$, giving the pentitol shown below.

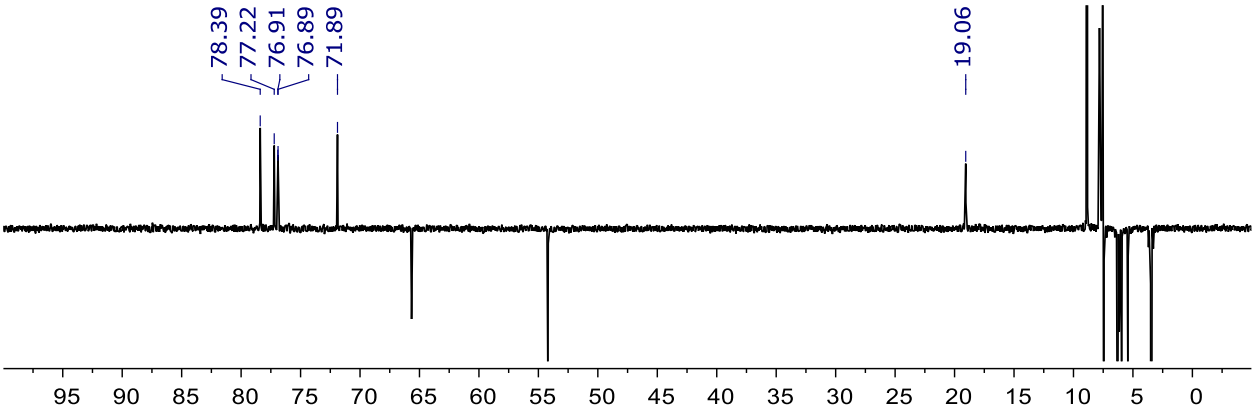

Figure 5.29: In situ $^{13}C\{^{1}H\}$ Attached Proton Test spectrum of 1-deoxy glucitol

Reduction of C_1-methoxy glucose 10a to pentitol 10b with deuterium labeling

Following Procedure 5B, 50 mg (0.07 mmol) Et_3Si-protected C_1-methoxy glucose was reduced with 24 µL Et_3SiD (0.15 mmol, 2.1 eq) in the presence of 3 mg (0.006 mmol, 9 mol%) $B(C_6F_5)_3$. After 12 h at room temperature, the sample was returned to the glovebox and 250 µL (1.5 mmol, 21 eq.) Et_3SiH was added. After 2 days, another NMR spectrum was acquired showing deuterium-labeled 1-deoxy glucitol **10b**.

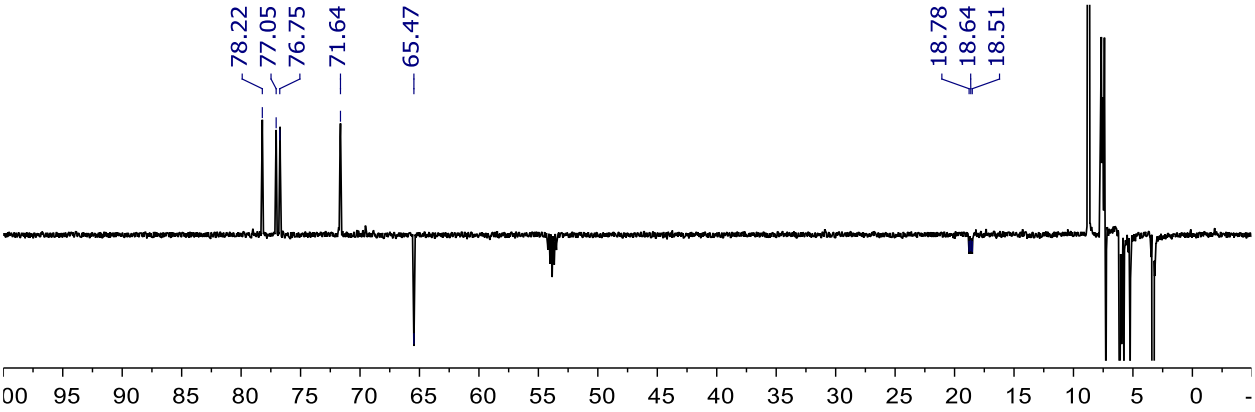

Figure 5.30: In situ $^{13}C\{^1H\}$ Attached Proton Test spectrum of deuterium-labeled 1-deoxy glucitol

Reduction of 2-methyl tetrahydropyran 29 to 1-hexanol and 2-hexanol

Following Procedure 5B, 40 mg (0.4 mmol) 2-methyl tetrahydropyran **29** was reduced with 47 µL (0.4 mmol, 1 eq.) Me_2EtSiH in the presence of 4 mg (0.008 mmol, 2 mol%) $B(C_6F_5)_3$. By integration of peaks in the $^{13}C\{^1H\}$ NMR spectrum, the ratio of silyl-protected 2-hexanol to 1-hexanol was 1:2.5.

Cyclization of 1,5-hexanediol 30a with [Ph_3C][BAr^F_4]

Following Procedure 5D, 11 mg (0.03 mmol) Et_3Si-protected 1,2-hexanediol **30a** was reduced by 4 (0.3 mmol, 1 eq.) µL Et_3SiH in the presence of 31 mg (0.3 mmol, 1 eq.) [Ph_3C][BAr^F_4], giving compound **30b**. In situ NMR spectra were then collected.

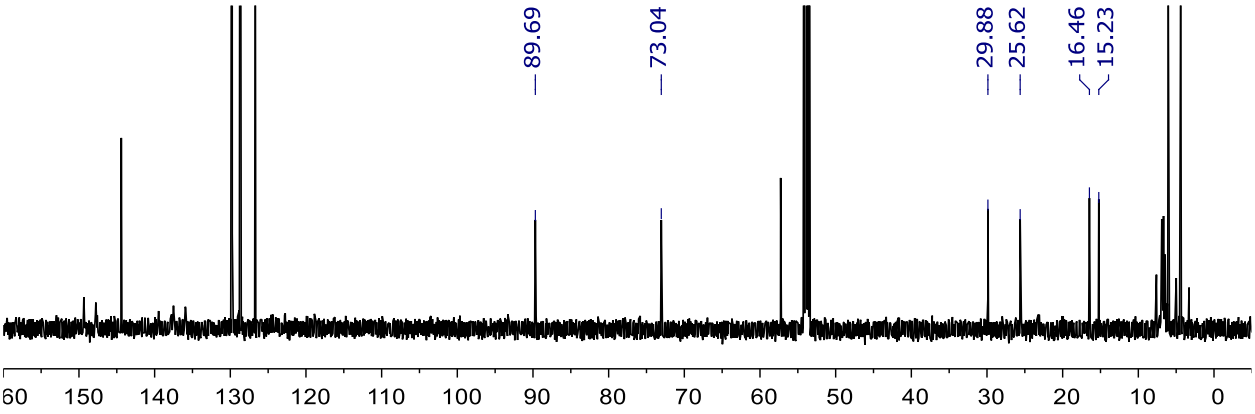

Figure 5.31: In situ $^{13}C\{^1H\}$ NMR spectrum of product resulting from cyclization of 1,5-hexanediol

Cyclization of 2,5-hexanediol 31a with [Ph_3C][BAr^F_4]

Following Procedure 5D, 11 mg (0.03 mmol) Et_3Si-protected 2,5-hexanediol **31a** was reduced by 4 µL (0.03 mmol, 1 eq.) Et_3SiH in the presence of 31 mg (0.03 mmol, 1 eq.) [Ph_3C][BAr^F_4], giving compound **31b**. In situ NMR spectra were then collected.

In situ:

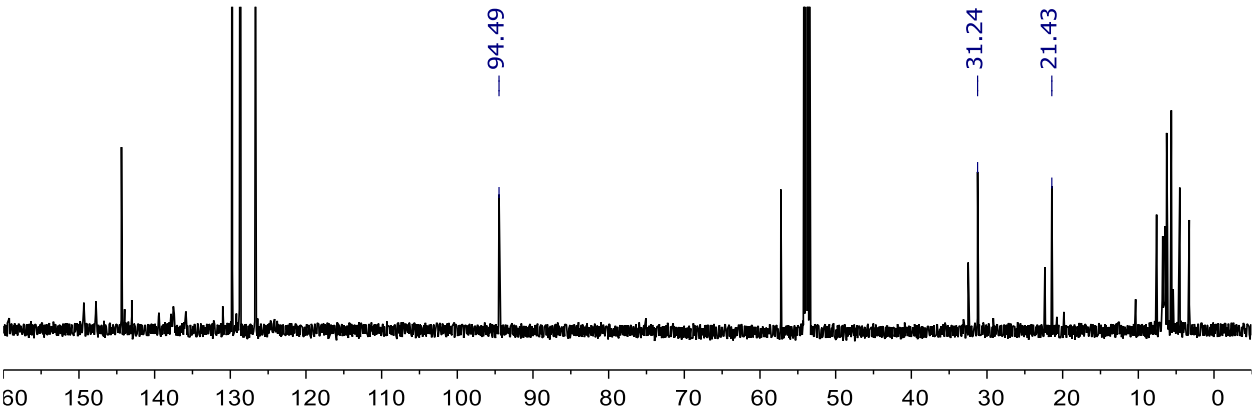

Figure 5.32: In situ $^{13}C\{^{1}H\}$ NMR spectrum of product resulting from cyclization of 2,5-hexanediol

Low temperature NMR study of 1-deoxy glucose reduction with 10% $B(C_6F_5)_3$

Following Procedure 5B, 50 mg (0.10 mmol) of Me_2EtSi-protected 1-deoxy glucose was treated with 51 µL (0.40 mmol, 4 eq.) Me_2EtSiH in the presence of 5 mg (0.01 mmol, 10 mol%) $B(C_6F_5)_3$. NMR spectra were acquired at various temperatures.

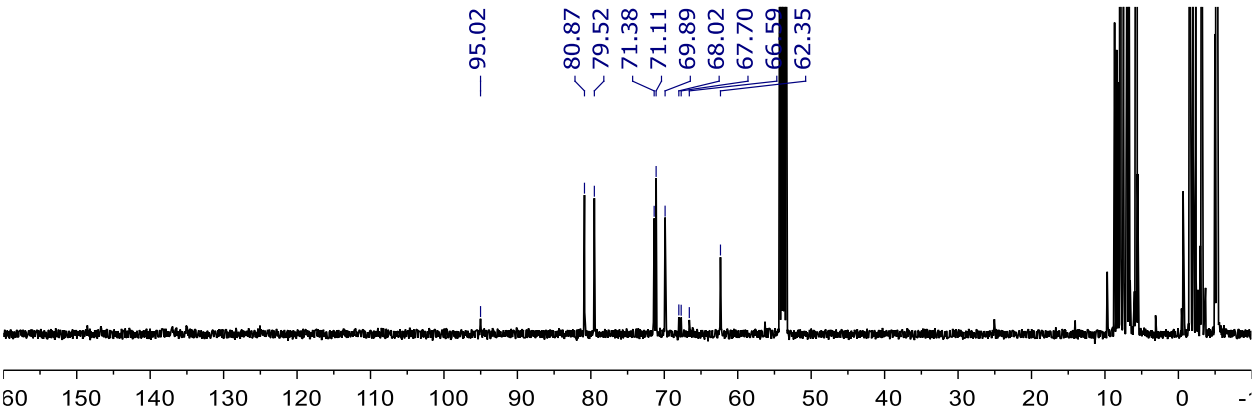

Figure 5.33: In situ NMR at -70°C of reduction of Me_2EtSi-protected 1-deoxy glucose with Me_2EtSiH 10 mol% $B(C_6F_5)_3$.

Low temperature NMR study of 1-deoxy glucose reduction with 50% B(C_6F_5)$_3$

Following Procedure 5B, 50 mg (0.10 mmol) of Me_2EtSi-protected 1-deoxy glucose was treated with 51 µL (0.40 mmol, 4 eq.) Me_2EtSiH in the presence of 25 mg (0.050 mmol, 0.5 eq) $B(C_6F_5)_3$. NMR spectra were acquired at various temperatures.

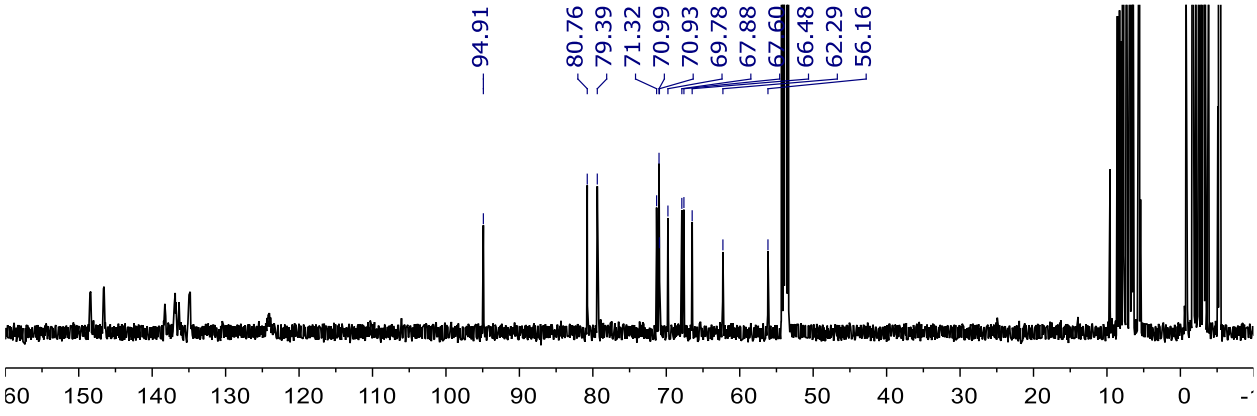

Figure 5.34: In situ NMR spectrum at -70°C of reduction of Me_2EtSi-protected 1-deoxy glucose with Me_2EtSiH and 50 mol % $B(C_6F_5)_3$.

Low temperature NMR spectrum of 6-deoxy, C_1-methoxy glucose reduction

Following Procedure 5B, 14 mg (0.080 mmol) unprotected 6-deoxy C_1-methoxy glucose **32** was treated with 100 µL (0.77 mmol, 10 eq.) Me_2EtSiH at in the presence of 15 mg (0.03 mmol, 0.4 eq.) $B(C_6F_5)_3$. A $^{13}C\{^1H\}$ NMR spectrum was acquired at -70°C.

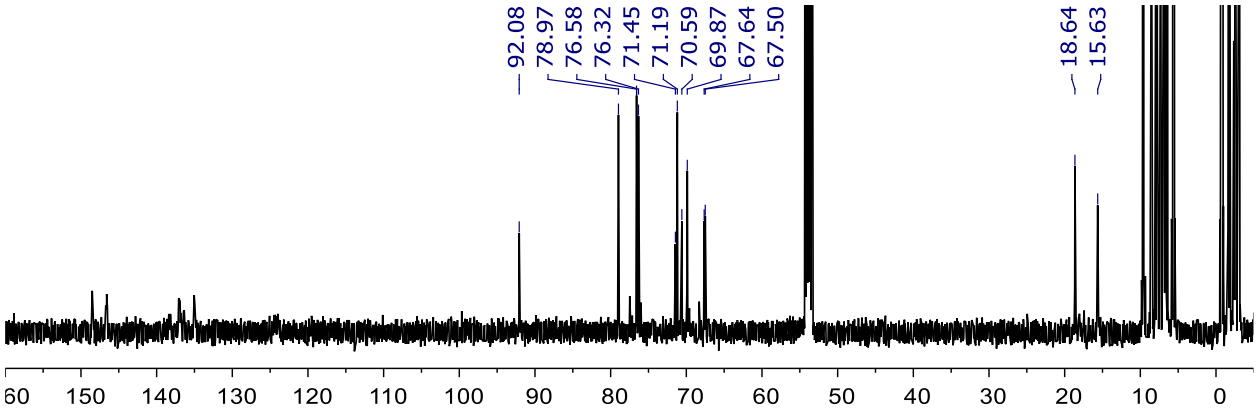

Figure 5.35: In situ NMR spectrum at -70°C of reduction of Me_2EtSi-protected 6-deoxy C_1-methoxy glucose with Me_2EtSiH 10 mol% $B(C_6F_5)_3$.

REFERENCES

Adlington, M. G.; Orfanopoulos, M.; Fry, J. L. *Tetrahedron Lett.* **1976**, *17*, 2955–2958.

Ahmed Foskey, T. J.; Heinekey, D. M.; Goldberg, K. I. *ACS Catal.* **2012**, *2*, 1285-1289.

Alonso, D. M.; Wettstein, S. G.; Dumesic, J. A. *Chem. Soc. Rev.* **2012**, *41*, 8075–8098.

Altomare, A.; Cascarano, G.; Giacovazzo, C.; Guagliardi, A.; Burla, M. C.; Polidori, G.; Camalli, M. *J. Appl. Cryst.* **1994**, *27*, 435.

Anderson, T. J.; Jones, G. D.; Vicic, D. A. *J. Am. Chem. Soc.* **2004**, *126*, 8100–8101.

Andrews, R. S.; Becker, J. J.; Gagné, M. R. *Angew. Chem. Int. Ed.* **2010**, *49*, 7274–7276.

Andrews, R. S.; Becker, J. J.; Gagné, M. R. *Angew. Chem. Int. Ed.* **2012**, *51*, 4140–4143.

Apple, D. C.; Brady, K. A.; Chance, J. M.; Heard, N. E.; Nile, T. A. *J. Mol. Catal. A* **1985**, *29*, 55-64

Arceo, E.; Marsden, P.; Bergman, R. G.; Ellman, J. A. *Chem. Commun.* **2009**, 3357-3359.

Barili, P. L.; Berti, G.; Catelani, G.; Cini, C.; D'Andrea, F.; Mastrorilli, E. *Carbohyd. Res.* **1995**, *278*, 43-57.

Barrett, C. J.; Dumesic, J. A.; Liu, Z. Y.; Roman-Leshkov, Y. *Nature* **2007**, *447*, 982-985.

Besson, M., Gallezot,P., Pinel, C. *Chem. Rev.* **2014**, *114*, 1827-1870.

Betteridge, P. W.; Carruthers, J. R.; Cooper, R. I.; Prout, K.; Watkin, D. J. *J. Appl. Cryst.* **2003**, *36*, 1487.

Blackwell, J. M.; Foster, K. L.; Beck, V. H.; Piers, W. E. *J. Org. Chem.* **1999**, *64*, 4887–4892.

Blaser, H. U. *Chem. Rev.* **1992**, *92*, 935–952.

Bourdreux, Y.; Lemetais, A.; Urban, D.; Beau, J.-M. *Chem. Comm.* **2011**, *47*, 2146–2148.

Cahiez, G.; Chaboche, C.; Duplais, C.; Moyeux, A. *Org. Lett.* **2008**, *11*, 277–280.

Cahiez, G.; Duplais, C.; Moyeux, A. *Org. Lett.* **2007**, *9*, 3253–3254.

Cárdenas, D. J. *Angew. Chem. Int. Ed.* **2003**, *42*, 384–387.

Carey, F. A.; Sundberg, R. J. *Advanced Organic Chemistry*; 4th ed.; Plenum Publishers: New York, 2000.

Chatani, N.; Ikeda, T.; Sano, T.; Sonoda, N.; Kurosawa, H.; Kawasaki, Y.; Murai, S. *J. Org. Chem.* **1988**, *53*, 3387–3389.

Chatani, N.; Shinohara, M.; Ikeda, S.-i.; Murai, S. *J. Am. Chem. Soc.* **1997**, *119*, 4303-4304.

Cheng, C.; Brookhart, M. *J. Am. Chem. Soc.* **2012**, *134*, 11304-11307

Cong, H.; Fu, G. C. *J. Am. Chem. Soc.* **2014**, *136*, 3788–3791.

Corma, A.; Iborra, S.; Velty, A. *Chem. Rev.* **2007**, *107*, 2411–2502.

DeShong, P.; Slough, G. A.; Elango, V. *Carbohydr. Res.* **1987**, *171*, 342–345.

DeShong, P.; Slough, G. A.; Elango, V.; Trainor, G. L. *J. Am. Chem. Soc.* **1985**, *107*, 7788-7790.

DeShong, P.; Soli, E. D.; Slough, G. A.; Sidler, D. R.; Elango, V.; Rybczynski, P. J.; Vosejpka, L. J. S.; Lessen,

Douvris, C.; Ozerov, O. V. *Science* **2008**, *321*, 1188-1190.

Du, Y.; Linhardt, R. J.; Vlahov, I. R. *Tetrahedron* **1998**, *54*, 9913–9959.

Ewing, G. J.; Robins, M. J. *Org. Lett.* **1999**, *1*, 635-636.

Fan, J.; De bruyn, M.; Budarin, V. L.; Gronnow, M. J.; Shuttleworth, P. S.; Breeden, S.; Macquarrie, D. J.; Clark, J. H. *J. Am. Chem. Soc.* **2013**, *135*, 11728–11731.

Farrugia, L. *J. Appl. Cryst.* **1997**, *30*, 565.

Feghali, E.; Cantat, T. *Chem. Commun.* **2014**, *50*, 862–865.

Fletcher, H. G., In: *Methods Carbohydr. Chem.*, 1962, Vol. 2; 1962, pp. 226-228.

Frisch, A. C.; Beller, M. *Angew. Chem. Int. Ed.* **2005**, *44*, 674–688.

Fry, J. L.; Orfanopoulos, M.; Adlington, M. G.; Dittman, W. P.; Silverman, S. B. *J. Org. Chem.* **1978**, *43*, 374–375.

Gallezot, P. *Chem. Soc. Rev.* **2012**, *41*, 1538-1558.

Geilen F. M. A., Engendahl, B., Harwardt, A., Marquardt, W., Klankermayer, J., Leitner, W. *Angew. Chem. Int. Ed.* **2010**, *149*, 5642-5646

Gevorgyan, V.; Liu, J.-X.; Rubin, M.; Benson, S.; Yamamoto, Y. *Tetrahedron Lett.* **1999**, *40*, 8919-8922.

Gevorgyan, V.; Rubin, M.; Benson, S.; Liu, J.-X.; Yamamoto, Y. *J. Org. Chem.* **2000**, *65*, 6179–6186.

Ghosh, P.; Fagan, P. J.; Marshall, W. J.; Hauptman, E.; Bullock, R. M. *Inorg. Chem.* **2009**, *48*, 6490-6500.

Giese, B.; Dupuis, J. *Angew. Chem. Int. Ed.* **1983**, *22*, 622–623.

Giese, B.; Dupuis, J. *Angew. Chem. Int. Ed.* **1983**, *22*, 622–623.

Giese, B.; Dupuis, J. *Tetrahedron Lett.* **1984**, *25*, 1349–1352.

Giese, B.; Dupuis, J.; Leising, M.; Nix, M.; Lindner, H. J. *Carbohydr. Res.* **1987**, *171*, 329–341.

Gong, H.; Andrews, R. S.; Zuccarello, J. L.; Lee, S. J.; Gagné, M. R. *Org. Lett.* **2009**, *11*, 879–882.

Gong, H.; Gagné, M. R. *J. Am. Chem. Soc.* **2008**, *130*, 12177–12183.

Gong, H.; Sinisi, R.; Gagné, M. R. *J. Am. Chem. Soc.* **2007**, *129*, 1908–1909.

Guo, Z.-W.; Hui, Y.-Z. *Synth. Commun.* **1996**, *26*, 2067-2073.

Gutsulyak, D. V.; Vyboishchikov, S. F.; Nikonov, G. I. *J. Am. Chem. Soc.* **2010**, *132*, 5950-5951.

Hartwig, J. F. *Organotransition Metal Chemistry: From Bonding to Catalysis*; University Science Books: Sausalito, 2010.

Higashibayashi, S.; Czechtizky, W.; Kobayashi, Y.; Kishi, Y. *J. Am. Chem. Soc.* **2003**, *125*, 14379–14393.

Hills, I. D.; Netherton, M. R.; Fu, G. C. *Angew. Chem. Int. Ed.* **2003**, *42*, 5749–5752.

Hoffman, R. A.; Forsen, S.; Gestblom, B. In *N.M.R. Basic Principles and Progress*, 1971; Vol. 71.

Hosomi, A.; Sakata, Y.; Sakurai, H. *Carbohydr. Res.* **1987**, *171*, 223–232.

Hosomi, A.; Sakata, Y.; Sakurai, H. *Tetrahedron Lett.* **1984**, *25*, 2383–2386.

Huber, G. W.; Iborra, S.; Corma, A. *Chem. Rev.* **2006**, *106*, 4044-4098.

In Hwan, O.; Gray, G. R. *Carbohydr. Res.* **1995**, *278*, 329-338.

Jensen, A. E.; Knochel, P. *J. Org. Chem.* **2001**, *67*, 79–85.

Jones, G. D.; Martin, J. L.; McFarland, C.; Allen, O. R.; Hall, R. E.; Haley, A. D.; Brandon, R. J.; Konovalova, T.; Desrochers, P. J.; Pulay, P.; Vicic, D. A. *J. Am. Chem. Soc.* **2006**, *128*, 13175–13183.

Jones, G. D.; McFarland, C.; Anderson, T. J.; Vicic, D. A. *Chem. Commun.* **2005**, 4211–4213.

Jones, G. S.; Scott, W. J. *J. Am. Chem. Soc.* **1992**, *114*, 1491–1492.

Joshi-Pangu, A.; Ganesh, M.; Biscoe, M. R. *Org. Lett.* **2011**, *13*, 1218-1221.

Kerr, R. A.; Service, R. F. *Science* **2005**, *309*, 101.

Komatsu, N.; Uda, M.; Suzuki, H.; Takahashi, T.; Domae, T.; Wada, M. *Tetrahedron Lett.* **1997**, *38*, 7215–7218.

Kozikowski, A. P.; Sorgi, K. L.; Wang, B. C.; Xu, Z. *Tetrahedron Lett.* **1983**, *24*, 1563–1566.

Kunkes, E. L.; Simonetti, D. A.; West, R. M.; Serrano-Ruiz, J. C.; Gärtner, C. A.; Dumesic, J. A. *Science* **2008**, *322*, 417–421.

Labinger, J. A.; Osborn, J. A. *Inorg. Chem.* **1980**, *19*, 3230–3236.

Lambert, J. B.; Shurvell, H. F.; Lightner, D. A.; Cooks, R. G. *Organic Structural Spectroscopy*; Simon & Schuster, 1998.

Lambert, J. B.; Zhang, S.; Ciro, S. M. *Organometallics* **1994**, *13*, 2430–2443.

Lambert, J. B.; Zhao, Y.; Wu, H. *J. Org. Chem.* **1999**, *64*, 2729–2736.

Larsen, C. H.; Ridgway, B. H.; Shaw, J. T.; Smith, D. M.; Woerpel, K. A. *J. Am. Chem. Soc.* **2005**, *127*, 10879–10884.

Lemieux, R. U.; Hayami, J. I. *Can J Chem* **1965**, *43*, 2162-2173.

Lemieux, R. U.; Hendriks, K. B.; Stick, R. V.; James, K. *J. Am. Chem. Soc.* **1975**, *97*, 4056-4062.

Lemieux, R. U.; Huber, G. *Can. J. Chem.* **1955**, *33*, 128-133.

Leroux, J.; Perlin, A. S. *Carbohydr. Res.* **1978**, *67*, 163–178.

Levy, D. E.; Tang, C. *The Chemistry of C-Glycosides*; Elsevier Science Ltd.: New York, 1995.

López-Pérez, A.; Adrio, J.; Carretero, J. C. *Org. Lett.* **2009**, *11*, 5514–5517.

Lu, Z.; Fu, G. C. *Angew. Chem. Int. Ed.* **2010**, *49*, 6676-6678.

Luh, T.-Y.; Leung, M.-k.; Wong, K.-T. *Chem. Rev.* **2000**, *100*, 3187-3204.

Mack, D. J.; Guo, B.; Njardarson, J. T. *Chem. Commun.* **2012**, *48*, 7844–7846.

Manolikakes, G.; Muñoz Hernandez, C.; Schade, M. A.; Metzger, A.; Knochel, P. *J. Org. Chem.* **2008**, *73*, 8422-8436.

Mascal, M.; Nikitin, E. B. *Angew. Chem. Int. Ed.* **2008**, *47*, 7924-7926.

Maurer, K.; Bohme, R. *Ber. Dtsch. Chem. Ges.* **1936**, *69B*, 1399-1410.

Meyer, N.; Lough, A. J.; Morris, R. H. *Chem. – A Eur. J.* **2009**, *15*, 5605–5610.

Mikami, K.; Lautens, M. *New Frontiers in Asymmetric Catalysis*; Wiley-Interscience, Inc.: Hoboken, N.J, 2007.

Miljkovic, M. *Electrostatic and Stereoelectronic Effects in Carbohydrate Chemistry*; Springer US: New York, 2014.

Mukhopadhyay, B.; Kartha, K. P. R.; Russell, D. A.; Field, R. A. *J. Org. Chem.* **2004**, *69*, 7758-7760.

Murai, T.; Furuta, K.; Kato, S.; Murai, S.; Sonoda, N. *J. Organomet. Chem.* **1986**, *302*, 249-254.

Netherton, M. R.; Fu, G. C. *Adv. Synth. Catal.* **2004**, *346*, 1525-1532.

Netherton, M. R.; Fu, G. C. In *Palladium in Organic Synthesis*, 2005; Vol. 14; pp 124-134.

Nichols, J. M.; Bishop, L. M.; Bergman, R. G.; Ellman, J. A. *J. Am. Chem. Soc.* **2010**, *132*, 12554-12555.

Nicotra, F. *Top. Curr. Chem.* **1997**, *187*, 55–83.

Nimmagadda, R. D.; McRae, C. *Tetrahedron Lett.* **2006**, *47*, 5755–5758.

Olah, G. A. In *Carbonium Ions*, Olah, G. A. Ed. Wiley: New York, 1970; Vol. 2, pp 655-782

Olah, G. A.; White, A. M. *J. Am. Chem. Soc.* **1969**, *91*, 5801-5810

Parks, D. J.; Blackwell, J. M.; Piers, W. E. *J. Org. Chem.* **2000**, *65*, 3090–3098.

Parks, D. J.; Piers, W. E. *J. Am. Chem. Soc.* **1996**, *118*, 9440–9441.

Pelczar, E. M.; Munro-Leighton, C.; Gagné, M. R. *Organometallics* **2009**, *28*, 663–665.

Petzold, K., Koschella, A., Klemm, D., Heublein, B., *Cellulose* **2003**, *10*, 251-269

Pieters, L. A. C.; Vlietinck, A. J. *J. Pharm. Biomed. Anal.* **1989**, *7*, 1405-1417

Powell, D. A.; Fu, G. C. *J. Am. Chem. Soc.* **2004**, *126*, 7788-7789.

Powell, D. A.; Maki, T.; Fu, G. C. *J. Am. Chem. Soc.* **2005**, *127*, 510–511.

Ragauskas, A. J.; Williams, C. K.; Davison, B. H.; Britovsek, G.; Cairney, J.; Eckert, C. A.; Jr, W. J. F.; Jason, P. H.; Leak, D. J.; Liotta, C. L.; Mielenz, J. R.; Murphy, R.; Templer, R.; Tschaplinski, T. *Science* **2006**, *311*, 484-489.

Robert, M. Oestreich, *Angew. Chem. Int. Ed.* **2013**, *52*, 5216-5218

Rolf, D.; Bennek, J. A.; Gray, G. R. *Carbohydr. Res.* **1985**, *137*, 183-196.

Román-Leshkov, J. N. Chheda, J. A. Dumesic, *Science* **2006**, *312*, 1933-1937

Roman-Leshkov, Y.; Barrett, C. J.; Liu, Z. Y.; Dumesic, J. A. *Nature* **2007**, *447*, 982–985.

Rosen, B. M.; Quasdorf, K. W.; Wilson, D. A.; Zhang, N.; Resmerita, A.-M.; Garg, N. K; Percec, V. *Chem. Rev.* **2011**, *111*, 1346–1416.

Rudolph, A.; Lautens, M. *Angew. Chem. Int. Ed.* **2009**, *48*, 2656–2670.

Ruppert, A. M.; Weinberg, K.; Palkovits, R. *Angew. Chem. Int. Ed.* **2012**, *51*, 2564–2601.

Schlaf, M. *Dalt. Trans.* **2006**, 4645–4653.

Schlaf, M.; Ghosh, P.; Fagan, P. J.; Hauptman, E.; Bullock, R. M. *Adv. Synth. Catal.* **2009**, *351*, 789–800.

Schlaf, M.; Thibault Michelle, E.; DiMondo, D.; Taher, D.; Karimi, E.; Ashok, D. *Int. J. Chem. React. Eng.*, 2009, *7*.

Scott, V. J.; Çelenligil-Çetin, R.; Ozerov, O. V. *J. Am. Chem. Soc.* **2005**, *127*, 2852-2853.

Sergeev, A. G.; Hartwig, H.F. *Science* **2011**, *332*, 439-442.

Serrano-Ruiz, J. C.; Braden, D. J.; West, R. M.; Dumesic, J. A. *Appl. Catal. B Environ.* **2010**, *100*, 184–189.

Sherry, B. D.; Fürstner, A. *Acc. Chem. Res.* **2008**, *41*, 1500–1511.

Smith, D. M.; Tran, M. B.; Woerpel, K. A. *J. Am. Chem. Soc.* **2003**, *125*, 14149–14152.

Smith, D. M.; Woerpel, K. A. *Org. Lett.* **2004**, *6*, 2063–2066.

Someya, H.; Ohmiya, H.; Yorimitsu, H.; Oshima, K. *Org. Lett.* **2007**, *9*, 1565–1567.

Stoddart, J. F. *Stereochemistry of Carbohydrates*; John Wiley & Sons, I., Ed.; New York, 1971; pp. 32–33.

Sustmann, R.; Lau, J.; Zipp, M. *Tet. Lett.* **1986**, *27*, 5207–5210.

T. A.; Le, T. X.; Anderson, G. B.; von Philipsborn, W.; Vöhler, M.; Rentsch, D.; Zerbe, O. *J. Organomet. Chem.* **2000**, *593-594*, 49–62.

Taher, D.; Thibault, M. E.; Di Mondo, D.; Jennings, M.; Schlaf, M. *Chem. Eur. J.* **2009**, *15*, 10132-10143.

Tatsuno, Y.; Yoshida, T.; Otsuka, S. *Inorg. Synth.* **1990**, *28*, 342-5.

Terao, J.; Kambe, N. *Acc. Chem. Res.* **2008**, *41*, 1545–1554.

Tolman, C. A. *Chem. Rev.* **1977**, *77*, 313-348.

Trainor, G. L.; Smart, B. E. *J. Org. Chem.* **1983**, *48*, 2447–2448.

Vechorkin, O.; Proust, V.; Hu, X. *J. Am. Chem. Soc.* **2009**, *131*, 9756-9766.

Wang, S.; Qian, Q.; Gong, H. *Org. Lett.* **2012**, *14*, 3352–3355.

Wasa, M.; Engle, K. M.; Yu, J.-Q. *Isr. J. Chem.* **2010**, *50*, 605-616.

Wellington, K. W.; Benner, S. A. *Nucleosides, Nucleotides and Nucleic Acids* **2006**, *25*, 1309–1333.

Werpy, T. and Petersen G., Top Value Added Chemicals from Biomass, Volume I, Results of Screening for Potential Candidates from Sugar and Synthesis Gas, US Department of Energy DOE/GO-102004-1992, August 2004

Wood, H. B.; Diehl, H. W.; Fletcher, H. G. *J. Am. Chem. Soc.* **1957**, *79*, 1986-1988.

Xia, Q.-H.; Ge, H.-Q.; Ye, C.-P.; Liu, Z.-M.; Su, K.-X. *Chem. Rev.* **2005**, *105*, 1603–1662.

Yang, G.; Schmieg, J.; Tsuji, M.; Franck, R. W. *Angew. Chem. Int. Ed.* **2004**, *43*, 3818–3822.

Yang, J.; Brookhart, M. *J. Am. Chem. Soc.* **2007**, *129*, 12656–12657.

Yang, J.; White, P. S.; Brookhart, M. *J. Am. Chem. Soc.* **2008**, *130*, 17509–17518.

Yang, W.; Grochowski, M. R.; Sen, A. *ChemSusChem* **2012**, *5*, 1218-1222.

Zhao, H.; Holladay, J. E.; Brown, H.; Zhang, Z. C. *Science* **2007**, *316*, 1597-1600.

Zhou, J.; Fu, G. C. *J. Am. Chem. Soc.* **2003**, *125*, 12527–12530.

Zhou, J.; Fu, G. C. *J. Am. Chem. Soc.* **2003**, *125*, 14726–14727.

Zhou, J.; Fu, G. C. *J. Am. Chem. Soc.* **2004**, *126*, 1340–1341.

Ziegler, J. E.; Zdilla, M. J.; Evans, A. J.; Abu-Omar, M. M. *Inorg. Chem.* **2009**, *48*, 9998-10000.